Pedro Manuel Francisco Valério

Mestre em Química Aplicada ao Património Cultural

Archaeometallurgical Study of Pre and Protohistoric Production Remains and Artefacts from Southern Portugal

Dissertação para obtenção do Grau de Doutor em
Conservação e Restauro, especialidade Ciências da Conservação

Orientador: Maria de Fátima Araújo, Investigadora Principal, Instituto Tecnológico e Nuclear
Co-orientador: Rui Jorge Cordeiro Silva, Professor Auxiliar, Faculdade de Ciências e Tecnologia
Co-orientador: António Monge Soares, Investigador Principal, Instituto Tecnológico e Nuclear

Júri:

Presidente: Prof. Doutor Fernando Jorge Pina
Arguentes: Prof. Doutor Salvador Rovira Llorens
Prof. Doutor João Luís Serrão da Cunha Cardoso

Vogais: Prof. Doutor João Carlos de Freitas de Senna-Martinez
Prof. Doutora Márcia Gomes Vilarigues
Doutor Luís Manuel Cerqueira Lopes Alves

FACULDADE DE CIÊNCIAS E TECNOLOGIA
UNIVERSIDADE NOVA DE LISBOA

Março de 2012

Archaeometallurgical Study of Pre and Protohistoric Production Remains and Artefacts from Southern Portugal

Copyright: Pedro Manuel Francisco Valério, Faculdade de Ciências e Tecnologia da Universidade Nova de Lisboa (FCT/UNL), Universidade Nova de Lisboa (UNL).

A Faculdade de Ciências e Tecnologia e a Universidade Nova de Lisboa têm o direito, perpétuo e sem limites geográficos, de arquivar e publicar esta dissertação através de exemplares impressos reproduzidos em papel ou de forma digital, ou por qualquer outro meio conhecido ou que venha a ser inventado, e de a divulgar através de repositórios científicos e de admitir a sua cópia e distribuição com objectivos educacionais ou de investigação, não comerciais, desde que seja dado crédito ao autor e editor.

Lisboa, Março de 2012

ACKNOWLEDGMENTS

This thesis was developed in the framework of the project "Early Metallurgy in the Portuguese Territory, EARLYMETAL" (PTDC/HIS/ARQ/110442/2008) financed by the Portuguese Science Foundation. The analytical work was conducted in several research units, namely (i) Grupo de Química Analítica e Ambiental (QAA - ITN); (ii) Centro de Investigação em Materiais/Instituto de Nanoestruturas, Nanomodelação e Nanofabricação (CENIMAT/I3N), Departamento de Ciências dos Materiais (DCM – FCT-UNL); and (iii) Departamento de Conservação e Restauro (DCR – FCT-UNL).

I wish to express my gratitude to my supervisors, M. Fátima Araújo (Instituto Tecnológico e Nuclear, ITN), Rui J.C. Silva (Faculdade de Ciências e Tecnologia da Universidade Nova de Lisboa, FCT-UNL) and A. Monge Soares (ITN) for guidance during this work. I would like to thank archaeologists and institutions that provided the artefacts for study, especially M. Almeida (Dryas); L. Barros (Museu Municipal de Almada); L. Berrocal-Rangel (Universidad Autónoma de Madrid); J.L. Cardoso (Universidade Aberta); M. Deus (Instituto de Gestão do Património Arquitectónico e Arqueológico); J. Dewulf; A. Gregório; R. Mataloto (UNIARQ); P. Rebelo, N. Neto, R. Santos and T. Fontes (NeoÉpica); T. Ricou (Universidade do Porto); A.I. Santos and L. Raposo (Museu Nacional de Arqueologia); F.J.C. Santos; A.C. Silva (Direcção Regional da Cultura do Alentejo); R. Silva (Museu Municipal de Torres Vedras); A.C. Valera (ERA Arqueologia) and R. Vilaça (Universidade de Coimbra).

Thanks also to my colleagues, E. Figueiredo, M.J. Furtado, J.M. Martins, G. Cardoso, R. Cardoso and F. Peralta, for the exchange of thoughts, ideas and friendship.

A special word to my family for providing me constant inspiration to carry out this work.

RESUMO

Este trabalho compreende um estudo multidisciplinar sobre a metalurgia antiga no sul de Portugal, sendo analisados 241 vestígios metalúrgicos e artefactos pertencentes maioritariamente ao Bronze Final (BF) e 1ª Idade do Ferro (1ª IF). A composição elementar foi determinada por espectrometria de fluorescência de raios X dispersiva de energias, sendo a caracterização microestrutural e dureza obtidas por microscopia óptica, microscopia electrónica de varrimento com microanálise por raios X e ensaios de dureza de Vickers.

Os resultados incluem a caracterização de escórias heterogéneas e imaturas (BF) contendo óxidos de estanho e inclusões metálicas (cobre e bronze) com teores reduzidos de ferro. A presença de minerais relíquia indica a co-redução de minérios de cobre, provavelmente, com cassiterite. A atmosfera pouco redutora destes processos resulta nos teores de ferro reduzidos dos artefactos do BF (<0.05%) face aos da 1ª IF (0.15-1.3%). A composição elementar distingue igualmente as colecções indígenas (bronzes binários, 10.0 ± 2.5% Sn) das Orientalizantes (bronzes binários, 5.1 ± 2.1% Sn, ternários e cobres). O teor de estanho reduzido dos bronzes tardios deverá resultar da utilização de sucata. As cadeias operatórias incluem ciclos de martelagem e recozimento, terminando com martelagem para aumentar a dureza. Os artefactos com teores elevados de estanho não foram trabalhados e não requerem uma resistência mecânica elevada, revelando a triagem de ligas. Determinados exemplares tardios apresentam uma dureza superior devido a operações de martelagem e recozimento mais eficientes, sugerindo que o teor reduzido de estanho seria compensado por um elevado conhecimento tecnológico.

Os artefactos em ouro Calcolíticos apresentam teores reduzidos de prata, enquanto os exemplares do BF e 1ª IF são maioritariamente constituídos por ligas com teores superiores de prata e cobre. A martelagem e recozimento de ouros Calcolíticos, bem como a soldadura por fusão parcial/difusão em fase sólida durante a 1ª IF encontram-se igualmente identificadas.

TERMOS CHAVE

Bronze; ouro; composição elementar; cadeia operatória; Bronze Final; 1ª Idade do Ferro

ABSTRACT

This work provides an integrated study of the ancient metallurgy in southern Portugal comprising the characterisation of 241 production remains and artefacts, mostly belonging to the Late Bronze Age (LBA) and Early Iron Age (EIA). Analytical studies involve energy dispersive X-ray fluorescence spectrometry (EDXRF) and micro-EDXRF to determine elemental composition, together with optical microscopy, scanning electron microscopy with X-ray microanalysis and Vickers microhardness testing for microstructural characterisation and hardness determination.

Main results include identification of heterogeneous and immature LBA slags containing tin oxides and metallic prills (copper and bronze) with low iron contents. Additionally, relic mineral inclusions indicate co-smelting of copper ores, probably with cassiterite. Poor reducing conditions shall be responsible by lower iron contents of LBA artefacts (<0.05%) when compared with EIA artefacts (0.15-1.3%). Further features distinguish these clusters – indigenous collection is composed mostly by binary bronzes (10.0 ± 2.5% Sn), while Orientalising collection also presents copper and leaded bronzes. Furthermore, latter binary bronzes exhibit lower tin contents (5.1 ± 2.1% Sn) probably due to the increased use of scrap. Operational sequences usually include cycles of forging and annealing, often completed with a final hammering that hardens the artefact. Higher tin content artefacts with typologies that do not require high mechanical strength were often left as-cast evidencing some selection of alloys. Despite being poorer in tin, some EIA artefacts exhibit higher hardness due to a more efficient use of hammering and annealing cycles, suggesting that low tin contents were not a problem for this type of artefacts.

Gold metallurgy analyses allow the identification of Chalcolithic gold with minor amounts of silver, while LBA and EIA gold present increased silver and copper contents, indicating the use of alloyed gold. Forging and annealing during the Chalcolithic, besides welding with partial melting/solid state diffusion during the EIA is also established.

KEYWORDS

Copper-based; gold; elemental composition; operational sequence; Late Bronze Age; Early Iron Age

INDEX OF CONTENTS

INDEX OF FIGURES

INDEX OF TABLES

SYMBOLS AND NOTATIONS

BA	Bronze Age
BCS	British Chemical Standards
BSE	BackScattered Electron imaging mode of SEM
CA	Copper Age or Chalcolithic
CENIMAT	Centro de Investigação de Materiais
DCM	Departamento de Ciências dos Materiais
DCR	Departamento de Conservação e Restauro
EBA	Early Bronze Age
EDXRF	Energy Dispersive X-Ray Fluorescence
EIA	Early Iron Age
HV	Vickers Hardness number
IA	Iron Age
ITN	Instituto Tecnológico e Nuclear
FCT	Faculdade de Ciências e Tecnologia
LBA	Late Bronze Age
MBA	Middle Bronze Age
OES	Optical Emission Spectroscopy
OM	Optical Microscopy
OM-BF	Optical Microscopy - Bright Field illumination
OM-DF	Optical Microscopy - Dark Field illumination
OM-Pol	Optical Microscopy - Polarised light
SAM	Studien zu den Anfängen der Metallurgie (SAM project)
SE	Secondary Electron imaging mode of SEM
SEM-EDS	Scanning Electron Microscopy with X-Ray Microanalysis
UNL	Universidade Nova de Lisboa

PUBLISHED WORK

Some contents of this work have been published and presented in scientific meetings.

Peer-reviewed papers:

1. Valério, P., Silva, R.J.C., Araújo, M.F., Soares, A.M.M., Barros L. 2012. A multianalytical approach to study the Phoenician bronze technology in the Iberian Peninsula – a view from Quinta do Almaraz. *Materials Characterization* 67, 74-82.
2. Figueiredo, E., Valério, P., Araújo, M.F., Silva, R.J.C., Soares, A.M.M. 2011. Inclusions and metal composition of ancient copper-based artefacts: a diachronic view by micro-EDXRF and SEM-EDS. *X-Ray Spectrometry* 40, 325-332.
3. Soares, A.M.M., Valério, P., Silva, R.J.C., Alves, L.C., Araújo, M.F. 2010. Early Iron Age gold buttons from South-Western Iberian Peninsula. Identification of a gold metallurgical workshop. *Trabajos de Prehistoria* 67/2, 501-510.
4. Valério, P., Silva, R.J.C., Soares, A.M.M., Araújo, M.F., Braz Fernandes, F.M., Silva, A.C., Berrocal-Rangel, L. 2010. Technological continuity in Early Iron Age bronze metallurgy at the South-Western Iberian Peninsula – a sight from Castro dos Ratinhos. *Journal of Archaeological Science* 37, 1811-1919.
5. Valério, P., Silva, R.J.C., Araújo, M.F., Soares, A.M.M., Braz Fernandes, F.M. 2010. Microstructural signatures of bronze archaeological artifacts from the southwestern Iberian Peninsula. *Materials Science Forum* 636-637, 597-604.

Other papers:

1. Valério, P., Alves, L.C., Soares, A.M.M., Araújo, M.F. 2010. Os metais dos Ratinhos. II. Os botões em ouro. In: Berrocal-Rangel, L., Silva, A.C. (Eds.) O Castro dos Ratinhos (Barragem do Alqueva, Moura). Escavações num povoado proto-histórico do Guadiana, 2004-2007. *O Arqueólogo Português Suplemento* 6, 381-388.
2. Valério, P., Araújo, M.F., Silva, R.J.C., Soares, A.M.M. 2010. Os metais dos Ratinhos I. A metalurgia do bronze. In: Berrocal-Rangel, L., Silva, A.C. (Eds.) O Castro dos Ratinhos (Barragem do Alqueva, Moura). Escavações num povoado proto-histórico do Guadiana, 2004-2007. *O Arqueólogo Português Suplemento* 6, 369-380.
3. Santos, F.J.C., Arez, L., Soares, A.M.M., Deus, M., Queiroz, P.F., Valério, P., Rodrigues, Z., Antunes, A.S., Araújo, M.F. 2008. O Casarão da Mesquita 3 (S. Manços, Évora): um sítio de fossas "silo" do Bronze Pleno/Final na Encosta do Albardão. *Revista Portuguesa de Arqueologia* 11, 55-86.

4. Ponte, T.R.N., Soares, A.M.M., Araújo, M.F., Frade, J.C., Ribeiro, I., Rodrigues, Z., Silva, R.J.C., Valério, P. in press. O Bronze Pleno do Sudoeste da Horta do Folgão (Serpa, Portugal). Os Hipogeus Funerários. *Revista Portuguesa de Arqueologia*.

5. Valério, P., Silva, R.J.C., Araújo, M.F., Soares, A.M.M., Barros L. in press. Influências orientalizantes na metalurgia do bronze do sul do território Português: estudo por micro-EDXRF, OM e SEM-EDS de artefactos da Quinta do Almaraz. *XELB.*

Scientific meetings:

1. Valério, P., Silva, R.J.C., Araújo, M.F., Soares, A.M.M., Barros, L. – Orientalising influences on bronze metallurgy at southern Portugal: Micro-EDXRF, OM and SEM-EDS evidences from Quinta do Almaraz. *1st International Congress Settlement and Mining Exploration in the Atlantic Western Europe*, Braga, Portugal, December 2010, 54.

2. Valério, P., Silva, R.J.C., Araújo, M.F., Soares, A.M.M., Barros, L. – Influências orientalizantes na metalurgia do bronze do sul do território Português: estudo por Micro-EDXRF, OM e SEM-EDS de artefactos da Quinta do Almaraz. *8º Encontro de Arqueologia do Algarve*, Silves, Portugal, October 2010, 25.

3. Valério, P., Araújo, M.F., Silva, R.J.C., Soares, A.M.M., Braz Fernandes, F.M. – A metalurgia do cobre no sul do território Português entre o Bronze Médio e a 1ª Idade do Ferro: teores de ferro e inclusões Cu-S. *VI Simpósio sobre Mineração e Metalurgia Históricas no Sudoeste Europeu*, Vila Velha de Ródão, Portugal, June 2010, 77.

4. Valério, P., Silva, R.J.C., Soares, A.M.M., Araújo, M.F., Braz Fernandes, F.M., Gregório, A., Rebelo, P., Neto, N., Santos, R., Fontes, T. – The beginning of bronze metallurgy in southern Portugal – Preliminary results from Entre Águas 5 (Serpa). *Archaeometallurgy: Technological, Economic and Social Perspectives in Late Prehistoric Europe*, Madrid, Spain, November 2009, 57.

5. Valério, P., Araújo, M.F., Silva, R.J.C., Soares, A.M.M., Silva, A.C., Berrocal-Rangel, L. – Composição química e microestrutural de artefactos metálicos do Castro dos Ratinhos (Moura, Portugal) – Bronze Final e 1ª Idade do Ferro, *IV Encontro de Arqueologia do Sudoeste Peninsular*, Huelva, Spain, November 2008, 489-513 (CD-ROM) (ISBN 978-84-92679-59-1).

6. Valério P., Alves, L.C., Soares, A.M.M., Berrocal-Rangel, L., Silva, A.C., Araújo, M.F. – Early Iron Age gold artefacts from Castro dos Ratinhos (Moura, Southern Portugal). *2nd International Conference Archaeometallurgy in Europe*. Aquileia, Italy, June 2007, 9 p. (CD-ROM) (ISBN 978-88-85298-61-3).

1. INTRODUCTION

The archaeometallurgical research presents a considerable importance in the archaeological field due to the relevant significance of metallurgy in the social and cultural organization of ancient cultures (Craddock, 1995). The study of this important component of the ancient material culture should incorporate different areas of knowledge, connecting analytical studies with the historical and cultural background revealed by archaeological contexts from which the artefacts and production remains were recovered.

The multidisciplinary study of these ancient materials should begin by identifying the different metallurgical issues evidenced by each chronological period, in order to significantly contribute to establish the metallurgical evolution of the studied region. Pre-historic and proto-historic times can be divided into different stages that imply progressively higher metallurgical knowledge. Generally, these phases comprise the use of native metals, the reduction of metallic ores and the production of alloys. Each one of these consecutive stages corresponds to a different chronological period that can differ from one region to another. However, the metallurgical issues involving each stage are common to virtually all regions of the Ancient World.

Metallic elements exploited during ancient times usually occur in the form of minerals, especially oxides and sulphides. Gold constitutes an exception since it is almost always present in the native form. Moreover, copper and silver can also be found in the native form often associated with their respective ores (e.g. cuprite (Cu_2O) and malachite ($Cu_2CO_3(OH)_2$) or cerargyrite (AgCl) and argentite (Ag_2S), respectively). Pre-historic communities in the Middle East start to use native metals during a premature phase of the Neolithic period. The earlier copper artefacts known are some beads, awls and fish-hooks from Çayönü Tepesi (Turkey), belonging to the end of the 8th millennium BC (Maddin *et al.*, 1991).

However, it is usually considered that the metallurgy only started with the exploitation of metallic ores, whose reduction significantly increased the amount of raw materials available to produce metallic artefacts. Copper obtained by early metallurgical processes presents an elemental composition similar to native copper, whereas it is often complicated to distinguish between smelting and melting slags. Consequently, it is very difficult to clearly identify the initial stages of the exploitation of metallic ores. According to the work of Renfrew (1983), smelting started in the Middle East during the 6th-5th millennia BC, but it was only during the 4th millennium BC that it began to present a real importance to those ancient communities. The 6500 BC slags from Çatal Höyök (Turkey) are probably the first evidence of ore smelting in the Middle East (Hauptmann,

2007). In Europe, a recent work (Radivojevic *et al.*, 2010) documents the earliest evidence of copper smelting at Belovode (Serbia), a Vinca culture site from the end of the 6th millennium BC.

In the Iberian Peninsula, the first evidence of the exploitation of copper ores belongs to the contexts from the first half of the 5th millennium BC of Cerro del Virtud, SE Spain (Ruíz-Taboada and Montero-Ruíz, 1999). However, this find is more than a millennium older than any other secure evidence of smelting in the region, so it is probable that copper ore smelting only occurred during the late 4th millennium BC (Roberts, 2008). The early sites with evidences of metallurgy in the Portuguese territory belong to the transition of the 4th to the 3rd millennium BC (Soares and Cabral, 1993), whereas the Copper Age or Chalcolithic (CA) corresponds to most of the 3rd millennium BC, namely around 3000-2250 BC.

The production and use of alloys was the following step within metallurgical evolution. Some of the metallic elements exploited during ancient times are commonly associated with others in nature. Native gold often presents high amounts of silver – a natural alloy called electrum, whereas copper ore can be found associated with arsenic (Mohen, 1990). Electrum was certainly one of the first alloys to be used during the pre-history. Similarly, arsenical coppers are present among the earlier contexts with evidences of metallurgy in some regions of the Iberian Peninsula (Ruíz-Taboada and Montero-Ruíz, 1999). However, in other regions such as the southern Portuguese territory these arsenical coppers only seem to appear by the end of the CA (Soares *et al.*, 1996).

The innovation of an alloy is related with the fact that it exhibits enhanced characteristics when compared with their individual metals. The possibility of attaining higher hardness or different colours was certainly among the first characteristics that were recognized by ancient metallurgists when producing copper-based or gold alloys. However, other characteristics such as lower melting temperature or higher castability of certain alloys were also exploited over time.

The bronze was certainly the more commonly utilised alloy during pre-historic times. The earlier bronze artefacts do not belong to a specific culture, instead being isolated discoveries from 3rd millennium BC sites at Bulgaria and Romania (Craddock, 1995). Consequently, the discovery of bronze alloy seems to be the outcome of an unintended reduction of polymetallic copper ores with significant amounts of tin. In the Iberian Peninsula, these mixed Cu-Sn ores are not as scarce as initially accepted (Hunt-Ortiz, 2003), being present in several mining areas (e.g. Toledo, Murcia and Sierra Morena) and displaying evidences of being used at a few pre-historic sites from central and southeastern regions (Rovira and Montero-Ruíz, 2003).

Bronze alloys were progressively introduced in the Portuguese territory during the Bronze Age (BA ~2250-800 BC), which is usually divided into the Early Bronze Age (EBA ~2250-1800 BC), Middle Bronze Age (MBA ~1800-1200 BC) and Late Bronze Age (LBA ~1200-800 BC). The EBA/MBA period did not introduce significant alterations among the copper-based metallurgy. Metallic artefacts maintain the tradition inherited from the end of the Chalcolithic, being composed of copper or arsenical copper (Soares *et al.*, 1996). The bronze artefacts only start to occur during the MBA but are still somewhat scarce among the archaeological record (Rovira, 2004).

The metallurgical background changes dramatically with the full adoption of bronze alloys during the LBA. This implementation coincides with a significant increase of typologies and number of metallic artefacts present in the archaeological record. During this period the Portuguese territory presents relations with other regions belonging to the Atlantic and Iberian traditions (Figure 1.1). A cultural regional tradition defines an area within which regular production and exchange of metalwork and pottery creates a stylistic regularity (Kristiansen, 2003). The Atlantic tradition includes the Northwestern Iberia, Western France and British Isles, which regarding the copper-based metallurgy are characterised by a significant use of leaded bronzes. However, the metallurgy at the Portuguese territory, as most of the Iberian Peninsula (Rovira, 2004), comprises mainly binary bronze alloys (Vilaça, 1997; Valério *et al.*, 2006; Figueiredo *et al.*, 2010).

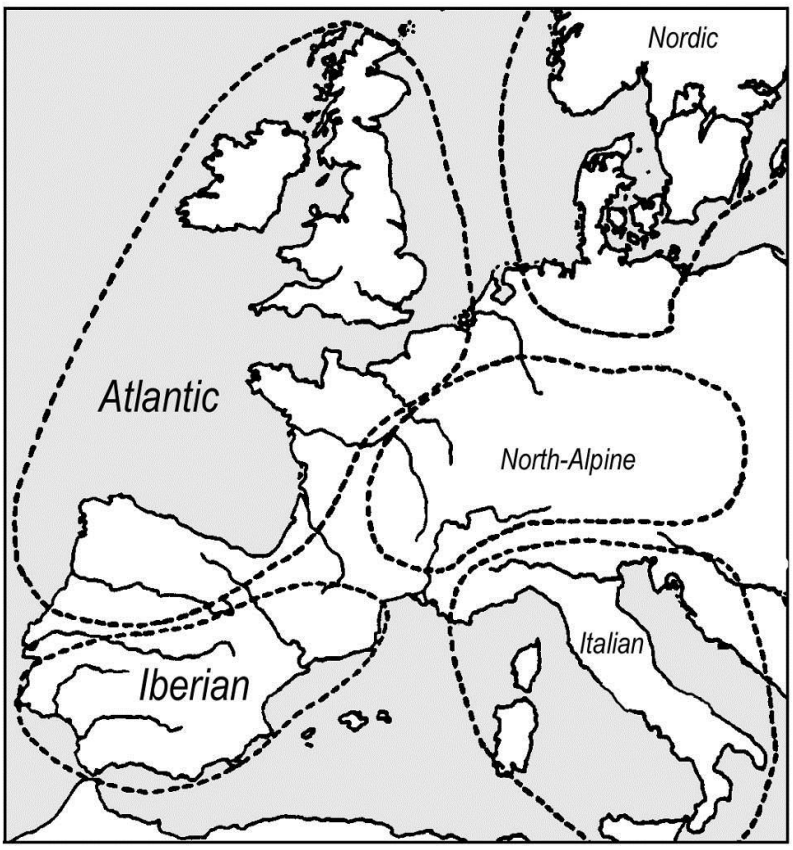

Figure 1.1. Schematic outline of regional traditions in LBA Europe (adapted from Kristiansen, 2003).

During the earliest centuries of the first millennium BC, the rich metallic resources of the Iberian Peninsula seem to have attracted people from the eastern Mediterranean region. The Phoenician trade routes include several intermediate regions along the Mediterranean Sea, such as Sardinia, North Africa, Italy and Sicily (Figure 1.2A). The increasingly stronger contacts with the Iberian Peninsula culminated with the establishment of Phoenician colonies along the southern and western seaboard during the late 9th and early 8th centuries BC (Figure 1.2). This occurrence initiated the Early Iron Age (EIA ~800-400 BC), a period characterised by introduction of new cultural and technological traditions brought by Mediterranean people, often called the Orientalising period. Metallurgy was among those innovations, including new practices, such as the lost wax method or the exploitation of silver through cupellation (Neville, 2007). However, studies regarding the EIA bronze metallurgy in the Iberian Peninsula are still rather scarce. In the southwestern region, the collections from the Orientalising settlements of Medellin and El Palomar already reveal a significant usage of leaded bronzes (Rovira *et al.*, 2005), but no comparable data is currently known concerning the Portuguese territory, except from a preliminary study concerning the Orientalising settlement of Quinta do Almaraz (Almada), which identified binary and leaded bronzes among the artefacts studied (Araújo *et al.*, 2004). The increased use of leaded bronzes was also recorded in the southeastern Iberian region (Montero-Ruíz, 2008), so it seems that this tendency might be widespread among areas with strong Orientalising influence.

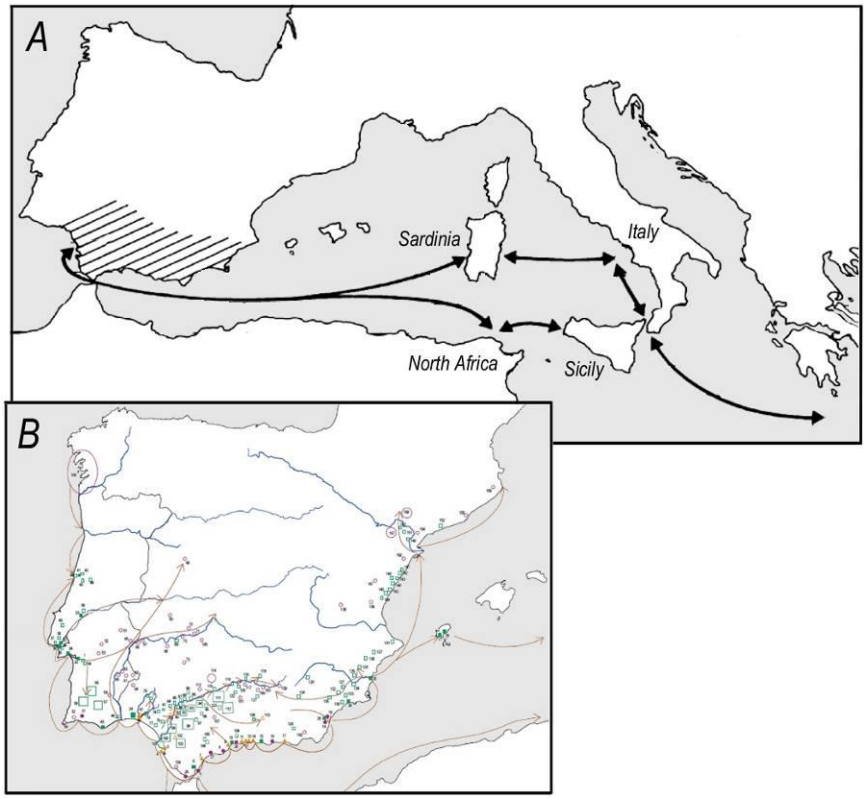

Figure 1.2. (A) Mediterranean trade routes on the basis of Ibero-Phoenician ivories and double-spring fibulae (adapted from Morgenroth, 1999); (B) Location of Phoenician and Orientalising settlements, together with trade routes at the Iberian Peninsula during the 8th-6th centuries BC (adapted from Pellicer-Catalán, 2000).

In fact, significant metallurgical studies regarding the pre-historic and proto-historic times at the Portuguese territory are very scant. Elemental compositions were obtained from the earlier study of gold artefacts by Hartmann (1982), in addition to the studies of Junghans *et al.* (1968; 1974) and Cofynn (1985) regarding copper-based artefacts. However, the chronology of metallic artefacts studied is often unreliable since it was obtained from typological comparisons and not from absolute dating. Moreover, the territory studied is too broad and regional differences were not taken into account. During the last decades several compositional studies were conducted regarding the copper-based metallurgy from the CA to the LBA (e.g. Cardoso *et al.*, 1992; Soares *et al.*, 1996; Vilaça, 1997; Cardoso, 2000; Melo, 2000; Araújo *et al.*, 2004; Sousa *et al.*, 2004; Gonçalves, 2005; Soares *et al.*, 2005; Valério *et al.*, 2006; Canha *et al.*, 2007; Figueiredo *et al.*, 2007; Valério *et al.*, 2007). However, the materials studied are mainly metallic artefacts and the few production remains present were only studied macroscopically. The study of ancient gold metallurgy at the Portuguese territory is even scarcer, with only a few studies regarding the elemental composition of artefacts (Alves *et al.*, 2002; Soares *et al.*, 2004). Despite some early microstructural analyses involving copper-based materials (Paço, 1955; Cardoso and Braz Fernandes, 1995; Soares *et al.*, 1996), it was only very recently that integrated studies involving the elemental composition and operational sequences of artefacts start to introduce more significant results concerning the metal production at the Portuguese territory (Figueiredo *et al*., 2010).

However, integrated studies regarding the southern region of the Portuguese territory have been absent. Despite some general idea about the evolution of the metallurgy in this region (Soares *et al.*, 1996) additional studies involving artefacts are needed to answer more precise and essential questions: What was the arsenic content of copper-based artefacts before the full adoption of bronze alloys? What was the evolution of the bronze alloys from the LBA to the EIA? There was any compositional difference between different typologies and functionalities? Which were the manufacturing operations involved? What was the evolution of the operational sequence? Did those operational sequences were able to produce harder materials? The present work intends to contribute to increase the knowledge regarding these and other important metallurgical issues.

A valuable collection of copper-based artefacts belonging to the southern region of the Portuguese territory was studied using a multiproxy approach comprising non-invasive and microanalytical techniques. The collection selected for study comprises mostly LBA and EIA artefacts, but some examples from the EBA/MBA were also studied. The elemental composition was determined by Micro-Energy Dispersive X-Ray Fluorescence (micro-EDXRF) analyses in minute cleaned areas of the metallic artefacts. This allows establishing the alloy composition with an insignificant interference to these cultural artefacts. The microstructural characterisation involved Optical Microscopy (OM) observations in the same cleaned areas, supported by Scanning Electron

Microscopy with X-Ray Microanalysis (SEM-EDS). This allows the identification of different phases, inclusions and casting defects, together with the manufacturing operations used to produce the artefacts. Finally, the hardness was determined by Vickers Microhardness Testing on selected artefacts to establish the effectiveness of the operational sequence.

Additionally, the elemental and microstructural characterisation of a significant number of LBA production remains (crucibles, tuyeres, moulds, metallic nodules and, especially, slags) contribute to resolve additional questions, such as: How was bronze alloy made? What were the operational conditions during smelting and casting operations? Did metallurgical operations were confined to a few locations or were commonly used in most settlements? This is an innovative approach concerning the metallurgy at the Portuguese territory. It will allow connecting the different metallurgical operations with the characteristics of the finished artefacts.

This work also includes the study of a collection of gold artefacts mainly belonging to the EIA, together with some examples from the LBA and the CA. The characterisation of these artefacts intends to determine the use and evolution of gold alloys at this southern region of the Portuguese territory, especially from the LBA until the EIA. Additionally, some microstructural analyses on a few selected artefacts intend to identify manufacturing procedures and welding operations during those ancient times.

The main contribution of this work is related with the recognition of the evolution of the copper-based metallurgy from the LBA to the EIA in the southern region of the Portuguese territory. The integrated study of production remains and metallic artefacts aims to provide a broad approach to different metallurgical issues, enabling a new insight into the Phoenician colonisation, especially about its influence on the indigenous metallurgy. Comparisons with coeval neighbouring regions will characterise intra-regional contacts and cultural exchanges among those ancient populations during the initial steps of the so-called Orientalising period.

2. MATERIALS AND METHODS

2.1. Materials

Ancient metallurgical materials can be divided into production remains and metallic artefacts. Production remains comprise all materials (e.g. crucibles, tuyeres, moulds, metallic nodules, ingots and slags) that resulted from the sequential steps involved in the production of artefacts. Generally, artefacts are finished products (ornaments, tools or weapons) that were used by ancient people in their daily life. Artefacts are often recovered in a fragmented state that can prevent the identification of its original functionality. Similarly, the accurate functionality of certain multipurpose artefacts, such as rings, hardly is attributable.

The following sections constitute an outline of the production remains, copper-based and gold objects studied in the present work. Special emphasis is given on the location of the archaeological sites, relevant chronologies, number and type of metallurgical materials.

2.1.1. Production remains

This collection is composed of 30 production remains, including crucibles, tuyeres, moulds, metallic nodules and slags, which belong to several LBA archaeological sites located at the southern region of the Portuguese territory (Figure 2.1).

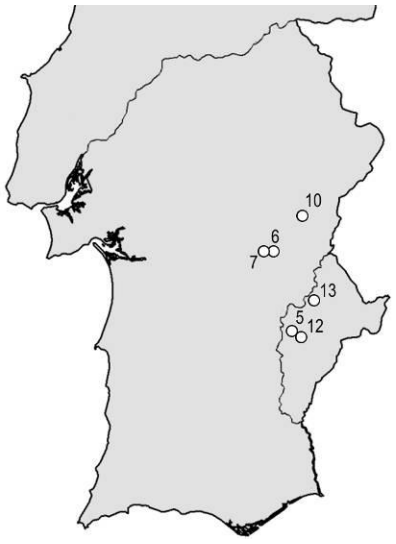

	Site	Chronology (BC)	LBA 1200-800
5	Salsa 3 (Serpa)		**2**
6	Casarão da Mesquita 3 (Évora)		**1**
7	Casarão da Mesquita 4 (Évora)		**6**
10	Martes (Redondo)		**2**
12	Entre Águas 5 (Serpa)		**18**
13	Castro dos Ratinhos (Moura)		**1**
		total	*30*

Figure 2.1. Number of production remains studied and location of each archaeological at the southern Portuguese territory.

2.1.2. Copper-based artefacts

The collection of 142 copper-based artefacts studied belongs to several archaeological sites located at the southern region of the Portuguese territory (Figure 2.2). These copper-based objects comprise 4 chronological periods (EBA, MBA, LBA and EIA), consequently covering a time span from the end of the 3rd millennium BC until the middle of the 1st millennium BC.

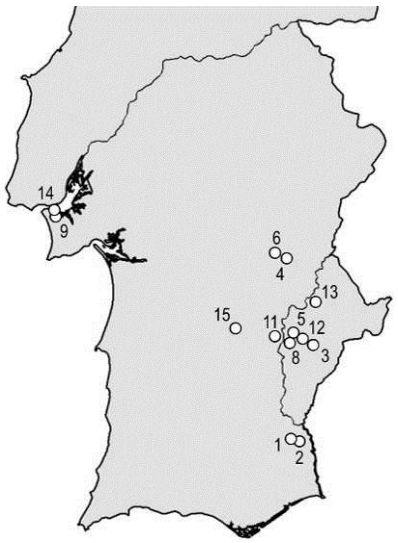

	Site	Chronology (BC)	EBA/MBA 2250-1200	LBA 1200-800	EIA 800-400
1	Anta do Malhão (Alcoutim)		**2**		
2	Soalheironas (Alcoutim)		**2**		
3	Horta do Folgão (Serpa)		**6**		
4	Monte da Cabida 3 (Évora)		**6**		
5	Salsa 3 (Serpa)			**2**	
6	Casarão da Mesquita 3 (Évora)			**2**	
8	Santa Margarida (Serpa)			**1**	
9	Quinta do Marcelo (Almada)			**2**	
11	Baleizão (Beja)			**19**	
12	Entre Águas 5 (Serpa)			**13**	
13	Castro dos Ratinhos (Moura)				**47**
14	Quinta do Almaraz (Almada)				**30**
15	Palhais (Beja)				**10**
		total	*16*	*39*	*87*

Figure 2.2. Number of copper-based artefacts studied by chronological period and archaeological site, including its location at the southern Portuguese territory (chronology of the period more significant regarding the metallurgical materials studied).

2.1.3. Gold artefacts and ingots

The collection of 69 gold objects mainly belongs to the period with strong Mediterranean influences (Figure 2.3). However, some examples that belong to earlier periods, namely the CA and LBA, were also studied in order to ascertain about the evolution of gold alloys at this southern region of the Portuguese territory.

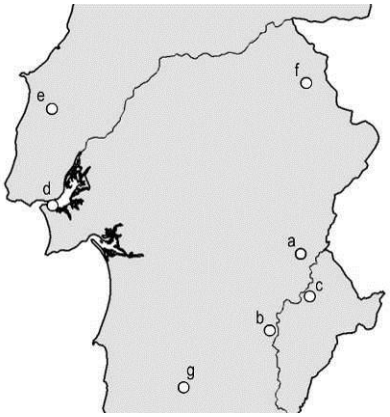

	Site	Chronology (BC)	CA 3000-2250	LBA 1200-800	EIA 800-400
a	Perdigões (Reguengos M.)		**12**		
b	Baleizão (Beja)			**11**	
c	Castro dos Ratinhos (Moura)				**8**
d	Quinta do Almaraz (Almada)				**1**
e	Outeiro Cabeça (Torres Vedras)				**31**
f	Fortios (Portalegre)				**5**
g	Fonte Santa (Ourique)				**1**
		total	*12*	*11*	*46*

Figure 2.3. Number of gold artefacts and ingots studied by chronological period and archaeological site, including its location at the southern Portuguese territory (chronology of the period more significant regarding the metallurgical materials studied).

2.2. Methodology

The methodology involved in this work comprises non-invasive and microanalytical techniques due to the archaeological and museological significance of the samples studied. The analytical techniques selected intent to determine elemental compositions, microstructural characteristics and hardness values of archaeological copper-based and gold artefacts. Initially, the production remains were analysed by EDXRF to identify significant elements that eventually could point out to the type of metal or alloy produced (Figure 2.4). Selected samples were further characterised by SEM-EDS, OM and micro-EDXRF to ascertain the type of metallurgical operation associated with each one, for instance smelting, alloying or recycling.

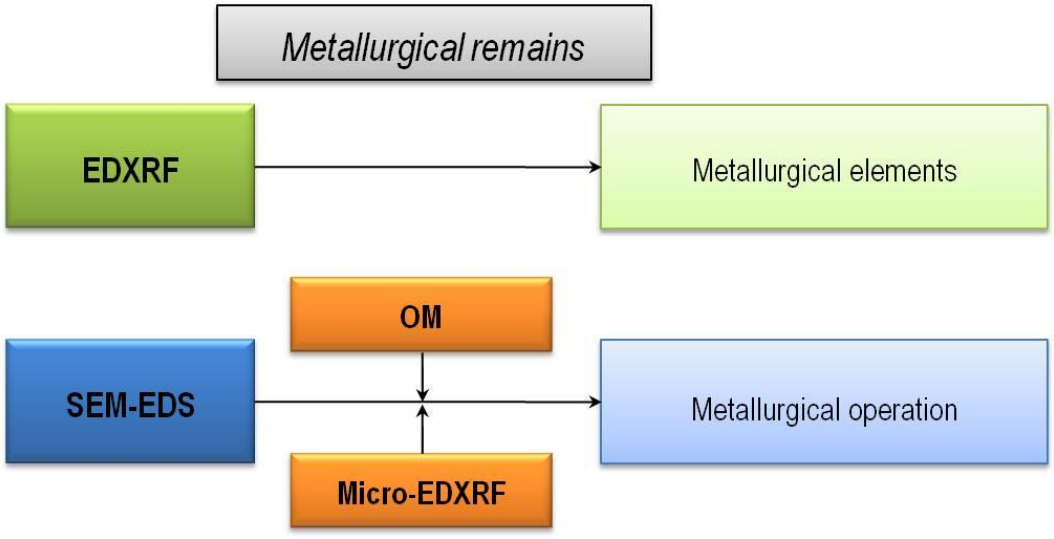

Figure 2.4. Methodology used to characterise the production remains studied in this work.

The archaeological copper-based artefacts that remained usually buried in the soil for a long period present a noteworthy corrosion layer enriched in specific elements. This enrichment results from selective corrosion processes originated by the different elemental electrochemical potentials and diverse stabilities of the corrosion products formed (Robbiola and Portier, 2006). For that reason, the elemental composition of copper-based archaeological artefacts can only be determined by the analysis of a surface previously cleaned from the corrosion layer. The majority of the copper-based artefacts included in this study were analysed by micro-EDXRF spectrometry (Figure 2.5). Since this technique is able to analyse merely a minute area (<100 μm), only a small area of the artefact must be cleaned from the superficial corrosion layer. Consequently, the elemental composition can be determined with an insignificant disturbance to the artefact. The few artefacts that could not be cleaned were analysed by EDXRF, but these results can only be considered semi-quantitatively due to the significant influence of the superficial corrosion layer. Additionally, the majority of the copper-based artefacts was characterised by OM observations to identify different phases, inclusions and operational sequences. The microstructural characterisation was assisted by SEM-EDS analyses of a few selected artefacts. Finally, the hardness of a significant number of copper-based artefacts was determined by Vickers Microhardness testing.

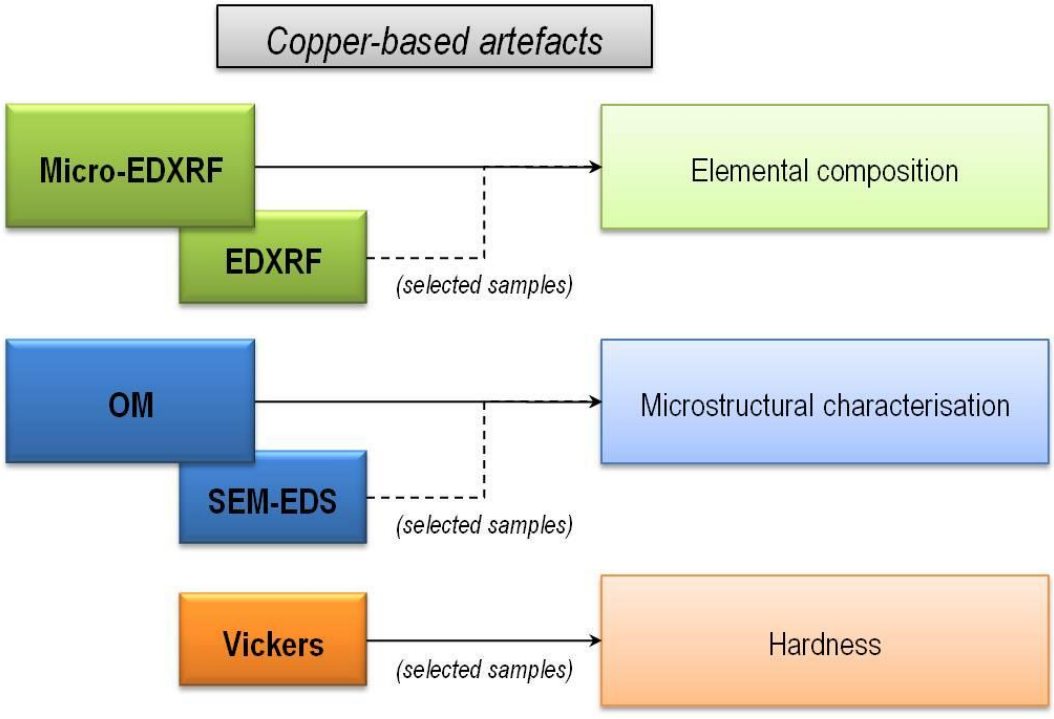

Figure 2.5. Methodology used to characterise the copper-based artefacts studied in this work (box dimensions are related with the significance of each analytical technique).

To avoid additional corrosion of the copper-based artefacts studied, the small cleaned areas were stabilised and sealed using a conventional conservation treatment applied after finishing the analytical study (Williamson and Nickens, 2000).

The analytical study of the archaeological gold artefacts had to rely on a completely non-invasive approach due to the extraordinary museological and archaeological significance of these artefacts. Despite archaeological gold artefacts exhibit a shallow surface layer depleted of less noble elements (Tate, 1986), it has been shown that the results from EDXRF analyses can be considered a good approximation to the composition of the original alloy (Araújo *et al.*, 1993). Finally, a few artefacts that were already fragmented could be sampled for OM and SEM-EDS characterisation to resolve particular issues, such as manufacturing and welding processes (Figure 2.6).

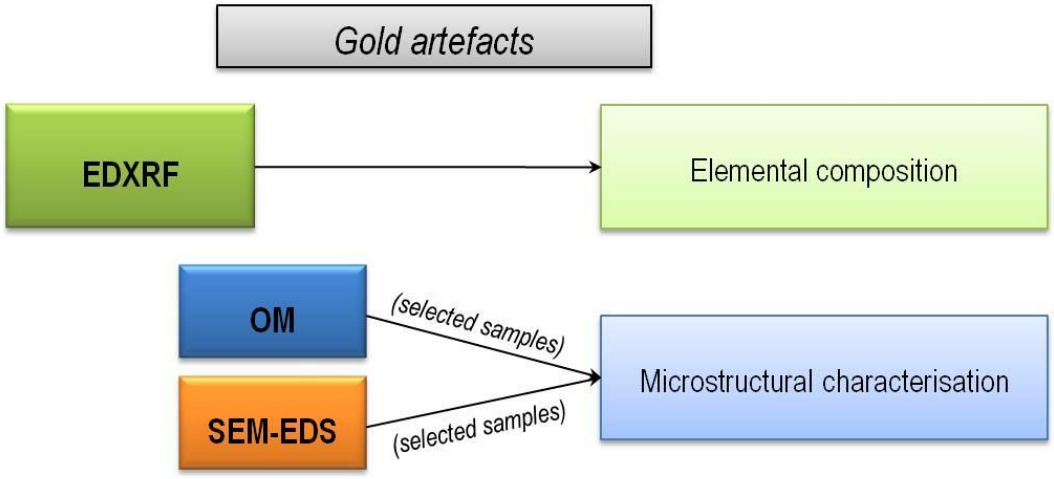

Figure 2.6. Methodology used to characterise the gold artefacts studied in this work (box dimensions are related with the significance of each analytical technique).

2.2.1. Energy Dispersive X-Ray Fluorescence Spectrometry

EDXRF analyses were conducted in a Kevex 771 spectrometer installed at Instituto Tecnológico e Nuclear (ITN). The spectrometer is equipped with a Rh X-ray tube as the primary excitation source. In addition, it comprises different secondary excitation targets and respective radiation filters to optimize the detection limits. The characteristic X-rays emitted by chemical elements present in the excited area of the sample (circular like outline with a diameter of about 2.5 cm) are measured in a liquid nitrogen cooled Si(Li) detector with a resolution of 175 eV at 5.9 keV (Mn-Kα). The samples are measured in a closed chamber with rather large dimensions (approximately, 35×35×10 cm^3), allowing the analysis of sizeable artefacts (Figure 2.7). The quantification procedure involves fundamental parameters and experimental calibration factors (Kevex, 1992). The experimental calibration factors were calculated through the analysis of certified reference

materials, whose composition should be similar to the composition of the sample to optimize the accuracy of the method. Artefacts and production remains included in this work were analysed using two experimental conditions in order to optimize detection limits (Table 2.1).

Figure 2.7. EDXRF spectrometer installed at ITN, including detail of the sample chamber with tray for large artefacts.

Table 2.1. Experimental conditions for EDXRF analyses of copper-based and gold samples (copper-based includes artefacts and production remains*; gold comprises artefacts and ingots).

Excitation	**Tube voltage (kV)**	**Current intensity (mA)**	**Live time (s)**	**Elements of interest (with respective X-ray peak)**
Copper-based				
Ag secondary target	35	0.5 (up to 3.0)*	300	Cu-Kα, Pb-Lβ, As-Kα and Fe-Kα
Gd secondary target	57	1.0 (up to 3.0)*	300	Sn-Kα
Gold				
Ag secondary target	35	0.5	300	Au-Lα and Cu-Kα
Gd secondary target	57	2.0	300	Ag-Kα

A certified reference material (Phosphor Bronze 551 Spectroscopic Standard from British Chemical Standards) was analysed using the same experimental conditions, to calculate the experimental calibration factors for the elements of interest of copper-based alloys. Moreover, the standard gold alloys 90Au-10Ag and Au90-Cu10 (Araújo *et al.*, 1993) were measured to calculate the experimental calibration factors for the elements of interest in gold alloys. These reference materials were used to calculate the quantification limits for the EDXRF analyses of copper-based and gold alloys (Table 2.2 and Table 2.3). The quantification limit for arsenic could not be accurately calculated due to spectral interferences among the As-Kα and Pb-Lα. The value attributed was estimated using elements with similar absorption and enhancement effects in the copper-based matrix.

Table 2.2. Quantification limits for EDXRF analyses of copper-based alloys (values in %; calculated as $10\times background^{0.5}$/sensitivity (IUPAC, 1978) using the certified reference material Phosphor Bronze 551).

Sn	Pb	As	Fe
0.02	0.10	0.10	0.05

Table 2.3. Quantification limits for EDXRF analyses of gold alloys (values in %; calculated as $10\times background^{0.5}$/sensitivity (IUPAC, 1978) using the standard alloys 90Au-10Ag and Au90-Cu10).

Ag	Cu
0.07	0.10

The accuracy of the EDXRF results of gold alloys was estimated through the quantification of the gold standards 80Au-20Ag and Au80-Cu20 (Table 2.4). The relative errors of the quantification of these two standards are below 6%, evidencing a good overall accuracy for the EDXRF method. However, relatively higher errors can be expected due to the non-flat geometry and slightly gold enriched surface of the gold artefacts studied.

Table 2.4. Accuracy of the EDXRF quantitative analyses of gold alloys (values in %; * mean value and standard deviation of 3 independent measurements).

Standard	Element	Certified	Obtained*	Relative error
80Au-20Ag	Au	80.2	81.0 ± 0.4	1%
	Ag	19.8	19.0 ± 0.4	4%
80Au-20Cu	Au	80.1	81.0 ± 1.2	1%
	Cu	19.9	19.0 ± 1.2	5%

2.2.2. Micro-Energy Dispersive X-Ray Fluorescence Spectrometry

Micro-EDXRF analyses were made in an ArtTAX Pro spectrometer belonging to the Departamento de Conservação e Restauro (DCR-FCT/UNL). This spectrometer is equipped with a low-power Mo X-ray tube, focusing polycapillary lens and silicon drift detector with a resolution of 160 eV at 5.9 keV (Mn-Kα). The polycapillary optics, CCD camera and accurate positioning system (Figure 2.8) enable an optimal lateral resolution that corresponds to a minute area of primary incident radiation in the sample (∅ < 100 μm) (Bronk *et al.*, 2001). The quantitative procedure was made through the WinAxil software, comprising fundamental parameters and experimental calibration factors (Canberra, 2003).

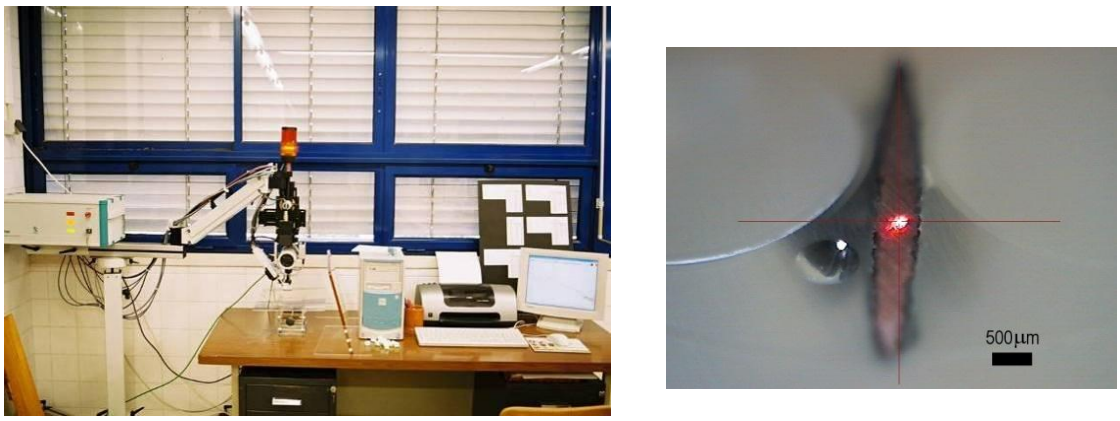

Figure 2.8. Micro-EDXRF spectrometer installed at DCR, including image of minute analysed area of artefact (red dot).

The preparation of the artefacts for micro-EDXRF analyses involved the cutting of a small section, which was mounted in epoxy resin, polished with SiC papers (P1000, P2500 and P4000) and finished with 1 μm and 1/4 μm diamond pastes. Alternatively, if the artefact cannot be sampled, it was prepared with a minicraft equipped with a rotary point of cotton impregnated with a diamond paste (7 μm and 1 μm). This process permits to remove the superficial corrosion layer in a small area (~3×3 mm^2) thus allowing the analysis of a clean metal surface of the artefact (Figure 2.9). The prepared areas of each artefact were analysed in 3 different spots using a tube voltage of 40 kV and a current intensity of 0.5 mA during 300 s of real measuring time (X-ray peaks of elements of interest: Fe-Kα, Cu-Kα, As-Kα, Pb-Lα and Sn-Lα).

Figure 2.9. Some examples of copper-based artefacts prepared for micro-EDXRF analyses.

The experimental calibration factors for the elements of interest of copper-based alloys were calculated through the analysis of the certified reference material Phosphor Bronze 551. Moreover, the Phosphor Bronze 551 was used to calculate the quantification limits for the micro-EDXRF analyses of copper-based alloys (Table 2.5).

Table 2.5. Quantification limits for micro-EDXRF analyses of copper-based alloys (values in %; calculated as $10\times background^{0.5}/sensitivity$ (IUPAC, 1978) using the certified reference material Phosphor Bronze 551).

Sn	Pb	As	Fe
0.50	0.10	0.10	0.05

The accuracy of the micro-EDXRF results of copper-based alloys was estimated using the quantification of the certified reference material Phosphor Bronze 552 from British Chemical Standards (Table 2.6). The micro-EDXRF technique exhibits a very good accuracy, presenting low relative errors regarding the elements of interest. The higher relative error obtained for iron, zinc and nickel is due to contents close to the quantification limit of the technique and spectral interferences (besides, zinc and nickel are usually bellow detection limits in the studied ancient metallic artefacts).

Table 2.6. Accuracy of the micro-EDXRF quantitative analyses of copper-based alloys (values in %; * mean value and standard deviation of 3 independent measurements).

Standard	Element	Certified	Obtained*	Relative error
BCS 552	Cu	87.7	88.3 ± 0.8	1%
	Sn	9.78	9.9 ± 0.4	1%
	Pb	0.63	0.62 ± 0.05	2%
	Fe	0.10	0.11 ± 0.01	10%
	Ni	0.56	0.63 ± 0.02	12%
	Zn	0.35	0.48 ± 0.02	39%

2.2.3. Optical Microscopy

OM observations were made in a Leica DMI 5000M optical microscope installed at Centro de Investigação de Materiais (CENIMAT-FCT/UNL). This optical microscope is equipped with several objectives that allow a wide range of magnifications (50× to 1000×) under bright field illumination (BF), dark field illumination (DF) and polarised light (Pol). Dark field illumination helps to recognize pores and cracks, while polarised light allows distinguishing among different components (e.g. copper oxides from copper sulphides). The microscope includes a motorized z-focus with parfocal function (automatic compensation of different focus level) that allows obtaining an image of slightly irregular areas. This is very important in the observation of artefacts that cannot be sampled, since the preparation of this type of materials always leaves a somewhat irregular surface. Furthermore, the optical lenses are set in an inverted position that facilitates the observation of large sized artefacts (Figure 2.10).

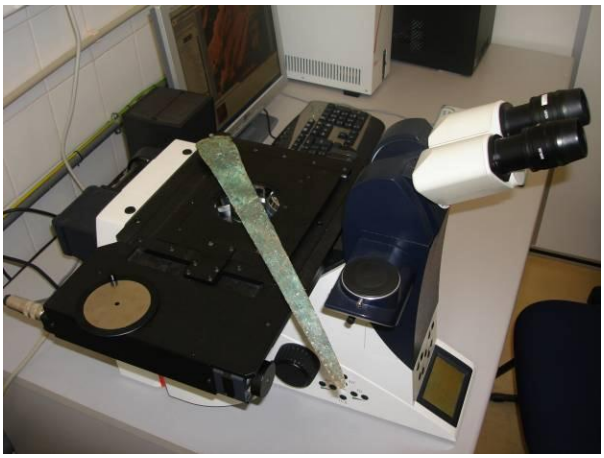

Figure 2.10. Leica DMI 5000M optical microscope installed at CENIMAT (the inverted design allows observation of artefacts with larger dimensions).

The preparation of the metallic artefacts for OM observations is equal to the used for the micro-EDXRF analyses. In fact, the same prepared area was almost always used for both techniques. The preparation comprises cutting of a small fragment, mounting in epoxy resin, polishing with SiC papers (P1000, P2500 and P4000) and finishing with 1 μm and 1/4 μm diamond pastes. Instead, a small area (~3×3 mm^2) was cleaned from corrosion products using a minicraft equipped with a rotary point of cotton impregnated with diamond pastes (7 μm and 1 μm). Initially, all samples were observed without etching, being afterwards etched with an aqueous ferric chloride solution to enhance the microstructural features, such as grain boundaries, annealing twins and slip bands.

2.2.4. Scanning Electron Microscopy with X-Ray Microanalysis

The SEM analyses were made in a Zeiss DSM 962 scanning electron microscope belonging to Centro de Investigação de Materiais (CENIMAT-FCT/UNL). This equipment is a conventional tungsten filament scanning electron microscope with secondary electron (SE) and backscattered electron (BSE) imaging modes. The equipment comprises also an Oxford Instruments INCAx-sight EDS spectrometer with an ultra-thin window to detect low atomic number elements ($Z < 5$). The semi-quantifications are made using the ZAF (atomic number, absorption and fluorescence) correction factors.

The selected artefacts and production remains were analysed with a gold coating, a carbon conductive bridge or copper tape bridge to prevent charge accumulation (Figure 2.11). The experimental conditions were 20 kV of accelerating voltage, approximately 3 A of filament current, 70 μA of emission current and a working distance of 25 mm. Most images were collected using BSE mode due to its high atomic number contrast, which allowed a better recognition of different phases, including non-metallic inclusions. The EDS analyses were also especially important to

identify the different elemental components in SEM-BSE observations, sometimes with the support of preceding OM images.

Figure 2.11. Zeiss DSM 962 SEM-EDS installed at CENIMAT.

2.2.5. Vickers Microhardness Testing

The microhardness was determined in a Zwick-Roell Indentec testing equipment installed at CENIMAT. The hardness of a material is defined by its resistance against the penetration by a harder material and in metals it is usually given by the Vickers Hardness number (HV), which is calculated by the load applied (F) over the surface area of the indentation (A) of a diamond pyramid into the metallic sample (Figure 2.12). Mounted copper-based archaeological artefacts were polished with 1 μm diamond paste and indented for 10 s with a low force of 0.2 kgf thus determining the microhardness (HV0.2). At least 3 indentations were made, being considered the average value of several measurements with a relative standard deviation better than 5%.

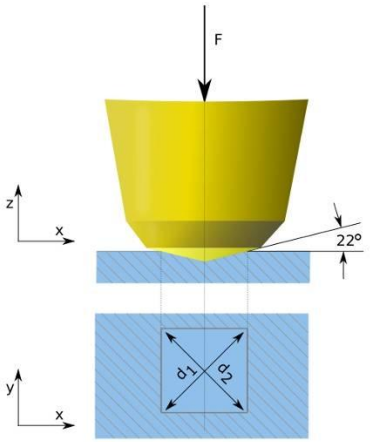

$$HV = \frac{F}{A} \approx \frac{1.8544F}{d^2}$$

(where d is the average of d_1 and d_2)

Figure 2.12. Vickers test scheme and calculation procedure (adapted from wikipedia.org/wiki/Vickers_hardness_test).

2.2.6. Minimizing the impact of analytical studies

The copper-based artefacts that were prepared for elemental and microstructural characterisation were later restored to avoid the increase of the corrosion processes. This was especially important for artefacts that exhibit an significant amount of chlorine – the outer corrosion layers of malachite ($Cu_2CO_3(OH)_2$) and cuprite (Cu_2O) are protective and stable, such as the more interior layer of cuprous chlorine (CuCl) under dry conditions (Walker, 1980). However, the removal of the outer corrosion layers facilitates the contact of moisture with the cuprous chlorine layer thus initiating the autocatalytic reaction known as bronze disease, which leads to the formation of paratacamite/atacamite ($4CuCl+4H_2O+O_2 \rightarrow 2Cu_2Cl(OH)_3+2HCl$).

The conservation treatment was applied to the areas of the artefacts that were previously cleaned for study, comprising the application of a corrosion inhibitor (benzotriazol dissolved in ethanol; 3% m/v), followed by an acrylic protector (Paraloid B-72 dissolved in acetone; 3% m/v). Afterwards, a mixture of pigments dissolved in the Paraloid B-72 solution was applied to replicate the coloration of the surrounding patina. The final protection of the area consisted of a microcrystalline wax dissolved in a paraffin-derived "*white spirit*". The artefacts were returned to the museum with an individual report consisting of the location of the interventioned area and the conservation treatment applied (Figure 2.13).

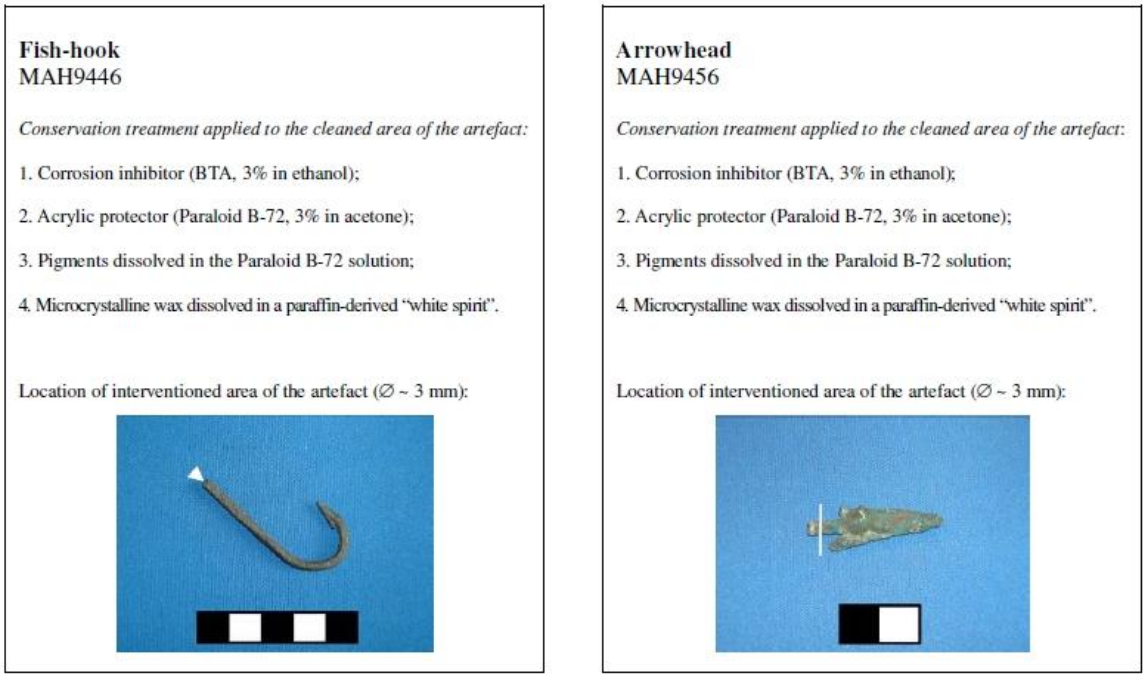

Figure 2.13. Examples of conservation treatment reports regarding archaeological copper-based artefacts.

3. PRODUCTION REMAINS

3.1. Introduction

The significant spread in the production of copper-based artefacts throughout the LBA is also noticeable in the number of production remains discovered among the archaeological record. The present introduction will summarize the most relevant technological characteristics of the production remains studied in this work, namely crucibles, tuyeres, moulds, metallic nodules and slags.

According to the archaeological record, ancient crucibles were usually made with non-refractory ceramic materials (Bayley and Rehren, 2007). These crucibles present thick walls in order to withstand the high firing temperatures used during metallurgical operations. Apart from being mechanically more resistant, thicker clay walls also reduce the heat transfer, thus inhibiting the heating from below. Consequently, early crucibles were covered with a pile of charcoal or wood and heated from above. This promotes an extensive vitrification and bloating of the inner and edge surfaces of the crucible, while the outer surface remains almost unchanged. Ancient metallurgical crucibles present two distinct technological functions – smelting and melting. The metallurgical residues that sometimes are still present in the crucibles result from the reaction of ore/metal with crucible fabrics and wood ash used for heating. The study of these metallurgical residues often allows classifying the type of metallurgical operation present in archaeological sites.

The introduction of forced air through blow pipes or bellows increases the furnace temperature thus improving the efficiency of the metallurgical process. Forced air enters the reaction zone through clay tubes – tuyeres. Unfortunately, these artefacts are often recovered in a very fragmented state that prevents the knowledge of its complete shape and size. Most known examples correspond to fragments that include the tip of the tuyere closer to the furnace. This end of the tuyere is more resilient since it becomes vitrified by heat. Sometimes it still exhibits residues of slagged material that permits to identify the type of metallurgy.

Ancient casting operations were conducted in open, bivalve or multiple moulds. Open moulds originate the loss of metal through oxidation and metal castings with flat upper surfaces (i.e. without reliefs), while multiple moulds can be used to cast several artefacts at once. The lost wax method was applied to cast more complex and, sometimes, finely decorated artefacts (Coghlan, 1975). Moulds were made of stone, clay or metal. Stone moulds were carved out of solid stone, while clay ones require the use of a wooden pattern of the artefact to be wrought. In the lost wax method this pattern was made of bees-wax and later melted down or burnt out. Stone moulds are more usual than clay moulds in the archaeological record probably because the first are more

resistant to the casting operation and can be used several times. By the other hand, metallic moulds are scarcer than the other two materials because they were more costly and, especially, since the metal mould could be recycled at the end of its useful life, thus disappearing from the archaeological record. A recent experimental study has determined that the proportions of metallic elements remaining in the moulds are systematic but impossible to predict (Kearns *et al.*, 2010). The propensity of an element to left traces in a mould is related with thermochemical properties, such as volatility, free energy of oxidation and chemical reactivity with the mould fabric. Generally, it was established that zinc exhibit the higher tendency to be enriched, being followed by lead and tin. By the contrary, copper was found to be present in relative proportions much lower than in the original alloy. Arsenic was not considered in this study but it is known to be highly volatile thus also exhibiting a higher tendency to become more enriched than copper (Craddock, 1995).

Metallic nodule is used as a broad term comprising melting and casting drops, as well as small droplets of metal found trapped in slag or crucible linings as result of two liquids immiscibility in certain temperature/composition ranges. Metallic nodules often contain useful information about the metallurgical process. The elemental composition gives indications about the type of metal being worked, while the cooling rate of the metallic nodule can be suggested by its microstructure. The latter provides additional information about the type of metallurgical operation that originated the nodule. A melting or casting drop will necessarily presents a high cooling rate, while a smelting nodule that remained attached to the slag in the crucible will exhibit a slow cooling rate.

Slags are mainly composed by complex silicates that resulted from reactions between ore/metal with crucible fabric and wood ash used for heating during smelting and melting operations. Generally, smelting slags tend to be richer in iron silicates while the melting slags are richer in non-ferrous silicates and wood ash (Tylecote, 1992). Furthermore, ancient smelting slags are very heterogeneous, containing all transitional stages between the thermal decomposition of ores up to the formation of metal phases (Hauptmann, 2007). The poor reducing conditions and low temperatures attained within the reaction vase during the earlier smelting operations prevent the formation of a fayalitic slag. Generally, the high viscosity of this immature slag causes the entrapment of numerous metallic nodules resulting in a high retention of metal. The study of LBA copper-based slags intends to identify the raw materials and process used in the production of bronze alloys, namely the co-smelting of copper ores with tin ores, smelting of tin ores with molten copper (cementation) or melting of metallic copper and tin in suitable proportions.

The following sections present the study of the several metallurgical debris recovered during archaeological excavations at the southern of the Portuguese territory.

3.2. Entre Águas 5[1]

Archaeological field works conducted during 2008 in the framework of the mitigation measures taken during the building up of the Serpa Dam led to the identification of Entre Águas 5 (Serpa). This archaeological site includes 3 hut floors and 6 pits, from where it was recovered a large collection of ceramic and lithic artefacts, in addition to metallic artefacts and metallurgical debris (Rebelo *et al.*, 2009). The typological characteristics of the negative structures and material culture recovered are familiar to the LBA. The radiocarbon dating of the context containing the above mentioned production remains point to the 10th-9th centuries BC.

The existence of a metallurgical workshop at this settlement is testified by the recovery from a single hut of several crucible fragments, a tuyere and numerous small clay fragments – "moulds?" (Figure 3.1). The crucibles 1374A and 1391A contain an handle with a quadrangular socket, in which a rod would be inserted to facilitate the handling of the crucible during metallurgical operations. This technological improvement is common in crucibles from the Eastern Mediterranean region since the beginning of metallurgy, but it is an unusual find in the archaeological record of the Iberian Peninsula (Urbina *et al.*, 2007). The collection from Entre Águas 5 contains another crucible (316) that might also have presented this innovation, but the handle is fragmented, not showing any sign of the socket.

The crucible 1374 presents a triangular shaped rim with a pouring lip that, eventually, will facilitate the transfer of the molten metal. The remaining set of crucibles comprises an edge (165) and three indistinct clay fragments (1373, 1374A1 and 1374A2). All crucibles exhibit heavily vitrified and slagged inner surfaces, sometimes with evident presence of metal oxides, which promptly indicate their use. Furthermore, their thick clay walls (up to ~2 cm) suggest that the heating was done from above, as it was common in these ancient metallurgical operations (Rovira, 2004).

A small chip of charcoal entrapped in the slagged material of the crucible 1374 was radiocarbon dated, Beta 26318: 2710±40BP – 980-810 cal BC (2σ). Considering also the chronology obtained from radiocarbon dating of other materials from the same context, it seems certain that this metallurgical workshop belongs to the later stages of the LBA.

[1] Part of the content from this section was previously published (Valério *et al.*, 2009).

Figure 3.1. Production remains from Entre Águas 5 (crucibles: 1374A; 1391A; 316; 1374; 165; 1373; 1374A1 and 1374A2; tuyere: 1374B and moulds: 1432A; 1432B1-2; 1342C1-10).

The tuyere 1374B from Entre Águas 5 is made of clay and exhibits a cylindrical typology that is very common among BA tuyeres at the Iberian Peninsula (Urbina *et al.*, 2007). Cylindrical tuyeres continue to be utilised during the EIA, but quadrangular tuyeres become increasingly more common among archaeological contexts of this period. The latter seem to result from the Phoenician colonisation because they are unknown at earlier archaeological records. Furthermore, a recent study involving a large collection of tuyeres recovered from the Phoenician settlement of La Fonteta, SE Spain (8th-7th centuries BC), established that quadrangular tuyeres predominate in contexts of iron production, whereas they are also present among copper-based metallurgical contexts (Renzi, 2007). The area closer to the air outlet of the tuyere 1374B is heavily vitrified and displays traces of slagged material and metal oxides, which prove that it was actually used in some type of metallurgical operation.

The mould fragments (1432A, 1432B1-2 and 1432C1-10) display thin clay walls and, in most cases, their inner surfaces are clearly scorched from contact with the molten metal during casting. However, these moulds are highly shattered, which prevents the recognition of the artefacts to be produced. None of the inner surfaces of these mould fragments present any sign of slagged material or metal oxides. The thin walls and highly shattered state of these mould fragments might be an indication of the use of the lost wax method, thus being an evidence of premature contacts of local communities with technology brought by Mediterranean people.

3.2.1. Crucibles

The slagged and clay surfaces of the crucibles were analysed by EDXRF to establish the elements that are enriched in the areas affected by the metallurgical operation (some examples in Figure 3.2). The results from the comparison of EDXRF spectra of slagged and clay surfaces of all crucibles from Entre Águas 5 are summarised in Table 3.1.

Table 3.1. Significant elements enriched in the slagged surfaces of crucibles from Entre Águas 5 (+: enriched element; the more discriminating elements are shaded).

Artefact	Type	Reference	Cu	Zn	As	Pb	Sn	Sb
crucible	socketed handle	1374A	+	+		+	+	+
crucible	socketed handle	1391A	+	+		+	+	+
crucible	socketed handle (?)	316	+				+	+
crucible	triangular rim	1374	+					
crucible	edge	165	+	+	+	+	+	
crucible	unknown	1373	+			+	+	
crucible	unknown	1374A1	+				+	+
crucible	unknown	1374A2	+			+	+	+

The enrichment of some elements in the slag depends on the highly heterogeneous nature of the metallurgical process. Wood ash is mainly composed of C, Mg, P, K and Ca (Etiégni and Campbell, 1991), consequently the enrichment observed of some of these elements results from reactions involving wood ash. Considering the elements that usually are present in ancient copper-based artefacts (Cu, Zn, As, Pb, Sn and Sb), it is important to mention that the significant volatility and high free energy of oxidation of Zn, in addition with its high reactivity with silicates of the clay, result in a high tendency to become enriched even if it is only present at trace level (Kearns *et al.*, 2010). Copper and tin are more indicative of the type of metallurgy involved with these ancient production remains despite presenting different tendencies to become enriched in the slagged material.

socketed handle crucible 1374A

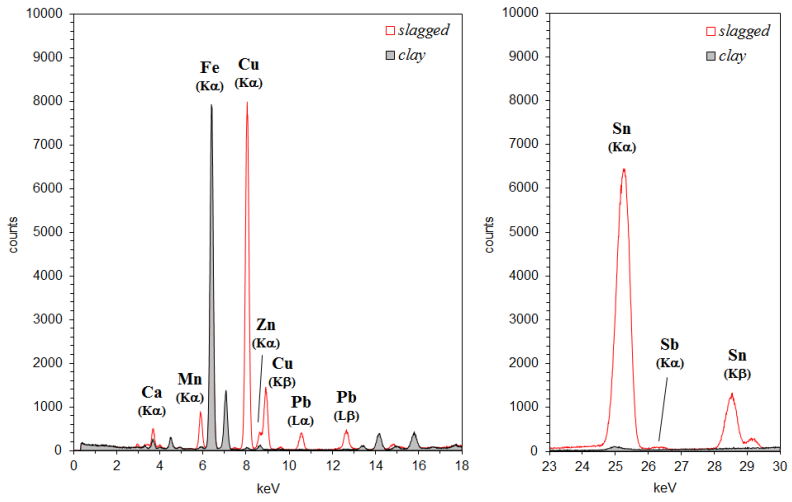

triangular rim crucible 1374

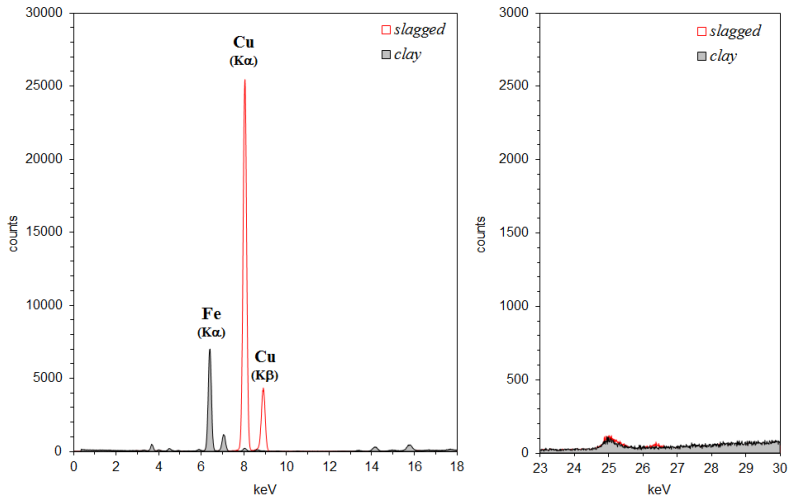

Figure 3.2. EDXRF spectra of slagged and clay surfaces of socketed handle crucible 1374A and triangular rim crucible 1374 from Entre Águas 5 (spectra of Ag and Gd secondary targets).

EDXRF results evidence that nearly all crucibles from Entre Águas 5 are testimonies of the practice of the metallurgy of bronze at the settlement. The triangular rim crucible is the exception, since it is only enriched in copper. The presence of a tip in this crucible suggests that the crucible

charge is supposed to be completely liquefied during pouring. By the contrary, the smelting of metallic ores hardly beneficiates from a crucible with a tip, given that ancient smelting produce high viscosity slags. It is feasible that this crucible results from a different operation in the bronze production process, e.g. melting the copper nodules obtained from a previous smelting of copper ores.

3.2.2. Slags

3.2.2.1. Slag 1374A-s

The sampling of the slag 1374A-s included the cutting of a complete segment of the socketed handle crucible 1374A, exposing the crucible fabric and slag layer cross-section from the base to the top of the reaction vase. The initial observation of the cross-section of the slag 1374A-s at low magnifications readily evidences its highly heterogeneous and porous nature including numerous globular inclusions of metals and oxides (Figure 3.3).

Figure 3.3. Crucible 1374A from Entre Águas 5 (detail of cross-section evidencing the crucible fabric and slag layer).

SEM-EDS and optical microscopy characterisation identified a very heterogeneous slag composed by a vitreous matrix of aluminium silicates with Na, Mg, K, Ca, Mn and Fe (Figure 3.4). This matrix is the result of reactions between metal and oxide melts with crucible fabric and charcoal ash. The abundant presence of magnetite (chemical formula: $Fe[II]Fe[III]_2O_4$) was also acknowledged, indicating an iron-rich slag under local oxidising conditions. This evidences the poor reducing atmosphere attained in the reaction vase during the metallurgical operation. Additionally, numerous globules of oxidised copper (cuprite and malachite), most likely formed from re-oxidising metallic copper indicate the limited control over the redox conditions. The

presence of metallic copper globules readily eliminates the possibility of bronze recycling. Bronze appears in metallic nodules that are sometimes partially or totally oxidised.

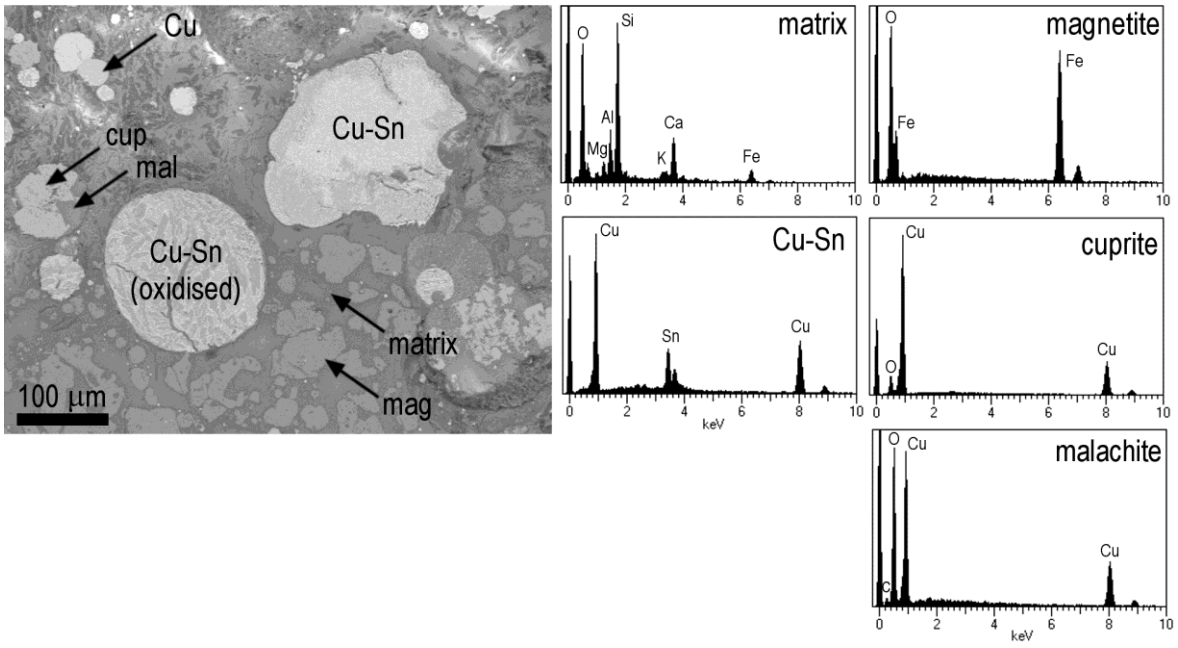

Figure 3.4. SEM-BSE image and EDS spectra of slag 1374A-s from Entre Águas 5 (mag: magnetite; cup: cuprite; mal: malachite; phases identified by approximate stoichiometry given by EDS).

A different region exhibits a similar vitreous matrix, numerous magnetite precipitations and small globular Cu-S formations with some iron (Figure 3.5). Cu-S inclusions evidence the existence of molten metal sulphide – matte. Smelting experiments conducted with copper oxides and carbonate ores with a significant amount of sulphides observed the presence of matte among the smelting remains (Hanning *et al.*, 2010). The presence of sulphides can be understood as a natural association with oxides and carbonates among the copper ores used.

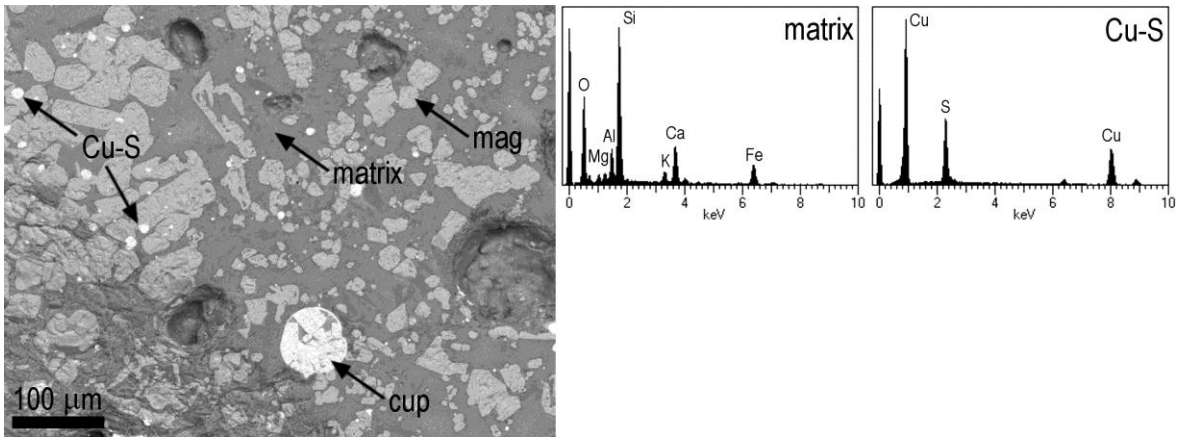

Figure 3.5. SEM-BSE image and EDS spectra of slag 1374A-s from Entre Águas 5 (mag: magnetite; cup: cuprite; phases identified by approximate stoichiometry given by EDS).

Further analysed areas are composed by a similar matrix (complex aluminium silicate) containing numerous tin oxide inclusions as globular and euhedral needles (Figure 3.6). Some regions present aluminium silicate crystallites (dark needles). The euhedral tin oxide inclusions are a secondary product resulting from the oxidation of tin in the molten phase. However, the copper nucleus present in some of these tin oxide inclusions suggests that both elements were present as metals in an oxidising environment, i.e. tin was oxidised leaving a metallic core of copper (Dungworth, 2000). The considerable abundance of tin oxide inclusions, together with the absence of metallic tin, is often seen as an evidence of the use of cassiterite instead of metallic tin to produce the bronze alloy (Rovira, 2004).

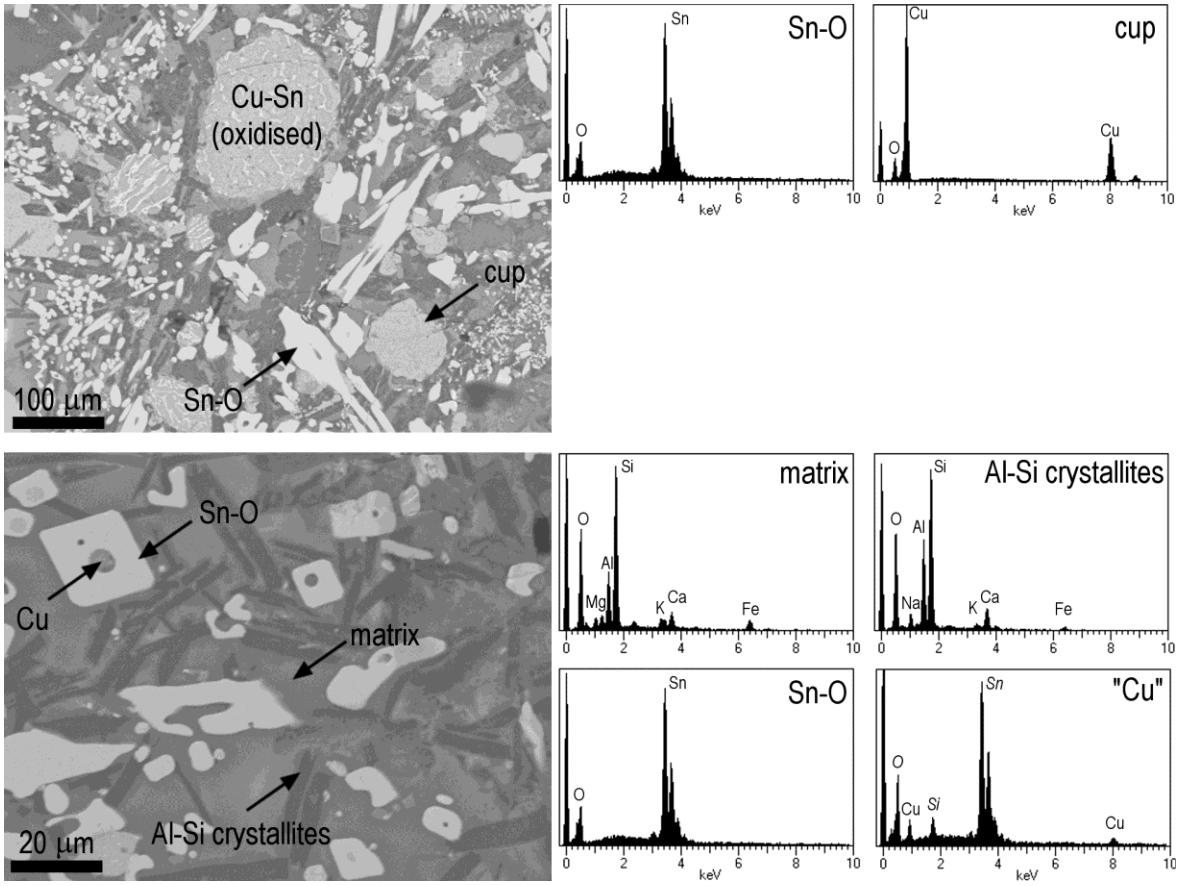

Figure 3.6. SEM-BSE images and EDS spectra of slag 1374A-s from Entre Águas 5 (cup: cuprite; phase identified by approximate stoichiometry given by EDS).

Metallic nodules are quite abundant in the slag 1374A-s, presenting variable dimensions (from a few micra up to 1mm) and different morphological characteristics (Figure 3.7). The high retention of metal in the slag is a common characteristic of primitive metallurgical processes that operate with the formation of immature slags. The high retention of metal derives from the high viscosity of these immature slags.

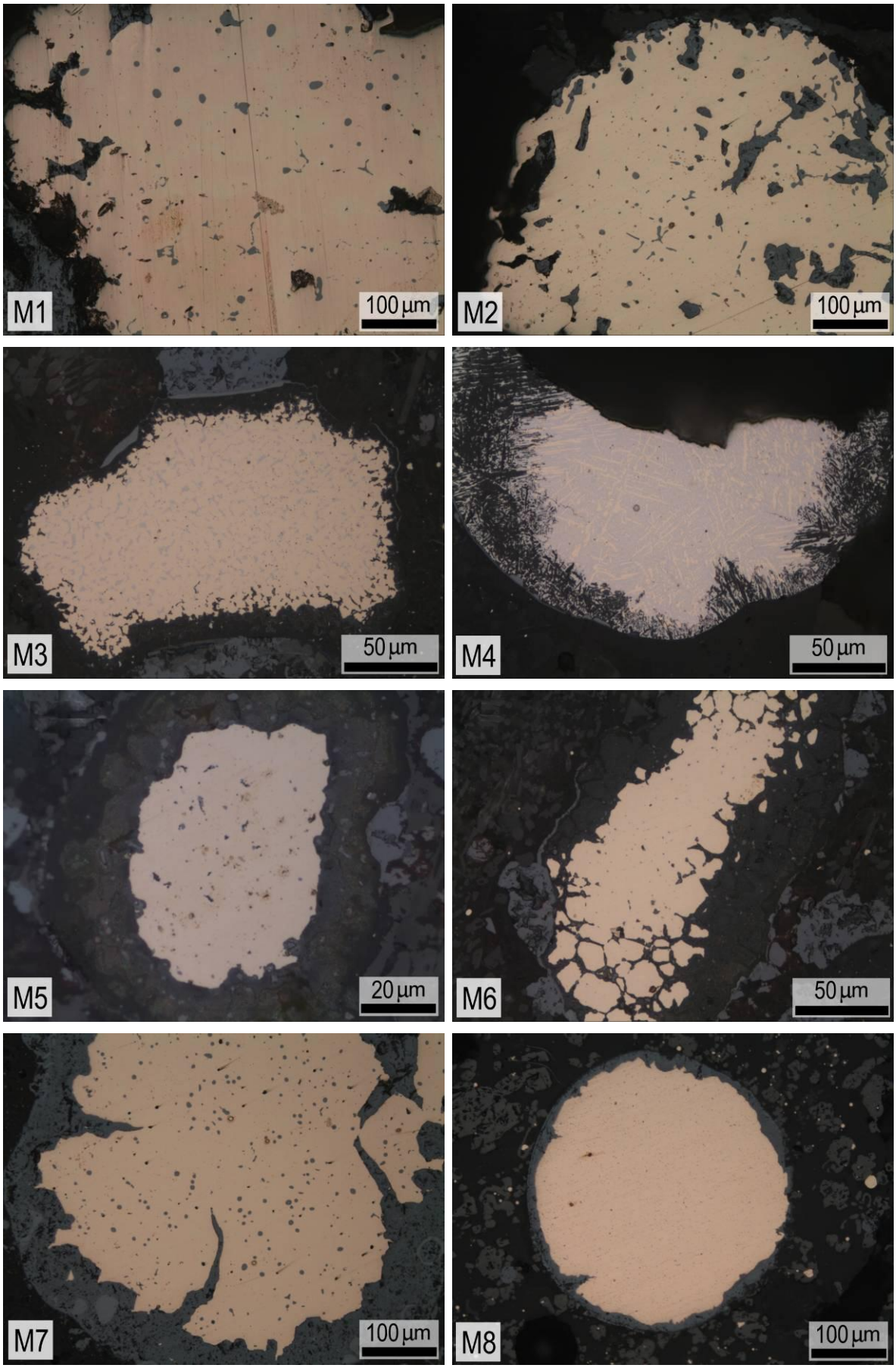

Figure 3.7. OM-BF images of metallic nodules entrapped in the slag 1374A-s from Entre Águas 5.

Generally, the microstructures of these nodules evidence the rather slow cooling rate of the slagged material – coarse granular microstructures (e.g. nodule M6, Figure 3.7). Occasionally, coarse microstructures facilitate the observation of coring (nodule M1, Figure 3.7). Another significant characteristic of the metallic nodules is their highly variable elemental composition, ranging from pure copper (copper nodule, Figure 3.4) to bronze with low or very high tin contents (Table 3.2). This variability is another evidence of the reasonably changeable conditions (T and pO_2) attained along the reaction vase. Additionally, the low iron content of these metallic nodules is very significant, since it evidences the poor reducing environment attained during this metallurgical operation. In the same manner that copper nodules, the presence of bronze nodules with very high tin contents (~25%) indicates that this slag was not produced by a bronze recycling operation because coeval alloys with such high tin contents are very uncommon. Additionally, a recent experiment involving the co-smelting of copper ores with cassiterite also originated a slag with numerous metallic inclusions showing particularly variable compositions, i.e. from pure copper up to bronzes with ~80% Sn (Rovira *et al.*, 2009).

Table 3.2. Results of SEM-EDS and micro-EDXRF analyses of metallic nodules from Entre Águas 5 (rem - remainder; nd - not detected)

Metallic nodule	SEM-EDS		micro-EDXRF			
	Cu (%)	Sn (%)	Sn (%)	Pb (%)	As (%)	Fe (%)
M1	rem	3.1	2.4	nd	<0.1	<0.05
M2	rem	-	5.8	0.7	nd	<0.05
M4	rem	24.6	-	-	-	-
M7	rem	3.8	3.5	0.6	0.2	<0.05
M9	rem	12.0	9.9	1.0	nd	<0.05
M10	rem	25.8	-	-	-	-

The SEM-EDS characterisation of these metallic nodules evidences the α phase with coring, together with numerous Cu-S and lead-rich inclusions (nodule M2, Figure 3.8). Some of the darker regions are copper oxides due to corrosion that is advancing from the outer rim to the interior of the nodule. Furthermore, bronze nodules that are richer in tin exhibit the characteristic α+δ eutectoid (e.g. nodule M3, Figure 3.8).

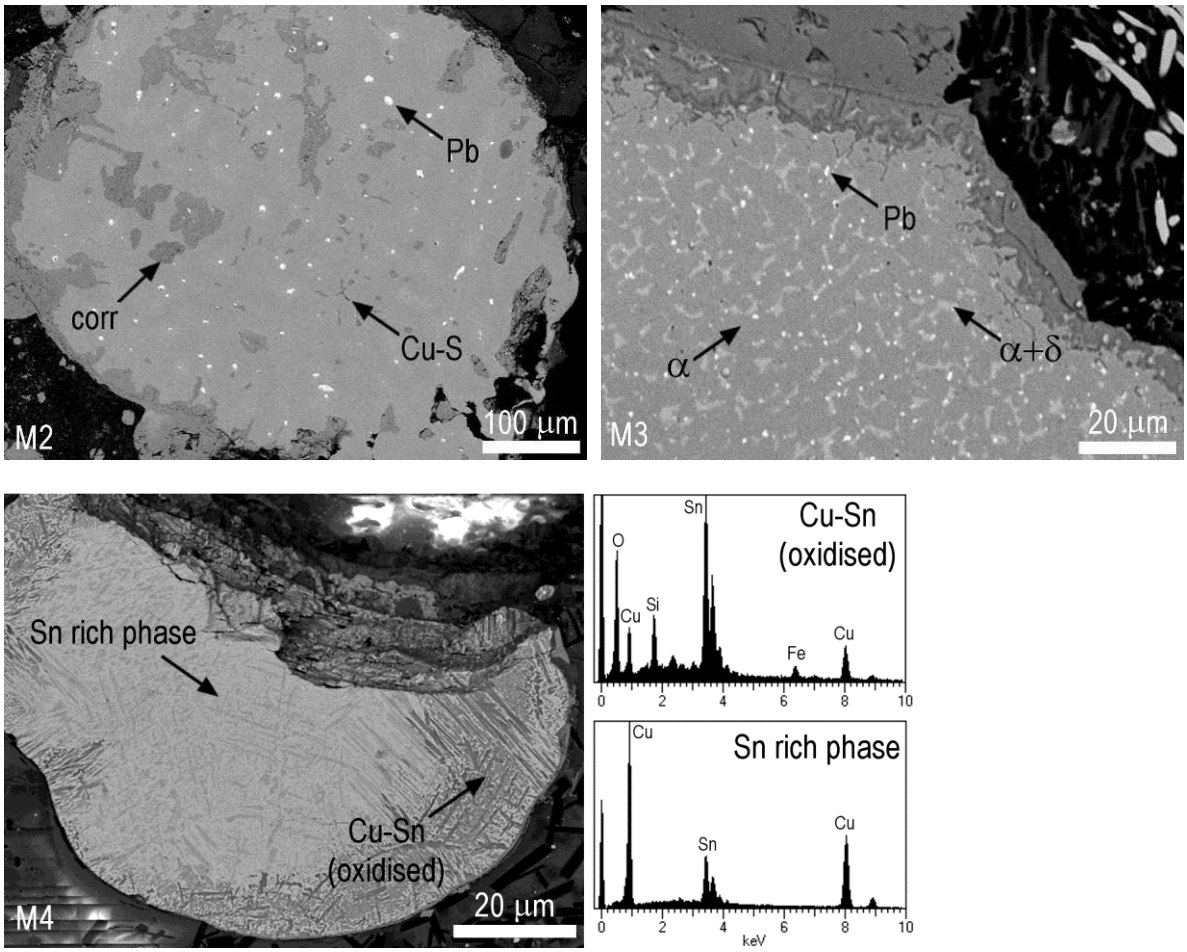

Figure 3.8. SEM-BSE images of metallic nodules entrapped in slag 1374A-s from Entre Águas 5.

3.2.2.2. Slag 1391A-s

The sampling of the slag 1391A-s included the cutting of a small segment of the socketed handle crucible 1391A, exposing the crucible fabric and slag layer cross-section in an area close to the top of the reaction vase (Figure 3.9).

Figure 3.9. Crucible 1391A from Entre Águas 5 (detail of the cross-section evidencing crucible fabric and slag layer).

SEM-EDS characterisation of the slag 1391A-s evidences a highly heterogeneous slag composed by a vitreous matrix (aluminium silicate with Na, Mg, K, Ca, Mn and Fe) with abundant copper inclusions, together with copper oxide and tin oxide precipitates (Figure 3.10). The weak reducing conditions attained during this metallurgical operation are quite obvious from the numerous magnetite inclusions spread all over the different iron-rich areas.

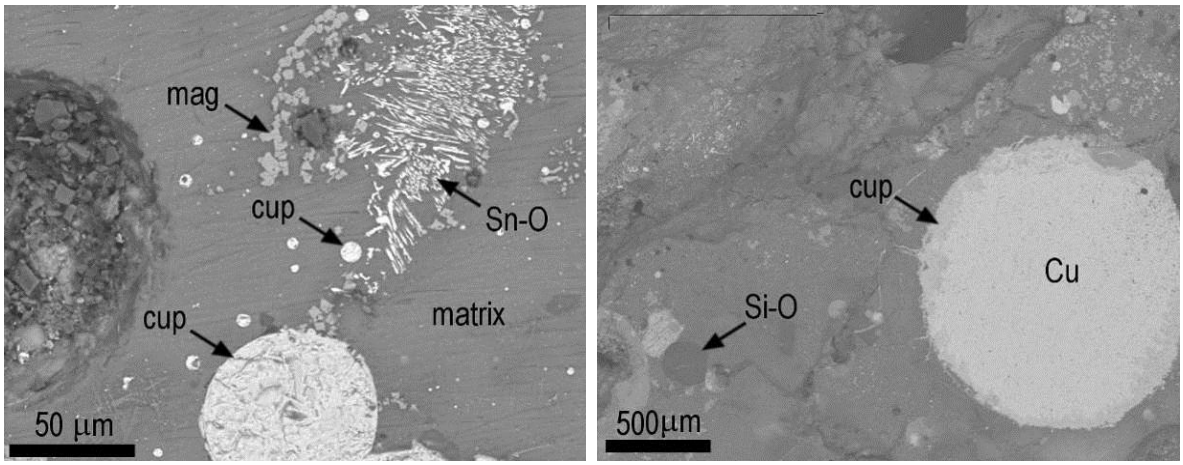

Figure 3.10. SEM-BSE images of slag 1391A-s from Entre Águas 5 (Si-O: silica nodule from crucible fabric; mag: magnetite; cup: cuprite; phases identified by approximate stoichiometry given by EDS).

The most valuable information is given by some relic mineral inclusions whose stoichiometry identified as mixed copper sulphides and oxides (Figure 3.11).

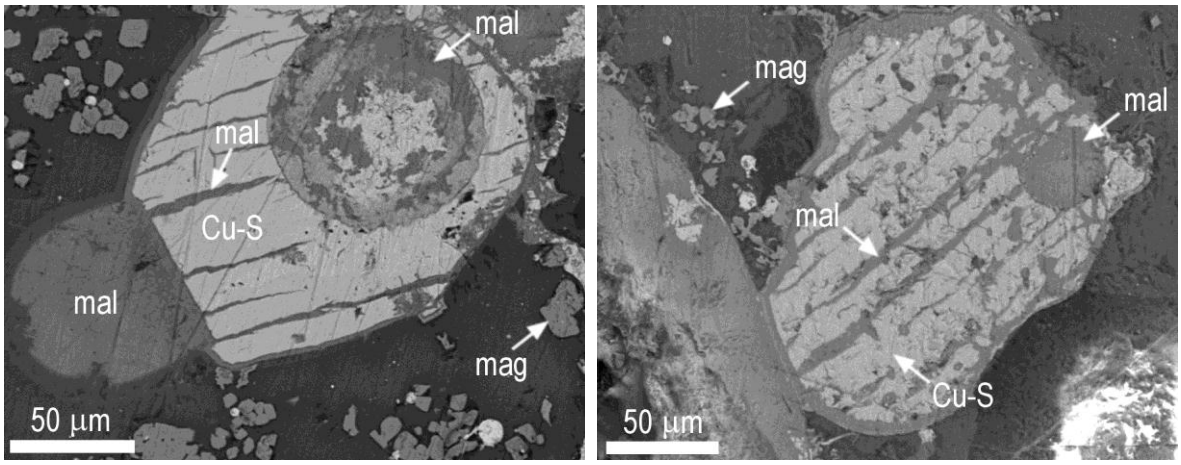

Figure 3.11. SEM-BSE images of slag 1391A-s from Entre Águas 5 (mag: magnetite; mal: malachite; phases identified by approximate stoichiometry given by EDS).

The morphology of these mineral inclusions is quite different from the more abundant globules of malachite, which most likely resulted from re-oxidising of metallic copper. During the metallurgical process, malachite minerals decompose into tenorite that is later reduced to cuprite. However, a particular high abundance of magnetite in these micro domains suggests a rather

oxidising atmosphere that seems to have prevented the complete reduction of these mineral inclusions. The presence of these relic copper minerals strongly suggests the smelting of copper oxide/carbonate ores with a significant amount of copper sulphides.

3.2.2.3. Slag 316-s

The sampling of the slag 316-s comprised the cutting of a small segment of the socketed handle crucible 316, exposing the crucible fabric and slag layer cross-section in the top area of the reaction vase (Figure 3.12).

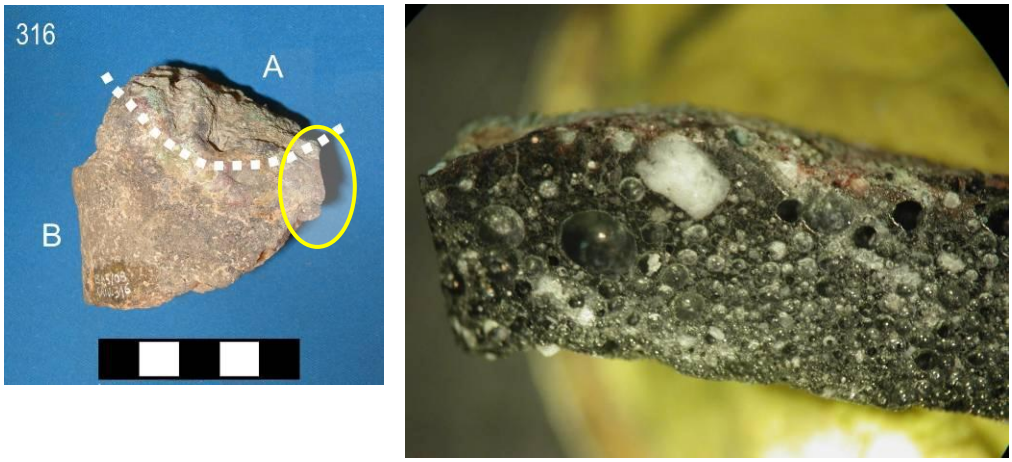

Figure 3.12. Crucible 316 from Entre Águas 5 (detail of the cross-section evidencing crucible fabric and slag layer).

The SEM-EDS characterisation of the slag 316-s identified a complex vitreous matrix of aluminium silicate with Na, Mg, K, Ca, Mn and Fe (Figure 3.13). This slag is highly heterogeneous, comprising many different phases and inclusions, namely euhedral tin oxide needles, copper prills and dendritic magnetite. The enlarged image evidence tin oxide and metallic copper converging into a bronze nodule.

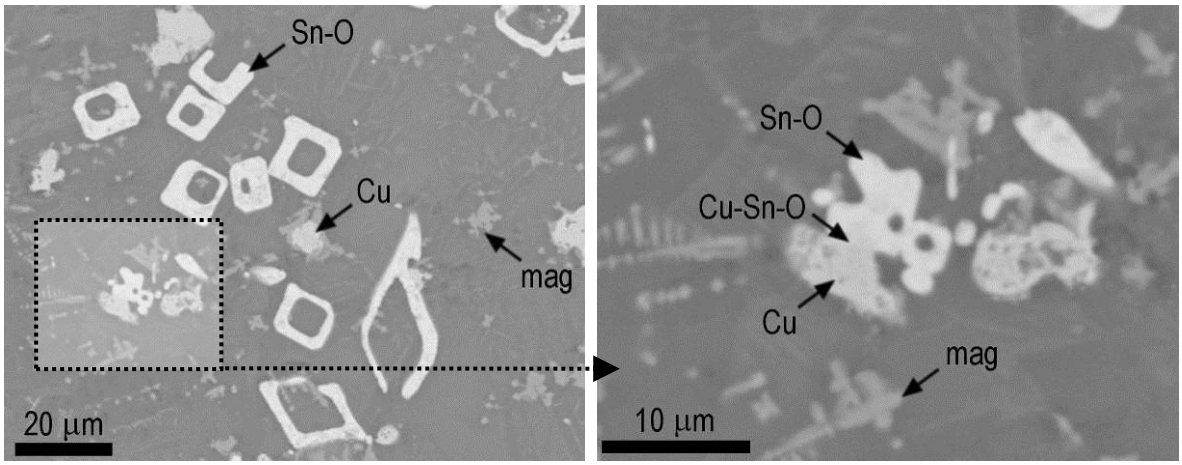

Figure 3.13. SEM-BSE images of the slag 316-s (mag: magnetite; phase identified by approximate stoichiometry given by EDS).

These results are comparable to the obtained from the other two socketed handle crucibles (i.e. euhedral needles of tin oxide, metallic and copper oxide inclusions and abundance of magnetite inclusions) suggesting that all these socketed handle crucibles were involved in a similar metallurgical operation.

3.2.2.4. Slag 1373-s

The slag 1373-s was obtained by cutting of a small segment of the crucible 1373 to expose a small cross-section the crucible fabric and slag layer. This slag comprises a thin layer of a complex vitreous matrix (aluminium silicate with Na, Mg, K, Ca, Mn and Fe) with a few globular inclusions of bronze (Figure 3.14).

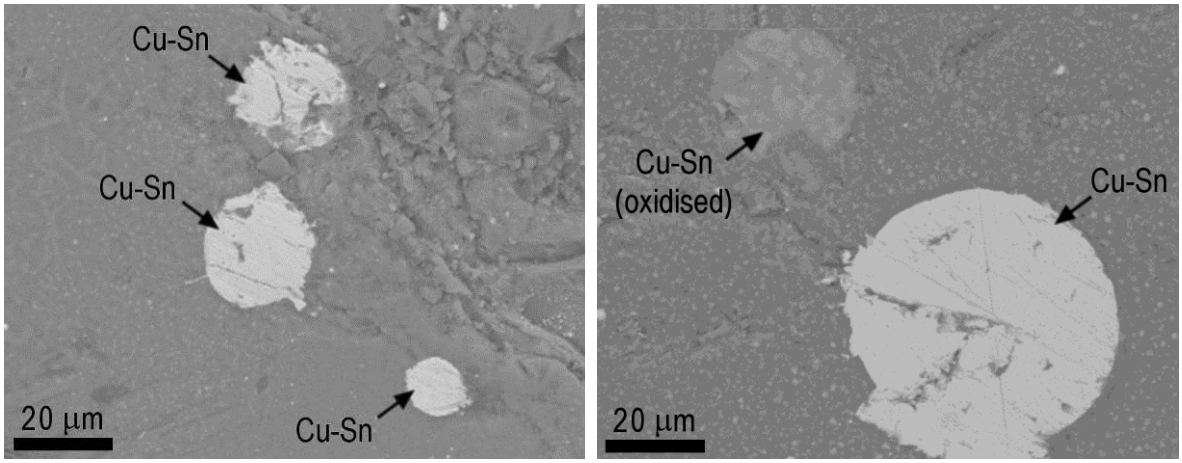

Figure 3.14. SEM-BSE images of the slag 1373-s.

3.2.2.5. Slag 1374A2-s

The characteristics of the slag 1374A2-s, obtained by cutting of a small segment of the crucible 1374A2, are very similar to the slags previously identified in the socketed handle crucibles. It is composed by a vitreous matrix (aluminium silicate with Na, Mg, K, Ca, Mn and Fe) with abundant magnetite inclusions, copper and copper oxide inclusions, globular and euhedral needles of tin oxide (Figure 3.15). This image shows a large copper prill with a bronze halo (oxidised) being surrounded by many tin oxide inclusions.

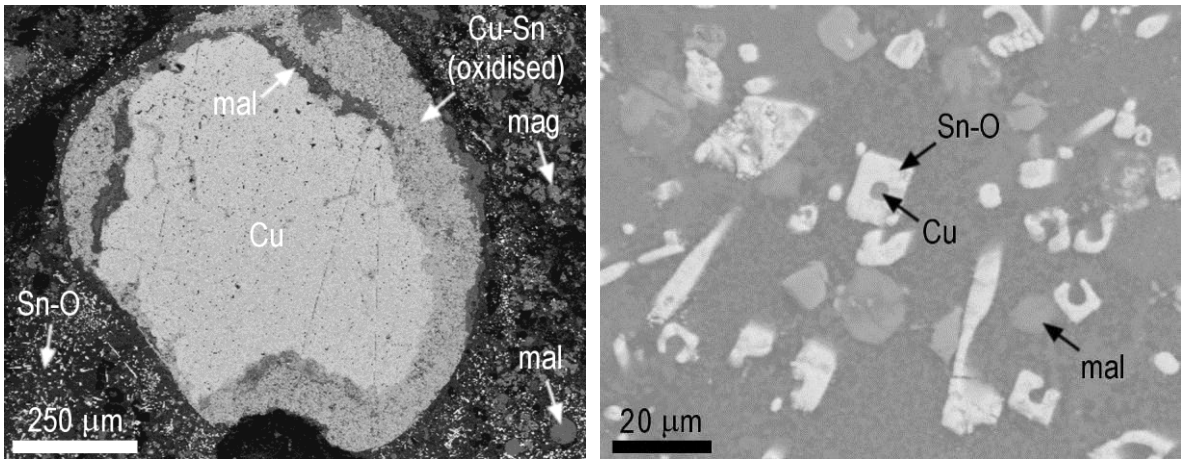

Figure 3.15. SEM-BSE images of the slag 1374A2-s (mag: magnetite; mal: malachite; phases identified by approximate stoichiometry given by EDS).

3.2.2.6. Slag 1374-s

The slag 1374-s was obtained by removing a small fragment of the slagged material present in the tip of the triangular rim crucible 1374. This slag is composed by a copper oxide/carbonate matrix with copper sulphide inclusions (Figure 3.16).

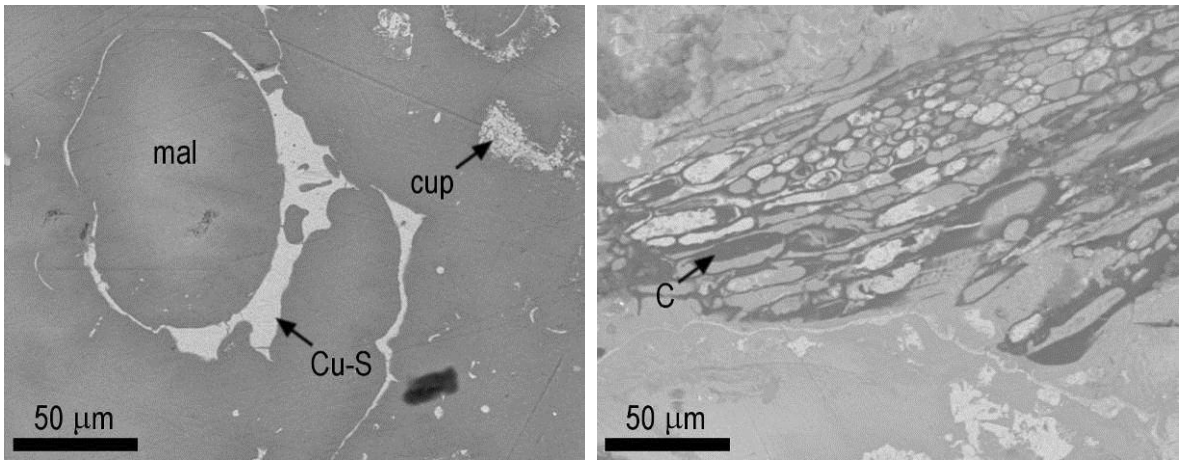

Figure 3.16. SEM-BSE images of the slag 1374-s (mal: malachite; cup: cuprite; phases identified by approximate stoichiometry given by EDS).

An uncommon silver inclusion was also identified, contrary to tin that was not detected (similarly to the results from the EDXRF analyses of this crucible). An interesting result was the morphological identification of the charcoal inclusion as belonging to the *Erica sp.* (heather)[2]. This species is very common in the southern Portuguese territory. According to a recent study (García-Martínez and Ros-Sala, 2010), *Erica sp.* presents one of the highest calorific powers among the

[2] The taxonomic identification of the charcoal inclusion was made by Paula Queiroz (Terra Scenica)

woods usually used as fuel in ancient metallurgical operations. The pouring tip of this crucible suggests that it supposed to handle some kind of liquefied material. Additionally, the charcoal inclusions are more commonly found in completely liquefied slags (Hauptmann, 2007). Therefore, these evidences seem to suggest that this crucible was used to melt copper, probably copper nodules previously obtained from the smelting of mixed oxide/sulphide copper ores.

3.2.3. Tuyere

EDXRF analyses of the slagged and clay surfaces of the tuyere 1374B identified some enrichment in Mn, Cu, Sn and Sb in the slagged area (Figure 3.17). The significant enrichment in copper and tin readily connects this tuyere with the metallurgy of bronze implemented within the crucibles recovered from the "metallurgical" hut at Entre Águas 5.

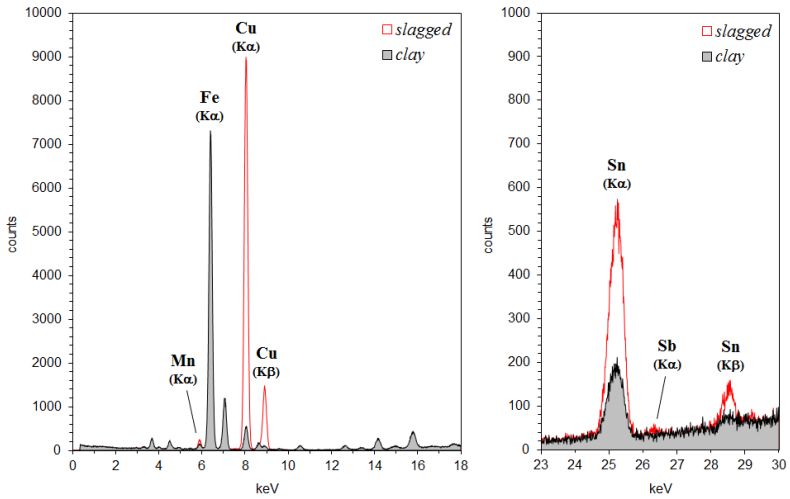

Figure 3.17. EDXRF spectra of slagged and clay surfaces of tuyere 1374B from Entre Águas 5 (spectra of Ag and Gd secondary targets).

3.2.4. Moulds

The comparison of the EDXRF spectra of inner and outer clay surfaces of mould fragments from Entre Águas 5 indicated that only some of them are slightly enriched in significant elements (Table 3.3). It is not surprising that the mould fragments exhibit less evidences of a metallurgical element since the casting operation usually originates fewer residues than smelting or melting/refining. The increased presence of tin over copper results from the lower tendency of copper to become enriched during the casting operation. Nevertheless, the enrichment of these elements in some of fragments clearly indicates that these moulds were used to cast bronze alloys. Regarding the Pb, it

should be noted that its higher vapour pressure and reactivity with mould fabric should produce more "residues" if these mould were related with the casting of leaded bronze alloys.

Table 3.3. Significant elements enriched in the inner surfaces of mould fragments from Entre Águas 5 (+: enriched element; the more discriminating elements are shaded).

Artefact	Type	Reference	Cu	Zn	As	Pb	Sn	Sb
mould	unknown	1432A					+	
mould	unknown	1432B1						
mould	unknown	1432B2					+	
mould	unknown	1432C1						
mould	unknown	1432C2						
mould	unknown	1432C3						
mould	unknown	1432C4						
mould	unknown	1432C5						
mould	unknown	1432C6						
mould	unknown	1432C7	+				+	
mould	unknown	1432C8				+	+	
mould	unknown	1432C9						
mould	unknown	1432C10						

3.3. Casarão da Mesquita 3 and 4[3]

During 2006, emergency archaeological excavations at Casarão da Mesquita 3 (Évora) exposed 49 pits, whose radiocarbon dating and ceramic typology integrate into the Middle/Late Bronze Age (Santos *et al.*, 2008). The material culture recovered at this site includes a mould for flat axes. In the following year, another 68 pits were identified during emergency archaeological excavations conducted at Casarão da Mesquita 4, Évora (Nunes *et al.*, 2007). This site is located only several hundred meters to west of Casarão da Mesquita 3, thus both locations are probably part of a much larger one. Artefacts recovered inside some of the negative structures from Casarão da Mesquita 4 comprises two small crucibles and two metallic nodules that can be ascribed to the BA.

The mould for flat axes from Casarão da Mesquita 3 (QC4/F8/C1) was carved in steatite stone. The recovered fragment corresponds to part of one valve, whose carved region match with the cutting edge of a flat axe (Figure 3.18). A black greasy powder sticking to the carved surface of the mould was identified as an organic dressing, which was probably obtained using a smoky flame from burning bones, i.e. *bone black* (Soares *et al.*, 2007). The "so-called" bone black used in old paintings contain as little as 10% carbon – more or less the same percentage determined for this dressing – the remainder being mainly calcium phosphate with a little calcium carbonate (Plesters,

[3] A preliminary work with some content from this section was previously published (Soares *et al.*, 2007).

1956). The presence of this dressing material attached to the mould after the long burial period is an exceptional circumstance. It allows a better knowledge of the materials used to protect the mould from high temperatures of casting during those ancient times.

Figure 3.18. Steatite mould from Casarão da Mesquita 3 (A: outline of the flat axe blade with ~4cm width).

The crucibles recovered at Casarão da Mesquita 4 are made of clay and exhibit relatively thick walls (Figure 3.19). The crucible 2600 belongs to a very shallow typology with a vitrified inner surface that clearly evidences the heating from above. Furthermore, both crucibles exhibit slagged inner surfaces with relics of metal oxides.

Figure 3.19. Crucibles from Casarão da Mesquita 4 (including detail of slagged inner surface from crucible 2600).

3.3.1. Crucibles

The comparison of the EDXRF analyses of the slagged and clay surfaces of the crucibles from Casarão da Mesquita 4 evidences the enrichment in Ca, Mn, Cu and Sn (Figure 3.21 and Figure 3.21). Additionally, the slagged surface of the shallow crucible 2600 seems to be enriched in iron (iron-rich slag?). The enrichment in calcium probably results from the reactions between wood-ash

and metal/oxides/crucible fabric, while the enrichment in copper and tin clearly indicate the relation of these crucibles with the metallurgy of bronze. This fact ascribes these metallurgical materials to the last centuries of the BA since the introduction of bronze in the southern region of the Portuguese territory was rather late, namely around 1400-1200 BC (Senna-Martinez, 2007).

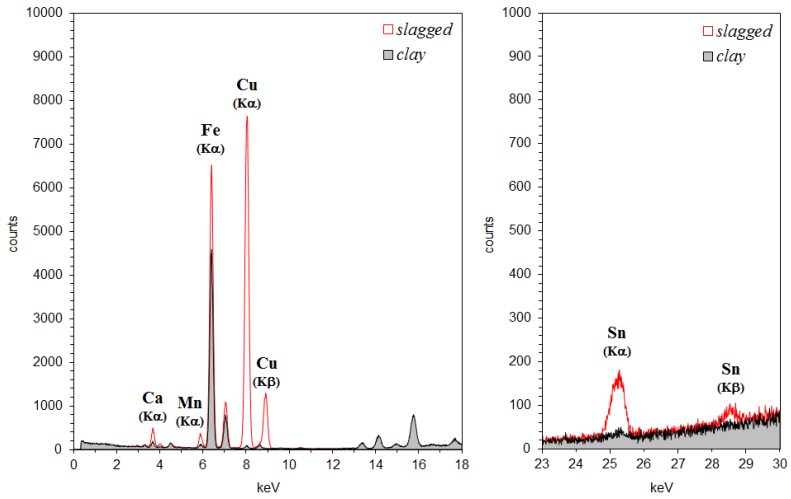

Figure 3.20. EDXRF spectra of slagged and clay surfaces of shallow crucible 2600 from Casarão da Mesquita 4 (spectra of Ag and Gd secondary targets).

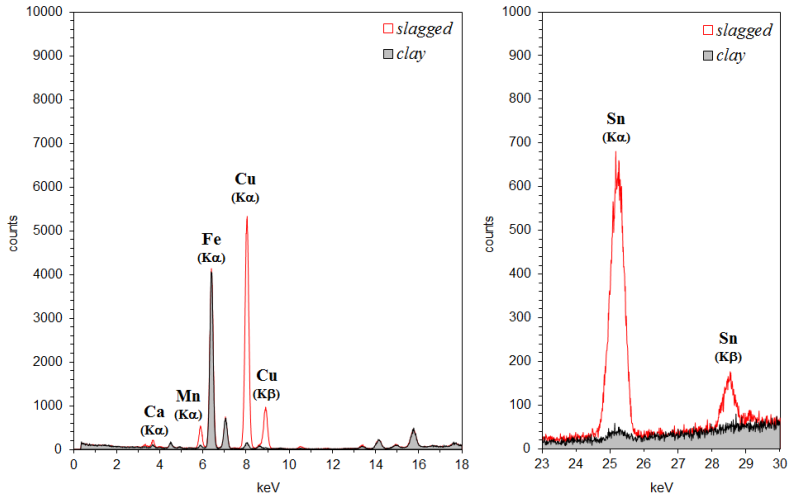

Figure 3.21. EDXRF spectra of slagged and clay surfaces of crucible edge 469 from Casarão da Mesquita 4 (spectra of Ag and Gd secondary targets).

3.3.2. Slags

3.3.2.1. Slag 2600-s

The sampling of the slag 2600-s included cutting a segment of the crucible 2600 to expose a cross-section of the slag layer. SEM-EDS characterisation identified a heterogeneous slag composed by a

complex vitreous matrix (aluminium silicate with Na, Mg, K, Ca, Mn and Fe) with abundant magnetite inclusions (Figure 3.22).

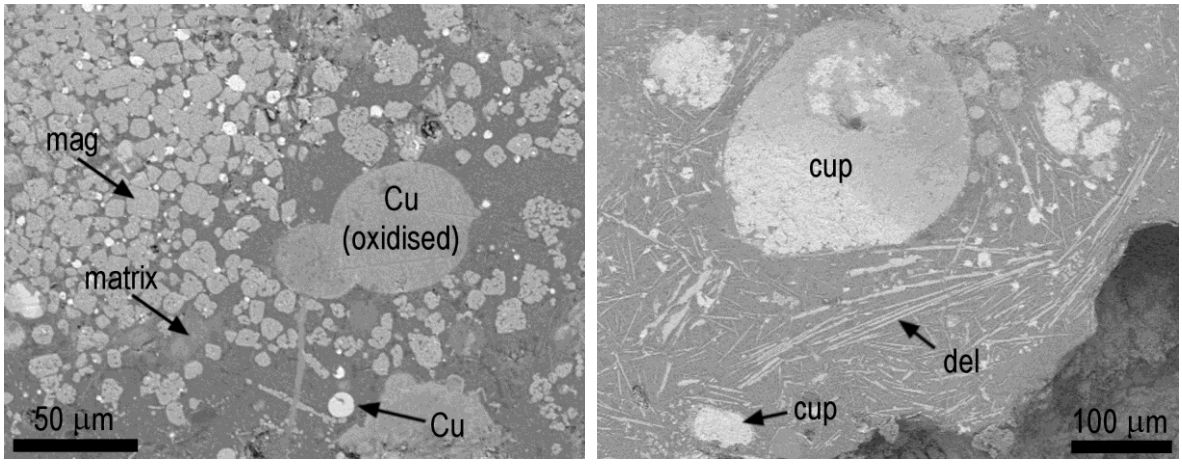

Figure 3.22. SEM-BSE images of slag 2600-s from Casarão da Mesquita 4 (mag: magnetite; cup: cuprite; del: delafossite; phases identified by morphology and approximate stoichiometry given by EDS).

Magnetite inclusions among this iron-rich slag evidence the oxidising conditions present at certain regions of the reaction vase. The shallow typology of the crucible 2600 makes more difficult to achieve a proper reducing atmosphere. Copper is present in various forms that evidence the different reactions among ore, metal, crucible fabric and wood ash, namely copper oxide, and metal. Additionally, copper is present as long needles of an iron rich phase, i.e. delafossite (chemical formula: $Cu[I]Fe[III]O_2$). Delafossite, cuprite and magnetite are usually present among ancient iron-rich slags formed under rather oxidizing conditions (Hauptmann, 2007). Tin could not be detected by SEM-EDS characterisation despite being slightly enriched in the slagged surface of the crucible (see EDXRF spectra, Figure 3.20).

3.3.2.2. Slag 469-s

The sampling of the slag 469-s included cutting a segment of the crucible 469 to expose a cross-section of the slag layer. The SEM-EDS characterisation identified a complex vitreous matrix (aluminium silicate with Na, Mg, K, Ca, Mn and Fe) with a few copper nodules (Figure 3.23). The relatively high iron content of these copper nodules (~0.8-1.2%) probably results from the superior reducing conditions in this micro domain. A second region was found to be especially rich in tin, containing both tin oxides and tin-rich nodules with a very variable composition, i.e. from copper to almost pure tin. The presence of metallic nodules with such different compositions, together with the absence of cassiterite needles, was used as an indicator of alloying of metallic copper and tin in EIA slags from Carmona, SW Spain (Rovira, 2005).

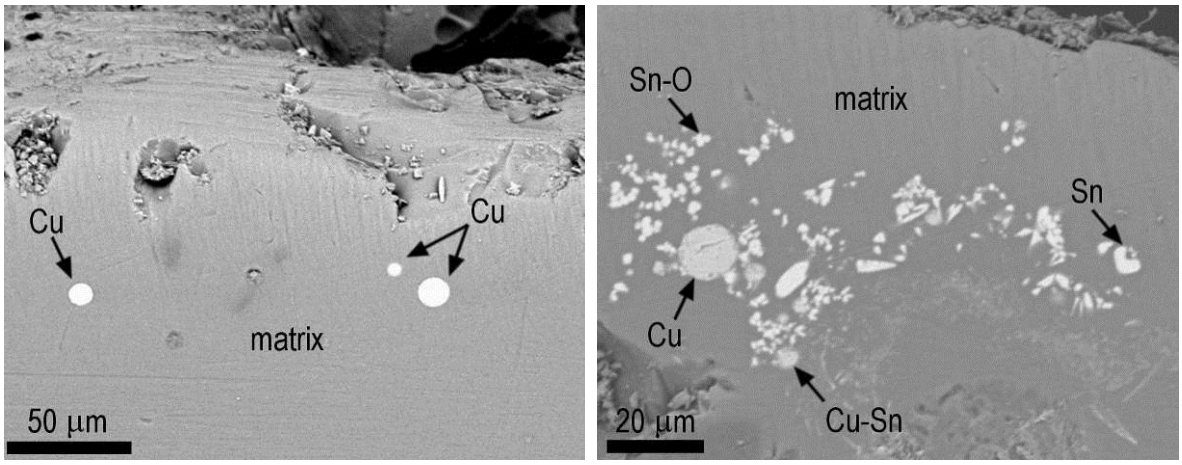

Figure 3.23. SEM-BSE images of slag 469-s from Casarão da Mesquita 4.

3.3.3. Mould

The steatite mould from Casarão da Mesquita 3 was analysed by EDXRF in the inner and outer surfaces in order to identify any significant production remains eventually present. Comparison of chemical elements present in both surfaces evidenced enrichment in Ca, Cu, Sn and Pb in the inner area (Figure 3.24). The enhanced content in Ca can result from the dressing material used. The presence of Cu and Sn establish that the mould was used to cast a bronze flat axe. Considering the chronology of this mould (i.e. ~1400-1200 BC), it probably constitutes one of the earliest known evidences of the practice of the bronze metallurgy at the southern Portuguese territory.

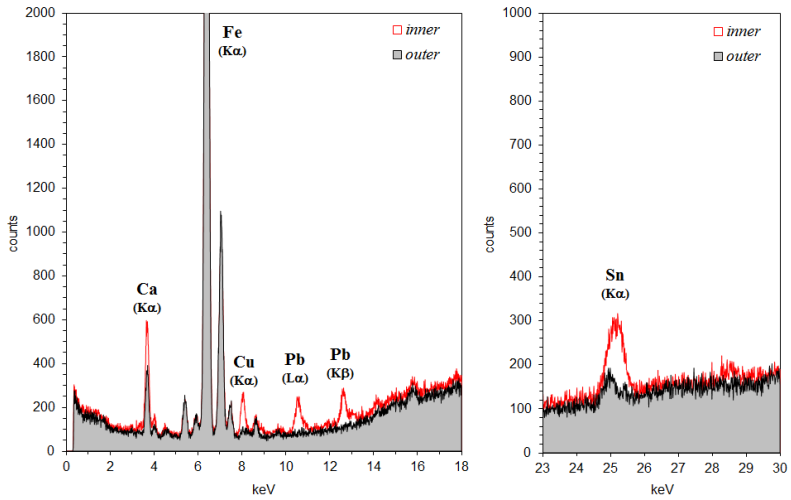

Figure 3.24. EDXRF spectra of inner and outer surfaces of mould from Casarão da Mesquita 3 (spectra of Ag and Gd secondary targets).

3.3.4. Metallic nodules

EDXRF analysis of the metallic nodule 41B from Casarão da Mesquita 4 indicates that it is mainly constituted by copper and tin, together with traces of iron. Optical microscopy observations reveal that the nodule is totally corroded, displaying an external layer composed mainly by malachite compounds (green areas) surrounding the inner core of cuprite compounds (Figure 3.25). Furthermore, higher magnifications disclose a relic fine dendritic microstructure that indicates a fast cooling rate. These characteristics are consistent with a small piece of molten bronze that fall from the crucible during a melting or pouring operation, thus cooling extremely fast due to the prompt temperature change and its very small dimension.

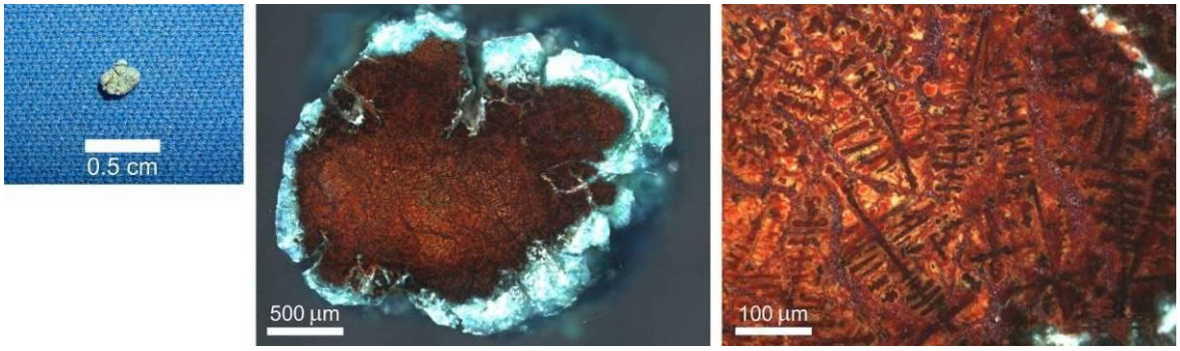

Figure 3.25. Microstructure of metallic nodule 41B from Casarão da Mesquita 4 (OM-Pol, non-etched).

Micro-EDXRF analysis of the metallic nodule 48A from Casarão da Mesquita 4 indicates that it is mainly composed by copper with traces of arsenic and iron (Table 3.4). Optical microscopy observations point to a microstructure of coarse Cu grains, large porosities, a small amount of twins and some copper oxide inclusions in the grain borders (Figure 3.26). The coarse microstructure evidences a slow cooling rate that is consistent with a smelting/melting nodule that was left in the crucible until it cools down. Copper oxide inclusions are very common among pre-historic copper artefacts, especially in those without a deoxidizing element, such as arsenic or tin. The somewhat poor reducing conditions achieved during those ancient smelting operations also originate metallic copper with very low iron contents (i.e. the nodule 48A presents Fe<0.05%).

Table 3.4. Results of micro-EDXRF analysis of metallic nodule from Casarão da Mesquita 4 (nd - not detected).

Sample	Cu (%)	Sn (%)	Pb (%)	As (%)	Fe (%)
48A	99.8	nd	nd	0.15	<0.05

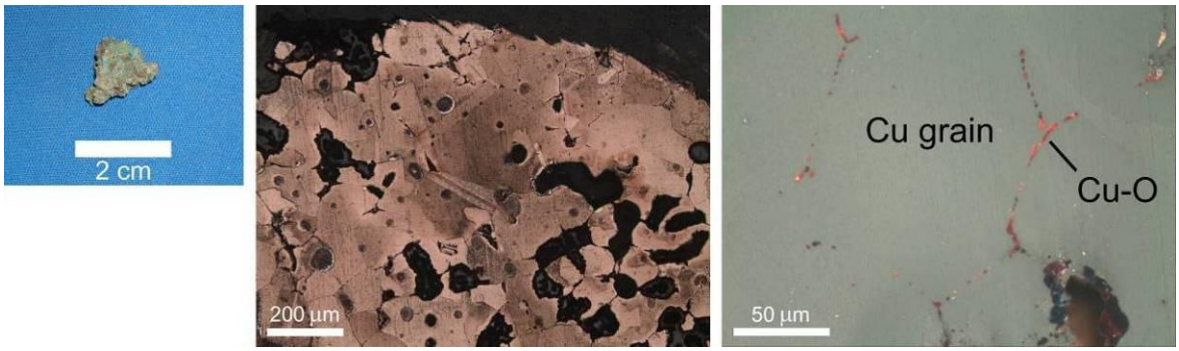

Figure 3.26. Microstructure of metallic nodule 48A from Casarão da Mesquita 4 (OM-BF, etched and OM-Pol, non-etched, respectively).

3.4. Salsa 3

The archaeological excavations at Salsa 3 (Serpa) were carried out from 2005 to 2007, revealing 2 hut floors and 8 pits, whose material culture can mostly be ascribed to the LBA (Deus *et al.*, 2009). The material culture recovered includes two production remains, namely a large mould and a metallic nodule (Deus *et al.*, 2009). The mould (Silo 4) was carved in stone and corresponds to a fragmented valve exhibiting the hilt section of a flat axe (Figure 3.27). The casting sprue, located at one end of the mould, undoubtedly indicates that this was a bivalve mould that was filled while in a vertical position.

Figure 3.27. Stone mould from Salsa 3 (A: outline of flat axe with ~4cm width; B: casting sprue).

3.4.1. Mould

EDXRF analyses of the carved surface of this mould did not show any significant levels of metals, i.e. copper is only present at trace level (similar to the one found in the outer surface of mould), while lead and tin were not identified.

3.4.2. Metallic nodule

The micro-EDXRF analyses of the metallic nodule 23 point to a bronze alloy with traces of lead, arsenic and iron (Table 3.5). However, these results should be considered merely indicative since the optical microscopy observations revealed a highly heterogeneous and corroded matrix (Figure 3.28). The microstructural characterisation also exposes a microstructure constituted by coarse α grains, suggesting a somewhat slow cooling rate, with coring (i.e. Cu content decreases along the grain section). The coarse grains are surrounded by smaller dendrites, clearly indicating that the final cooling rate of this nodule was much faster. Cu-S inclusions are present along regions between the larger grains. A possible explanation is that this metallic nodule corresponds to a smelting nodule that was removed from the crucible in the first stages of the cooling process, thus originating a much higher cooling rate. Another explanation concerns a partial remelting of the nodule (only the tin richer regions were melted down) with a later fast cooling rate. Finally, its low iron content (<0.05%) is indicative of the poor reducing conditions during the smelting of the copper present in this nodule.

Table 3.5. Results of micro-EDXRF analysis of metallic nodule from Salsa 3.

Sample	Cu (%)	Sn (%)	Pb (%)	As (%)	Fe (%)
23	85.4	14.5	0.10	<0.10	<0.05

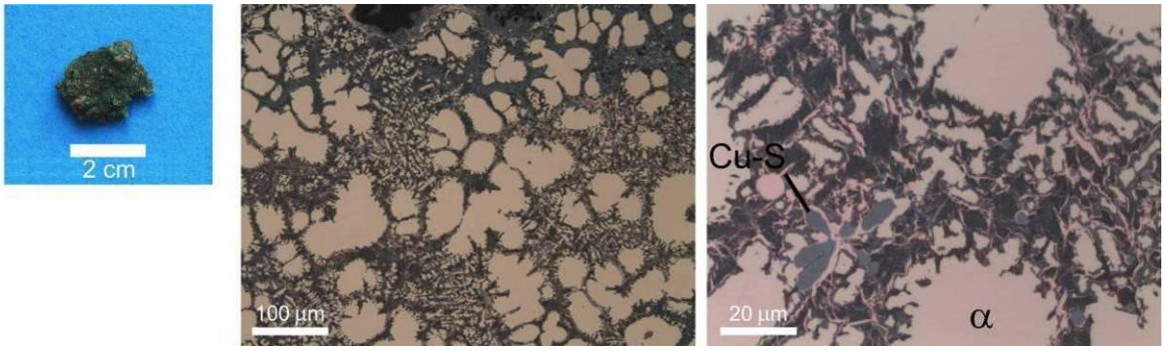

Figure 3.28. Microstructure of metallic nodule 23 from Salsa 3 (OM-BF, non-etched).

3.5. Martes

The archaeological site of Martes (Redondo) corresponds to a LBA settlement, possibly fortified, and located at the top of an hill (Calado and Mataloto, 2001). Archaeological excavations recovered two highly shattered production remains – a clay crucible and a stone mould. The clay crucible (M1) comprises half of a fragmented socketed handle and a small part of the inner wall of the reaction vase (Figure 3.29). This typologically more advanced socketed handle crucible must have been very similar to the socketed handle crucibles recovered at Entre Águas 5.

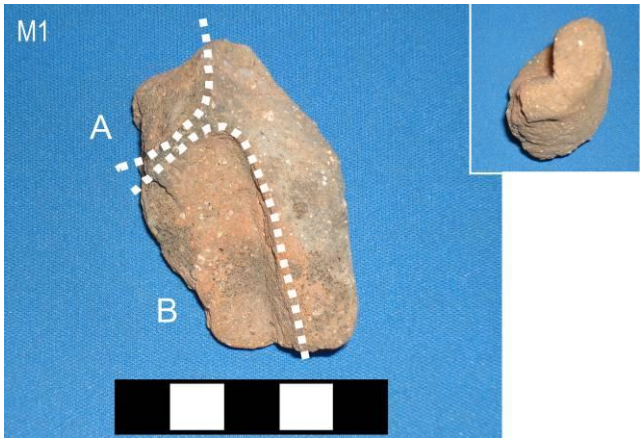

Figure 3.29. Crucible M1 from Martes (A: reaction area; B: fragmented handle; detail of the socket).

The stone mould (M2) comprises a fragmented valve of a bivalve mould for casting several artefacts (Figure 3.30). At least 3 faces of the mould still present recognisable carved surfaces, but it is impossible to distinguish the complete shape of the artefacts to be produced. Face A exhibits one hole to insert a dowel for the correct alignment of the two valves, while face C presents a straight channel, which was probably carved to serve as pouring channel.

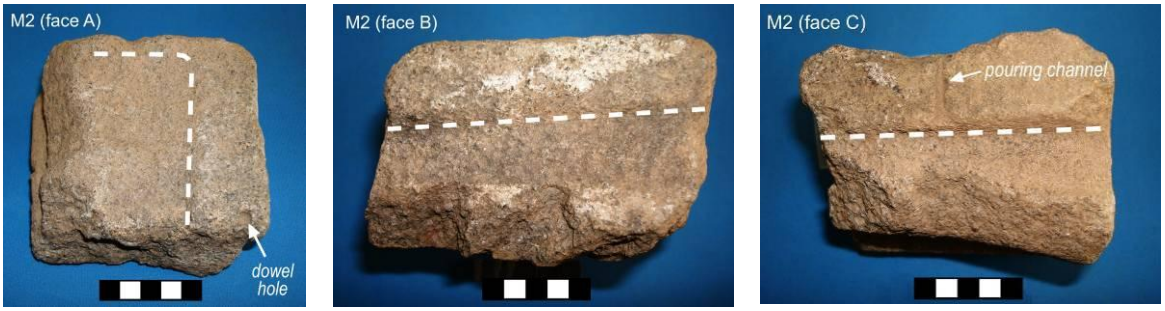

Figure 3.30. Stone mould M2 from Martes (outline of recognisable carved surface at faces A, B and C).

3.5.1. Crucible

The comparison of the EDXRF analyses of the vitrified and clay surfaces of this crucible evidence the enrichment in K, Ca, Mn, Cu, Pb and Sn (Figure 3.31). These results indicate the relation of this socketed handle crucible with the metallurgy of bronze. The relatively higher enrichment in Pb results from the much higher propensity of this element to become enriched in this type of metallurgical debris than tin or copper (Kearns *et al.*, 2010). Furthermore, the lack of slagged material still adhering to the clay in the reaction vase prevents a more detailed study, as the one conducted at the crucibles from Entre Águas 5.

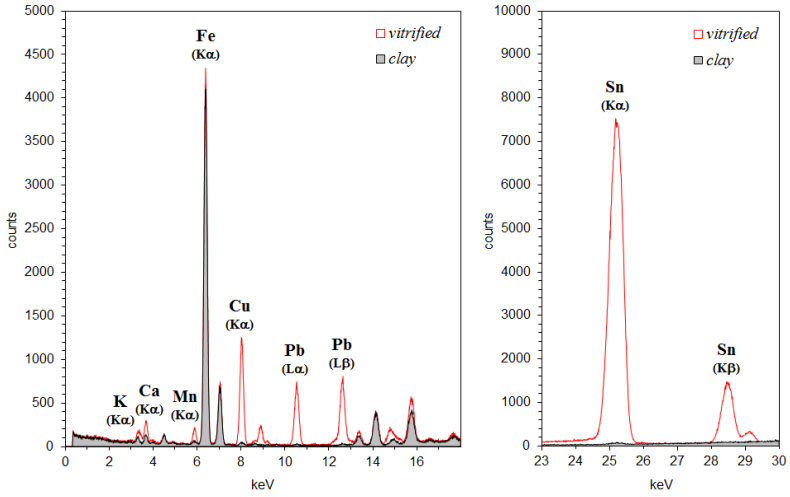

Figure 3.31. EDXRF spectra of vitrified and clay surfaces of socketed handle crucible M1 from Martes (spectra of Ag and Gd secondary targets).

3.5.2. Mould

Several EDXRF analyses of the carved surfaces of this mould were unable to identify any production remains. Unfortunately, prehistoric moulds often do not present evidences of metallurgical contamination because these residues can easily be leached during the long burial time or removed during the discovery and cleaning of the artefact.

3.6. Castro dos Ratinhos

The archaeological excavations conducted from 2004 to 2007 at Castro dos Ratinhos (Moura) recovered a mould for "carp-tongue" swords belonging to the 12th-9th centuries BC (Berrocal-Rangel and Silva, 2010). The mould (R1/Ic/L1) comprises a fragment of one of the two valves that originally should compose the mould, while the carved region corresponds to the tip section of the blade (Figure 3.32). The material elected to make this mould was sandstone since it is a relatively soft material that facilitates the carving operation.

Figure 3.32. Sandstone mould from Castro dos Ratinhos (A: outline of leaf-shaped blade with ~2.5cm width).

3.6.1. Mould

The EDXRF analyses of the inner and outer surfaces of the mould indicate that the carved area is enriched in K, Ca, Cu, Sn and Pb (Figure 3.33). The enrichment of K and Ca might be related with some kind of dressing material used to protect the mould from the high temperature of molten metal during pouring. The enrichment of copper, tin and lead in the carved surface indicates the casting of a bronze sword.

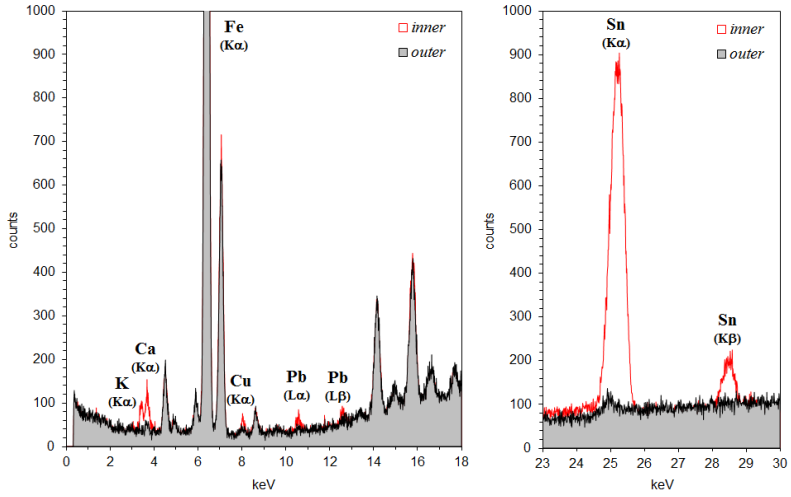

Figure 3.33. EDXRF spectra of inner and outer surfaces of mould from Castro dos Ratinhos (spectra of Ag and Gd secondary targets).

3.7. Discussion

The integration of results obtained from the study of the production remains allows some important considerations about the LBA copper-based metallurgical technology at this region of the Southwestern Iberian Peninsula. First of all, it must be taken into account that the knowledge of nowadays regarding those ancient communities is often incomplete. For instance, despite the extensive archaeological works conducted at Castro dos Ratinhos, it is believed that only a small part of the site was actually excavated. Taking this into account, the obtained results seem to establish that the majority of the LBA sites present evidences of the practice of metallurgical activities (Figure 3.34). Furthermore, smelting/alloying and casting activities were often present at the same location (Salsa 3 presents a metallic nodule whose microstructure suggests a smelting origin, thus both smelting and casting activities could have been carried out at this site). The coordinated practice of smelting/alloying and casting activities at the same location can probably explain the shortage of ingots among the archaeological record since metal obtained from smelting/alloying could be melted down and directly poured into a mould.

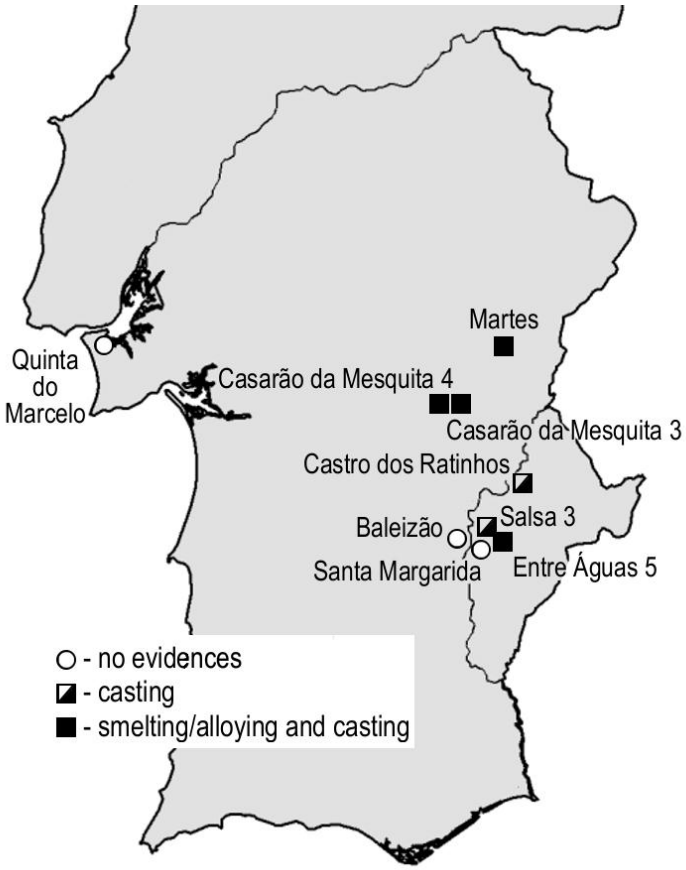

Figure 3.34. Type of metallurgical operations among the LBA archaeological sites studied.

Moreover, the relatively small number of production remains among the archaeological record suggests a small scale production, consistent with the one established at other coeval regions, namely the LBA central Portuguese territory, where it is believed that copper-based metallurgy was conducted at a domestic scale (Senna-Martinez and Pedro, 2000).

The moulds studied are commonly made of soft stones (e.g. steatite or sandstone), while most crucibles are composed of ceramic materials. Some of the production remains show evolved typologies (multipurpose mould and socketed handle crucibles) that suggest a rather skilled metallurgical knowledge. Almost all production remains could be directly connected with the metallurgy of bronze, with the exception of the triangular crucible from Entre Águas 5 that only exhibits traces of copper. Nonetheless, to fully understand the meaning of the obtained results, it is imperative to begin by establishing the current state of the art regarding the ancient bronze production at the Iberian Peninsula.

The archaeological record indicates that smelting operations were usually conducted in open-mouthed ceramic vessels from the CA until the Pre-roman period, whereas the only significant change was a general trend to increase the size of the crucibles (Rovira, 2002). These crucibles

were filled with succeeding charges of crushed ore and charcoal. Due to the crucible open shape and, sometimes, overwork of the tuyeres, the redox conditions were far from ideal. Furthermore, silica or iron oxides were not added to the charge as fluxes and consequently no fayalitic slag was formed. Therefore, the ceramic crucible must be shattered at the end of the process, to recover the metallic nodules formed among this immature and high viscosity slag. Metallic nodules are then melted inside another crucible and poured into a mould or left to cool as an ingot. The study of several crucibles and slags from the MBA metallurgical site of Peñalosa (SW Spain), suggests that smelting was done in flat ceramic vessels that present heavily slagged inner surfaces, while melting of metallic nodules was conducted in deeper vessels exhibiting thinner slag layers (Moreno-Onorato *et al.*, 2010).

The emergence of bronze does not seem to introduce any technological innovation regarding the smelting operations at the Iberian Peninsula because bronzes can be produced by co-smelting of copper and tin ores. Experimental trials established that the bronze alloy can be obtained through the direct reduction of copper and tin ores, using a crucible, tuyeres and charcoal as fuel (Rovira *et al.*, 2009). It is only during the IA that the archaeological record begin to presents some evolved furnaces, but this transformation is not swift nor generalized, even among the regions with strong Phoenician influence (Gómez-Ramos, 1999).

The somewhat scarce analytical studies of slags at the Iberian Peninsula seem to indicate that the production of bronzes begin with co-smelting (Rovira, 2005). This process continues to be generally utilised at least until the transition to the EIA. An example is the LBA/EIA socketed handle crucible from Las Camas (Madrid), whose abundance of cassiterite and cuprite, together with the absence of metallic tin indicated a co-smelting process. During the transition of the LBA to the EIA the cementation of metallic copper with cassiterite is evident from the slags at Gusendo de los Oteros (NW Spain). The LBA socketed handle crucible from Cerro de San Cristobal (Central Spain) was also used to smelt cassiterite with metallic copper (Rodriguez-Diaz *et al.*, 2001). At the present moment, the first example in the archaeological record of alloying copper with tin emerge in an 8th-7th centuries BC slag from Carmona, Andalusia (Rovira, 2005).

The analytical evidences obtained from the metallurgical debris from Entre Águas 5 indicate the co-smelting of copper ores and cassiterite. The copper ores exploited were oxides and carbonates with significant amounts of sulphides. The source of tin is not entirely certain, but analytical and archaeological evidences strongly point to the use of cassiterite instead of metallic tin. However, the 10th-9th centuries BC triangular rim crucible containing a copper-rich slagged material with no tin does not seems to fit into this metallurgical scenery. It is possible that this crucible was used to melt copper nodules obtained from a previous reduction of copper ores. The presence of a lip

greatly simplifies pouring of the molten metal into the mould. The use of metallic copper implies a new method other than the co-smelting for the production of bronze alloys at Entre Águas 5. Perhaps, these dissimilar metallurgical methods belong to slightly different chronological occupations of the settlement, which could not be differentiated through radiocarbon dating.

The analytical data obtained from slagged crucible remains from Casarão da Mesquita 4 do not produce conclusive results about the type of method used in production of the bronze alloy. However, the common feature of all these slags is their highly heterogeneous and immature nature, which results from the poor and changeable redox conditions attained within the reaction vase. This characteristic feature of LBA metallurgy from the Iberian Peninsula originates a high viscosity slag with a high retention of metal, e.g. an crucible slag from the BA necropolis of Valdegalaroza (SW Spain) exhibit ~8% of copper (Pérez *et al.*, 2002). The majority of metallic nodules produced exhibit very low iron contents since the redox conditions were not sufficient to reduce the iron impurities present in the process. Therefore, these ancient smelting operations would produce a metal with very low iron content (Craddock and Meeks, 1987). Finally, an important consideration was to find out that none of these production remains point to the recycling of bronze artefacts.

4. COPPER-BASED ARTEFACTS

4.1. Early and Middle Bronze Age – some case studies

4.1.1. Introduction

During the early stages of this period the copper-based artefacts still present a relatively small number of typologies despite being already known for about one millennium. The archaeological record is mostly composed by awls, axes, saws, daggers, arrows, needles and some ornamental artefacts. Throughout the 2nd millennium BC there are small alterations in the typological panorama of metallic artefacts, the major novelty being the introduction of swords. Additionally, ornaments become more frequent, fact that can be understood as an evidence of the increased importance of metal as a prestige material (Rovira, 2004).

The so-called Southwestern Bronze Age corresponds roughly to 2250-1200 BC, which is usually divided in EBA (2250-1800 BC) and MBA (1800-1200 BC). The copper-based metallurgy from this period is still poorly understood. An important and still unique revision, based mostly on semi-quantitative analyses, established that this period did not bring any technological innovation – copper-based artefacts with significant arsenic contents are common since the middle of the 3rd millennium BC, when arsenical coppers seem to substitute copper artefacts (Soares *et al.*, 1996).

The introduction of arsenical coppers (As>2%) was understood as a metallurgical innovation (Craddock, 1995). The addition of arsenic to copper greatly improves the mechanical properties of the metal (Figure 4.1), but the enhanced increase of hardness is better achieved for very high arsenic contents (~7%), which usually are not found in ancient artefacts (Lechtman, 1996). In equilibrium conditions copper can dissolve up to 8% arsenic before the formation of the arsenic-rich γ phase (Figure 4.1), but under the relatively fast cooling rates commonly used this γ phase has been observed in alloys with only 2% As (Northover, 1989). The significant presence of the arsenic-rich phase will make the alloy increasingly brittle. Arsenical coppers can be produced by the co-smelting of copper and arsenic ores (Lechtman and Klein, 1999). A fragment of pyrite ore associated with arsenopyrite, recovered from the Late Copper Age contexts at Castelo Velho de Safara (Moura), suggests that the co-smelting process was used at this region (Soares *et al.*, 1985). The study of Late Copper Age copper-based artefacts and ores from Porto das Carretas (Mourão), evidence that the artefacts present significant amounts of arsenic, while this element was not present in the ores (Valério *et al.*, 2007). However, smelting experiments had demonstrated that it is possible to obtain arsenical coppers from ores with low arsenic content (Hanning *et al.*, 2010; Hauptmann, 2007). The higher affinity of arsenic with metallic copper than with slag will naturally produce an alloy richer in this element.

Several other archaeometallurgical evidences seem to be pointing in a different direction regarding the role of arsenic in copper. Most artefacts from the MBA Argaric Culture present arsenic contents bellow the values that are actually required to enhance the mechanical properties of copper, 3-4% As (Rovira, 2004). Additionally, the Iberian archaeological sites with the earlier evidences of copper metallurgy present both copper and arsenical copper artefacts, suggesting that coppers do not precede arsenical coppers (Ruíz-Taboada and Montero-Ruíz, 1999). CA and EBA/MBA copper artefacts from southern Portugal analysed by the SAM project (Junghans *et al.*, 1968; 1974) exhibit a lognormal distribution of arsenic contents, which resembles the natural distribution of minor and trace elements in minerals (Müller *et al.*, 2007). All these evidences suggest that the arsenic content is not an intentional addition, instead resulting from its natural variability in the copper ores exploited. In addition, the increased variability of the arsenic content in the archaeological panorama is an outcome from the poor control over the metallurgical processes, together with the probable remelting of artefacts – experimental studies had demonstrated that arsenic losses during recycling could be up to 50% (Tylecote *et al.*, 1977).

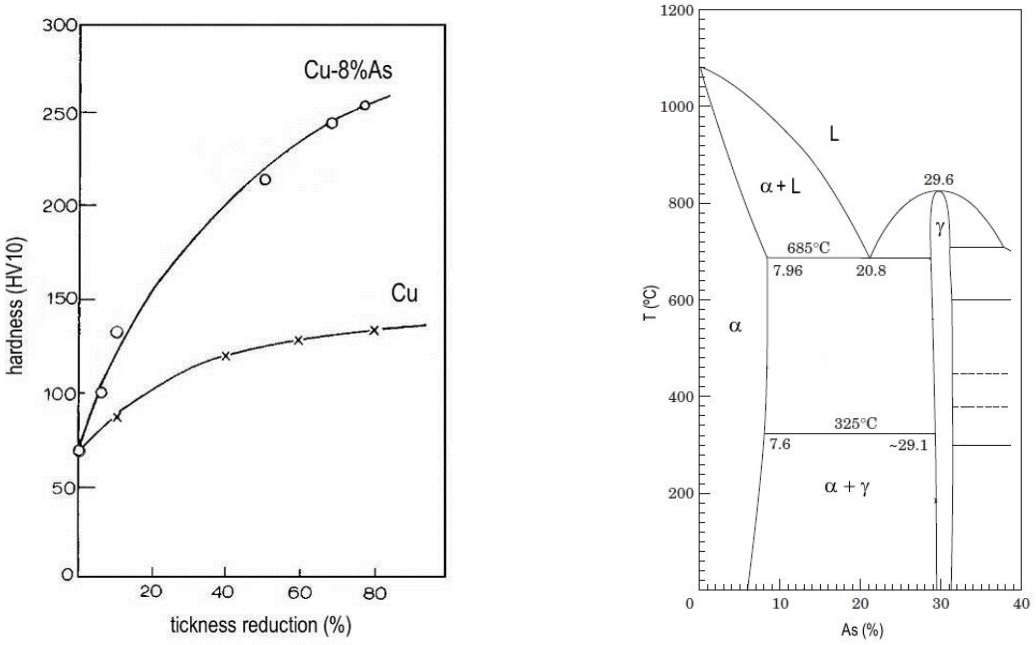

Figure 4.1. The hardness increase of copper and arsenical copper alloy by cold hammering (adapted from Coffyn, 1985) and copper-rich section of Cu-As phase diagram in equilibrium conditions evidencing the formation of the arsenic-rich γ phase at As-richer alloys (adapted from Subramanian and Laughlin, 1988).

Bronze artefacts constitute a small part of the EBA/MBA artefacts and present a considerable compositional heterogeneity indicating a very poor control over the metallurgical process (Hunt-Ortiz, 2003). It is possible that this novelty was initially more appreciated by the unique appearance of bronze rather than due to its mechanical properties (Montero-Ruíz, 1994). One of the first evidences of bronze metallurgical operations in this region is the mould for flat axes from Casarão da Mesquita 3 presented in this work. A recent work (Senna-Martinez, 2007) based on typological

data, together with the belief of a diffusion of the bronze metallurgy from the north to the south (i.e. sources of tin are located in the northern Portugal) led to the proposal of a late introduction of the bronze metallurgy in the southern region of the Portuguese territory (~1400-1200 BC).

In general, operational sequences of the early phase of the EBA/MBA still present a strong Chalcolithic influence (i.e. most artefacts are only subjected to mechanical work), while the use of forging and annealing cycles gradually increases, thus becoming the more frequently used operational sequence by the end of the MBA period (Rovira, 2004). This does not mean that the use of mechanical and thermal treatments to improve the resistance of metallic artefacts was an innovation of the EBA/MBA. In fact, the majority of the copper artefacts from the Chalcolithic site of Valencina de la Concepción (SW Spain) were subjected to successive levels of thermal and mechanical treatments, i.e. casting, forging, annealing and final forging, evidencing a direct relation between the complexity of the manufacturing procedure and the hardness of the product (Nocete *et al.*, 2008).

The results on some EBA/MBA artefacts are presented in the following sections. Despite not belonging to the main theme of the present work, it was considered important to characterise a few artefacts from a period before the full development of the bronze alloys, to identify some aspects of the arsenical copper metallurgy at the south of the Portuguese territory.

4.1.2. Anta do Malhão and Soalheironas

The archaeological works conducted during 2004 at the megalithic necropolis of Anta do Malhão (Alcoutim) revealed a latter utilisation (Cardoso and Gradim, 2009). The characteristics of the burial uncovered, together with the typologies of the materials recovered from excavations, specifically ceramics and metals, situate the grave in the transition of the CA to the BA (~2250-2000 BC). The copper-based artefacts recovered correspond to a long and narrow dagger and a Palmela point, AM/1 and AM/2 respectively (Figure 4.2). The dagger has a hilt without riveting, which is a characteristic inherited from the Chalcolithic period.

During 2005, archaeological excavations on a small hill facing the Guadiana River uncovered 32 cists containing a small number of ceramic and metallic offerings (Cardoso and Gradim, 2008) – the MBA necropolis of Soalheironas (Alcoutim). The copper-based collection comprises a dagger (Soa/1) and a throwing tip (Soa/2: arrow?) with the remainder of the riveting hole (Figure 4.2).

Figure 4.2. Copper-based artefacts belonging to the archaeological sites of Anta do Malhão and Soalheironas.

The copper-based weapons were analysed by micro-EDXRF to establish their elemental composition (Table 4.1). Results indicate that these weapons are composed of arsenical copper alloys (i.e. As > 2%) with comparable arsenic contents (2.0 – 3.4%). Moreover, the only metallic impurity detected by micro-EDXRF analyses was iron, which is present at very low concentrations (<0.05%).

Table 4.1. Results of micro-EDXRF analyses of copper-based artefacts from Anta do Malhão and Soalheironas (values in %; nd: not detected).

Type	Artefact	Reference	Context	Cu	As	Pb	Sn	Fe
Weapon	Dagger	AM/1	EBA	96.6	3.4	nd	nd	<0.05
Weapon	Arrow	AM/2	EBA	97.8	2.2	nd	nd	<0.05
Weapon	Dagger	Soa/1	MBA	96.9	3.1	nd	nd	<0.05
Weapon	Arrow (?)	Soa/2	MBA	98.0	2.0	nd	nd	<0.05

Microstructural characterisation by OM and SEM-EDS identified the common features of these artefacts, such as deformed equiaxial grains with annealing twins and slip bands (Table 4.2). Other regular feature is the presence of reddish inclusions at OM-Pol observations, later identified by SEM-EDS as being copper and arsenic oxides. These oxide inclusions are present in higher amount in the dagger from Soalheironas. Furthermore, both arrows (Soa/2 and AM/2) present monophasic microstructures, whereas the two daggers (Soa/1 and AM/1) exhibit a second phase rich in arsenic. In the microstructure of the dagger from Soalheironas, this As-rich phase is present at intergranular regions (bluish areas of OM-BF image at Figure 4.3C) with an homogeneous morphology, clearly different from the $\alpha+\gamma$ eutectic of the dagger from Anta do Malhão (Figure 4.3A). The manufacture of these artefacts included mechanical and thermal operations, namely forging and annealing. The final forging procedure was applied with different intensities in each artefact, evident in deformed twins and slip bands densities.

Table 4.2. OM and SEM-EDS characterisation of copper-based artefacts from Anta do Malhão and Soalheironas (*: % given by micro-EDXRF; s: segregation bands; t: annealing twins; sb: slip bands; d: heavily deformed inclusions; C: Casting; A: Annealing; F: Forging; FF: Final Forging; ↑: high amount; ↓: low amount).

Type	Artefact	Reference	As*	Phases	As (EDS)	Inclusions	Features		Manufacture
Weapon	Dagger	AM/1	3.4	α α+γ↓	5.2; 6.8 9.6; 27.9	Cu-As-O	equiaxial	t, sb, d	C+(F+A)+FF↓
Weapon	Arrow	AM/2	2.2	α	-	Cu-As-O	equiaxial	s, t, sb, d	C+(F+A)+FF↓
Weapon	Dagger	Soa/1	3.1	α As-rich	- -	Cu-As-O↑	equiaxial	t, sb(?)	C+(F+A)+FF?
Weapon	Arrow (?)	Soa/2	2.0	α	-	Cu-As-O	equiaxial	s, t, sb, d	C+(F+A)+FF↓

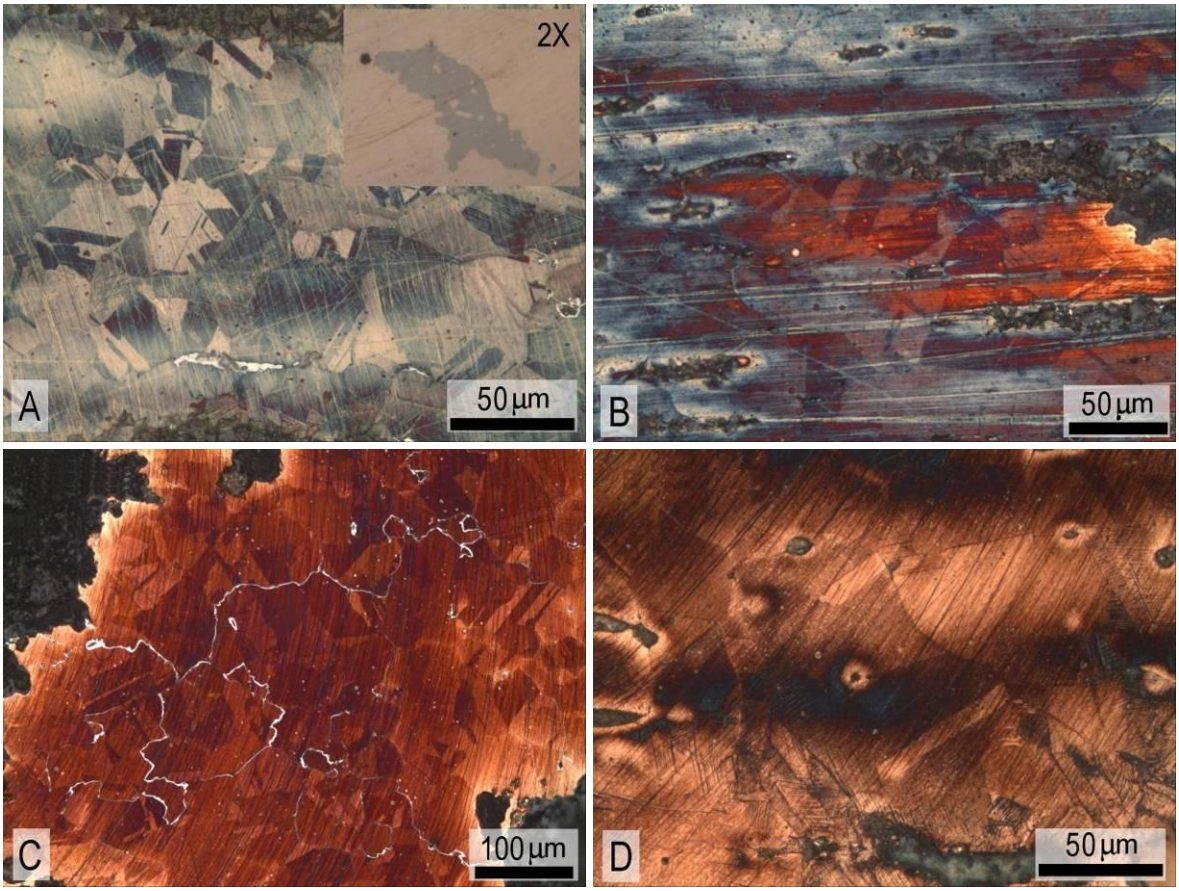

Figure 4.3. Microstructures of copper-based artefacts from Anta do Malhão and Soalheironas (A: dagger AM/1 with detail on α+γ eutectic; B: arrow AM/2; C: dagger Soa/1; D: arrow Soa/2; all OM-BF, etched).

The SEM-EDS analyses performed at the dagger from Anta do Malhão allow a better characterisation of the As-rich phase. According to the equilibrium diagram of the Cu-As system (Figure 4.1), for hypoeutectic alloys, after the α-Cu primary phase solidification, the second transformation comprises the liquid eutectic decomposition into α+γ, where γ is the Cu_3As intermetallic, 29.6% As (Subramanian and Laughlin, 1988). SEM-EDS analyses of the dagger AM/1 characterise this α+γ eutectic (Figure 4.4A) as being composed by α islands (with ~11% As)

surrounded by the γ intermetallic with ~28% As. The quantification of the α island is overestimated since it also include some of the surrounding arsenic-rich γ intermetallic. The α phase closer to this α+γ eutectic is richer in arsenic (with ~6% As) than the overall alloy (3.4%), evidencing the original segregation of arsenic in the α matrix during cooling. Copper and arsenic oxide inclusions display a very elongated morphology (Figure 4.4B), indicating the high deformation applied during the manufacture of this dagger.

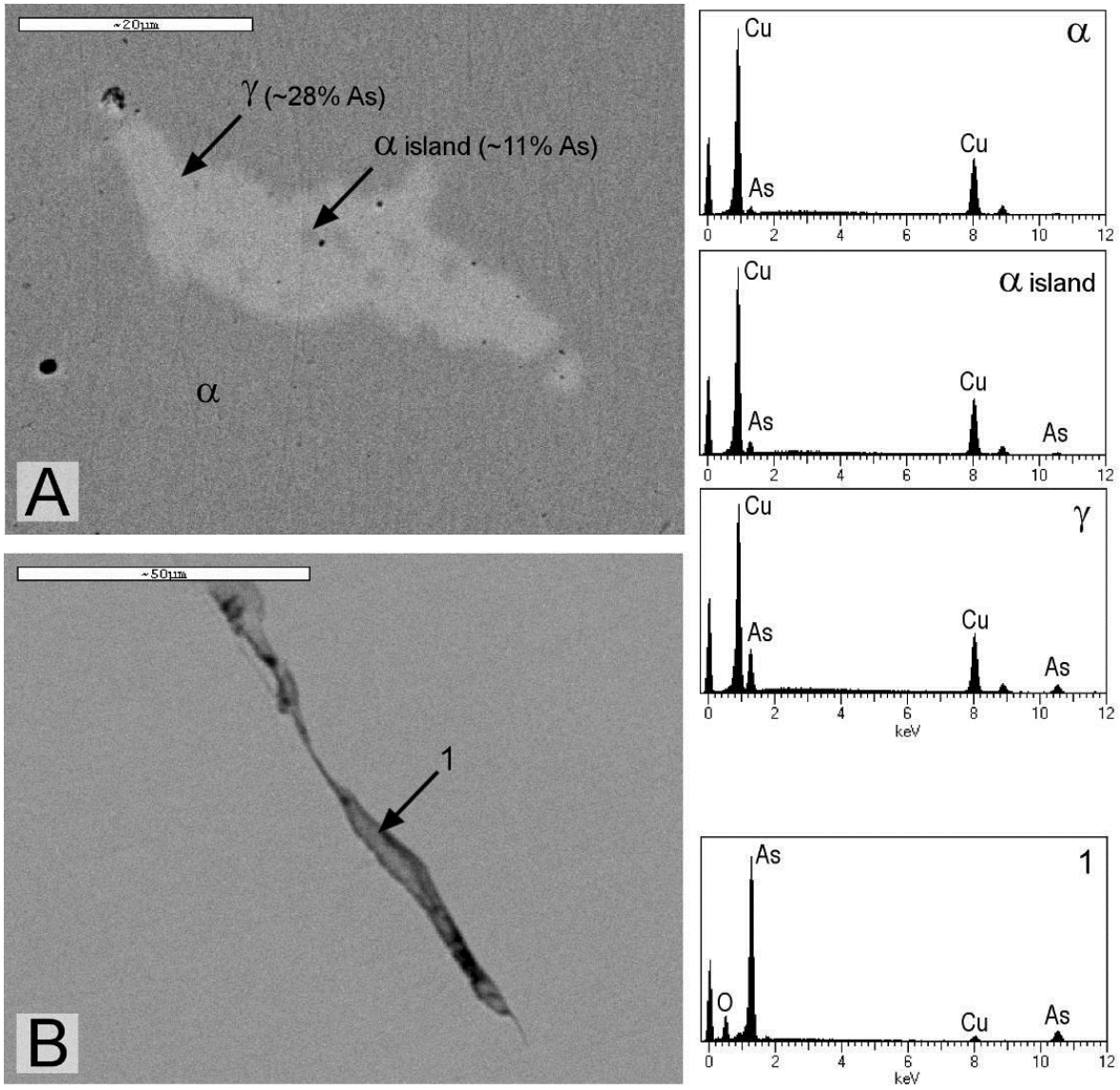

Figure 4.4. Microstructure of dagger AM/1 from Anta do Malhão (A and B: SEM-BSE images with EDS spectra of α phase; α island; γ intermetallic; 1: Cu-As-O inclusion).

4.1.3. Horta do Folgão[4]

During 2009, archaeological excavations conducted at Horta do Folgão (Serpa) discovered several negative structures mostly attributed to the BA (Ponte *et al.*, in press). The hypogeum 3 enclosed the skeletal remains of an adult together with a sword (F/1) with a riveting hilt containing, at least, 6 rivets, although 4 of them (F/2 to F/5) are now detached from the main body (Figure 4.5). Additionally, a small awl (F/6) was recovered from the hypogeum 2, containing also the skeletal remains of an adult female. The radiocarbon dating of the skeletal remains from hypogeum 3 allows including the burial into the 18th-16th centuries BC.

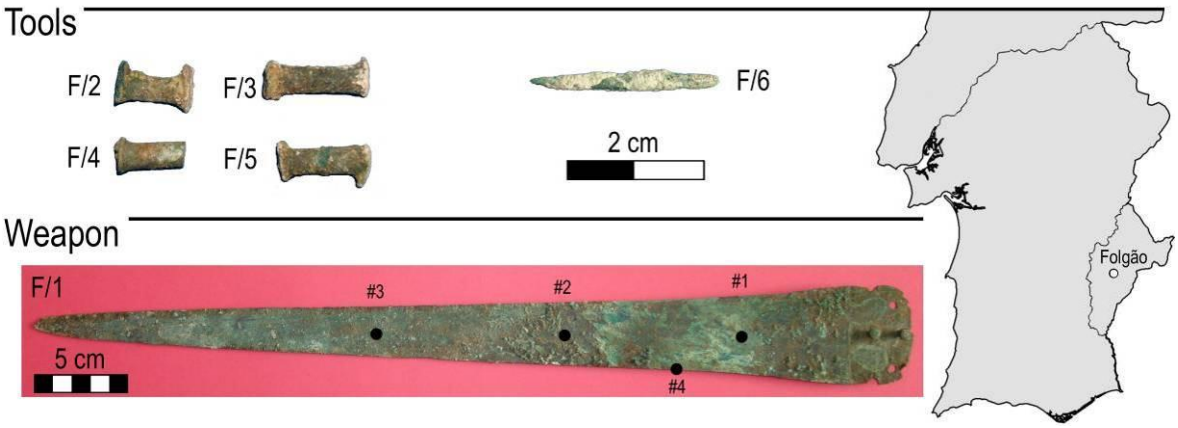

Figure 4.5. Copper-based artefacts belonging to the archaeological site of Horta do Folgão (sword with analysis spots).

Taking into account the size of the sword, it was considered important to study more than one area to ascertain about possible differences concerning elemental composition and manufacturing procedures. For that reason, several areas located along the blade were prepared for analysis – 3 areas are lined up in the main axis of the sword, while the last is situated at the edge of the blade (see Figure 4.5). The end section of the sword was intentionally discarded since the corrosion phenomena at this thinner region of the sword make the preparing operation more hazardous regarding the stability of the artefact. The awl and 1 rivet were also prepared for micro-EDXRF analysis, while the remaining rivets were analysed by EDXRF without any preparation procedure (Table 4.3).

The different areas of the sword present analogous elemental results indicating that the body of the blade is constituted by an homogeneous copper alloy with about 4.2% arsenic. The rivet exhibits a significant arsenic content (3.0%), while the awl presents a lower value (1.6%). Iron is the only noteworthy metallic impurity, being present at very low levels (<0.05%).

[4] A preliminary work with the content from this section was previously published (Ponte *et al.*, in press).

Table 4.3. Results of micro-EDXRF and EDXRF analyses of copper-based artefacts from Horta do Folgão (values in %;*: EDXRF analysis; nd: not detected; vest: <2; +: [2, 15]; ++: >15).

Type	Artefact	Reference	Context	Cu	As	Pb	Sn	Fe
Tool	Awl	F/6	BA	98.3	1.6	nd	nd	<0.05
Tool	Rivet*	F/2	18th-16th	++	+	nd	nd	vest
Tool	Rivet*	F/3	18th-16th	++	+	nd	nd	vest
Tool	Rivet	F/4	18th-16th	97.0	3.0	<0.10	nd	<0.05
Tool	Rivet*	F/5	18th-16th	++	+	nd	nd	vest
Weapon	Sword	F/1 *#1*	18th-16th	96.0	4.0	nd	nd	<0.05
		F/1 *#2*		96.0	4.0	nd	nd	<0.05
		F/1 *#3*		95.5	4.5	nd	nd	<0.05
		F/1 *#4*		95.5	4.5	nd	nd	<0.05
		F/1 *average*		95.8	4.2	nd	nd	<0.05

The microstructural characterisation using OM and SEM-EDS establish the different phases present, along with the common inclusions and manufacturing characteristics of each studied artefact (Table 4.4).

Table 4.4. OM and SEM-EDS characterisation of copper-based artefacts from Horta do Folgão (*: % given by micro-EDXRF; s: segregation bands; t: annealing twins; sb: slip bands; d: heavily deformed inclusions; C: Casting; A: Annealing; F: Forging; FF: Final Forging; ↑: high amount; ↓: low amount).

Type	Artefact	Reference	As*	Phases	As (EDS)	Inclusions	Manufacturing characteristics		
Tool	Awl	F/6	1.6	α As-rich↓	<0.10; 5.7 18.6	Cu-As-O	equiaxial	s↑, t, sb	C+(F+A)+FF
Tool	Rivet	F/4	3.0	α	2.3; 3.6	Cu-As-O	equiaxial	s, t, d	C+(F+A)
Weapon	Sword	F/1	4.2	α As-rich	- -	Cu-As-O	equiaxial	s, t, sb	C+(F+A)+FF

At the awl, segregation bands evidence an heavily cored microstructure where the regions richer in arsenic (brighter areas) correspond to regions that were the last to solidify in the original dendritic microstructure (Figure 4.6A). SEM-EDS analyses were able to quantify the segregation of the α phase, i.e. arsenic contents varying from <0.10% to ~6%. Additionally, a second phase rich in arsenic was also identified, but the arsenic content determined (~19%) should be underestimated since it might include the surrounding α phase poorer in As. Such a heavy segregation in an alloy with an overall arsenic content (1.6% As) well below its solubility limit (~7-8% As, in equilibrium) evidences a fast cooling rate after pouring the alloy in the mould. This fast cooling rate is according with the very small size of the artefact, but suggests that there was not any intent to control its cooling. Manufacturing characteristics include also deformed equiaxial grains with annealing twins and slip bands evidencing mechanical and thermal operations.

Evidently, annealing was not sufficient to homogenize the microstructure of this awl. According to some authors (Northover, 1989), the annealing of arsenical coppers during ancient times were conducted with temperatures of about 300-400ºC. This range of temperatures is noticeably lower than the temperature necessary to homogenize this type of alloys in a reasonable time, i.e. ~600-700ºC. Additionally, as the segregation intensity is the determinant factor regarding the homogenisation of arsenical coppers (Budd, 1991), this heavily segregated microstructure will require an even higher temperature to become fully homogenized.

SEM-EDS analyses identify the common inclusions of copper and arsenic oxides (Figure 4.6D). Experimental works showed that during the melting operation arsenic will effectively detain oxygen (Northover, 1989), thus giving especially significance to the use of a reducing atmosphere during the melting of this type of alloys. The presence of arsenic prevents the significant formation of copper oxides, but arsenic retained in these oxidised inclusions will not contribute to the improving of the mechanical properties of the alloy.

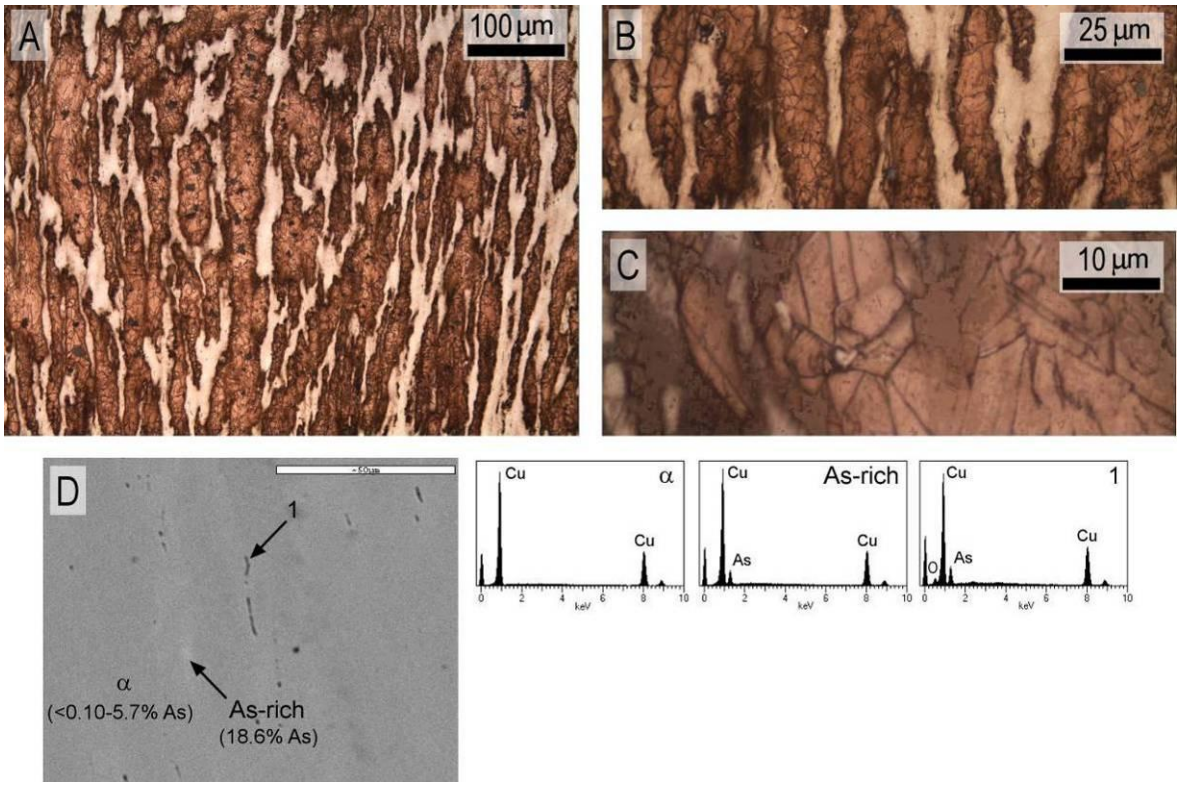

Figure 4.6. Microstructure of the copper-based awl F/6 from Horta do Folgão (A to C: OM-BF, etched; D: SEM-BSE image with EDS spectra of α phase; As-rich phase; 1: Cu-As-O inclusion).

The sword presents a deformed equiaxial microstructure with annealing twins and slip bands (Figure 4.7). The microstructural characteristics of the different areas along the blade point to a general operational sequence comprising forging and annealing cycles, plus a final forging

operation. However, the different areas observed also revealed certain dissimilar microstructural features. The edge of the blade (area #4) shows a much smaller grain size than the central section (areas #1 and #3), establishing the higher deformation applied, definitely to obtain an edge with an increased hardness. Additionally, the central section closer to the tip of the blade (area #3) exhibits more slip bands than the section closer to the handle (area #1) suggesting a higher final deformation in a longitudinal direction of the blade. Similarly to the awl, the microstructure of the sword includes a second phase rich in arsenic (bluish areas of OM images from Figure 4.7).

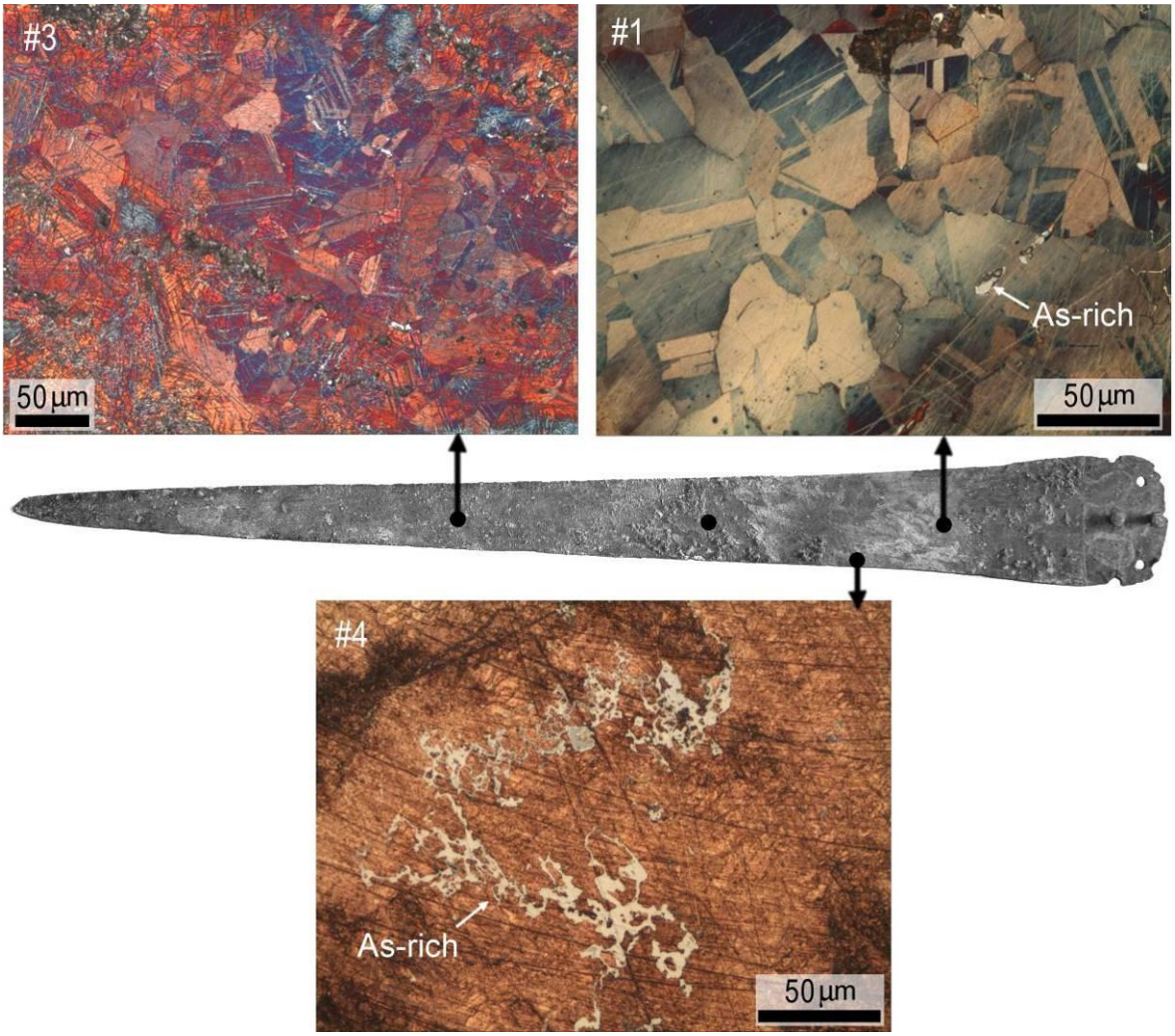

Figure 4.7. Microstructure of the copper-based sword F/1 from Horta do Folgão (areas #1, #3 and #4; OM-BF, etched).

The rivet presents long segregation bands and heavily elongated inclusions (Figure 4.8) evidencing the high deformation applied during its manufacture. Despite the heavy contrast from etching, SEM-EDS analyses establish that arsenic variations in the α phase are minor (~3 to 5%), while the As-rich phase seems to be absent. This microstructure is not as heavily segregated as the one from the awl. It is also composed by equiaxial grains from recrystallization annealing, which was probably used to soften the material in order to allow further deformation. At the end, this will

result in a tougher material that is required for riveting the hilt of the sword. The high deformation induced by the riveting process is clearly visible in the microstructure of its head section (Figure 4.8A – top left area).

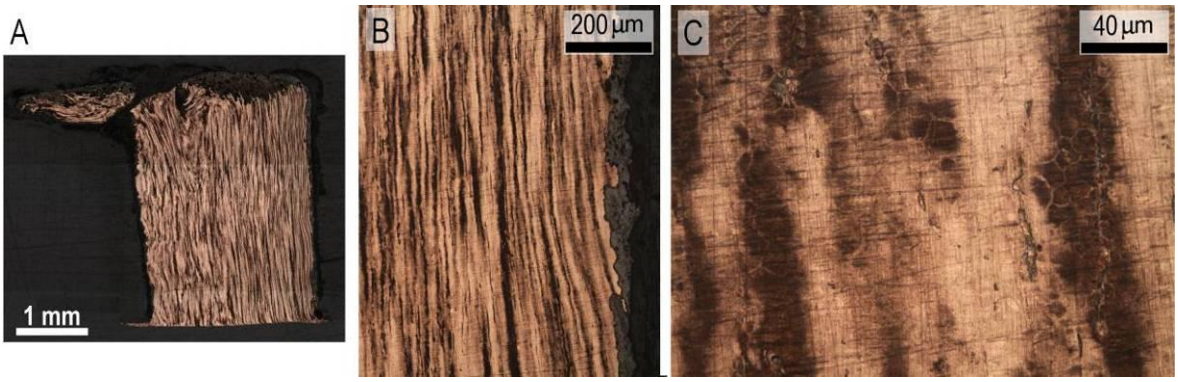

Figure 4.8. Microstructure of the copper-based rivet F/4 from Horta do Folgão (all OM-BF, etched).

4.1.4. Monte da Cabida 3

During 2009, archaeological works at Monte da Cabida 3 (Évora) uncovered several female burials containing a small collection of copper-based artefacts (Soares *et al.*, 2009). The radiocarbon analyses were able to date this necropolis into the 15th-13th centuries BC. The copper-based collection from Monte da Cabida 3 is composed by 6 artefacts, namely 3 needles (MCAB/M1, MCAB/M1 and MCAB/M3) and 3 small fragments of unknown functionality (MCAB3/M8, MCAB3/M9 and MCAB3/L11, Figure 4.9).

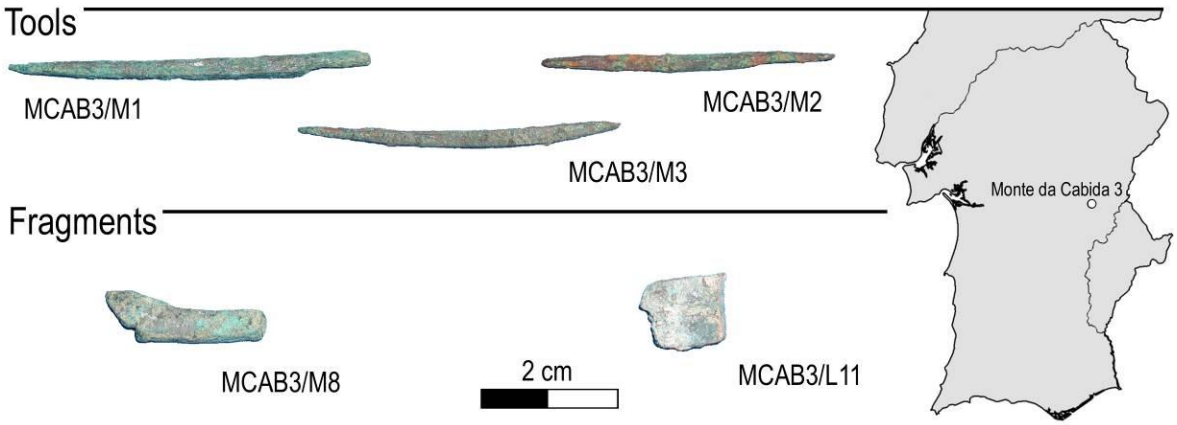

Figure 4.9. Copper-based artefacts belonging to the archaeological sites of Monte da Cabida 3.

Results of micro-EDXRF analyses indicate that all needles and the fragment MCAB3/M8 are composed by arsenical copper alloys (Table 4.5). The composition of the fragment MCAB3/L11 stands out of this set, being a pure copper with a considerably low arsenic content (<0.10%) and

somewhat higher iron content (0.33%) since all remaining artefacts present iron contents below the quantification limit (<0.05%).

Table 4.5. Results of micro-EDXRF analyses of copper-based artefacts from Monte da Cabida 3 (values in %; nd: not detected).

Type	Artefact	Reference	Context	Cu	As	Pb	Sn	Fe
Tool	Needle	MCAB3/M1	15th-13th	97.2	2.8	<0.10	nd	<0.05
Tool	Needle	MCAB3/M2	15th-13th	94.1	5.9	<0.10	nd	<0.05
Tool	Needle	MCAB3/M3	15th-13th	94.6	5.4	<0.10	nd	<0.05
Unknown	Fragment	MCAB3/M8	15th-13th	97.4	2.6	<0.10	nd	<0.05
Unknown	Fragment	MCAB3/M9	15th-13th	99.0	1.0	<0.10	nd	<0.05
Unknown	Fragment	MCAB3/L11	15th-13th	99.6	<0.10	<0.10	nd	0.33

The microstructural characterisation of these artefacts by OM and SEM-EDS is summarized in Table 4.6. Most microstructures exhibit deformed equiaxial grains with annealing twins and different densities of slip bands, except for the fragment MCAB3/M9 that appears to be hammered after casting. The inclusions more common are copper and arsenic oxides (e.g. Figure 4.10E3), while the fragment MCAB3/L11 presents a low amount of Cu-S inclusions.

Table 4.6. OM and SEM-EDS characterisation of copper-based artefacts from Monte da Cabida 3 and Salsa 3 (*: % given by micro-EDXRF; s: segregation bands; t: annealing twins; sb: slip bands; d: heavily deformed inclusions; C: Casting; A: Annealing; F: Forging; FF: Final Forging; ↑: high amount; ↓: low amount).

Type	Artefact	Reference	As*	Phases	As (EDS)	Inclusions	Features		Manufacture
Tool	Needle	MCAB3/M1	2.8	α As-rich	4.1 26.2	Cu-As-O	equiaxial	t, sb	C+(F+A)+FF
Tool	Needle	MCAB3/M2	5.9	α As-rich	5.4 27.1	Cu-As-O	equiaxial	t, sb	C+(F+A)+FF
Tool	Needle	MCAB3/M3	5.4	α As-rich	- -	Cu-As-O	equiaxial	t, sb	C+(F+A)+FF
Unknown	Fragment	MCAB3/M8	2.6	α	-	Cu-As-O	equiaxial	s, t, sb, d	C+(F+A)+FF
Unknown	Fragment	MCAB3/M9	1.0	α	-	Cu-As-O	equiaxial	s	C+F
Unknown	Fragment	MCAB3/L11	<0.10	α	-	Cu-S↓	equiaxial	t	C+(F+A)

The needles from Monte da Cabida 3 present very similar microstructures evidencing the use of forging and annealing cycles, plus a final forging operation (Figure 4.10). Annealing conditions were enough to recrystallize and partly homogenize the as-cast coring since segregation bands are absent. The As-rich phase is still present, mostly in the intergranular regions of the annealed grains of these needles.

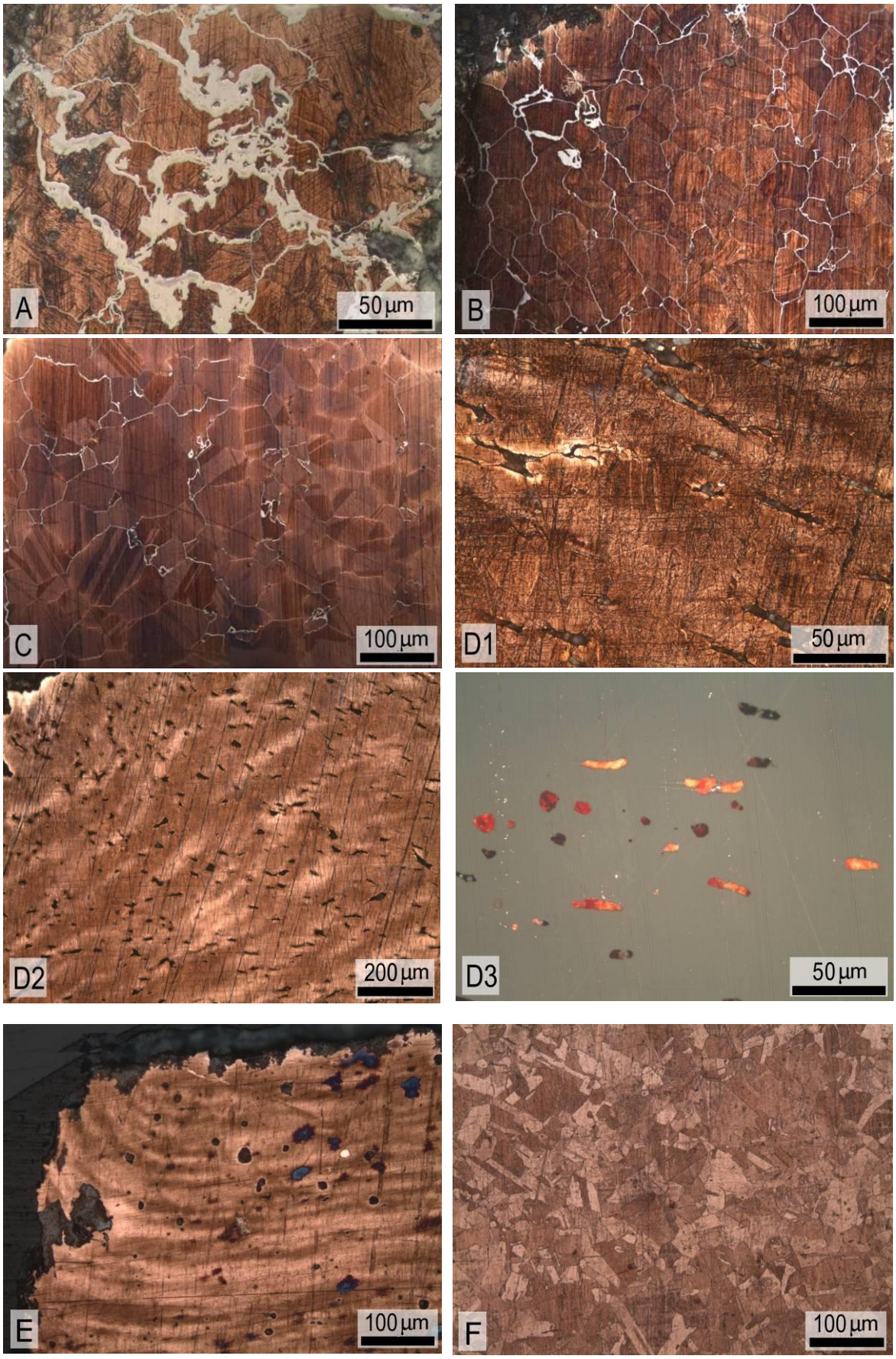

Figure 4.10. Microstructures of copper-based artefacts from Monte da Cabida 3 (A: needle MCAB3/M1; B: needle MCAB3/M2; C: needle MCAB3/M3; D1 to D3: fragment MCAB3/M8; E: fragment MCAB3/M9; F: fragment MCAB3/L11; all OM-BF, etched, excluding E2: OM-Pol, non-etched).

Contrary, the As-rich phase is absent at the fragment MCAB3/M8 despite the similar arsenic content and operational sequence. This might be related with a slower cooling rate during solidification of the fragment MCAB3/M8 that minimized the inverse segregation of arsenic. In general, a higher efficiency of forging and annealing cycles will also assist the alloy homogenisation.

Segregation bands are quite evident at the fragments MCAB3/M8 and MCAB3/M9 (Figure 4.10D2 and E) evidencing the initial forging of the as-cast microstructure. In the first case, annealing was probably made at a low temperature that was not sufficient to homogenise as-cast segregation despite the relatively low arsenic content, whereas in the second fragment no evidences of annealing were found. By the contrary, the fragment MCAB3/L11 exhibits very well recrystallized grains with annealing twins.

Additional SEM-EDS analyses were made on artefacts whose microstructure contains the As-rich phase in order to better characterise it. This As-rich phase seems to form a homogeneous layer close to the surface of the artefact, while becoming only present in intergranular regions at deeper regions (see Figure 4.11A: from bottom left to top right of SEM-BSE image we are looking at progressively deeper regions).

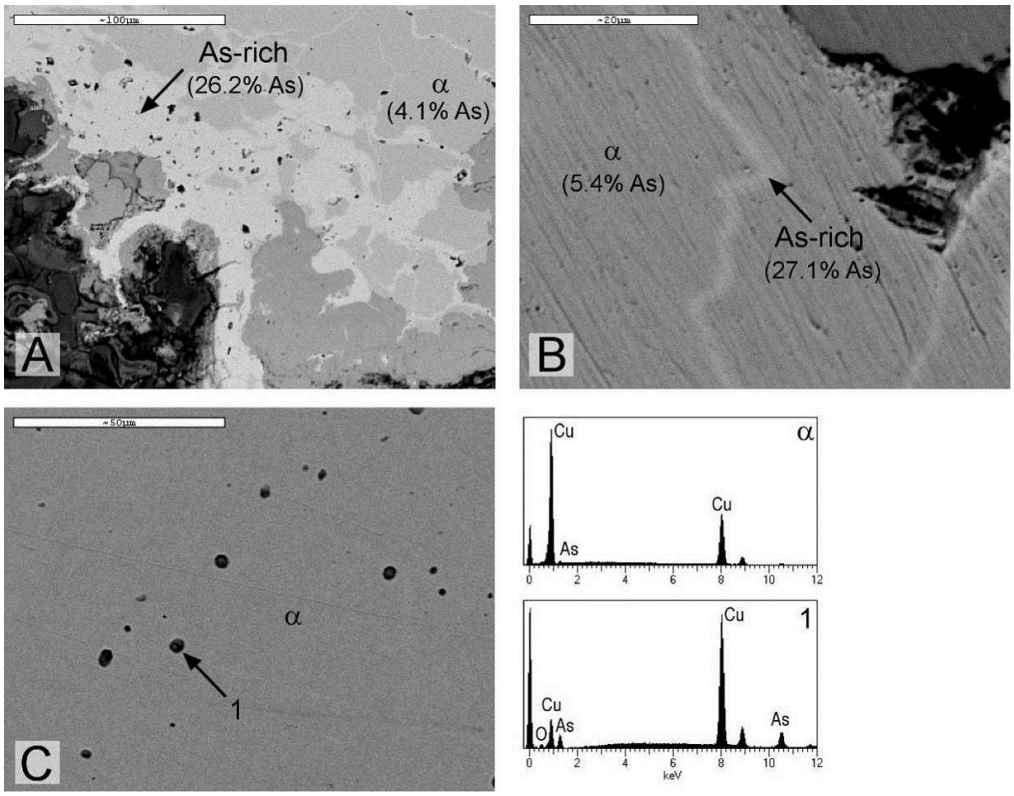

Figure 4.11. Microstructures of needles MCA3/M1 and MCAB3/M2 (A, B and C: SEM-BSE images with EDS spectra of α phase; 1: Cu-As-O inclusion with reduced intensity of low energy peaks due to topographic effects).

The enrichment in superficial regions of the artefact suggests inverse segregation during the solidification of the alloy. The As-rich phase presents a similar composition in both artefacts (~26% and ~27% As) that correspond almost to the composition of the γ intermetallic (29.6% As). However, the copper arsenic system can segregate the α+γ eutectic (e.g. see the microstructure of the dagger AM/1, Figure 4.3A), but not the pure γ intermetallic seen here surrounding the α grains. A previous work also identified this γ intermetallic at intergranular regions, suggesting that it can precipitate from solid solution over archaeological times, thus being the result of post depositional alteration (Budd and Ottaway, 1995). Therefore, the presence of this γ intermetallic along the grain boundaries results from long term precipitation in As richer regions of the α grains.

The relatively high iron content and uncommon Cu-S inclusions of the fragment MCAB3/L11 introduce some doubts regarding its actual integration in the MBA of the southern Portuguese region. It should be mentioned that the site of Monte da Cabida 3 also presents other contexts from the Roman period. However, the elemental characteristics should not be used to determine the chronological data of individual artefacts, so in the absence of more definitive answers, this artefact will still be included among the discussion of materials belonging to this period.

4.2. Late Bronze Age

4.2.1. Introduction

This period is especially characterised by a remarkable increase in the number of metal artefacts recovered from the archaeological record, being a *testimony to a flourishing metal industry* (Tylecote, 1992). It coincides with the full adoption of the bronze alloy that substitutes coppers and arsenical coppers. Typologies become more diversified, in particular with the production of more complex and finer artefacts. Their production is an outcome of the development of increasingly more versatile and advanced casting technologies, such as the use of a core for hollow casting, the utilization of multifaceted moulds and the heating of the mould prior to pouring.

Generally, the Western European region was divided into two different metallurgical traditions. LBA communities from regions around the Mediterranean Sea, such as Sardinia, Sicily, Italy and Greece (Giardino, 1995; Hook, 2007; Kayafa, 2003), as well as, most of the Iberian Peninsula (Rovira, 2004), were using a technology of binary bronzes. On the other hand, the majority of metallic artefacts from LBA Atlantic Europe, such as the British Isles, Western France and Northwestern Iberia, were composed by leaded bronzes, i.e. Pb>2% (Rovira and Gómez-Ramos, 1998). Lead enhances the fluidity of the molten bronze alloy and increases the temperature solidification range, thus facilitating the casting of large and/or complex artefacts. Additionally, the significant use of leaded bronzes can also be understood as an outcome from a shortage of tin, as at the LBA central Iberian Peninsula (Delibes de Castro *et al.*, 2001).

However, extensive sources of tin could be found during ancient times in the Northwestern region of the Iberian Peninsula (Penhallurick, 1986). Mediterranean regions imported tin from neighbouring areas. Low tin bronze alloys produced at the northeastern Italy during a local crisis in the trade of tin are a good indication of the importance of tin supply within the Mediterranean region (Giumlia-Mair, 2005a). The southern region of the Portuguese territory could obtain tin from the neighbouring area at north. The tin could be traded by copper obtained at the common copper sources of the southern region (Coffyn, 1985).

Similarly to arsenical copper, the bronze alloy exhibits a much higher strength and increased capability to strain hardening by cold working than copper (Figure 4.12). The strain hardening effect of additions of tin or arsenic to copper is rather similar, especially for worked alloys, allowing an increase up to 4-5 times in the hardness of the material (Figure 4.12). Despite their comparable mechanical properties, bronzes replaced arsenical coppers within a relatively short period (~300-400 years) throughout the entire European and Middle Eastern world (Tylecote, 1992). Several reasons have been pointed out to explain the abandonment of arsenical coppers,

namely the higher volatility of arsenic, the instability and toxicity of the As_2O_3 produced and the higher complexity of arsenic minerals over cassiterite (Mohen, 1990).

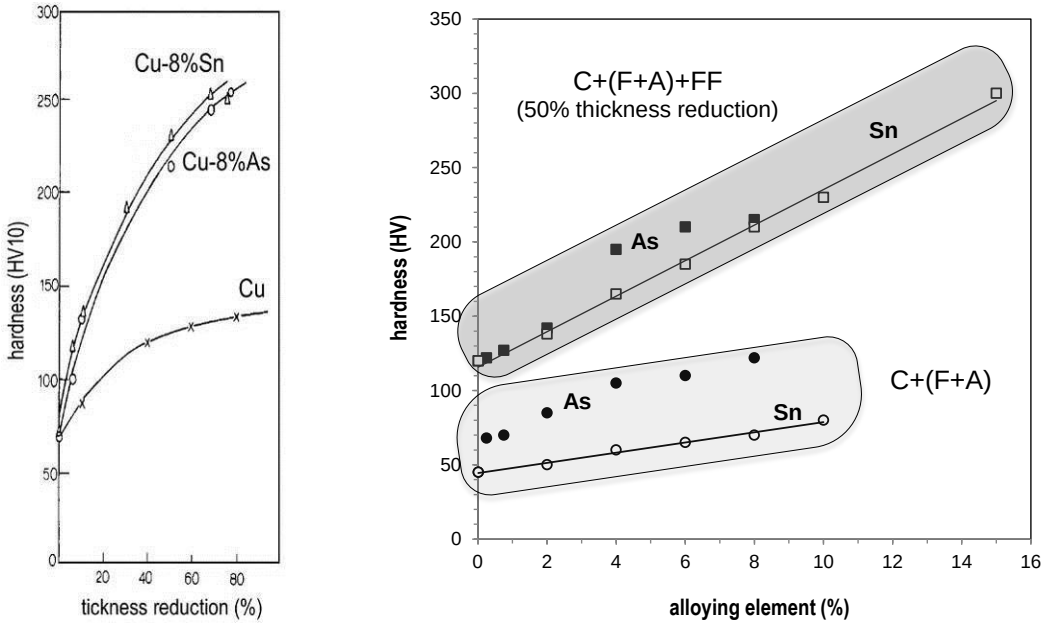

Figure 4.12. The hardness increase of copper, Cu-8%As and Cu-8%Sn alloys by cold hammering (adapted from Tylecote, 1996) and the effect of tin and arsenic additions on the hardness of worked and annealed (C+(F+A)) and work hardened (C+(F+A)+FF) copper-based alloys (adapted from Tylecote, 1986).

The temperature needed to melt a bronze is lower than to melt copper, while the high temperature solidification range of the bronze alloy results in a better castability, which improves significantly as tin content increases (Figure 4.13).

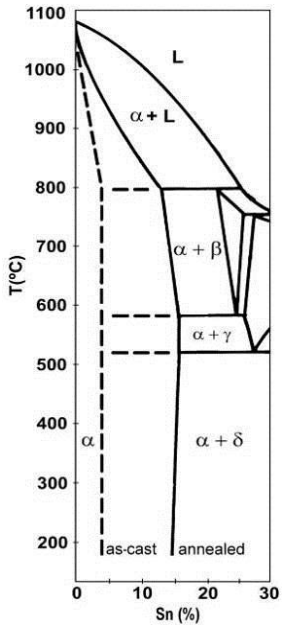

Figure 4.13. Copper-rich section of Cu-Sn phase diagram evidencing the shift of the α "solvus" line between a situation close to the equilibrium (annealed) and a fast solidification (as-cast), (adapted from Hanson and Pell-Walpole, 1951).

However, under the usual casting conditions, a second phase rich in tin (δ phase) starts to develop from very low tin contents (~4-5% Sn). A significant presence of this δ phase in the alloy makes the artefact brittle and much more difficult to hammer. The annealing operation softens the metal by dissolution of δ phase into α phase, but for tin contents higher than ~14% some δ phase is always present. Therefore, the control over the tin content of a bronze alloy is very important to obtain an artefact with high mechanical properties, which is especially significant, even in those ancient times, for some tools and weapons.

At the southern region of the Portuguese territory the LBA corresponds to the period between the end of the 2nd millennium BC and the beginning of the next, approximately 1200-800 BC. The elemental and microstructural characterisation of numerous LBA artefacts from this region will be presented in the following sections. The results typify the metallurgical technology present in this important region, located amongst the Atlantic and Mediterranean metallurgical traditions, thus allowing for the first time its integration into the metallurgical panorama of the LBA Iberian Peninsula.

4.2.2. Entre Águas 5

In addition to the significant collection of production remains that were presented in the previous section, the archaeological works at Entre Águas 5 (Serpa) also exposed several copper-based artefacts (Rebelo *et al.*, 2009).

The collection of 13 copper-based artefacts from Entre Águas 5 is mainly composed by ornaments, namely small beads (e.g. 1127a), a bracelet (314a) and two fibula fragments (411 and 1384a) (Figure 4.14). The tools are merely represented by a needle (491a) and a small awl (1554). Most of these artefacts came from the same archaeological context of the metallurgical production remains (hut X). The bracelet, fibula pin, needle and a fragment 314 belong to other archaeological contexts, although with a similar chronology (i.e. 10th-9th centuries BC).

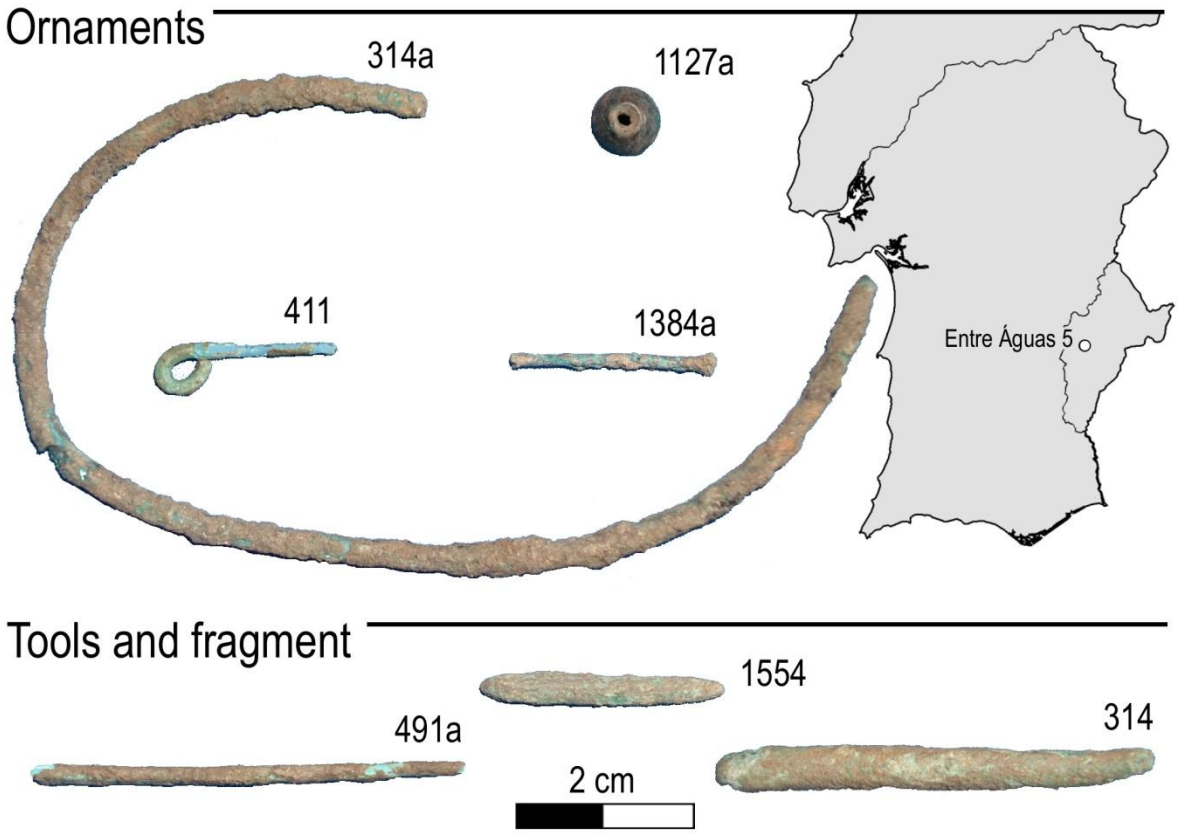

Figure 4.14. Copper-based artefacts belonging to the archaeological site of Entre Águas 5.

Selected artefacts from Entre Águas 5 were analysed by micro-EDXRF to determine the elemental composition (Table 4.7). Due to the advanced corrosion processes in the bead 1410, it was impossible to obtain the clean metallic alloy for micro-EDXRF analysis. Similarly, it was considered that the nail with a gold head 1495b should not be sampled nor cleaned for micro-EDXRF analysis due to its significant museological value, being analysed by EDXRF to identify the main alloy constituents.

Compositional results point out to binary bronze alloys, apart from the bead 1127a that is constituted by copper with very low tin content (1.6%). Lead is the main metallic impurity with contents up to 0.7%, while arsenic and iron present mostly values below the quantification limits (0.10% and 0.05%, respectively).

Table 4.7. Results of micro-EDXRF and EDXRF analyses of copper-based artefacts from Entre Águas 5 (values in %; *: EDXRF analysis; nd: not detected; vest: <2; +: [2, 50]; ++: >50).

Type	Artefact	Reference	Context	Cu	Sn	Pb	As	Fe
Ornament	Bead	1037	10th-9th	88.8	11.1	nd	<0.10	<0.05
Ornament	Bead	1127a	10th-9th	97.6	1.6	0.49	0.33	<0.05
Ornament	Bead*	1410	10th-9th	++	+	nd	nd	vest
Ornament	Bracelet	314a	10th-9th	94.6	5.0	0.27	<0.10	<0.05
Ornament	Fibula (axe?)	1384a	10th-9th	91.5	8.3	0.10	<0.10	<0.05
Ornament	Fibula (pin?)	411	10th-9th	89.6	10.3	nd	nd	<0.05
Tool	Needle	491a	10th-9th	93.1	5.9	0.69	0.20	<0.05
Tool	Awl	1554	10th-9th	88.3	11.6	nd	nd	<0.05
Tool	Nail*	1495b	10th-9th	++	+	nd	nd	vest
Unknown	Ring (open)	1388	10th-9th	84.3	15.5	0.20	<0.10	<0.05
Unknown	Ring (open)	1425	10th-9th	87.1	12.7	0.12	<0.10	<0.05
Unknown	Fragment	314	10th-9th	90.1	9.5	0.20	<0.10	<0.05
Unknown	Fragment	1250	10th-9th	92.2	7.7	nd	<0.10	<0.05

This small collection of bronzes presents an average tin content of 9.7 ± 3.2% (Figure 4.15). The distribution of tin contents among ornaments, tools and rings is by no means statistically significant, but it is useful to demonstrate that the higher tin artefacts are rings (1388 and 1425), while the only "unalloyed" copper is an ornament (1127a). Theoretically, rings and ornaments do not require a high mechanical strength, so the "abnormal" tin content of these artefacts might be related with their functionality. However, the reduced number of studied artefacts prevents any further considerations about the selection of alloys according to different artefact typologies.

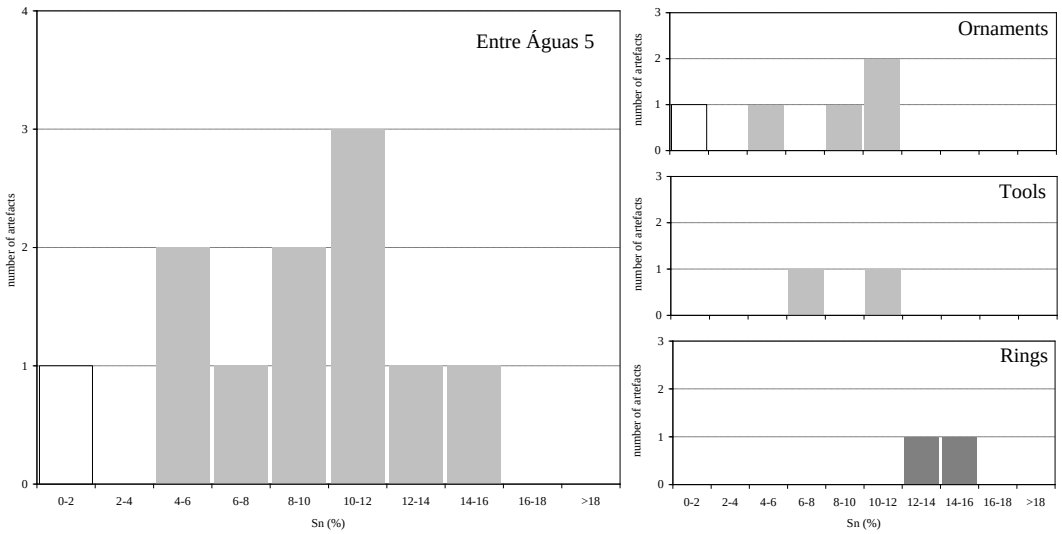

Figure 4.15. Distribution of tin contents in copper-based artefacts from Entre Águas 5 (white columns symbolize "unalloyed" copper artefacts, while darker columns symbolize artefacts with higher tin contents).

Most artefacts were further analysed by OM to identify its operational sequence, which is given by the type of microstructure, presence of annealing twins, inclusion morphologies and slip bands density (Table 4.8). All studied artefacts exhibit a deformed equiaxial microstructure with annealing twins, evidencing the use of forging and annealing operations. The considerable occurrence of Cu-S inclusions is another common feature to this collection. It must be noted that the classification of the amount of Cu-S inclusions is somewhat subjective because it derives from observation and comparison of OM images. However, it is rather significant that the artefacts from Entre Águas 5 present a considerable occurrence of these Cu-S inclusions since the analytical study of production remains from this site (previous chapter) established the co-smelting of copper oxide and carbonate ores with significant amounts of sulphides.

Table 4.8. OM characterisation of copper-based artefacts from Entre Águas 5 (*: % given by micro-EDXRF; t: annealing twins; sb: slip bands; d: heavily deformed inclusions; C: Casting; A: Annealing; F: Forging; FF: Final Forging; ↑: high amount; ↓: low amount).

Type	Artefact	Reference	Sn*	Phases	Inclusions	Features		Manufacture
Ornament	Bead	1037	11.1	α	Cu-S↑	equiaxial	t, sb, d	C+(F+A)+FF
Ornament	Bead	1127a	1.6	α	Cu-S↑	equiaxial	t, sb	C+(F+A)+FF↓
Ornament	Bracelet	314a	5.0	α	Cu-S↑	equiaxial	t, d	C+(F+A)
Ornament	Fibula (axe?)	1384a	8.3	α	Cu-S	equiaxial	t	C+(F+A)+FF
Ornament	Fibula (pin?)	411	10.3	α	Cu-S↑	equiaxial	t, sb	C+(F+A)+FF
Tool	Needle	491a	5.9	α	Cu-S↑	equiaxial	t, sb	C+(F+A)+FF↑
Tool	Awl	1554	11.6	α	Cu-S↑	equiaxial	t, sb, d	C+(F+A)+FF
Unknown	Ring (open)	1388	15.5	α, α+δ	Cu-S↑	equiaxial	t, sb	C+(F+A)+FF
Unknown	Ring (open)	1425	12.7	α	Cu-S↑	equiaxial	t, sb	C+(F+A)+FF
Unknown	Fragment	314	9.5	α	Cu-S↑	equiaxial	t, sb	C+(F+A)+FF
Unknown	Fragment	1250	7.7	α	Cu-S↑	equiaxial	t, sb	C+(F+A)+FF

Microstructural characterisation shows that the use of a final forging operation is equally used among ornaments, tools, rings and fragments. However, some microstructures display a higher density of characteristic slip bands (Figure 4.16) than others (Figure 4.17). This indicates a different amount of final deformation applied to some artefacts. The alloy with the higher tin content (ring 1388, 15.5%) corresponds to the only microstructure that is not completely homogenized, with a high amount of the α+δ eutectoid distributed along the ring microstructure (Figure 4.16C).

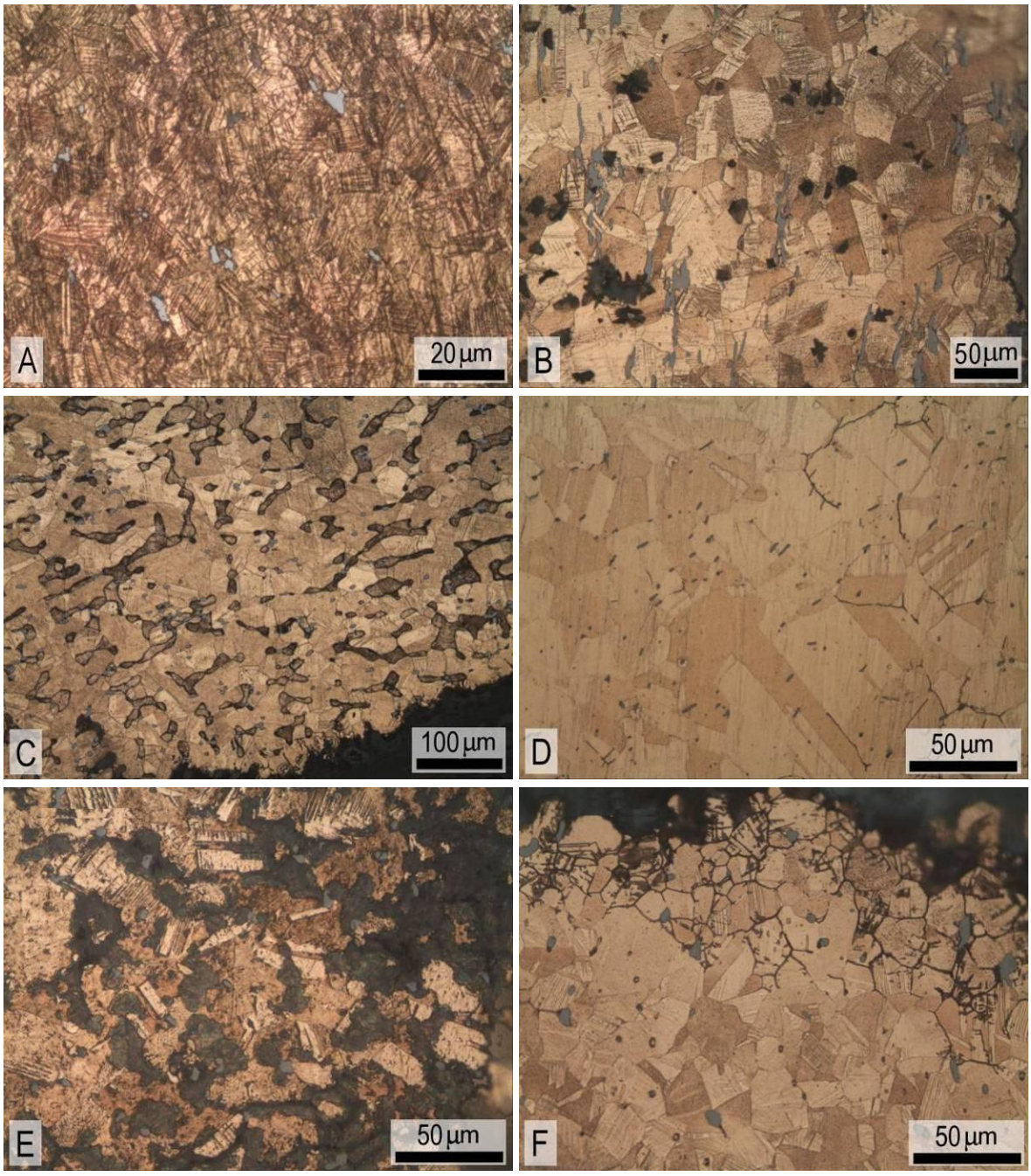

Figure 4.16. Microstructures of copper-based tools, rings and fragments from Entre Águas 5 (A: needle 491a; B: awl 1554; C: ring 1388; D: ring 1425; E: fragment 314; F: fragment 1250; all OM-BF, etched).

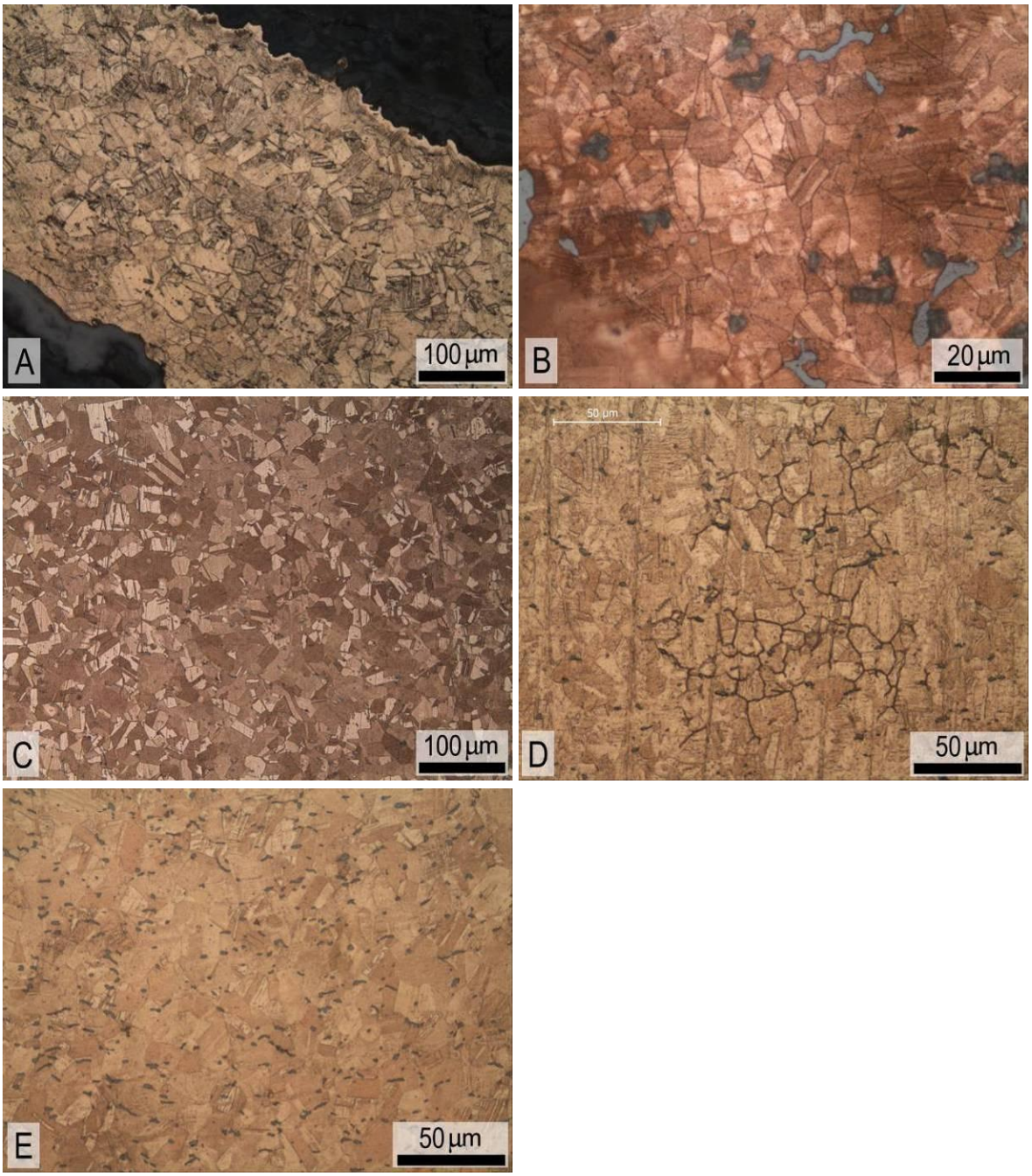

Figure 4.17. Microstructures of copper-based ornaments from Entre Águas 5 (A: bead 1037; B: bead 1127a; C: bracelet 314a; D: fibula axe(?) 1384a; E: fibula pin(?) 411; all OM-BF, etched).

SEM-EDS analysis of the ring 1388 shows the high amount of Cu-S inclusions, the α+δ eutectoid displaying an interdendritic morphology and more corroded in the regions closer to the surface (Figure 4.18). Semi-quantitative SEM-EDS point analysis indicate an α phase with 14.0% Sn, while the α+δ eutectoid analysed attained 22.5% Sn.

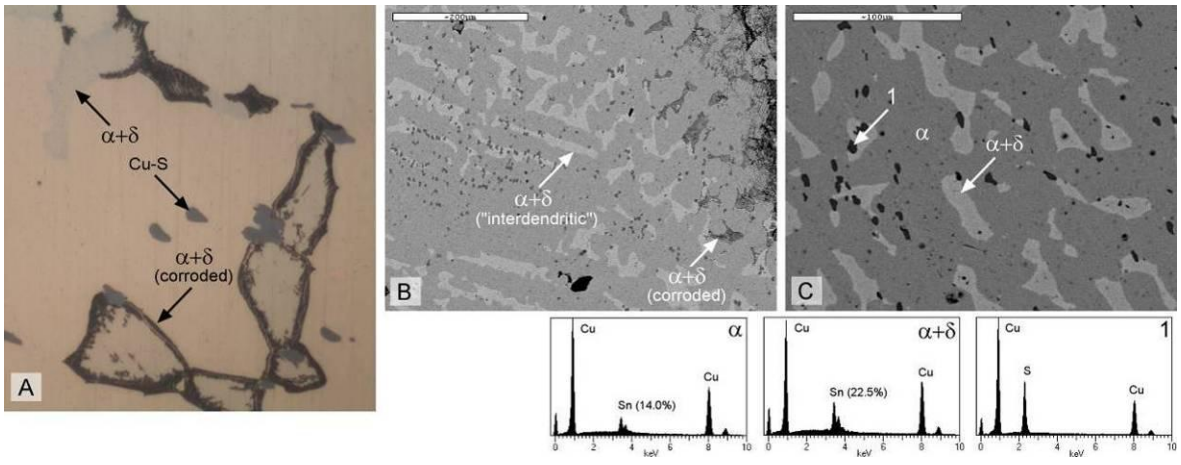

Figure 4.18. Microstructure of ring 1388 from Entre Águas 5 (A: OM-BF, non-etched; B and C: SEM-BSE images with EDS spectra of α phase; α+δ eutectoid; 1: Cu-S inclusion).

The Vickers testing of selected artefacts evidences that most artefacts present comparable hardness, except for the well recrystallized bracelet 314a that exhibits a much lower value, 79 HV0.2 (Table 4.9). It seems that the final forging procedure actually produces a harder material, but other factors like, tin content, recrystallized grain size and different phases also influence the hardness of the material. The high hardness of the ring 1388 (163 HV0.2) is a clear example of the effect of high tin contents, jointly by α phase saturation in tin and by precipitation of the harder δ phase. However, the high hardness of the needle 491a (154 HV0.2) evidences that even low tin content bronzes can be effectively strain hardened by final forging, i.e. it presents a very high amount of slip bands (Figure 4.16A). Regarding the differences among different typologies/functionalities of the artefacts, one must rely on a much higher number of samples to obtain reliable conclusions (a comparison involving data from all studied collections will be presented among the discussion).

Table 4.9. Vickers microhardness of copper-based artefacts from Entre Águas 5 (relevant elemental and microstructural data obtained by micro-EDXRF and OM analyses is also presented).

Type	Artefact	Reference	Sn (%)	Phases	Manufacture	HV0.2
Ornament	Bead	1037	11.1	α	C+(F+A)+FF	148
Ornament	Bracelet	314a	5.0	α	C+(F+A)	79
Ornament	Fibula (axe?)	1384a	8.3	α	C+(F+A)+FF	146
Ornament	Fibula (pin?)	411	10.3	α	C+(F+A)+FF	166
Tool	Needle	491a	5.9	α	C+(F+A)+FF↑	154
Unknown	Ring (open)	1388	15.5	α, α+δ	C+(F+A)+FF	163
Unknown	Ring (open)	1425	12.7	α	C+(F+A)+FF	126
Unknown	Fragment	1250	7.7	α	C+(F+A)+FF	139

4.2.3. Baleizão

A collection of metallic artefacts was accidentally discovered during 2004 at the neighbourhood of Baleizão (Beja). This metallic collection comprises some gold and copper-based materials, the latter presenting typologies that are familiar to the LBA period of the Portuguese territory (Vilaça and Lopes, 2005).

The collection of 20 copper-based artefacts from Baleizão includes a serpentine fibula (392/26) (Figure 4.19), which is a typology very common during the LBA (Arruda, 2008). Tools comprise 3 flat axes (392/7, 392/8 and 392/9) plus a remarkable set of 7 balance weights (392/19 to 392/25) (Figure 4.19). These balance weights include bitroncoconical – some with a piercing to insert the *pondarium*, in addition to discoidal and octahedral shapes. Bitroncoconical and discoidal typologies are usually found in LBA contexts, while the octahedral shape seems to be very rare, with only another known exemplar at the Portuguese territory – the balance weigh from the LBA site of Monte do Trigo, Castelo Branco (Vilaça, 2003).

Additionally, the collection from Baleizão contains 8 rings (e.g. 392/10, 392/11 and 392/129) (Figure 4.19) most of them closed, while others are open. It is impossible to ascertain if the latter were manufactured as "open" rings or resulted from a breakage. Contrary, it is certain that closed rings were cast in circular moulds since it is generally accepted that bronze sections cannot be joined through heating and forging (Sarabia-Herrero *et al.*, 1996).

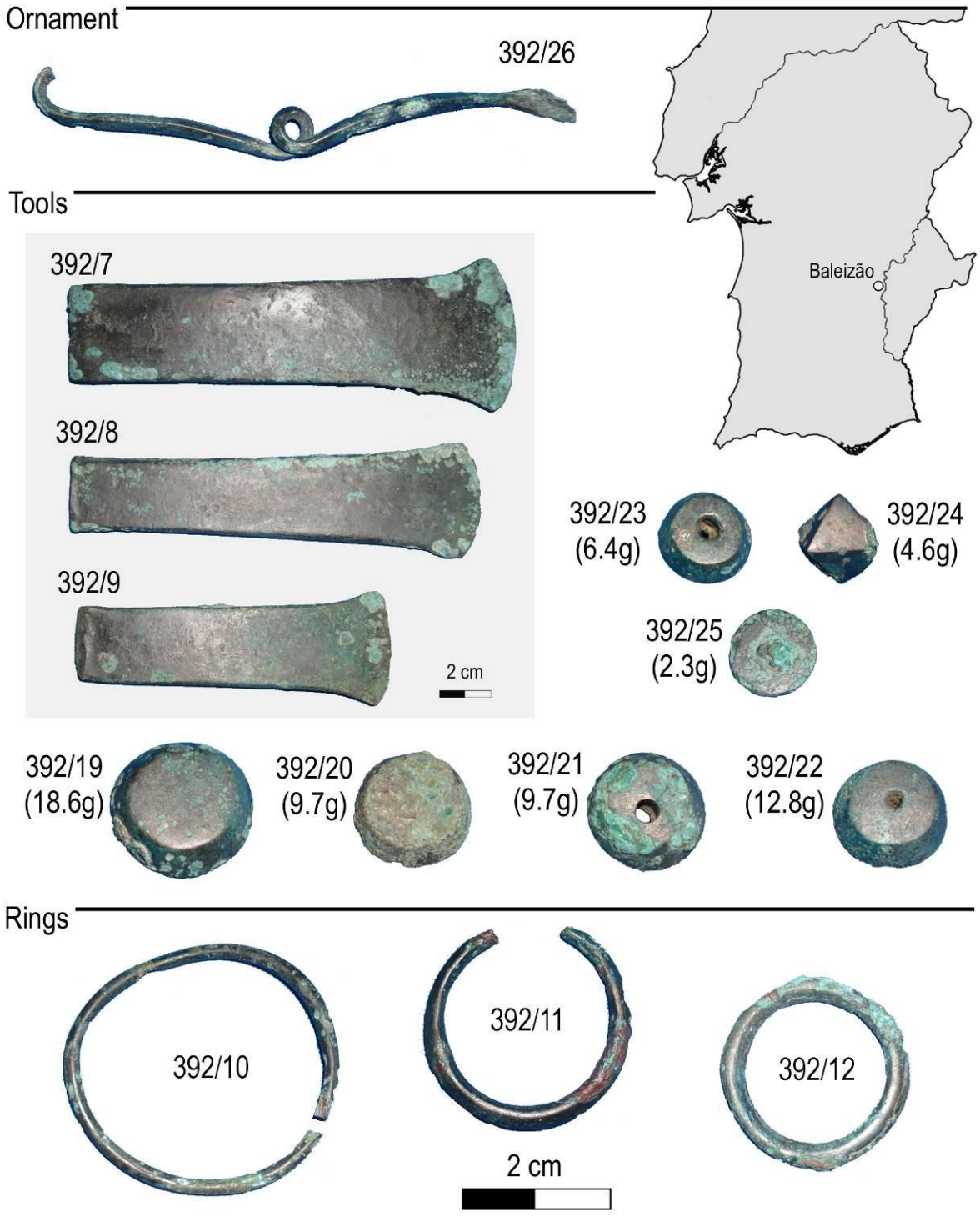

Figure 4.19. Copper-based artefacts belonging to the archaeological site of Baleizão.

Copper-based artefacts from Baleizão were analysed by micro-EDXRF to determine their elemental composition (Table 4.10). Only one balance weight was cleaned for the micro-EDXRF analyses due to the relevant archaeological and museological significance of these artefacts. The remaining were analysed by EDXRF to identify the main alloy constituents. EDXRF analyses also established that one of the rings (392/14) is composed by a copper-zinc alloy. Although a few pre-

Roman brasses are known at the Iberian Peninsula, these only seem to occur since the 6th century BC among Orientalising contexts (Montero-Ruíz and Perea, 2007). As a consequence, the ring 392/14 was not included in this study since brasses are out of the scope of this work.

Table 4.10. Results of micro-EDXRF and EDXRF analyses of copper-based artefacts from Baleizão (values in %; *: EDXRF analysis; nd: not detected; vest: <2; +: [2, 50]; ++: >50).

Type	Artefact	Reference	Context	Cu	Sn	Pb	As	Fe
Ornament	Fibula (Serpentine)	392/26	LBA	90.7	9.1	nd	0.12	<0.05
Tool	Axe (flat)	392/7	LBA	87.3	12.5	nd	0.14	<0.05
Tool	Axe (flat)	392/8	LBA	88.8	11.0	nd	0.17	<0.05
Tool	Axe (flat)	392/9	LBA	88.6	11.0	0.20	0.13	<0.05
Tool	Weight (bitronc.)*	392/19	LBA	++	+	vest	vest	vest
Tool	Weight (bitronc.)*	392/20	LBA	++	+	vest	nd	vest
Tool	Weight (bitronc.)*	392/21	LBA	++	+	vest	vest	vest
Tool	Weight (bitronc.)*	392/22	LBA	++	+	vest	vest	vest
Tool	Weight (bitronc.)*	392/23	LBA	++	+	vest	vest	vest
Tool	Weight (octahedral)*	392/24	LBA	++	+	vest	vest	vest
Tool	Weight (discoidal)	392/25	LBA	91.4	8.4	nd	0.19	<0.05
Unknown	Ring (open)	392/10	LBA	89.9	10.0	nd	<0.10	<0.05
Unknown	Ring (open)	392/11	LBA	89.8	10.1	nd	0.10	<0.05
Unknown	Ring (closed)	392/12	LBA	91.7	8.1	0.17	nd	<0.05
Unknown	Ring (closed)	392/13	LBA	92.1	7.9	nd	nd	<0.05
Unknown	Ring (closed)	392/15	LBA	89.7	10.1	nd	0.15	<0.05
Unknown	Ring (open)	392/16	LBA	89.2	10.6	nd	0.12	<0.05
Unknown	Ring (closed)	392/17	LBA	88.7	11.1	0.19	<0.10	<0.05
Unknown	Ring (closed)	392/18	LBA	86.6	12.9	0.23	0.18	<0.05

Artefacts analysed by micro-EDXRF are composed by binary bronze alloys with low metallic impurity contents, namely lead (up to 0.23%) and arsenic (up to 0.19%), while Fe always present contents below the quantification limit (0.05%). Tin contents present a narrow normal distribution around an average value of 10.2 ± 1.6% (Figure 4.20). Once more, the distribution of tin contents among ornaments, tools and rings is by no means statistically significant, but it is useful to exemplify that in this collection, tools and rings display an analogous distribution of tin contents.

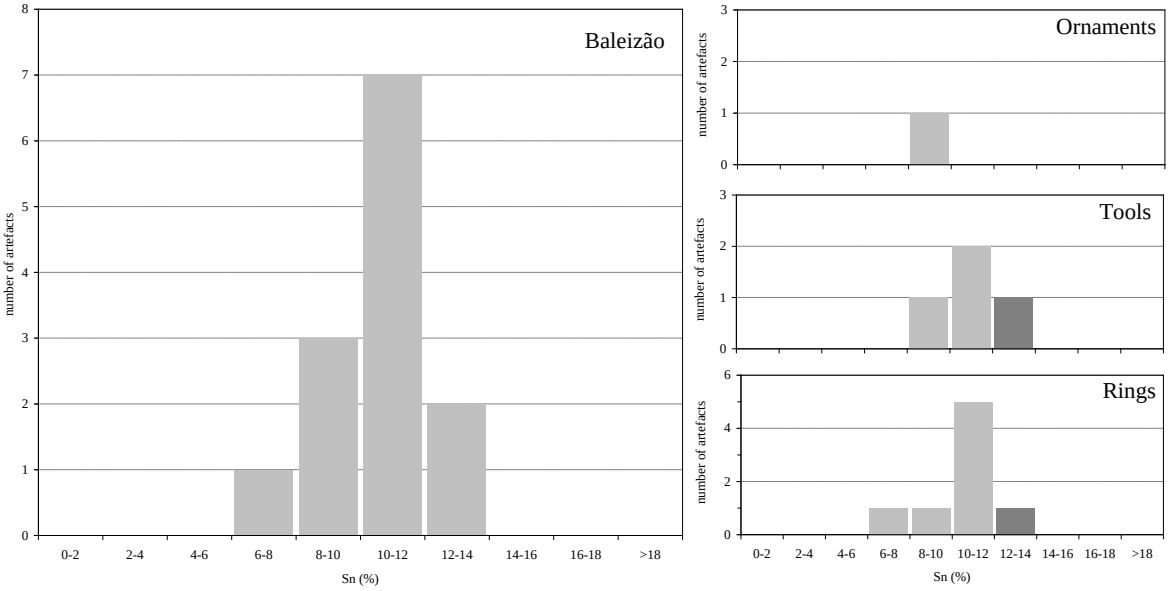

Figure 4.20. Distribution of tin contents in copper-based artefacts from Baleizão (darker columns symbolize artefacts with higher tin contents).

The type of microstructure, phases present, annealing twins and slip bands density, plus common inclusions were determined by OM observations (Table 4.11). The occurrence of Cu-S inclusions is a common feature of these microstructures, whereas the α+δ eutectoid is scarcer, being only present in a few (axe 392/7, weight 392/25, ring 392/11 and ring 392/18). The presence of α+δ eutectoid in annealed alloys with low tin contents (i.e. 392/11: 10.1%) evidences the low efficiency of the forging and annealing cycles in homogenising the alloy.

Table 4.11. OM characterisation of copper-based artefacts from Baleizão (*: % given by micro-EDXRF; t: annealing twins; sb: slip bands; d: heavily deformed inclusions; C: Casting; A: Annealing; F: Forging; FF: Final Forging; ↑: high amount; ↓: low amount).

Type	Artefact	Reference	Sn*	Phases	Inclusions	Features		Manufacture
Ornament	Fibula (Serpentine)	392/26	9.1	α	Cu-S↓	equiaxial	t, sb	C+(F+A)+FF
Tool	Axe (flat)	392/7	12.5	α, α+δ	Cu-S	equiaxial	t	C+(F+A)
Tool	Axe (flat)	392/8	11.0	α	Cu-S	equiaxial	t	C+(F+A)
Tool	Axe (flat)	392/9	11.0	α	Cu-S	equiaxial	t	C+(F+A)
Tool	Weight (discoidal)	392/25	8.4	α, α+δ	Cu-S	dendritic		C
Unknown	Ring (open)	392/10	10.0	α	Cu-S	equiaxial	t, sb	C+(F+A)+FF
Unknown	Ring (open)	392/11	10.1	α, α+δ	Cu-S↓	equiaxial	t, sb	C+(F+A)+FF
Unknown	Ring (closed)	392/12	8.1	α	Cu-S↑	dendritic		C
Unknown	Ring (closed)	392/13	7.9	α	Cu-S	equiaxial	t, sb	C+(F+A)+FF
Unknown	Ring (closed)	392/15	10.1	α	Cu-S	equiaxial	t, sb	C+(F+A)+FF
Unknown	Ring (open)	392/16	10.6	α	Cu-S	equiaxial	t, sb	C+(F+A)+FF
Unknown	Ring (closed)	392/17	11.1	α	Cu-S↑	equiaxial	t, sb	C+(F+A)+FF
Unknown	Ring (closed)	392/18	12.9	α, α+δ	Cu-S	equiaxial	t	C+(F+A)

Some of the artefacts from Baleizão exhibit the characteristic features of as-cast microstructures, namely dendrites with coring (Figure 4.21). However, despite the similar low tin contents of both alloys, the ring 392/12 presents a monophasic microstructure (Figure 4.21B), whereas the weight 392/25 display the α+δ eutectoid (Figure 4.21A), probably due to a faster cooling rate.

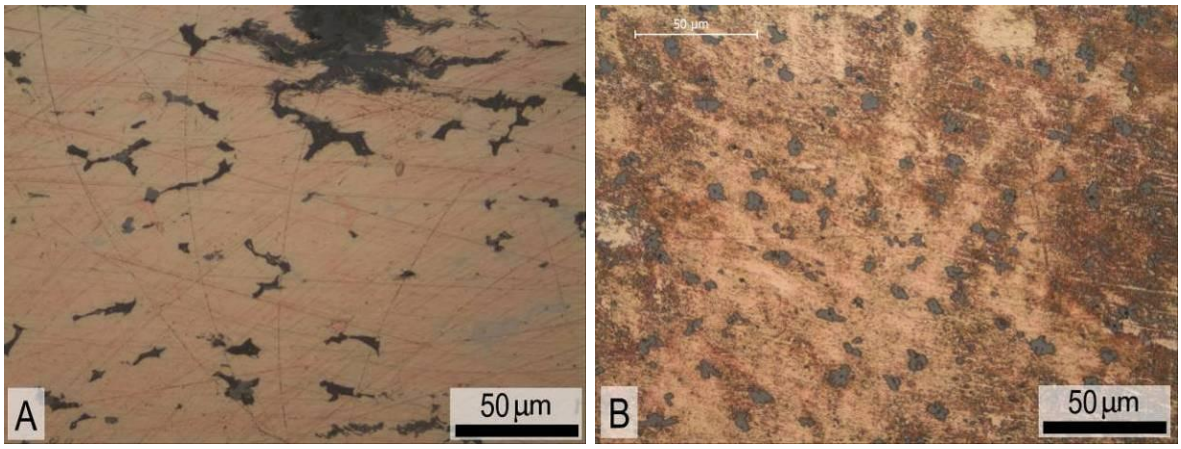

Figure 4.21. Microstructures of copper-based artefacts from Baleizão, showing characteristic as-cast features (A: weight 392/25; B: ring 392/12; OM-BF, non-etched and OM-BF, etched, respectively).

The axes 392/7, 392/8 and 392/9 present deformed equiaxial grains with annealing twins (Figure 4.22A, B and C, respectively), evidencing the use of forging and annealing operations. The density of the annealing twins is much lower in the axe 392/8, which is certainly related with the position of sampling. All axes were sampled at the blunt end since the blades were highly corroded. However, the axe 392/8 was sampled in a longitudinal area, which is obviously less deformed than the transversal areas sampled in the other two axes. The ring 392/18 display a comparable operational sequence (i.e. forging and annealing operations), but the high amount of the α+δ eutectoid present (Figure 4.22D) indicates that the annealing conditions were not sufficient to completely homogenize the alloy.

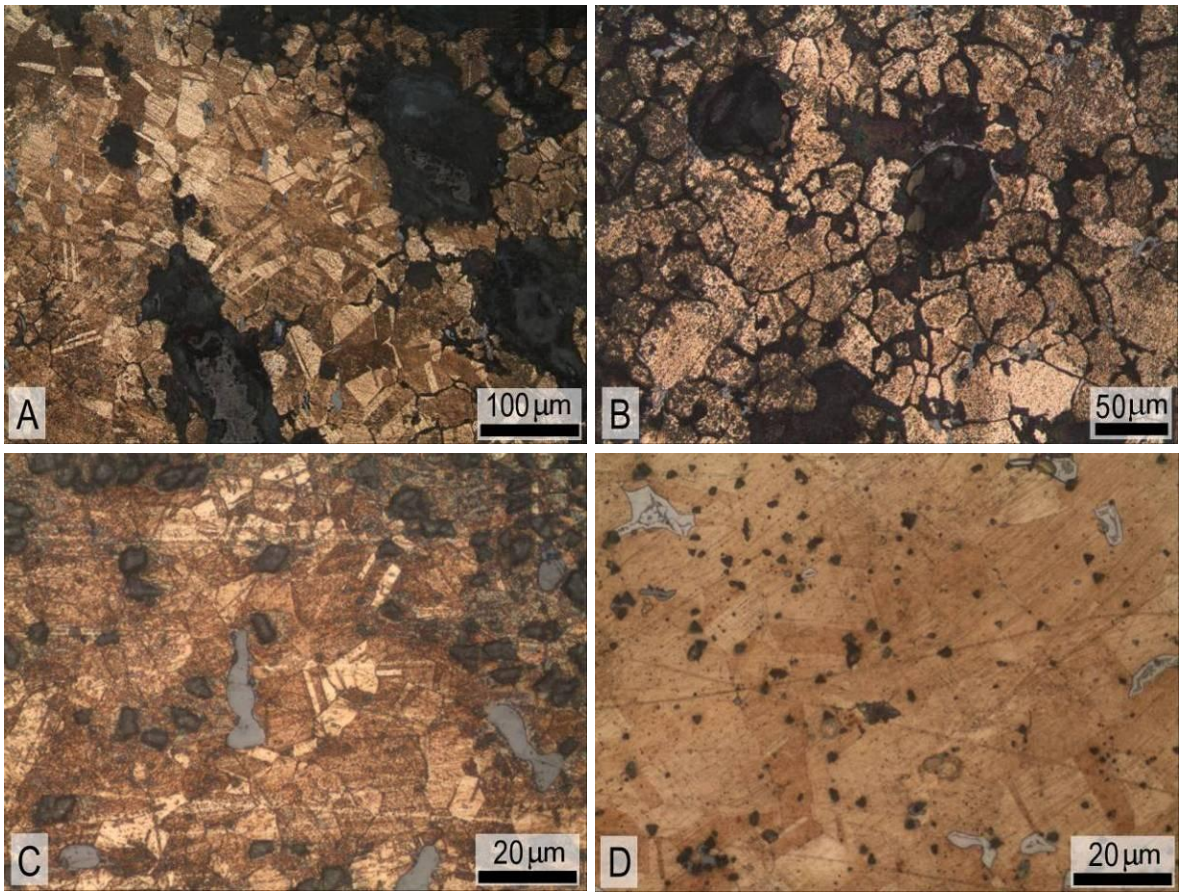

Figure 4.22. Microstructures of copper-based artefacts from Baleizão with forging and annealing work (A: axe 392/7; B: axe 392/8; C: axe 392/9; D: ring 392/18; all OM-BF, etched).

The fibula and most of the rings present deformed equiaxial microstructures with annealing twins and slip bands (Figure 4.23). The variable efficiency of the forging plus annealing cycles is very obvious from the different grain sizes present, ranging from the better (ring 392/16, Figure 4.23E) to the poorly worked (ring 392/10, Figure 4.23B). The presence of slip bands indicates that the operational sequence ended with a final forging operation, whose intensity can generally be related with the density of the slip bands.

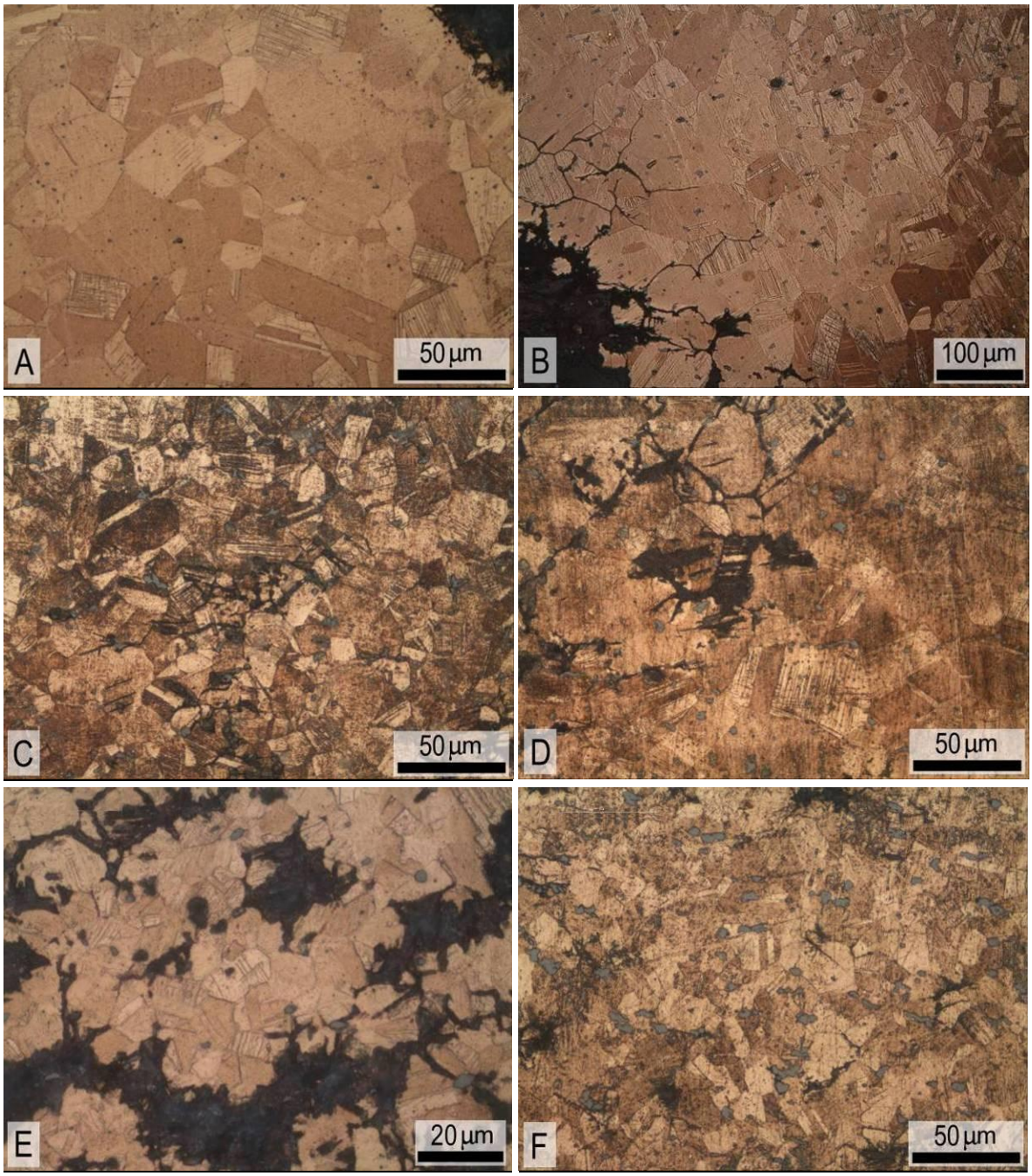

Figure 4.23. Microstructures of copper-based artefacts from Baleizão with forging, annealing and final forging work (A: fibula 392/26; B: ring 392/10; C: ring 392/13; D: ring 392/15; E: ring 392/16; F: ring 392/17; all OM-BF, etched).

The microstructure of the ring 392/11 was further investigated by SEM-EDS. Previous OM observations had already established that the annealing operation was not sufficient to completely homogenize the alloy since the $\alpha+\delta$ is still present. In addition, SEM-BSE images and EDS analyses evidence some coring (Figure 4.24B – spot analyses (α_1 and α_2) show different tin contents), which indicates non-equilibrium solidification conditions, typical of as-cast alloys. Therefore, this microstructure is the result of an initial high heterogeneity from "as-cast" segregation, followed by poor annealing conditions (i.e. not enough temperature or time of

operation). Some minute Pb rich inclusions were also identified (Cu-Pb eutectic formed at 326 ºC with ~99.9% Pb content; the Cu and Sn peaks in EDS spectrum of the Pb inclusion are mainly from the surrounding Cu-Sn matrix).

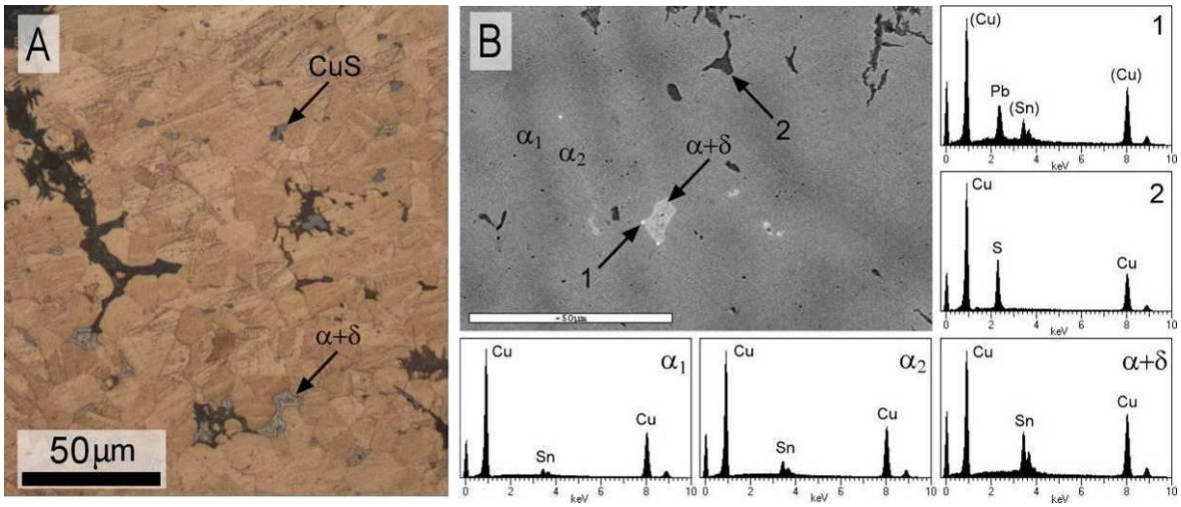

Figure 4.24. Microstructure of ring 392/11 from Baleizão (A: OM-BF, etched; B: SEM-BSE image with EDS spectra of α phase (α_1 and α_2: coring); α+δ eutectoid; 1: Pb rich inclusion; 2: Cu-S inclusion).

Vickers testing of selected artefacts evidences variable hardness despite similar tin contents and operational sequences (Table 4.12). The lower hardness of the ring 392/10 (99 HV0.2) is certainly related with the larger grain size of this microstructure (Figure 4.23B), which, as was already mentioned, evidences the poor efficiency of the forging and annealing operations. The higher hardness obtained at the ring 392/11 (129 HV0.2) is probably due to the presence of the harder δ phase (additionally, the heterogeneous distribution of this δ phase among the microstructure of the ring produced a lower confidence HV0.2 mean). Finally, the even higher hardness of the fibula 392/26 (154 HV0.2) might be related to a superior final deformation evidenced by the higher density of slip bands (Figure 4.23A).

Table 4.12. Vickers microhardness of copper-based artefacts from Baleizão (HV0.2 values in italic mean that the relative standard deviation of measurements is among 5-10%; relevant elemental and microstructural data obtained by micro-EDXRF and OM analyses is also presented).

Type	Artefact	Reference	Sn (%)	Phases	Manufacture	HV0.2
Ornament	Fibula (Serpentine)	392/26	9.1	α	C+(F+A)+FF	154
Unknown	Ring (open)	392/10	10.0	α	C+(F+A)+FF	99
Unknown	Ring (open)	392/11	10.1	α, α+δ	C+(F+A)+FF	*129*

4.2.4. Other artefacts

The archaeological sites of Salsa 3, Casarão da Mesquita 3, Santa Margarida and Quinta do Marcelo produced a small number of copper-based artefacts that were grouped in this section.

The majority of the material culture recovered by archaeological excavations carried out at Salsa 3 (Serpa) belongs to LBA contexts (Deus *et al.*, 2009). The metallic set comprises an awl (S3/F5) and a small fragment (S3/N18) that probably belonged to a needle (Figure 4.25).

The archaeological excavations at Casarão da Mesquita 3 (Évora)[5] recovered two copper-based artefacts (Santos *et al.*, 2008) – a small bead (CMQT3/F42) and a fragment of a blade (CMQT3/F49) with the riveting hole (Figure 4.25).

Archaeological works conducted during 2008 at Santa Margarida (Serpa) revealed several LBA negative structures (Deus *et al.*, in press), whereas a copper-based tranchet (or pendant?) was recovered at the surface layer (SM1, Figure 4.25).

During 1986, archaeological works conducted at Quinta do Marcelo (Almada) identified a seasonal settlement that was probably related with gold digging activities at the Tagus estuary (Barros, 1998). Radiocarbon dating points out to a LBA occupation belonging to the 11th–9th centuries BC. The copper-based artefacts consist of a tranchet (QM/0001, surface recovery) and a fragment (QM/1531), possibly from the blade of a knife (Figure 4.25).

[5] A preliminary work with some content from this section was previously published (Santos *et al.*, 2008).

Figure 4.25. Copper-based artefacts belonging to the archaeological sites of Casarão da Mesquita 3, Santa Margarida, Salsa 3 and Quinta do Marcelo.

The elemental characterisation using EDXRF and micro-EDXRF analyses indicates that the artefacts from Casarão da Mesquita 3, Santa Margarida, Salsa 3 and Quinta do Marcelo are constituted by binary bronze alloys, except for the awl from Salsa 3 that is composed by an arsenical copper alloy (Table 4.13).

The micro-EDXRF results establishes that the bronze artefacts are composed of alloys with tin contents (~10%) close to the values obtained in other LBA sites studied in this work. The relatively high iron content (0.25%) of the tranchet from Quinta do Marcelo differentiates it from the remaining LBA artefacts, which usually present lower iron contents (<0.05%). However, it is possible that the tranchet belongs to a later chronology since it was recovered at the surface level.

Contrary, the awl from Salsa 3 might belong to an earlier period since it is composed by an arsenical copper.

Table 4.13. Results of micro-EDXRF and EDXRF analyses of copper-based artefacts from Casarão da Mesquita 3, Santa Margarida, Salsa 3 and Quinta do Marcelo (values in %; *: EDXRF analysis; nd: not detected; vest: <2; +: [2, 50]; ++: >50).

Type	Artefact	Reference	Context	Cu	Sn	Pb	As	Fe
Ornament	Bead*	CMQT3/F42	LBA	++	+	nd	nd	vest
Ornament	Pendant (?)	SM/1	LBA	88.8	10.0	0.12	0.97	<0.05
Tool	Blade (?)*	CMQT3/F49	LBA	++	+	vest	vest	vest
Tool	Awl	S3/F5	LBA(?)	95.8	nd	nd	4.1	<0.05
Tool	Needle (?)	S3/N18	LBA	90.6	7.6	0.76	0.17	<0.05
Tool	Knife (?)	QM/1531	11th-9th	92.5	7.3	0.18	nd	<0.05
Tool	Tranchet	QM/0001	11th-9th	90.5	8.8	0.36	nd	0.25

Optical microscopy observations identified some common features of these bronze alloys as being constituted by monophasic microstructures (the α+δ eutectoid present at the needle S3/N18 is only residual) with Cu-S inclusions, despite presenting rather different operational sequences (Table 4.14). The awl S3/N18 presents microstructural characteristics that are common to other arsenical copper artefacts analysed at the previous chapter, namely Cu-As-O inclusions among an equiaxial microstructure with annealing twins and slip bands.

Table 4.14. OM characterisation of copper-based artefacts from Santa Margarida, Salsa 3 and Quinta do Marcelo (*: % given by micro-EDXRF; t: annealing twins; sb: slip bands; d: heavily deformed inclusions; C: Casting; A: Annealing; F: Forging; FF: Final Forging; ↑: high amount; ↓: low amount).

Type	Artefact	Reference	Sn*	Phases	Inclusions	Features		Manufacture
Ornament	Pendant (?)	SM/1	10.0	α	Cu-S	coarse	-	C+A
Tool	Awl	S3/F5	-	α	Cu-As-O	equiaxial	t, sb, d	C+(F+A)+FF
Tool	Needle (?)	S3/N18	7.8	α, α+δ↓	Cu-S	equiaxial	t, sb	C+(F+A)+FF
Tool	Knife (?)	QM/1531	7.3	α	Cu-S↑	equiaxial	t, sb, d	C+(F+A)+FF↑
Tool	Tranchet	QM/0001	8.8	α	Cu-S	equiaxial	t	C+(F+A)

The "pendant" SM/1 has a coarse microstructure (Figure 4.26A) that can either result from a very slow cooling rate after pouring or from a latter thermal treatment. However, considering that the pendant seems to be unfinished (i.e. it still exhibits some casting seams) and do not exhibits any traces of ever being used, it is more likely that its microstructure resulted from a controlled cooling during casting.

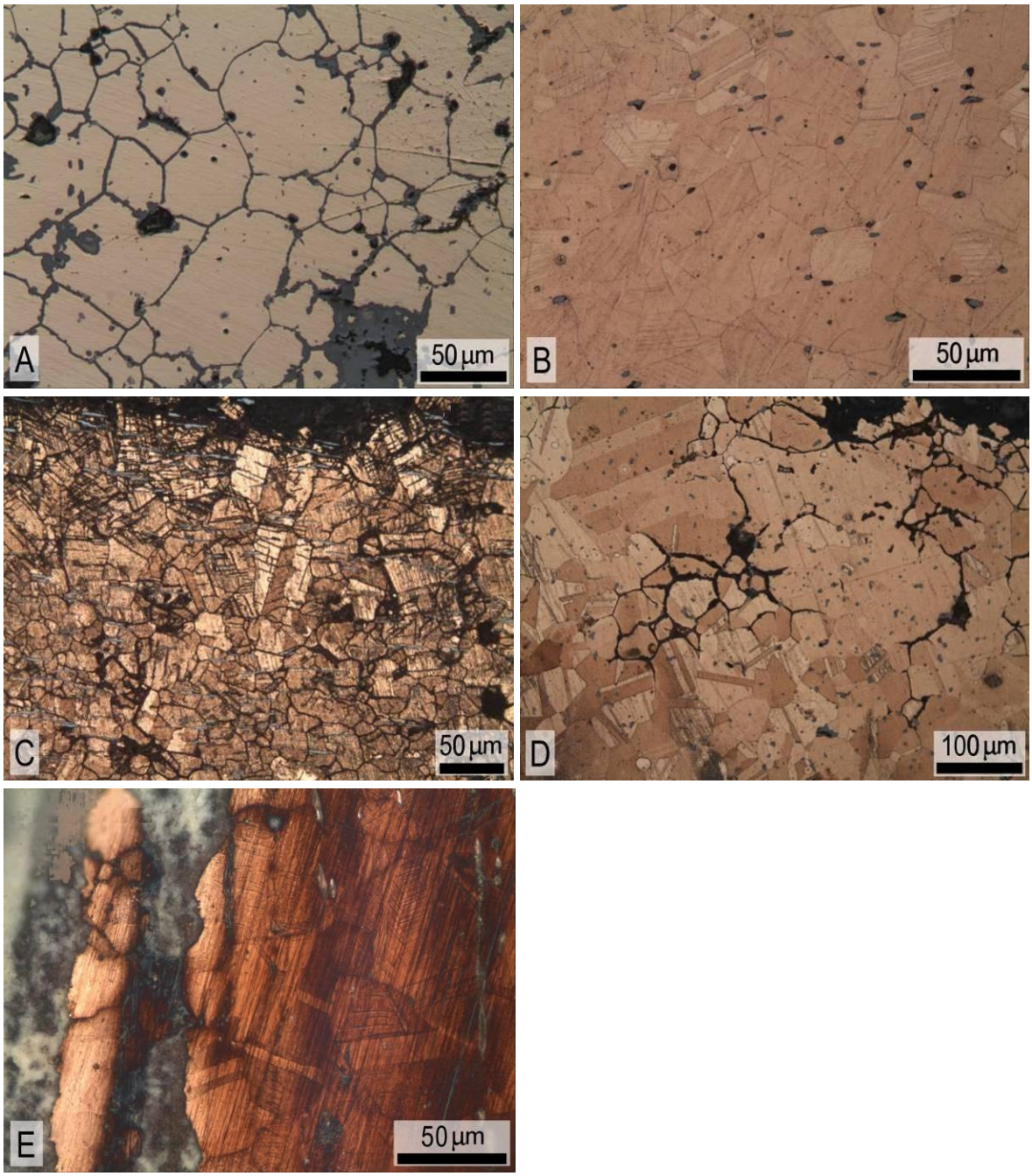

Figure 4.26. Microstructures of copper-based artefacts from Santa Margarida, Salsa 3 and Quinta do Marcelo (A: pendant SM/1; B: needle S3/N18; C: knife QM/1531; D: tranchet QM/0001; E: awl S3/F5; pendant SM/1: BF, non-etched; remaining: OM-BF, etched).

The needle S3/N18 and the knife QM/1531 exhibit deformed equiaxial microstructures (Figure 4.26B and C) from forging and annealing cycle(s). Additionally, the knife presents highly deformed Cu-S inclusions and a high density of slip bands, evidencing the high deformation applied throughout the entire manufacturing procedure and during the final forging operation, respectively. The tranchet QM/0001 displays annealed grains with exceptionally variable sizes (Figure 4.26D). The abnormal grain growth identified in some regions of this microstructure was

probably induced by a high annealing temperature, which indicates a rather poor control over this heat treatment.

Vickers testing of selected artefacts evidences the hardening effect of the final forging procedure since the needle S3/N18 presents a much higher hardness than the recrystallized tranchet QM/0001 (Table 4.15). Additionally, the exceptionally strong thermal treatment applied to the tranchet QM/0001 originated a very large grain size, resulting in a softer material, as proven by the very low Vickers microhardness (94 HV0.2).

Table 4.15. Vickers microhardness of copper-based artefacts from Salsa 3 and Quinta do Marcelo (relevant elemental and microstructural data obtained by micro-EDXRF and OM analyses is also presented).

Type	**Artefact**	**Reference**	**Sn (%)**	**Phases**	**Manufacture**	**HV0.2**
Tool	Needle (?)	S3/N18	7.8	α, $\alpha+\delta\downarrow$	C+(F+A)+FF	149
Tool	Tranchet	QM/0001	8.8	α	C+(F+A$\uparrow$)	94

4.3. Early Iron Age

4.3.1. Introduction

The foundation of the first Phoenician colonies in the southern and western seaboard regions of the Iberian Peninsula during the late 9th and early 8th century BC (Barros and Soares, 2004; González de Canales *et al.*, 2006; Neville, 2007; Nijboer and Van der Plicht, 2006; Torres-Ortiz, 1998) initiated a period of plentiful cultural and technological interactions. Phoenician people belong to a region where bronzes were known for a very long time. In fact, the bronze alloy was already used at the Eastern Mediterranean region since around 2600 BC. Furthermore, at the time of the Phoenician implantation at the Iberian Peninsula, weapons and tools from the Eastern Mediterranean region were often made with iron, whereas the bronze alloy was more related with ornaments and cult artefacts (Mohen, 1990).

During the following centuries there was an increase in the exploitation of the rich mineral resources of the Iberian Peninsula, including of iron, silver and tin. In general, most Phoenician sites at the Iberian Peninsula show archaeological evidences of metallurgical activities (Neville, 2007), either concerning the exploitation of mineral resources or the production of metallic artefacts, e.g. Quinta do Almaraz, Almada (Araújo *et al.*, 2004), Cerro da Rocha Branca, Silves (Gomes, 1993), Monte Romero, SW Spain (Kassianidou, 1993) and La Fonteta, SE Spain (Renzi *et al.*, 2009). Innovative metallurgical practices were introduced, as for instance the lost wax technique for casting complex artefacts. Moreover, new artefact typologies related to Mediterranean traditions and culture emerge (e.g. tweezers for body treatment or some specific types of fibula for vestment tighten). However, acculturation appears to have been a slow and selective process, very dependent on the social-economic and cultural development of local societies (Sieso, 2005).

The good castability properties of leaded bronze alloys seem to be better understood. Contrasting with its apparent indiscriminate use at the LBA Atlantic world, leaded bronzes become more related to ornaments from the southwestern Iberian Peninsula (Montero-Ruíz *et al.*, 2003). This situation has also been recorded in the southeastern region (Montero-Ruíz, 2008), evidencing that the increased use of leaded bronzes was widespread among the areas that experienced a strong Orientalising influence.

Another important alteration regarding the alloy composition at Southwestern Iberian Peninsula seems to involve the general use of alloys somewhat poorer in tin (Rovira, 1995). The elemental composition of latter Orientalising bronze sets becomes more comparable to collections from related Mediterranean areas, such as Sardinia, Italy and Sicily (Giardino, 1995; Hook, 2007; Ingo *et*

al., 2006). However, there has been a general lack of metallurgical studies concerning this important period of the Iberian Peninsula.

The following sections will present the result of several metallic collections belonging to the Early Iron Age. The results aim to contribute to fill that gap by establishing the evolution of the copper-based metallurgical technology at the southern Portuguese territory and ascertaining about the actual outcome of the Mediterranean influences in this region.

4.3.2. Castro dos Ratinhos[6]

The archaeological works at Castro dos Ratinhos (Moura) revealed a complex fortified system implanted on top of an elevated ridge in the left bank of the Guadiana River (Berrocal-Rangel and Silva, 2010). The different contexts of this settlement can be ascribed to a period from the LBA until the Orientalising period. Radiocarbon dating established that the earlier contexts belong to the 12th-9th centuries BC, whereas the latter contexts comprise the end of the 9th century BC and the 8th century BC (Soares and Martins, 2010). Being contemporary of the first Phoenician colonies in the Iberian coastal areas, the latter phase of this settlement already present some Orientalising traces, such as habitat structures with a rectangular plan, imported wheel-turned pottery (red slip ware and amphorae) and iron artefacts.

The collection of 47 copper-based artefacts comprises mostly ornaments, tools and rings, which belong mainly to the latter 8th century BC contexts. Ornaments include a bead, belt-locks, fibulae, a necklace-lock and a pendant. Fibulae are among the most common and interesting artefacts, including 1 serpentine (B1/IIc/M2), 2 double-spring (C1/Ia/M1 and C1/Ib/M3) and, possibly, 1 *Bencarrón* type fibula (M3/IIb/M1) (Figure 4.27). The serpentine fibulae are frequent in the LBA Portuguese archaeological contexts, whereas double-spring fibulae present an extensive period of utilization that continues up to the Iron Age (Arruda, 2008). It is during the period of increasing Orientalising contacts that other types emerge in the Iberian Peninsula, such as *Alcores*, *Bencarrón* and *Acebuchal* fibulae (Ponte, 2006). Finally, one should underline two small conical heads (D1/Ib/M3 and N3/Ic/M1) that might also belong to fibulae (Figure 4.27).

The collection of tools consists of chisels, fish-hook, knives, awl, nails, needles, tweezers and a balance weight (Figure 4.27). The balance weight (C1/sup/M1) exhibits a bitroncoconical shape, being the more common typology in the Portuguese territory during the 12th-9th centuries BC (Vilaça, 2003). Chronologically latter balance weights also present cubic, zoomorphic and

[6] Part of the content from this section was previously published (Valério *et al*., 2010a; 2010b; 2010c).

anthropomorphic typologies, while are frequently constituted by lead instead of copper-based alloys (e.g. 2 cubic balance weights composed by lead from Quinta do Almaraz (Valério *et al.*, 2003). Finally, a considerable number of artefacts from this collection present an unknown functionality, namely 7 fragments and 9 rings, comprising open (fragmented?), coiled and closed examples (Figure 4.27).

Figure 4.27. Copper-based artefacts belonging to the archaeological site of Castro dos Ratinhos (A: *Bencarrón* fibula from Carmona evidencing the flat bow ending as a conical head, adapted from Almagro-Bash, 1966).

Table 4.16. Results of micro-EDXRF and EDXRF analyses of copper-based artefacts from Castro dos Ratinhos (values in %; *: EDXRF analysis; nd: not detected; vest: <2; +: [2, 50]; ++: >50).

Type	Artefact	Reference	Context	Cu	Sn	Pb	As	Fe
Ornament	Bead*	B1/IIc/M3	12th-9th	++	+	vest	nd	vest
Ornament	Bead*	C1/IIa/M2	9th-8th	++	+	vest	vest	vest
Ornament	Belt-lock	A1/Ib/M1	9th-8th	89.6	10.3	nd	0.18	<0.05
Ornament	Belt-lock	A1/IIa/M4	9th-8th	88.8	11.1	nd	<0.10	0.06
Ornament	Fibula (*Bencarrón*)	M3/IIb/M1	9th-8th	89.9	9.8	0.16	0.13	<0.05
Ornament	Fibula (Double-spring)*	C1/Ia/M1	9th-8th	++	+	vest	vest	vest
Ornament	Fibula (Double-spring)	C1/Ib/M3	9th-8th	93.3	6.3	nd	0.43	<0.05
Ornament	Fibula (Serpentine)	B1/IIc/M2	12th-9th	87.3	12.8	nd	nd	<0.05
Ornament	Fibula (conical head)	D1/Ib/M3	9th-8th	84.1	15.9	nd	nd	<0.05
Ornament	Fibula (conical head)*	N3/Ic/M1	9th-8th	++	+	vest	nd	vest
Ornament	Fibula (spring)*	B1/IIc/M4	12th-9th	++	+	nd	nd	vest
Ornament	Fibula (spring)*	C1/Sup/M2	12th-9th	++	+	vest	vest	vest
Ornament	Necklace-lock	D1/Ib/M1	9th-8th	90.0	9.4	0.30	0.12	0.14
Ornament	Pendant	D1/IIa/M2	9th-8th	91.4	8.3	0.17	<0.10	<0.05
Tool	Chisel	A1/IIa/M3	9th-8th	90.3	9.5	0.18	<0.10	<0.05
Tool	Chisel	C1/Ic/M1	9th-8th	88.3	11.4	0.19	0.15	<0.05
Tool	Chisel	D1/IIa/M3	9th-8th	89.5	10.2	nd	0.23	<0.05
Tool	Fish-hook	D2/Ic/M1	9th-8th	90.6	9.2	0.10	<0.10	<0.05
Tool	Knife	A2/IIc/M1	12th-9th	95.1	4.9	nd	nd	<0.05
Tool	Knife*	B1/IIc/M1	12th-9th	++	+	vest	vest	vest
Tool	Nail	A2/IIa/M1	9th-8th	90.1	9.6	nd	<0.10	0.16
Tool	Nail	B1/IIa/M1	9th-8th	90.3	9.4	nd	0.10	0.11
Tool	Needle	A1/IIa/M1	9th-8th	91.4	8.3	0.10	0.11	<0.05
Tool	Needle	C1/Ib/M2	9th-8th	89.2	10.3	0.18	0.29	<0.05
Tool	Needle	C1/IIa/M1	9th-8th	91.4	8.5	nd	nd	<0.05
Tool	Needle	D1/Ib/M2	9th-8th	92.3	7.2	0.30	0.19	<0.05
Tool	Needle	R1/IIc/M1	9th-8th	93.0	6.9	nd	nd	<0.05
Tool	Awl	C1/Ib/M4	9th-8th	93.6	6.3	nd	0.10	<0.05
Tool	Tweezers	D1/IIc/M2	12th-9th	90.3	9.6	nd	<0.10	<0.05
Tool	Weight (bitronc.)	C1/Sup/M1	9th-8th	84.2	15.5	0.18	<0.10	<0.05
Weapon	Dagger*	D2/IIb/M1	9th-8th	++	+	nd	vest	vest
Unknown	Ring (closed)	A4/Ia/M1	9th-8th	85.7	14.3	nd	<0.10	<0.05
Unknown	Ring (closed)	B1/IIa/M2	9th-8th	85.7	13.7	nd	0.51	<0.05
Unknown	Ring (closed)	B1/Ic/M1	9th-8th	92.2	7.8	nd	<0.10	<0.05
Unknown	Ring (closed)	C2/Ic/M1	9th-8th	88.4	10.5	0.97	0.16	<0.05
Unknown	Ring (coiled)	Q1/Ib/M1	9th-8th	88.8	10.8	0.16	0.18	<0.05
Unknown	Ring (open)	D1/IIa/M4	9th-8th	86.9	12.7	0.18	0.14	<0.05
Unknown	Ring (open)	D1/IIc/M1	12th-9th	89.3	10.7	nd	nd	<0.05
Unknown	Ring (open)	D2/IIa/M2	9th-8th	86.8	13.1	nd	0.12	<0.05
Unknown	Ring (open)	N3/IId/M1	9th-8th	89.1	10.3	0.15	0.16	<0.05
Unknown	Fragment*	D1/IIa/M1	9th-8th	++	+	vest	nd	vest
Unknown	Fragment	D2/IIa/M3	9th-8th	89.4	9.3	1.3	<0.10	<0.05
Unknown	Fragment	S1/Ia/M1	9th-8th	91.6	8.3	nd	<0.10	<0.05
Unknown	Fragment	A1/IIa/M2	9th-8th	90.1	9.7	0.14	0.10	<0.05
Unknown	Fragment	D2/IIa/M1	9th-8th	86.5	13.5	nd	nd	<0.05
Unknown	Fragment	D2/IIa/M4	9th-8th	90.7	8.5	0.80	<0.10	<0.05
Unknown	Fragment*	D2/IIa/M5	9th-8th	++	+	vest	vest	vest

The alloy composition of the majority of these artefacts was determined by micro-EDXRF analyses conducted at areas cleaned from the superficial corrosion layer (Table 4.16). The artefacts that could not be cleaned nor sampled were analysed by EDXRF to identify the main alloy constituents.

Results indicate that the collection of metallic artefacts from Castro dos Ratinhos is entirely composed of copper-tin alloys with impurities of lead, arsenic and iron. The quantitative analyses point to bronze alloys with very low impurity contents, namely of lead (only 3 artefacts present contents above 0.30%) and arsenic (only 2 artefacts present contents above 0.29%). Furthermore, iron is always present in remarkably low concentrations (<0.05%), except in 3 artefacts (necklace-lock and nails: 0.11-0.14%) that belong to latter 8th century BC contexts.

Regarding the distribution of the main alloying element, results indicate that the collection present a normal like distribution with an average of 10.1 ± 2.5% (Figure 4.28). Despite no noticeable differences between the alloy type in ornaments and tools, it should be noted that the few examples presenting higher tin contents (12-14%) are rings and other artefacts (e.g. conical heads, serpentine fibula and balance weight) that usually do not require high mechanical strength.

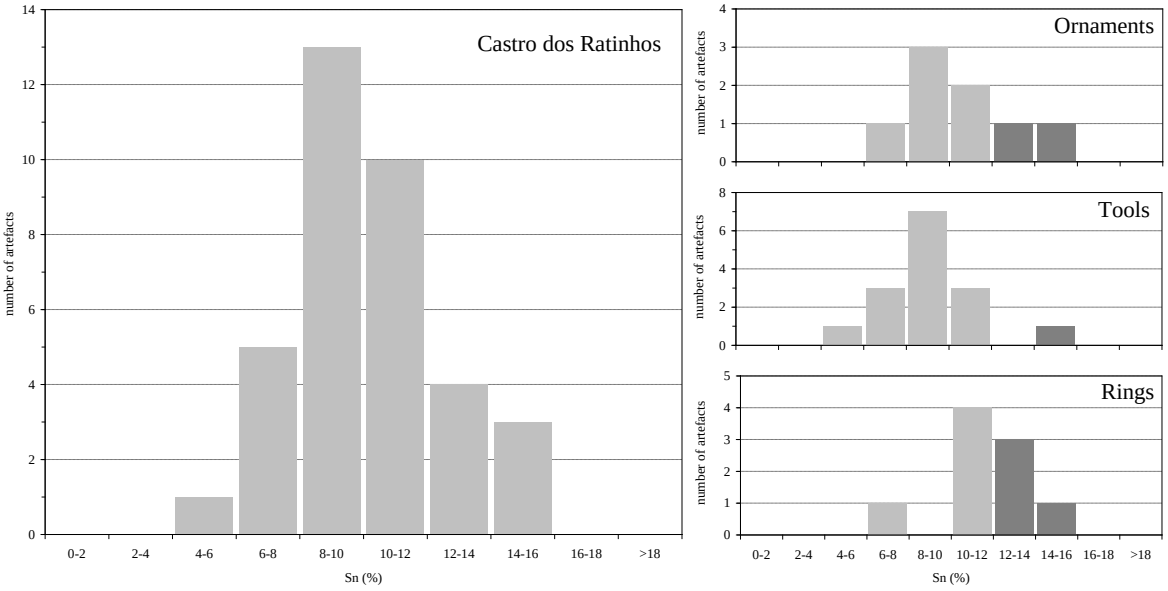

Figure 4.28. Distribution of tin contents in copper-based artefacts from Castros dos Ratinhos (darker columns symbolize ornaments, tools and rings with higher tin contents).

Selected artefacts were analysed by OM to identify different phases and common inclusions. In addition, operational sequences were established with the characteristic signatures of annealing and hammering operations, namely type of microstructure, annealing twins, inclusion morphologies and slip bands density (Table 4.17).

Table 4.17. OM characterisation of copper-based artefacts from Castro dos Ratinhos (*: % given by micro-EDXRF; t: annealing twins; sb: slip bands; d: heavily deformed inclusions; C: Casting; A: Annealing; F: Forging; FF: Final Forging; ↑: high amount; ↓: low amount).

Type	Artefact	Reference	Sn*	Phases	Inclusions	Features		Manufacture
Ornament	Fibula (Double-spring)	C1/Ib/M3	6.3	α	Cu-S	equiaxial	t, sb	C+(F+A)+FF↑
Ornament	Fibula (conical head)	D1/Ib/M3	15.9	α, α+δ	Cu-S	dendritic	-	C
Ornament	Fibula (conical head)	N3/Ic/M1	-	α	-	dendritic	-	C
Ornament	Necklace-lock	D1/Ib/M1	9.4	α, α+δ	Cu-S↑	equiaxial	t, sb	C+(F+A)+FF
Ornament	Pendant	D1/IIa/M2	8.3	α	Cu-S	coarse	-	C
Tool	Knife	A2/IIc/M1	4.9	α	Cu-S↑	equiaxial	t, sb, d	C+(F+A)+FF
Tool	Needle	A1/IIa/M1	8.3	α	Cu-S↑	equiaxial	t, sb	C+(F+A)+FF↑
Tool	Needle	C1/Ib/M2	10.3	α	Cu-S↑	equiaxial	t, sb	C+(F+A)+FF↑
Tool	Needle	C1/IIa/M1	8.5	α	Cu-S↑	equiaxial	t	C+(F+A)
Tool	Needle	D1/Ib/M2	7.2	α	Cu-S	equiaxial	t, sb	C+(F+A)+FF↓
Tool	Needle	R1/IIc/M1	6.9	α	Cu-S↑	equiaxial	t	C+(F+A)
Tool	Awl	C1/Ib/M4	6.3	α	Cu-S↑	equiaxial	t, sb	C+(F+A)+FF↓
Tool	Weight (bitronc.)	C1/Sup/M1	15.5	α, α+δ	Cu-S	coarse	-	C
Unknown	Ring (closed)	A4/Ia/M1	14.3	α, α+δ	Cu-S	dendritic	-	C
Unknown	Ring (open)	D1/IIa/M4	12.7	α, α+δ	Cu-S↑	equiaxial	t, sb	C+(F+A)+FF↑
Unknown	Ring (open)	D1/IIc/M1	10.7	α, α+δ	Cu-S↑	equiaxial	t	C+(F+A)↓
Unknown	Ring (open)	D2/IIa/M2	13.1	α, α+δ	Cu-S	coarse	sb	C+A↓+F
Unknown	Ring (open)	N3/IId/M1	10.3	α	Cu-S↑	coarse	sb	C+A↓+F
Unknown	Fragment	S1/Ia/M1	8.3	α	Cu-S	equiaxial	t, sb	C+(F+A)+FF↑
Unknown	Fragment	A1/IIa/M2	9.7	α, α+δ	Cu-S	equiaxial	t	C+(F+A)
Unknown	Fragment	D2/IIa/M4	8.5	α	Cu-S	equiaxial	t	C+(F+A)

"As-cast" artefacts from Castro dos Ratinhos account for about 25% of the analysed artefacts, comprising mainly ornaments plus 1 weight and 1 ring. These artefacts present as-cast microstructures constituted by dendritic structures or coarse grains (Figure 4.29). Faster cooling rates originate dendritic microstructures with evident primary and secondary arms. As the cooling rates diminish, the microstructures become more homogenized, exhibiting progressively coarser dendrites that ultimately develop into coarse grains at very slow cooling rates (as seen in Figure 4.29).

The "as-cast" artefacts with higher tin contents (~14-16%) exhibit the characteristic α+δ eutectoid in the regions that were the last to solidify (Figure 4.29A and E), with the exception of the ring (Figure 4.29C), in which the interdendritic regions are completely corroded. A closer observation of the microstructure of the weight also reveals the coring of the α grains (Figure 4.29F). During

solidification sulphur was segregated into the liquid phase due to its low solubility in copper, precipitating as Cu_2S in the last regions to solidify. Therefore, Cu-S inclusions are often close to the $\alpha+\delta$ eutectoid (e.g. see Figure 4.29F).

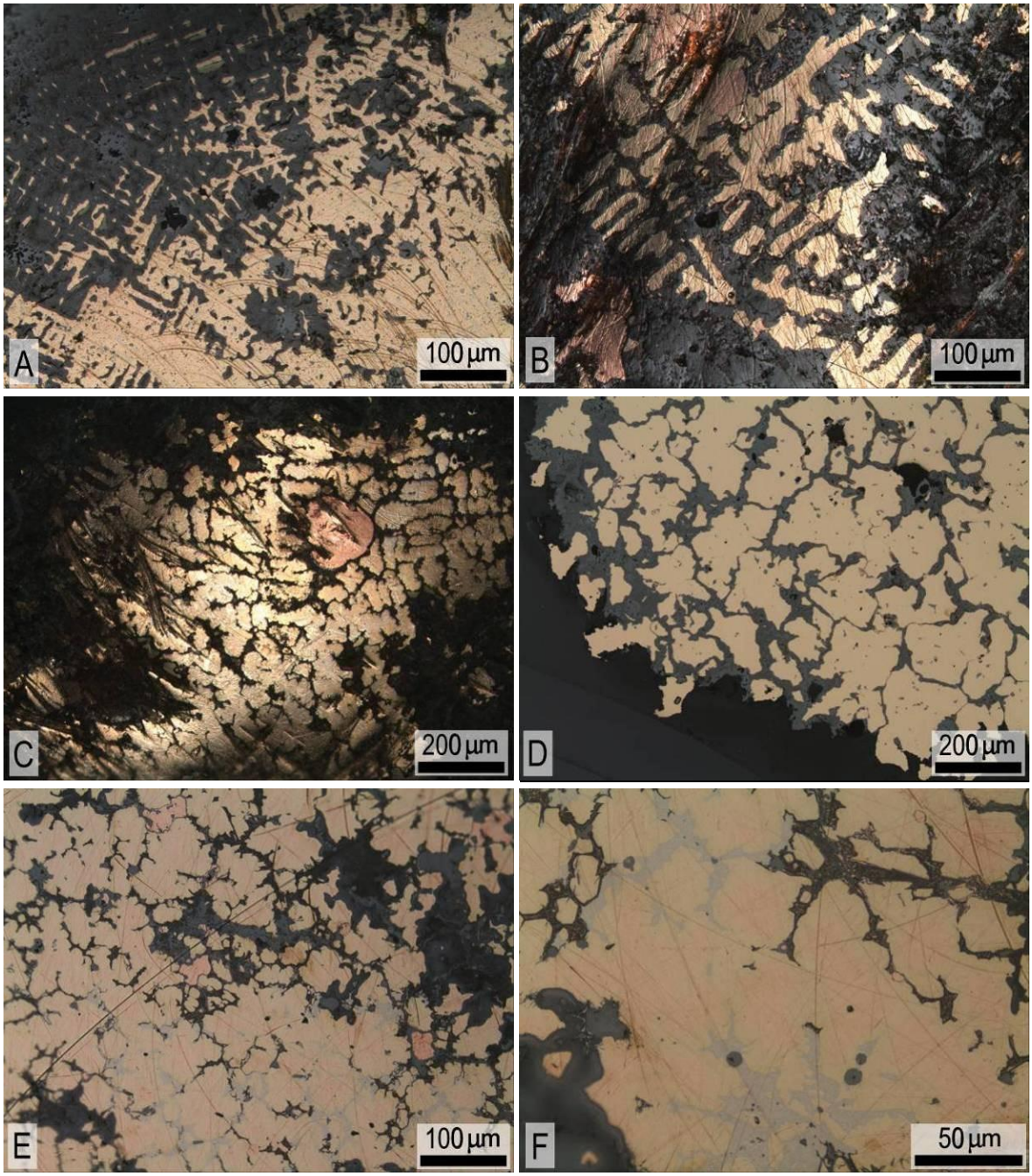

Figure 4.29. Microstructures of copper-based artefacts from Castros dos Ratinhos, generally showing the effect of increasingly slower cooling rates on "as-cast" microstructures (A: conical head D1/Ib/M3; B: conical head N3/Ic/M1; C: ring A4/Ia/M1; D: pendant D1/IIa/M2; E and F: weight C1/Sup/M1; all OM-BF, non-etched).

Some of these microstructures present "inclusions" of metallic copper (appearing pink in BF illumination) that derives from long term redeposition. This corrosion process of bronzes is characterized by tin oxide formation and metallic copper redeposition at internal regions where

oxygen concentration is low. These copper "inclusions" are commonly found in archaeological bronze alloys and are frequently used as an indicator of long term corrosion (Bosi *et al.*, 2002).

The rings D2/IIa/M2 and N3/Id/M1 present a rather unusual type of microstructure among the collections studied, being partially homogenized and deformed (Figure 4.30). This type of microstructures might result from a deficient annealing process due to low temperature (under critical deformation for recrystallization) or insufficient time of operation. In any case, the high density of slip bands in both microstructures indicates that these rings were finished by forging. Furthermore, certain slip bands appear to be distorted indicating that the final hammering was probably performed to bend the ring. Other significant characteristics include the islands of the $\alpha+\delta$ eutectoid present in the ring with high tin content (13.1%), clearly indicating the principal direction of development of the original dendrites. Additionally, the ring D2/IIa/M2 exhibits an abnormal density of large pores originated by degasification during the cooling. This type of casting defects is unusual among the artefacts studied, indicating a poorer control over the temperatures of the mould and molten metal during pouring. Copper sulphide inclusions are more resistant to the alteration processes and some still remain in the corroded regions.

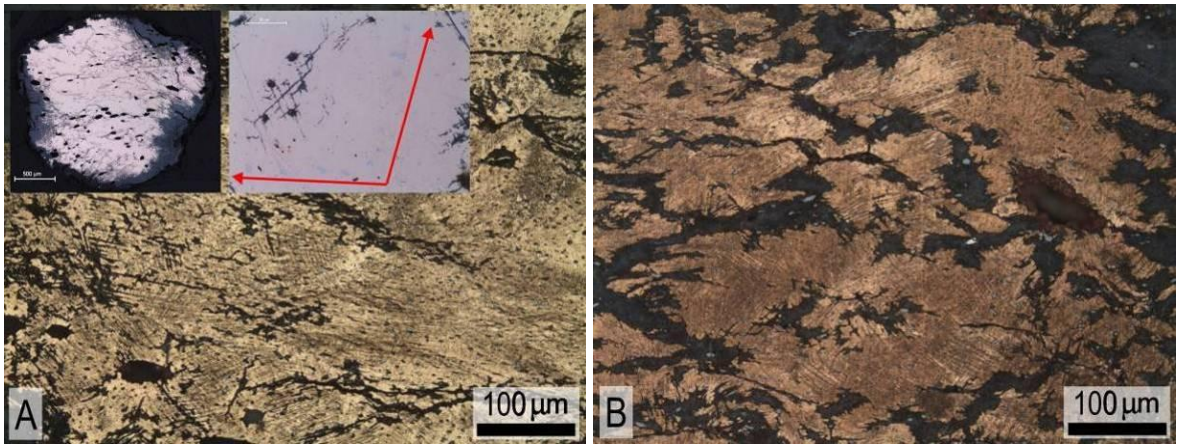

Figure 4.30. Microstructures of copper-based artefacts from Castro dos Ratinhos with "annealing" and forging work (A: ring D2/IIa/M2 and B: ring N3/Id/M1; both OM-BF, etched).

Artefacts that were subjected to forging and annealing cycle(s) present deformed equiaxial microstructures with annealing twins (Figure 4.31). This particular type of manufacturing procedure accounts for about 25% of the analysed artefacts. Cu-S inclusions are common in all these microstructures, whereas the ring D1/IIc/M1 exhibit the $\alpha+\delta$ eutectoid (Figure 4.31D), despite a relatively low tin content (10.7% Sn). Corrosion evidences a residual dendritic microstructure, which is superimposed by recrystallized grains only in the regions closer to the surface (Figure 4.31C). Consequently, the thermomechanical treatments were probably only applied as a surface finishing of the ring.

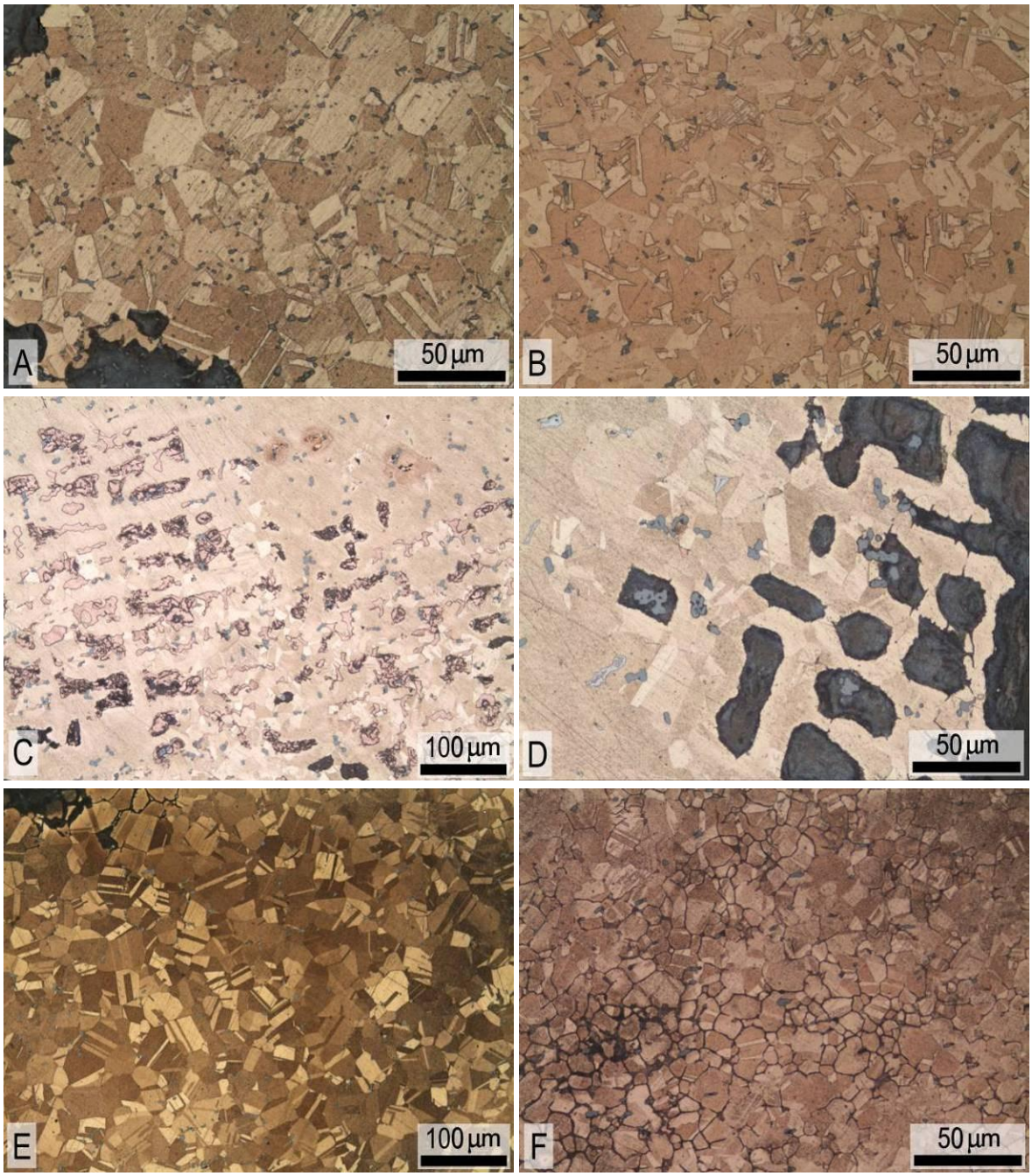

Figure 4.31. Microstructures of copper-based artefacts from Castros dos Ratinhos with forging and annealing work (A: needle C1/IIa/M1; B: needle R1/IIc/M1; C and D: ring D1/IIc/M1; E: fragment A1/IIa/M2; F: fragment D2/IIa/M4; all OM-BF, etched).

The type of microstructure more common at Castro dos Ratinhos (with a frequency of around 40%) presents equiaxial grains with annealing twins and slip bands (Figure 4.32). The presence of slip bands imply a manufacture finished with a final forging, which intensity can be related with the density of the slip bands, e.g. the flat fragment S1/Ia/M1 (Figure 4.32G) clearly suffered a much higher final deformation than the awl C1/Ib/M4 (Figure 4.32E).

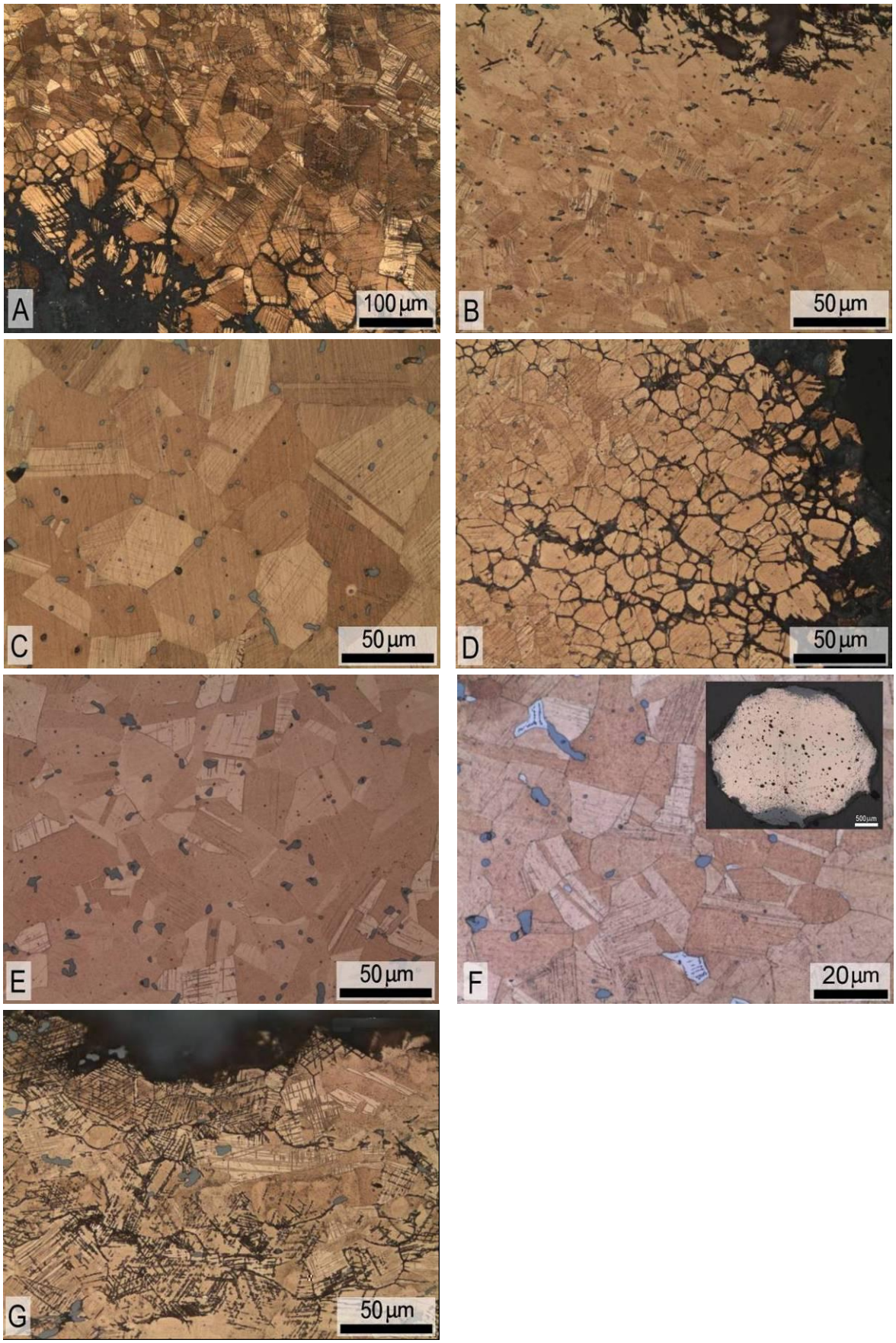

Figure 4.32. Microstructures of copper-based artefacts from Castros dos Ratinhos with forging, annealing and final forging work (A: fibula C1/Ib/M3; B: needle A1/IIa/M1; C: needle C1/Ib/M2; D: needle D1/Ib/M2; E: awl C1/Ib/M4; F: ring D1/IIa/M4; G: fragment S1/Ia/M1; all OM-BF, etched).

In the microstructure of the flat fragment S1/Ia/M1 (Figure 4.32G) is very clear that intragranular corrosion along crystallographic planes evidence the slip bands, being a very useful indicator of corroded microstructures that were kept in a strain hardening condition. Besides, these microstructures present comparable characteristics to the ones already described, such as common Cu-S inclusions and α+δ eutectoid in the alloys with higher tin contents (e.g. ring D1/IIa/M4, 12.7% Sn Figure 4.32F). Furthermore, the ring D1/IIa/M4 exhibits a high density of large pores (Figure 4.32F) due to a significant degasification during the casting operation. This seems to be a rather uncommon characteristic among the collection of copper-based artefacts studied.

A particularly remarkable microstructure was selected for further study by SEM-EDS – the knife A2/IIc/M1 exhibits heavily deformed grains, annealing twins and a few slip bands (Figure 4.33). Furthermore, copper sulphide inclusions are very elongated, clearly evidencing the high total deformation applied to obtain the final artefact shape. This indicates an operational sequence that comprises several forging and annealing cycles (high total deformation) followed by a rather limited final forging procedure. SEM-EDS analyses reveal Sn-O inclusions associated with some Cu-S inclusions. Tin oxide inclusions are less deformed probably due to their higher hardness. Tin oxide inclusions can be non-reacted ore or could also result from partial tin oxidation during melting (Klein and Hauptmann, 1999). The oxide inclusions would normally be transferred to the slag but a low casting temperature would prevent this occurring (Dungworth, 2000).

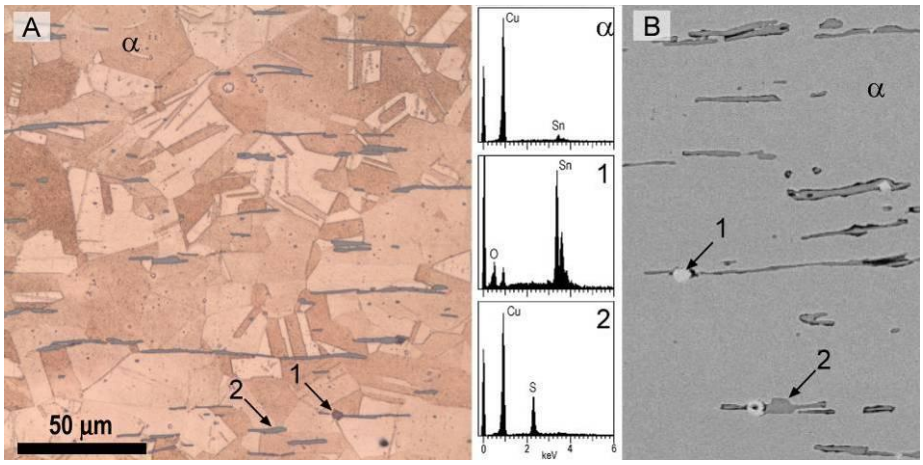

Figure 4.33. Microstructure of the knife A2/IIc/M1 from Castro dos Ratinhos (A: OM-BF, etched; B: SEM-BSE with EDS spectra of α phase; 1: Sn-O inclusion; 2: Cu-S inclusion).

Another noteworthy example (necklace-lock D1/Ib/M1) also displays a worked microstructure overlaying few remaining dendrites (Figure 4.34). The presence of cored dendrites together with some α+δ eutectoid in a bronze alloy with relatively low tin content (9.4%), point to an incomplete recrystallization and homogenisation of the microstructure due to either a short time or low temperature of the annealing operation. It should be noted that recrystallization starts to take place

at around 500 ºC, while homogenisation of the tin microsegregation is only achieved at slightly higher temperatures, such as that of 650-700 ºC (Northover, 2004). The presence of iron, in this case associated with Cu-S inclusions, reflects the relatively higher content of this element in the alloy (0.14%). Lead is dispersed in small Pb rich globules due to its low miscibility in molten bronze (in this case, the Cu and Sn peaks in the EDS spectrum of the Pb inclusion are mainly from the surrounding Cu-Sn matrix).

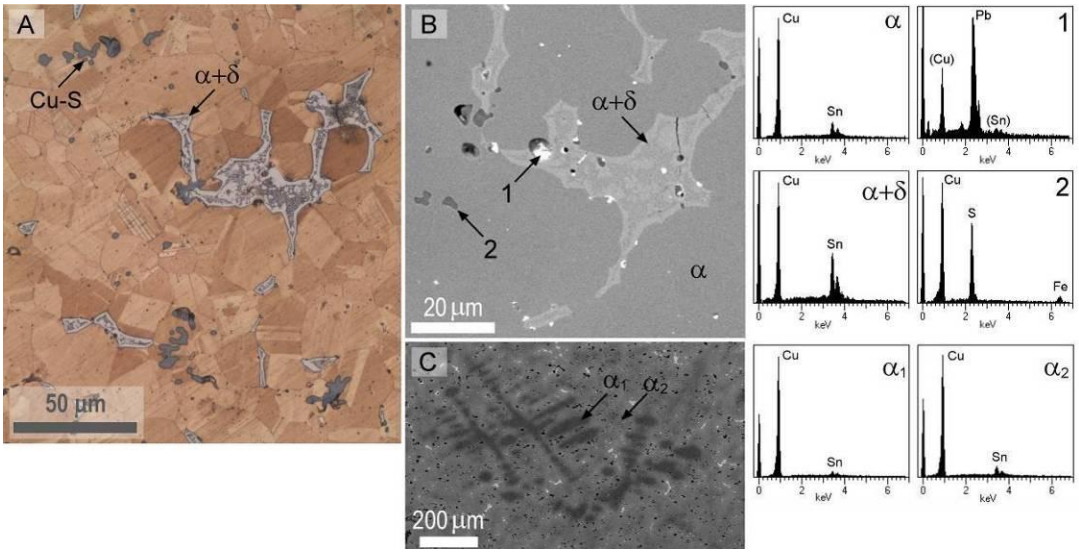

Figure 4.34. Microstructure of the necklace-lock D1/Ib/M1 from Castro dos Ratinhos (A: OM-BF, etched; B and C: SEM-BSE with EDS spectra of α phase (α_1 and α_2: coring); α+δ eutectoid; 1: Pb rich inclusion; 2: Cu-S-Fe inclusion).

The Vickers microhardness of selected copper-based artefacts from Castro dos Ratinhos is presented in Table 4.18. The single as-cast artefact (pendant D1/IIa/M2) tested presents the lowest hardness (78 HV0.2) among the collection due to its coarse microstructure (Figure 4.29D). Other low hardness artefacts include the group of annealed artefacts (Figure 4.31), together with others with a less significant final forging procedure (needle D1/Ib/M2 and awl C1/Ib/M4; Figure 4.32D and E, respectively). By the contrary, artefacts with higher hardness (needle A1/IIa/M1, needle C1/Ib/M2 and fragment S1/Ia/M1; Figure 4.32B, C and G, respectively) exhibit higher deformation and/or smaller grain size. Despite a higher final deformation, the low hardness of the fibula C1/Ib/M3 (101 HV0.2) is most likely due to its larger grain size (Figure 4.32A).

The numerous needles tested evidence that a same typology can present very different hardness values, in this case varying from 94 to 192 HV0.2. The intensity of the final forging seems to be the controling factor regarding the hardness since the other significant factors (phases, tin content and grain size) seem to be rather similar in all these needles. The presence of the harder δ phase do not seem to be very significant, probably because when it is present it is always in very low amounts that do not produce a significant increase in the overall hardness of the material.

Table 4.18. Vickers microhardness of copper-based artefacts from Castro dos Ratinhos (relevant elemental and microstructural data obtained by micro-EDXRF and OM analyses is also presented).

Type	Artefact	Reference	Sn (%)	Phases	Manufacture	HV0.2
Ornament	Fibula (Double-spring)	C1/Ib/M3	6.3	α	C+(F+A)+FF↑	101
Ornament	Necklace-lock	D1/Ib/M1	9.4	α, α+δ	C+(F+A)+FF	124
Ornament	Pendant	D1/IIa/M2	8.3	α	C	78
Tool	Knife	A2/IIc/M1	4.9	α	C+(F+A)+FF	125
Tool	Needle	A1/IIa/M1	8.3	α	C+(F+A)+FF↑	192
Tool	Needle	C1/Ib/M2	10.3	α	C+(F+A)+FF↑	164
Tool	Needle	C1/IIa/M1	8.5	α	C+(F+A)	94
Tool	Needle	D1/Ib/M2	7.2	α	C+(F+A)+FF↓	100
Tool	Needle	R1/IIc/M1	6.9	α	C+(F+A)	108
Tool	Awl	C1/Ib/M4	6.3	α	C+(F+A)+FF↓	95
Unknown	Ring (open)	D1/IIa/M4	12.7	α, α+δ	C+(F+A)+FF↑	142
Unknown	Ring (open)	D1/IIc/M1	10.7	α, α+δ	C+(F+A)↓	108
Unknown	Fragment	S1/Ia/M1	8.3	α	C+(F+A)+FF↑	160
Unknown	Fragment	A1/IIa/M2	9.7	α, α+δ	C+(F+A)	94
Unknown	Fragment	D2/IIa/M4	8.5	α	C+(F+A)	100

4.3.3. Quinta do Almaraz[7]

Archaeological excavations conducted during 1988 on an elevated platform over the Tagus estuary revealed the site of Quinta do Almaraz, Almada (Barros *et al.*, 1993). This settlement is considered one of the ancient Phoenician foundations of the west coast of the Iberian Peninsula (Melo *et al.*, in press). The material culture includes a valuable collection of copper-based, iron and gold artefacts, together with a significant amount of production remains (i.e. slags, crucibles and tuyeres) that point to a local metallurgy of iron, silver and gold (Araújo *et al.*, 2004). The site was already occupied during the LBA, but the archaeometallurgical materials largely belong to latter contexts. The radiocarbon dating established that the metallurgical material culture can generally be ascribed to the 9th-7th centuries BC, even though a small part might belong to a wider period that continues up to the 5th century BC (Barros and Soares, 2004).

The collection of copper-based artefacts selected for study comprises 30 artefacts, mostly ornaments and tools. The ornaments are bracelets and fibulae (Figure 4.35), the latter being too incomplete to allow a secure identification. Nevertheless, some of the fibulae fragments

[7] Part of the content from this section was previously published (Valério *et al.*, 2012).

(MAH4414, MAH9622 and MAH10114) are compatible with the *Acebuchal* type, which is a typology very frequent in the Portuguese territory during the EIA (Ponte, 2006).

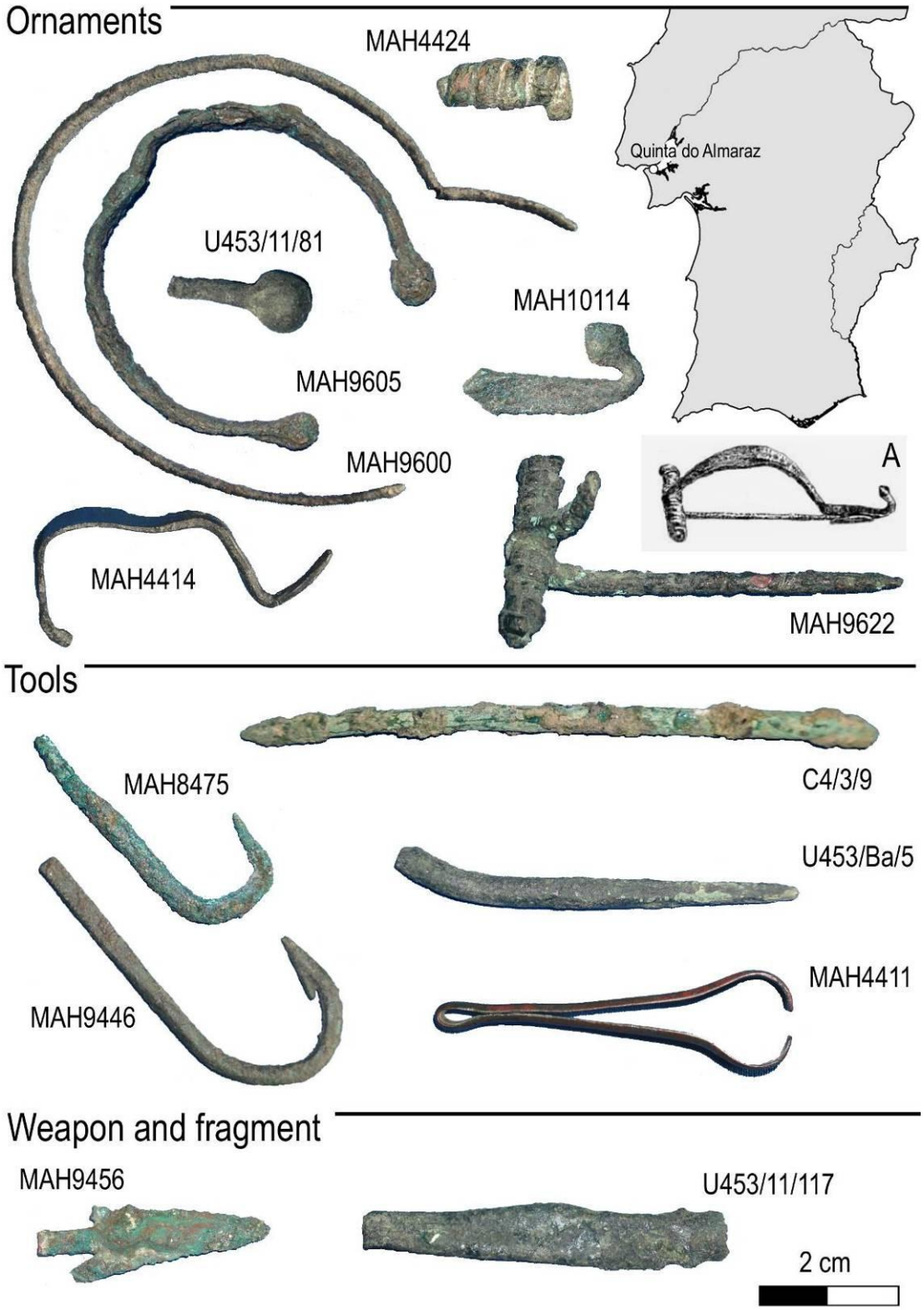

Figure 4.35. Copper-based artefacts belonging to the archaeological site of Quinta do Almaraz (A: *Acebuchal* fibula from the Iberian Peninsula, adapted from Almagro-Bash, 1966).

Tools comprise several typologies that are rather common among indigenous typologies (e.g. fish-hooks, awls, rivets and handles), whereas the tweezers (MAH4411) are relatively rare (Figure 4.35). Unsurprisingly, fish-hooks are among the more frequent typologies recovered from this riverside settlement. Fish-hooks studied present two different types – with or without barb (e.g. MAH9446 and MAH8475, respectively), which might indeed correspond to some chronological evolution (Melo *et al.*, in press). This collection of copper-based artefacts is completed by an arrowhead (MAH9456) and several fragments of unknown functionality, e.g. U453/11/7 (Figure 4.35).

The collection from Quinta do Almaraz was analysed by micro-EDXRF to determine the alloy composition (Table 4.19). The artefacts that could not be cleaned were analysed by EDXRF to identify the main constituents of the alloy.

The results evidence the presence of different groups of copper-based materials, namely "unalloyed" coppers (Sn <2% and Pb <2%), binary bronzes (Sn >2% and Pb <2%) and ternary bronzes (Sn and Pb >2%). These groups present similar contents of metallic impurities – arsenic is below detection limits in almost all artefacts, while iron present rather higher contents (0.4 ± 0.3%) when compared to the other studied collections.

Table 4.19. Results of micro-EDXRF and EDXRF analyses of copper-based artefacts from Quinta do Almaraz (values in %; *: EDXRF analysis; nd: not detected; vest: <2; +: [2, 50]; ++: >50).

Type	Artefact	Reference	Context	Cu	Sn	Pb	As	Fe
Ornament	Bracelet	MAH9600	9th-7th	93.8	5.3	0.19	nd	0.68
Ornament	Bracelet*	MAH9605	9th-7th	++	+	nd	nd	vest
Ornament	Bracelet	U453/11/81	LBA	93.8	5.9	nd	nd	0.27
Ornament	Fibula (*Acebuchal?*)	MAH4414	9th-7th	98.8	nd	0.24	0.66	0.25
Ornament	Fibula (*Acebuchal?*)	MAH9622	9th-7th	92.9	6.2	0.66	nd	0.24
Ornament	Fibula (pin)	A12/34A	9th-7th	90.9	8.0	0.19	nd	0.80
Ornament	Fibula (pin-rest)*	MAH10114	9th-7th	++	+	vest	nd	vest
Ornament	Fibula (pin-rest)*	A12/8/31A	9th-7th	++	+	vest	nd	vest
Ornament	Fibula (pin-rest)*	K311/4/17	9th-7th	++	+	vest	nd	vest
Ornament	Fibula (spring)	MAH4424	9th-7th	94.1	5.0	0.58	nd	0.29
Tool	Fish-hook*	MAH8475	9th-7th	++	+	nd	nd	vest
Tool	Fish-hook	MAH9446	9th-7th	91.5	2.4	5.9	nd	0.16
Tool	Fish-hook*	A12/8/31B	9th-7th	++	+	vest	nd	vest
Tool	Fish-hook	J274/4/19	9th-7th	92.0	7.2	0.16	nd	0.58
Tool	Awl	C4/3/9	9th-7th	94.3	5.3	0.23	nd	0.16
Tool	Awl	U453/Ba/5	LBA	95.6	3.2	0.63	nd	0.42
Tool	Rivet	J294/5/10	9th-7th	97.8	1.2	<0.10	nd	0.91
Tool	Rivet (?)	A12/34B	9th-7th	99.7	nd	<0.10	<0.10	0.21
Tool	Situla handle	MAH4403	EIA	99.6	nd	<0.10	<0.10	0.36
Tool	Tweezers	MAH4411	9th-7th	88.9	6.2	4.6	nd	0.27
Weapon	Arrowhead	MAH9456	9th-7th	91.5	8.1	0.20	nd	0.15
Unknown	Fragment	A12/4/19A	9th-7th	97.0	1.4	1.1	nd	0.45
Unknown	Fragment	U453/11/117	LBA	98.1	1.4	0.10	nd	0.31
Unknown	Fragment	A12/4/19B	9th-7th	96.7	2.2	0.60	0.10	0.36
Unknown	Fragment	A12/8/31A	9th-7th	99.3	nd	0.41	nd	0.27
Unknown	Fragment	J282/4/12A	9th-7th	97.8	1.6	0.18	nd	0.37
Unknown	Fragment	A12/8/31B	9th-7th	90.8	7.7	0.16	nd	1.3
Unknown	Fragment	J282/10/32A	9th-7th	94.1	4.8	0.55	nd	0.50
Unknown	Fragment	J282/6/18A	9th-7th	96.1	3.0	0.28	nd	0.64
Unknown	Fragment*	K311/4/17	9th-7th	++	+	nd	nd	vest

The ternary bronzes are represented by a fish-hook (MAH9446: 5.9% Pb) and a tweezers (MAH4411: 4.6% Pb), whereas artefacts constituted by "unalloyed" copper seem to be more related with tools than with ornaments (Figure 4.36). However, binary bronzes still constitute the more representative group at Quinta do Almaraz, but exhibiting a lower average tin content (5.4 ± 2.0%), with no noticeable difference among ornaments and tools (Figure 4.36).

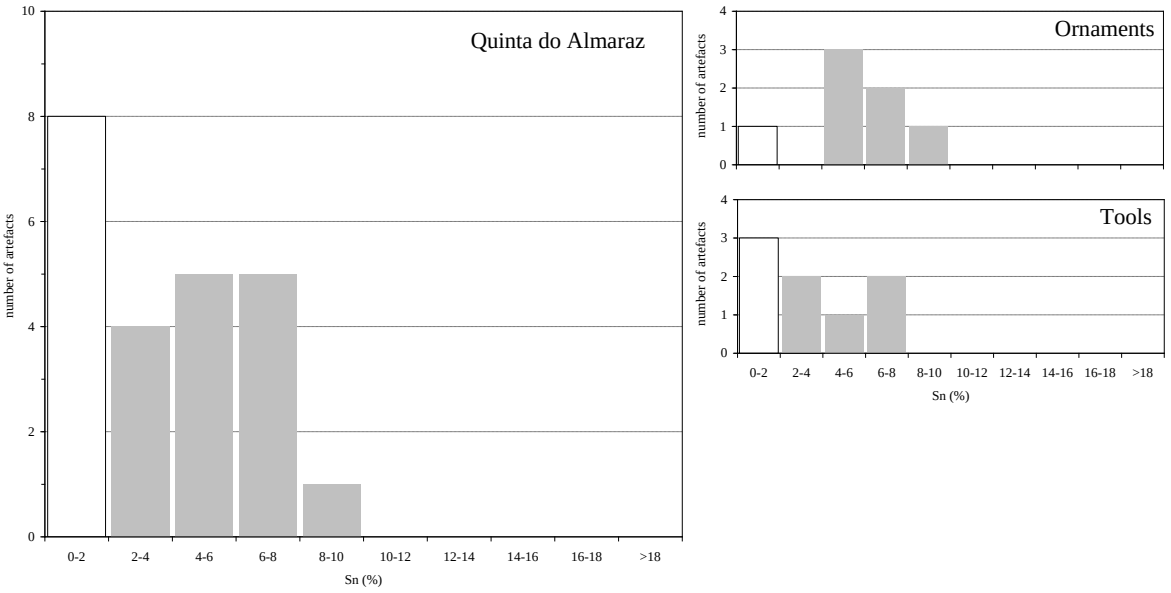

Figure 4.36. Distribution of tin contents in copper-based artefacts from Quinta do Almaraz (white columns symbolize "unalloyed" copper artefacts).

The OM characterisation evidences the microstructural homogeneity of this collection, i.e. the artefacts present monophasic and deformed equiaxial microstructures with Cu-S inclusions and having undergone forging and annealing procedures (Table 4.20).

Table 4.20. OM characterisation of copper-based artefacts from Quinta do Almaraz (*: % given by micro-EDXRF; t: annealing twins; sb: slip bands; d: heavily deformed inclusions; C: Casting; A: Annealing; F: Forging; FF: Final Forging; ↑: high amount; ↓: low amount; +: tail of arrowhead).

Type	Artefact	Reference	Sn*	Phases	Inclusions	Features		Manufacture
Ornament	Bracelet	MAH9600	5.3	α	-	equiaxial	t, sb	C+(F+A)+FF↓
Ornament	Bracelet	U453/11/81	5.9	α	Cu-S	equiaxial	t, sb	C+(F+A)+FF↑
Ornament	Fibula (*Aceb.?*)	MAH4414	nd	α	Cu-S	equiaxial	t	C+(F+A)
Ornament	Fibula (*Aceb.?*)	MAH9622	6.2	α	Cu-S	equiaxial	t, sb	C+(F+A)
Ornament	Fibula (pin)	A12/34A	8.0	α	Cu-S	equiaxial	t, sb	C+(F+A)+FF↓
Ornament	Fibula (spring)	MAH4424	5.0	α	Cu-S	equiaxial	t, sb	C+(F+A)+FF↑
Tool	Fish-hook	MAH9446	2.4	α	Cu-S	equiaxial	t, sb	C+(F+A)+FF
Tool	Fish-hook	J274/4/19	7.2	α	Cu-S	equiaxial	t	C+(F+A)
Tool	Awl	C4/3/9	5.3	α	Cu-S	equiaxial	t, sb	C+(F+A)+FF↑
Tool	Awl	U453/Ba/5	3.2	α	Cu-S↑	equiaxial	t, sb	C+(F+A)+FF
Tool	Rivet	J294/5/10	1.2	α	Cu-S	equiaxial	t, sb	C+(F+A)+FF
Tool	Rivet (?)	A12/34B	nd	α	Cu-S	equiaxial	t, sb	C+(F+A)+FF
Tool	Situla handle	MAH4403	nd	α	Cu-S	equiaxial	t, d	C+(F+A)
Tool	Tweezers	MAH4411	6.2	α	Cu-S	equiaxial	t, sb	C+(F+A)+FF
Weapon	Arrowhead^{+}	MAH9456	8.1	α	Cu-S	equiaxial	t	C+(F+A)
Unknown	Fragment	A12/4/19A	1.4	α	Cu-S↑	equiaxial	t, d	C+(F↑+A)
Unknown	Fragment	U453/11/117	1.4	α	Cu-S	equiaxial	t, d	C+(F↑+A)
Unknown	Fragment	A12/4/19B	2.2	α	Cu-S	equiaxial	t	C+(F+A)
Unknown	Fragment	A12/8/31A	nd	α	Cu-S↑	equiaxial	t	C+(F+A)
Unknown	Fragment	J282/4/12A	1.6	α	Cu-S	equiaxial	t, d	C+(F+A)
Unknown	Fragment	A12/8/31B	7.7	α	Cu-S↑	equiaxial	t	C+(F+A)
Unknown	Fragment	J282/10/32A	4.8	α	Cu-S	equiaxial	t, sb	C+(F+A)+FF
Unknown	Fragment	J282/6/18A	3.0	α	Cu-S	equiaxial	t, sb	C+(F+A)+FF↑

The absence of the α±δ eutectoid might not reflect an actual improvement in the efficiency of the annealing operation, instead being more related with the low Sn contents of these bronze alloys. Actually, reduced Sn contents result in minor quantities of the α+δ eutectoid, which under usual casting conditions arise from very low tin contents (as seen at the phase diagram, Figure 4.13). Additionally, minor α+δ eutectoid contents can be more easily homogenized into a monophasic α matrix through thermal treatment.

Microstructures with twined grains (Figure 4.37 and Figure 4.38) resulting from forging and annealing operations belong mostly to fragments of unknown functionality and represent about 43% of the collection. The fibula MAH4414 and the situla handle MAH4403 exhibit rather larger

grain sizes due to lower deformation intensity and/or extreme annealing conditions (Figure 4.37A and C).

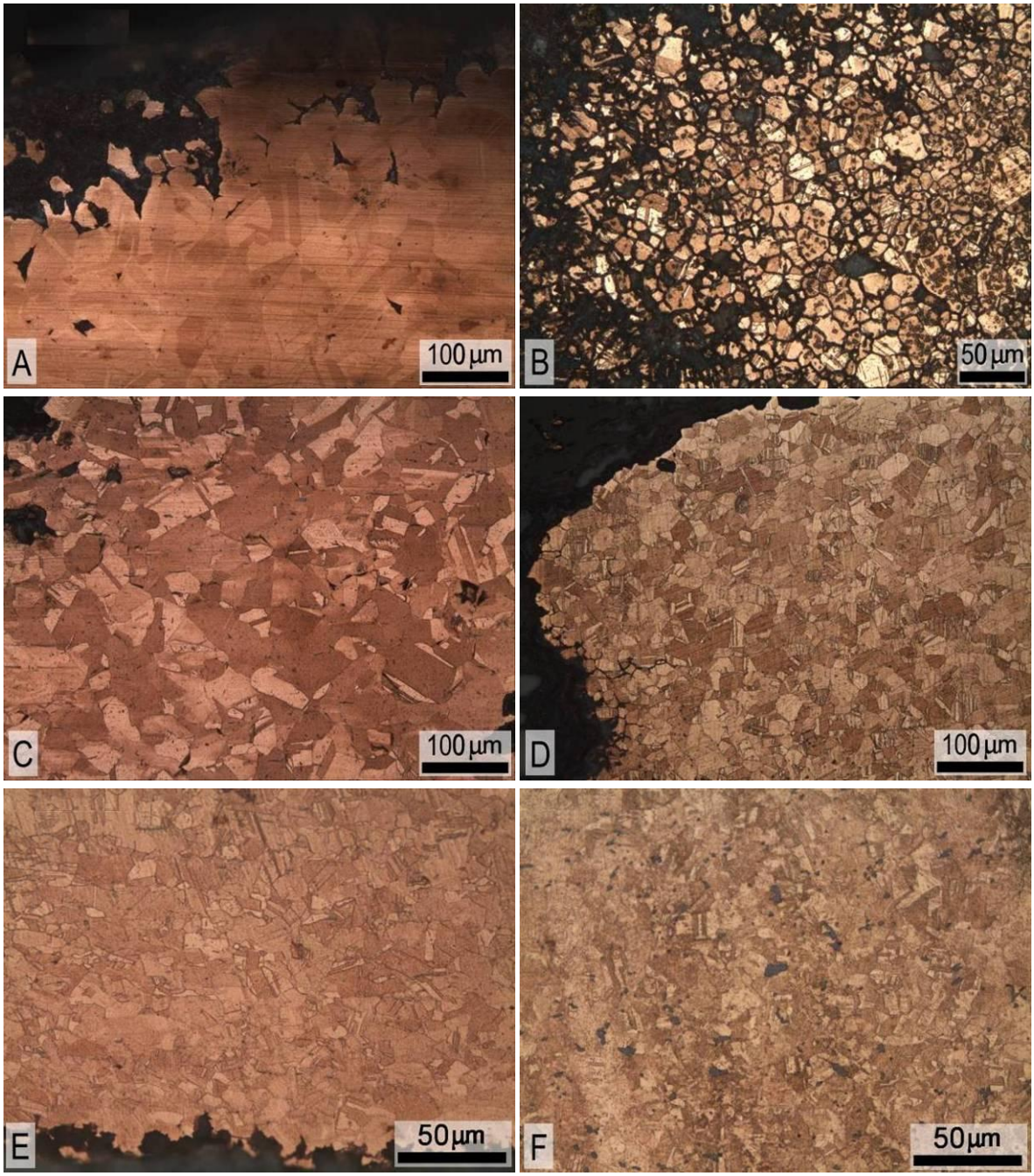

Figure 4.37. Microstructures of copper-based artefacts from Quinta do Almaraz with forging and annealing work (A: fibula MAH4414; B: fish-hook J274/4/19; C: situla handle MAH4403; D: arrowhead MAH9456; E: fragment J282/4/12A and F: fragment A12/8/31B; all OM-BF, etched).

A particular group of fragments, also exhibiting deformed equiaxial microstructures with annealing twins, revealed further interesting microstructural features (Figure 4.38). Cu-S morphologies consist on more or less elongated inclusions set along the original axe of the fragment, which indicate the deformation carried out – a bar was initially flattened and subsequently folded. Grains

with very different sizes also determine an uneven deformation of certain areas, e.g. inner and outer fold regions of fragment U453/11/117. These characteristics clearly establish a peculiar manufacture procedure consisting on the use of a thin sheet of metal that is folded in order to form a bar with a thicker section. However, the specific purpose of this type of folded fragments is still unclear (e.g. could they correspond to a particular typology of artefacts?).

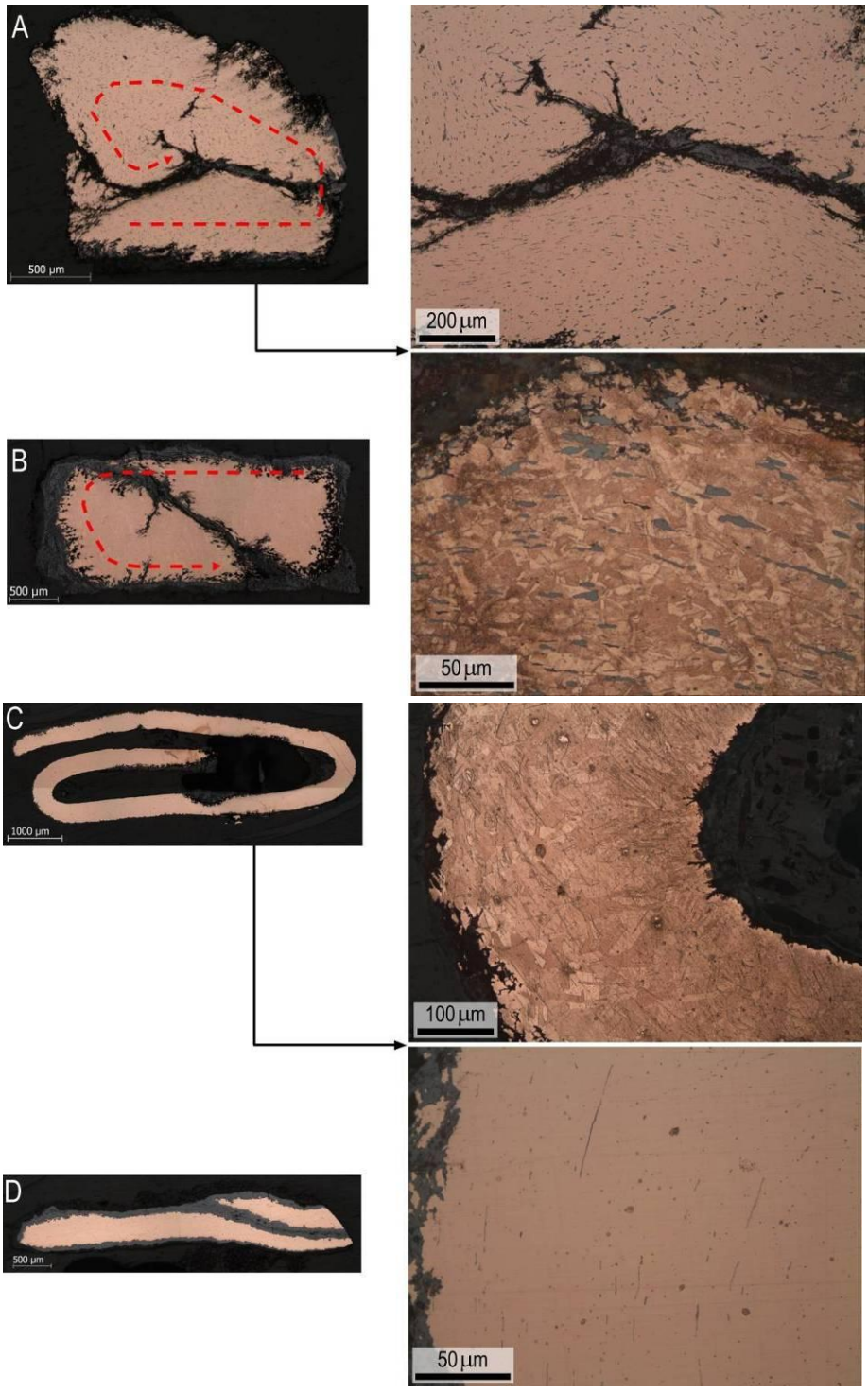

Figure 4.38. Microstructures of copper-based artefacts from Quinta do Almaraz composed by sheet metal folded upon itself (A: fragment A12/4/19A; B: fragment A12/8/31A; C: fragment U453/11/117; D: fragment A12/4/19B; all OM-BF, non-etched, except A2 and C1: OM-BF, etched).

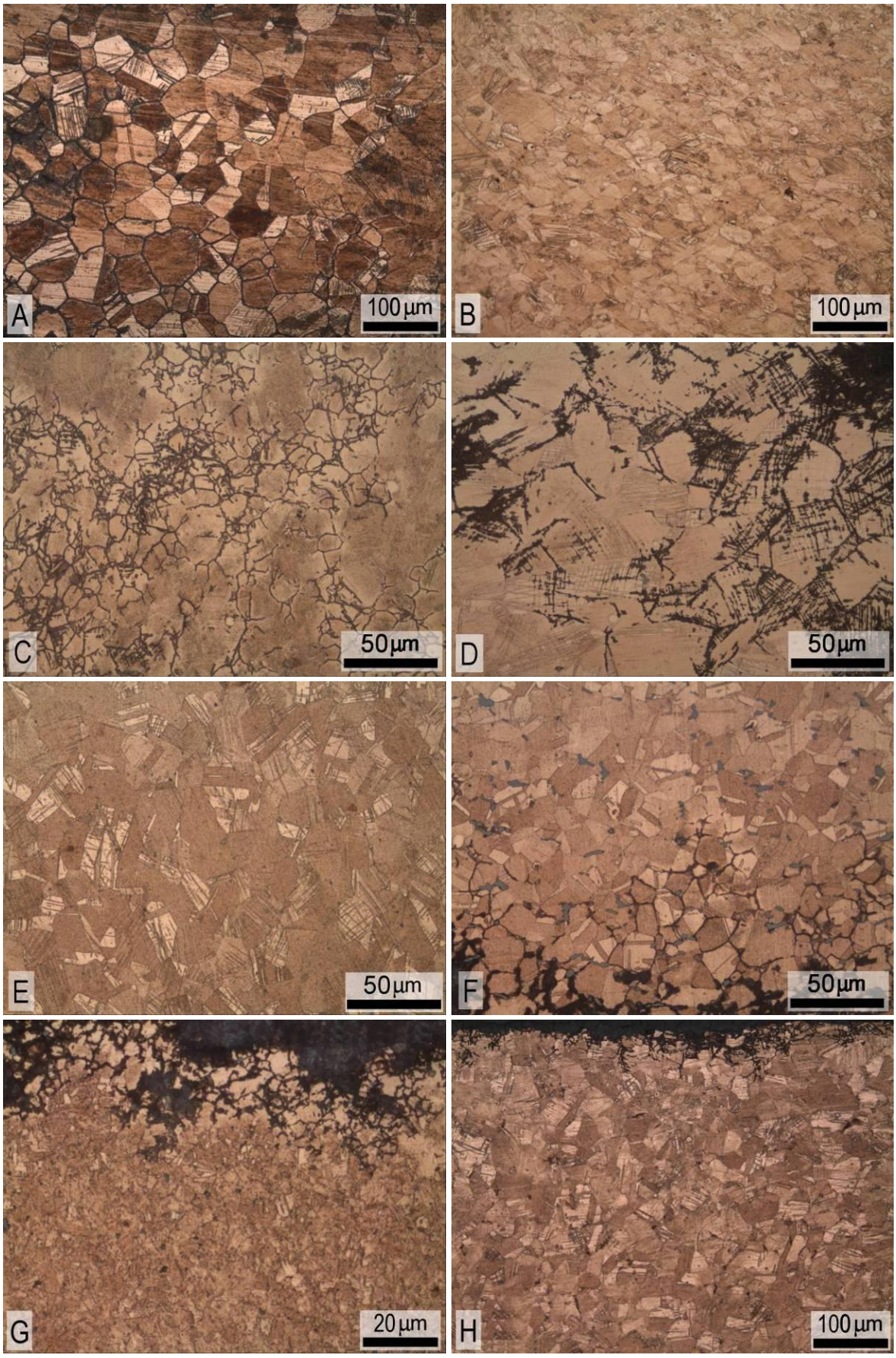

Figure 4.39. Microstructures of copper-based artefacts from Quinta do Almaraz with forging, annealing and final forging work (A: bracelet MAH9600; B: bracelet U453/11/81; C: fibula pin A12/32A; D: fibula spring MAH4424; E: awl C4/3/9; F: awl U453/Ba/5; G: fragment J282/10/32A; H: fragment J282/6/18A; all OM-BF, etched).

The type of microstructure more common presents recrystallized grains with annealing twins and slip bands, accounting for 57% of the set (Figure 4.39). The slip band density evidently increases from the bracelet MAH9600 and fibula pin A12/32A, up to the fibula spring MAH4424 and awl C4/3/9 (Figure 4.39A, C and D, respectively). The higher level of Cu-S inclusions of the awl U453/Ba/5 (Figure 4.39F) should also be mentioned, as well as the considerably small grain size of the fragment J282/10/32A (Figure 4.39G), which indicates more efficient forging and annealing cycles.

The microstructures identified in two fragments from Quinta do Almaraz (deformed equiaxial grains with variable features along the section) are consistent with the microstructure of a rivet (Figure 4.40). The head of the rivet J294/5/10 present heavily deformed grains with much smaller size due to the higher deformation, probably induced by the riveting process. The higher deformation of certain regions is also noticeable by corrosion paths (Figure 4.40B, head), which most likely resulted from preferential corrosion of more impure regions and, currently, enhances the original deformation of the microstructure.

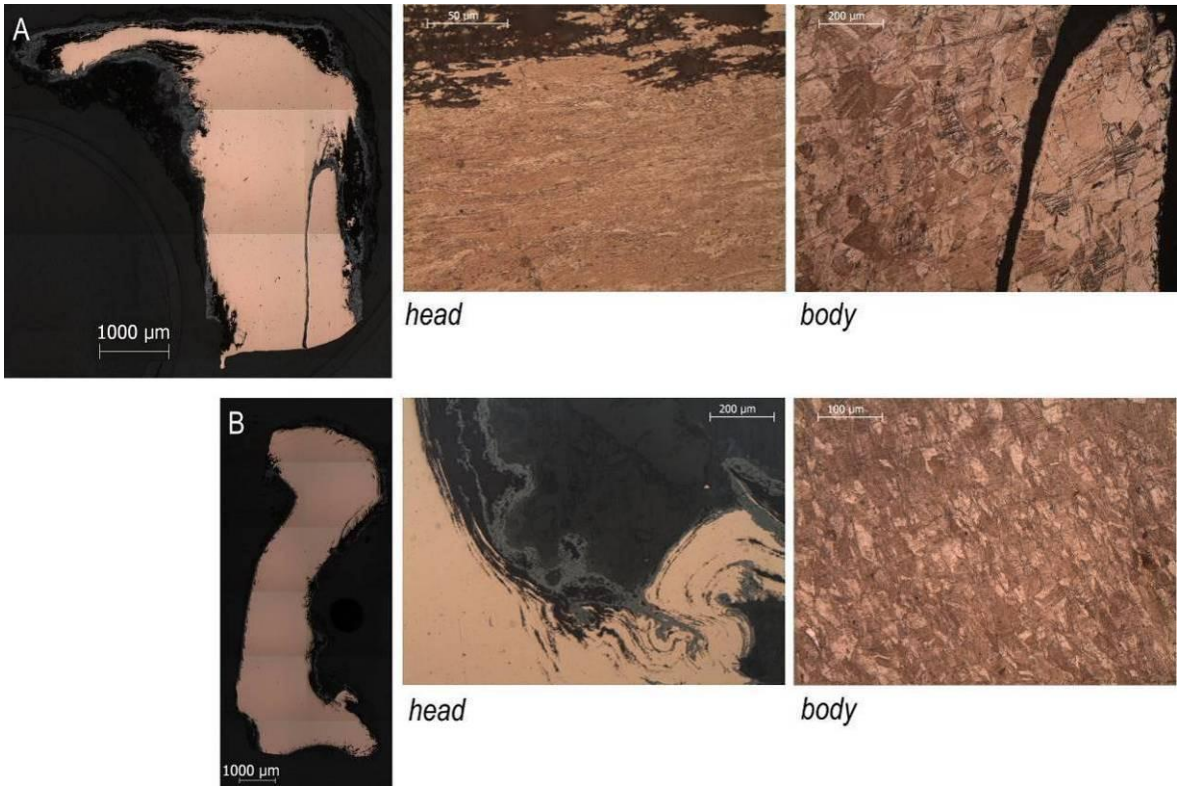

Figure 4.40. Microstructures of copper-based rivets from Quinta do Almaraz (A: J294/5/10; B: A12/34B).

SEM-EDS analyses on the fibula MAH9622 (0.66% Pb), fish-hook MAH9446 (5.9% Pb) and tweezers MAH4411 (4.6% Pb) evidence the enhanced presence of lead rich inclusions from binary to ternary bronze alloys (Figure 4.41). For low Pb contents, these inclusions present mainly

globular morphologies dispersed along the microstructure due the low miscibility of lead in bronze. At higher Pb contents, these low melting point inclusions highlight the primary interdendritic regions that were the last to solidify. In these microstructures, the common Cu-S inclusions were also identified, being sometimes associated with Fe-S inclusions especially for alloys with higher Fe contents. However, these Cu-S/Fe-S inclusions cannot be differentiated from Cu-S inclusions with SEM-BSE images.

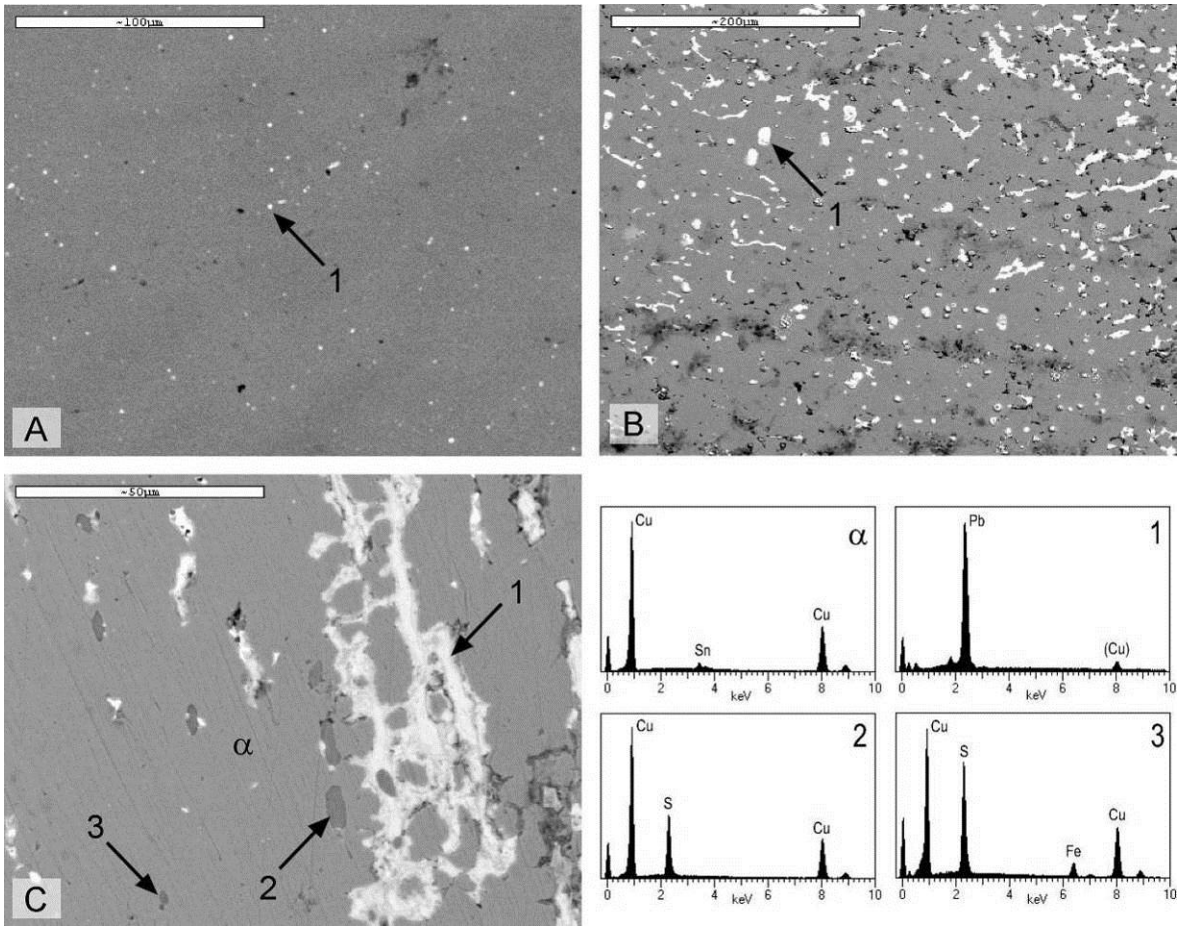

Figure 4.41. Microstructures of (A) fibula MAH9622; (B) fish-hook MAH9446; (C) tweezers MAH4411 from Quinta do Almaraz (SEM-BSE images with EDS spectra of α phase; 1: Pb rich inclusion; 2: Cu-S inclusion; 3: Cu-S/Fe-S inclusion).

Vickers testing on selected artefacts from Quinta do Almaraz shows a collection with highly variable hardness – from 97 to 237 HV0.2 (Table 4.21). Despite their relatively low tin contents (~5-6% Sn) some of these bronzes exhibit a very high hardness. The high value of the fibula MAH4424 (221 HV0.2) is certainly related with a tougher final deformation, as evidenced by a high density of slip bands (Figure 4.39D). On the other hand, the high hardness of the fragment J282/10/32A (237 HV0.2) should be more related with extremely efficient forging and annealing cycles, proven by a very small grain size (Figure 4.39G). The importance of the grain size is also evident in the high hardness of the recrystallized fragment A12/8/31B (158 HV0.2).

Microstructures with very small grain size rely on a very good control over the annealing procedure since too much time or temperature will readily produce a large grain size microstructure, such as the one of the situla handle MAH4403 (Figure 4.37C). Finally, it should be mentioned that the low hardness of the arrowhead MAH9456 (97 HV0.2) corresponds to the tail and not to the head, which could not be sampled due to conservational issues.

Table 4.21. Vickers microhardness of copper-based artefacts from Quinta do Almaraz (relevant elemental and microstructural data obtained by micro-EDXRF and OM analyses is also presented).

Type	Artefact	Reference	Sn (%)	Phases	Manufacture	HV0.2
Ornament	Bracelet	U453/11/81	5.9	α	C+(F+A)+FF↑	204
Ornament	Fibula (*Aceb.?*)	MAH9622	6.2	α	C+(F+A)	103
Ornament	Fibula (spring)	MAH4424	5.0	α	C+(F+A)+FF↑	221
Tool	Awl	C4/3/9	5.3	α	C+(F+A)+FF↑	142
Tool	Awl	U453/Ba/5	3.2	α	C+(F+A)+FF	113
Tool	Rivet	J294/5/10	1.2	α	C+(F+A)+FF	117
Tool	Rivet (?)	A12/34B	nd	α	C+(F+A)+FF	140
Weapon	Arrowhead	MAH9456	8.1	α	C+(F+A)	97
Unknown	Fragment	A12/4/19A	1.4	α	C+(F↑+A)	150
Unknown	Fragment	A12/8/31A	nd	α	C+(F+A)	108
Unknown	Fragment	J282/4/12A	1.6	α	C+(F+A)	133
Unknown	Fragment	A12/8/31B	7.7	α	C+(F+A)	158
Unknown	Fragment	J282/10/32A	4.8	α	C+(F+A)+FF	237
Unknown	Fragment	J282/6/18A	3.0	α	C+(F+A)+FF↑	158

4.3.4. Palhais

During 2008, emergency archaeological excavations conducted at the site of Palhais (Beja) uncovered a rectangular structure, 1 cremation and 3 inhumation tombs that certainly belong to a much larger necropolis. The copper-based artefacts were recovered from two inhumation tombs, whose material culture ascribes to the 6th century BC – besides the typological significant copper-based collection the tombs also contained iron weapons, vitreous bead necklace, silver bead necklace with pendant, a scarab naming *Amun-Re* and circular scaraboid (Santos *et al.*, 2009).

The collection of 10 copper-based artefacts (Figure 4.42) is composed by typologies that are unique in the Portuguese Proto-historic record, such as the two toilet instrument sets, comprising *scalptorium* (nail-cleaner?), spatula and spoon (ear-scoop?). The belt-lock should also be

mentioned since it is decorated with palm leaves, a motif characteristic of the Eastern Mediterranean region, where it was a fertility symbol related with the *Astarté* divinity. An almost exact replica of this belt-lock was found at the 7th-6th centuries BC necropolis of Cruz del Negro (Monteagudo, 1953). The fibula belongs to the *Alcores* type, exhibiting a flat bow with a decoration pattern of circles, also observed in some of the elements from the toilet sets. The *Alcores* fibulae are very common in the Southwestern Iberian Peninsula, being related with the *Béncarron* type, which is present at Castro dos Ratinhos.

Figure 4.42. Copper-based artefacts belonging to the archaeological site of Palhais (A: *Alcores* fibula from Collado de los Jardines, SE Spain, adapted from Almagro-Bash, 1966).

The elemental composition of the metallic collection from Palhais was determined by micro-EDXRF analyses (Table 4.22). The belt-lock was not sampled nor cleaned due to its relevant archaeological and museological significance. Additionally, the advanced state of corrosion at the wire and ring also prevented their quantitative analysis. These artefacts were analysed by EDXRF to establish the main constituents of the alloy.

Table 4.22. Results of micro-EDXRF and EDXRF analyses of copper-based artefacts from Palhais (values in %; *: EDXRF analysis; nd: not detected; vest: <2; +: [2, 50]; ++: >50).

Type	Artefact	Reference	Context	Cu	Sn	Pb	As	Fe
Ornament	Belt-lock*	S2/M6	EIA	++	+	vest	nd	vest
Ornament	Fibula (*Alcores*)	S1/M1	EIA	93.3	6.1	0.12	0.17	0.34
Tool	*Scalptorium*	S1/M4	EIA	95.4	2.9	0.14	0.71	0.78
Tool	*Scalptorium*	S2/M8	EIA	97.0	2.0	<0.10	<0.10	0.92
Tool	Spatula	S1/M2	EIA	95.0	3.2	0.15	0.77	0.85
Tool	Spoon	S1/M3	EIA	90.4	8.3	0.76	<0.10	0.51
Tool	Spoon	S2/M7	EIA	96.9	2.2	<0.10	<0.10	0.82
Tool	Rod	S1/M5	EIA	93.0	6.0	0.33	<0.10	0.52
Tool	Wire*	S2/M9	EIA	++	vest	nd	nd	vest
Unknown	Ring*	S2/M10	EIA	++	+	nd	vest	vest

This collection of artefacts is constituted by binary bronze alloys with a low average tin content (4.4 ± 2.4%). The low tin content of some of these alloys (especially, *scalptoria*, spatula and spoon) results in lower castability (due to higher *liquidus* and *solidus* temperatures, as well as narrow temperature solidification range), in addition to lower strength and less capability to strain hardening through cold work. Some of the common metallic impurities present low contents, namely of lead and arsenic. However, the iron contents are rather high (0.7 ± 0.2%) being only comparable to the values from the collection of Quinta do Almaraz (0.4 ± 0.3%).

Optical microscopy observations of these bronze alloys identified deformed equiaxial microstructures with annealing twins and slip bands (Table 4.23). In addition, the presence of copper sulphide inclusions in a monophasic α matrix is a common feature to all observed microstructures. Microstructural characteristics indicate that the manufacture of artefacts included one or more cycles of forging and annealing. Moreover, artefacts were finished with a more or less evident final hammering operation that would leave the alloy in a more strain hardened condition. This final hammering operation might intent to produce a harder material or to remove any surface imperfections, whereas this latter option would probably only produce microstructural deformation in areas located closer to the surface.

Table 4.23. OM characterisation of copper-based artefacts from Palhais (*: % given by micro-EDXRF; t: annealing twins; sb: slip bands; d: heavily deformed inclusions; C: Casting; A: Annealing; F: Forging; FF: Final Forging; ↑: high amount; ↓: low amount).

Type	Artefact	Reference	Sn*	Phases	Inclusions	Features		Manufacture
Ornament	Fibula (*Alcores*)	S1/M1	6.1	α	Cu-S	equiaxial	t, sb	C+(F+A)+FF↑
Tool	Scalptorium	S1/M4	2.9	α	Cu-S	equiaxial	t, sb, d	C+(F+A)+FF
Tool	Scalptorium	S2/M8	2.0	α	Cu-S	equiaxial	t, sb, d	C+(F+A)+FF↓
Tool	Spatula	S1/M2	3.2	α	Cu-S	equiaxial	t, sb, d	C+(F+A)+FF
Tool	Spoon	S1/M3	8.3	α	Cu-S↑	equiaxial	t, sb, d	C+(F+A)+FF
Tool	Spoon	S2/M7	2.2	α	Cu-S	equiaxial	t, sb, d	C+(F+A)+FF↓
Tool	Rod	S1/M5	6.0	α	Cu-S↑	equiaxial	t, sb, d	C+(F+A)+FF

Microstructures present different grain sizes (e.g. the *scalptorium* S2/M8 exhibit noticeable smaller grain size, Figure 4.43C) as result from variations in the processing parameters. These variations consist of different deformation levels induced by hammering and diverse heat treatment conditions (temperature and/or time of operation). Copper sulphide inclusions are often elongated along the preferential deformation plane of the artefact, evidencing the higher deformation applied through the entire process. These elongated morphologies indicate the working of an originally larger cross-sectioned bar into a thinner rod, consequently discarding the possibility of the casting of the artefact into its final shape. As it was noticeable along the microstructural characterisation of the artefacts studied in this work, the intergranular corrosion is a regular characteristic of archaeological bronze alloys. This type of corrosion advances faster along the grain boundaries, being clearly visible in the regions closer to the cross-section surface (e.g. Figure 4.43G). Additionally, the archaeological bronze artefacts that were finished by hammering often present intragranular corrosion, which progresses mainly along preferential crystallographic planes (e.g. Figure 4.43H). Intragranular corrosion evidences the slip bands, especially in the regions more altered, being a very useful indicator of the type of manufacturing process.

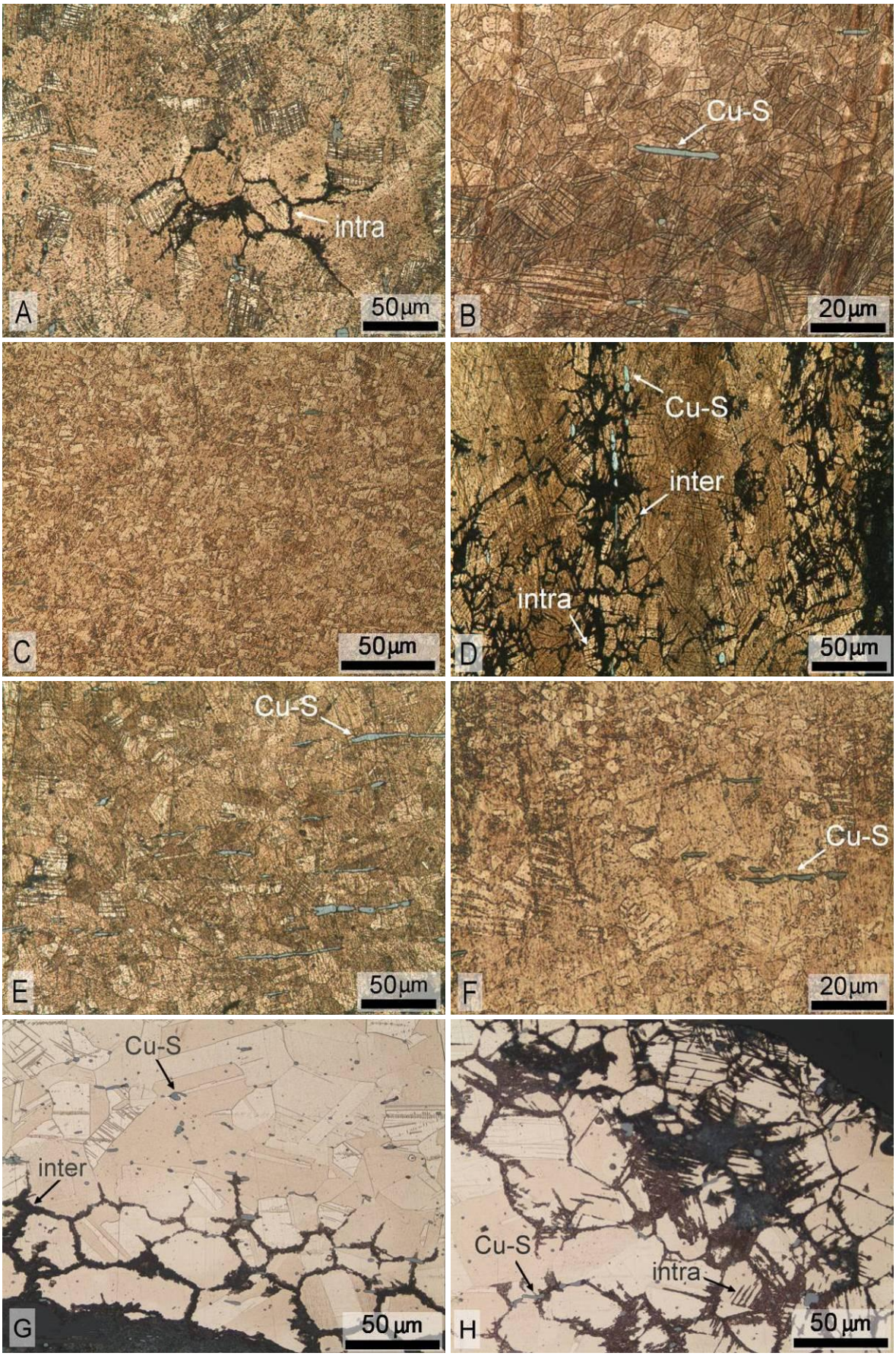

Figure 4.43. Microstructures of copper-based artefacts from Palhais, evidencing forging, annealing and final forging work (A: fibula S1/M1; B: *scalptorium* S1/M4; C: *scalptorium* S2/M8; D: spatula S1/M2; E: spoon S1/M3; F: spoon S2/M7; G and H: rod S1/M5; inter: intergranular corrosion; intra: intragranular corrosion; all OM-BF, etched).

The rod S1/M5 was selected for further characterisation by SEM-EDS (Figure 4.44). This study identified Pb rich inclusions dispersed in small globules (Cu and Sn peaks in EDS spectrum of the Pb rich inclusion are mainly from the surrounding Cu-Sn matrix) due to the relatively low Pb content (0.33%). Cu-S inclusions were also identified, often in association with Fe-S inclusions.

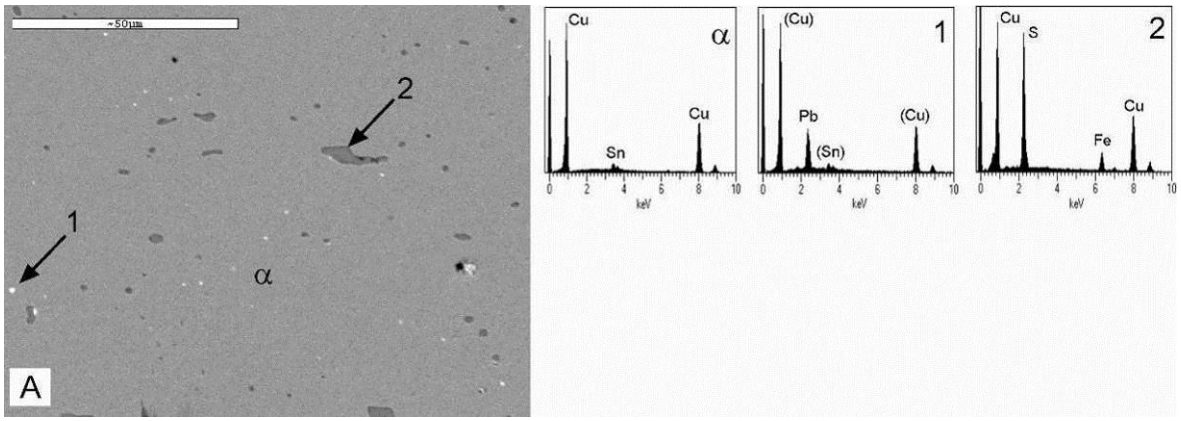

Figure 4.44. Microstructure of rod S1/M5 from Palhais (A: SEM-BSE image with EDS spectra of α phase; 1: Pb rich inclusion; 2: Cu-S/Fe-S inclusion).

The rod S1/M5 was submitted to Vickers testing to determine the hardness of the material (Table 4.24). Despite the final forging procedure applied during the manufacture of this rod, the obtained hardness is rather low (114 HV0.2). Therefore, it seems that the final deformation was not enough to compensate soften produced by an intense annealing operation, as evidenced by the rather large grain size of this microstructure (Figure 4.43G and H).

Table 4.24. Vickers microhardness of copper-based artefacts from Castro dos Ratinhos (relevant elemental and microstructural data obtained by micro-EDXRF and OM analyses is also presented).

Type	Artefact	Reference	Sn (%)	Phases	Manufacture	HV0.2
Tool	Rod	S1/M5	6.0	α	C+(F+A)+FF	114

4.4. Discussion

Despite the small number of copper-based artefacts from the EBA/MBA that were studied, their elemental compositions allow some important considerations regarding the metallurgy at the southern Portuguese territory before the full development of bronzes. Obtained results permit an initial incorporation of the EBA/MBA metallurgy of the southern Portuguese region in the already known metallurgy of neighbouring areas from the Iberian Peninsula.

The study established that the local EBA/MBA artefacts usually present significant contents of arsenic, while the majority of them were manufactured with forging and annealing operations (Figure 4.45). The operational sequences C+(F+A) and C+(F+A)+FF were considered together since the existence or not of the final forging operation in these type of large artefacts seems to be more related with the area analysed (e.g. edge versus centre of the blade) than with an actually different method of manufacture. The results establish that most artefacts were manufactured with forging and annealing, despite some evidences of a rather primitive control of the different metallurgical operations. Inverse segregation of arsenic indicates uncontrolled cooling rates during the casting operation, which difficult any latter homogenisation heat treatment. Arsenic oxide inclusions indicate not enough reducing environment during melting. Additionally, the use of reduced temperatures during the annealing procedure results in heterogeneous microstructures containing segregation bands and arsenic-rich phases. The arsenic retained in oxide inclusions and arsenic-rich phases reduces the arsenic content of the α-phase solid solution, thus decreasing the actual improvement of mechanical properties.

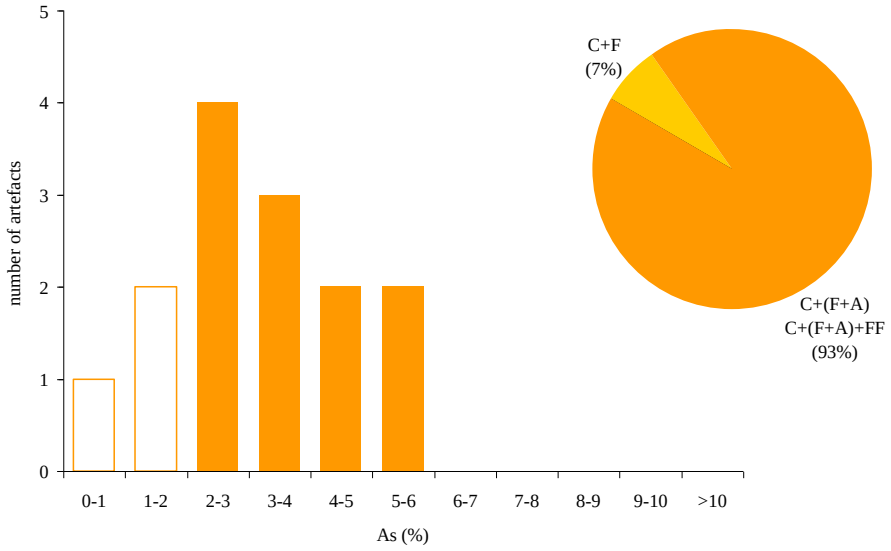

Figure 4.45. Distribution of arsenic contents and frequencies of operational sequences in EBA/MBA artefacts studied (n=14; white column symbolize artefacts with arsenic content below the limit usually utilised for arsenical copper alloys).

According to Rovira (2004), the frequencies of operational sequences applied during the EBA and MBA at the Iberian Peninsula still exhibit a strong Chalcolithic influence despite the increased utilization of the annealing operation (Figure 4.46). Almost 40% of the MBA artefacts were still produced by cold forging instead of by the more complete manufacturing procedure that involves one or more forging and annealing cycles.

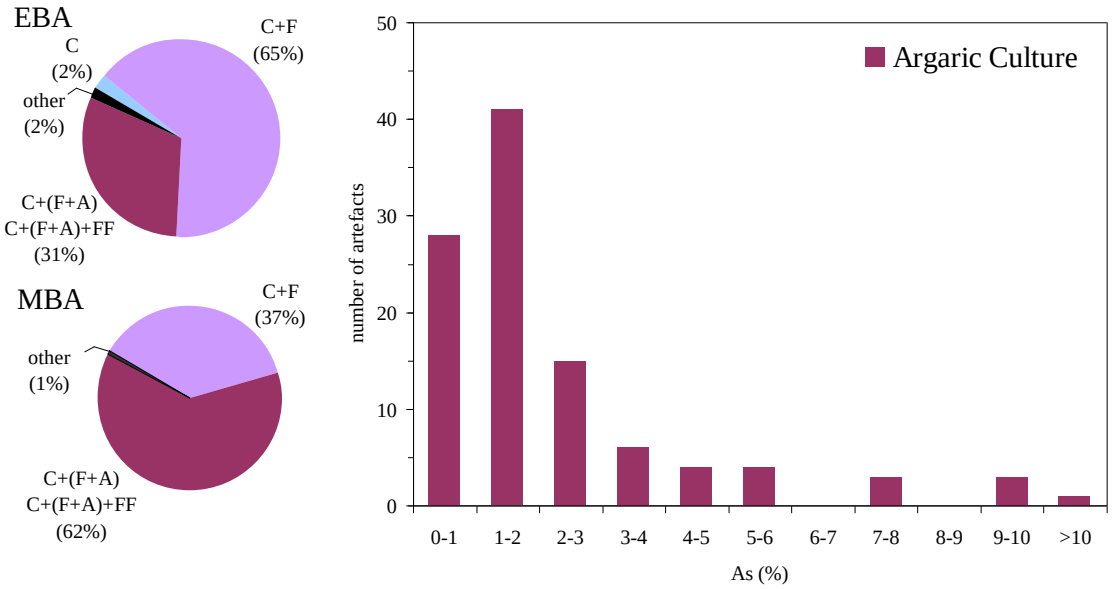

Figure 4.46. Relative frequencies of operational sequences (other comprise C+A and C+A+F) applied during the EBA and MBA at the Iberian Peninsula and distribution of arsenic contents in copper-based artefacts belonging to the Argaric Culture (modified from Rovira, 2004).

This consideration clearly differs from the results obtained for the EBA/MBA artefacts from the southern Portuguese territory, which were mostly manufactured with forging and annealing cycles. In fact, the combined use of mechanical and thermal operations was already commonly used among certain regions during the CA (see for instance Valencina de la Concepción, SW Spain, Nocete, 2008). This might imply some regional differences regarding the metallurgical technology, but the reduced number of EBA/MBA artefacts analysed from the southern Portuguese territory prevents any further conclusions.

The integration of the compositional results from the southern Portuguese territory in the metallurgy of the Iberian Peninsula was made by comparison with the statistically significant collection of metallic artefacts from the Argaric Culture at southeastern Spain (Figure 4.46). This last collection can be considered representative of the southwestern region, in the sense that the majority of these also exhibit low arsenic content (Hunt-Ortiz, 2003). The distribution of arsenic contents of EBA/MBA artefacts from the southern Portuguese territory is comparable to results from the Argaric Culture. However, the Portuguese collection seems to exhibit a somewhat higher frequency of artefacts with increased arsenic content (2-6%), which might be related with the typologies and the relatively small number of artefacts studied. A previous work had already evidence the higher arsenic content of some Chalcolithic typologies, namely Palmela points, saws, long awls and tanged daggers (Müller *et al.*, 2007). The lighter colour of arsenical copper can be easily identified and chosen for specific typologies. This selection can either be related with the colour of this alloy or with the knowledge of the toughen effect of arsenic in copper. Alternatively, the fact that mostly analysed artefacts become from burials can also explain the higher arsenic

contents. Contrary to the artefacts recovered from settlements, burial offerings were removed from circulation at the time of burial. Considering that the recycling of scrap was already carried out during those ancient times, it is certain that common artefacts will endure more recycling cycles during their larger life span (Rovira, 2004). Each melting of an arsenical copper alloy induces arsenic losses by oxidation and evaporation of As_2O_3 fumes. The efficient control of the reducing atmosphere during melting and annealing has important consequences in the arsenic content of copper-based artefacts (Mckerrell and Tylecote, 1972).

The sustained study of additional EBA/MBA artefacts and production remains in a near future will certainly provide a clearer characterisation of the evolution of the copper-based metallurgy in this region throughout the 2nd millennium BC. This could provide a better understanding about the "origin" of arsenic in copper artefacts, whereas it will possibly identify the introduction and spread of bronze alloys within the southern Portuguese territory.

The composition of the copper-based artefacts belonging to the following chronological period changes considerably, with the substitution of copper and arsenical copper by bronze alloys during the LBA. Furthermore, the composition of LBA and EIA artefacts analysed in the present work, unmistakably discriminate two different clusters, which will be designated as "indigenous" and "orientalising" (Figure 4.47).

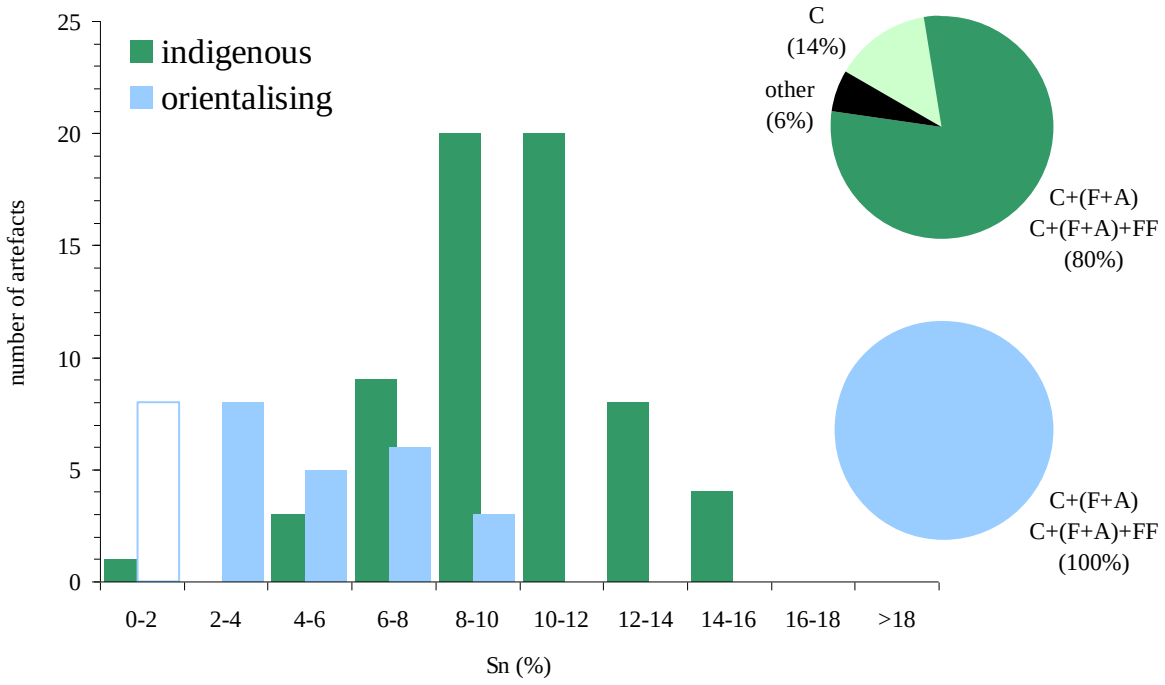

Figure 4.47. "Indigenous" *versus* "orientalising" – distribution of tin contents and frequencies of operational sequences (other comprise C+A and C+A+F) in copper-based artefacts from the "indigenous" cluster (Entre Águas 5, Baleizão, Santa Margarida, Salsa 3, Quinta do Marcelo and Castro dos Ratinhos) and "orientalising" cluster (Quinta do Almaraz and Palhais).

The "indigenous" cluster is composed by artefacts from Entre Águas 5, Baleizão, Santa Margarida, Salsa 3, Quinta do Marcelo and Castro dos Ratinhos (65 artefacts). This cluster designates a metallurgy characterised by the presence almost exclusive of binary bronze alloys. Leaded bronzes are absent and only 1 exemplar is composed by unalloyed copper. These binary bronzes present "suitable" tin contents, that is to say a "normal" distribution with an average of 10.0 ± 2.5% Sn. Furthermore, alloys with higher tin contents were utilised in typologies that do not require high mechanical strength, such as rings ("finger-rings"?), balance weights and fibulae. Considering similar casting conditions, an increased tin content results in a more significant presence of the α+δ eutectoid, which make the alloy more brittle and difficult to toughen by forging. Furthermore, this α+δ eutectoid is always present for tin concentrations above ~14%. Therefore, functional tools and ornaments usually present lower tin contents that can easily be thermally homogenized. The higher tin content of rings, balance weights and fibulae could also be associated with their colouring, i.e. as-cast artefacts with increased tin concentrations present a more yellowish-brown tint that could be considered more suitable for prestige artefacts (Giumlia-Mair, 2005b). All these features indicate not only a good control over the tin content of the bronze alloy, but also an advanced knowledge over the mechanical and physical implications of tin additions to copper.

The cluster of "orientalising" metallurgy is composed by artefacts from the chronological latter sites of Quinta do Almaraz and Palhais (30 artefacts). However, it is especially remarkable to verify that the metallurgy in attendance at Castro dos Ratinhos (coeval with Quinta do Almaraz) is not related with this "orientalising" cluster. In fact, despite the obvious Mediterranean influences present at this settlement, its artefacts are strongly correlated with the metallurgy inherited from the LBA. Regarding the "orientalising" cluster, the compositional results evidence the growing importance of unalloyed coppers (relative frequency of 27%) and leaded bronzes (relative frequency of 7%), even if binary bronzes are still the favoured alloy (relative frequency of 66%). The distribution of the tin contents in these binary bronzes is also different, presenting lower values with an average of 5.1 ± 2.1% Sn (Figure 4.47). An experimental work established that the recycling of a bronze alloy diminishes its tin content, i.e. a bronze with 9.5% Sn was reduced to 3.1% Sn after a few melting procedures (Sarabia-Herrero, 1992). The reduction is due to the preferential oxidation of tin during melting. Consequently, the significant use of bronze scrap without adding fresh tin might explain the presence of EIA low tin bronzes. It should be noted that none of the LBA production remains from the southern Portuguese region analysed in this work point to the recycling of bronze artefacts. Furthermore, only a comprehensive study of EIA production remains could clarify this issue.

The iron content additionally discriminates the "indigenous" and "orientalising" clusters, given that artefacts from the latter set clearly present higher iron contents (Figure 4.48). The increase of the iron contents of artefacts was also identified when comparing LBA and Phoenician-Iberian bronzes from SE Spain, namely from 0.04% to 0.27%, respectively (Craddock and Meeks, 1987). The iron content of bronze artefacts has been used as a technological indicator of the smelting process all over the Mediterranean region (Ingo *et al.*, 2006). The difference was understood to be the result of more efficient copper smelting furnaces employed by Orientalising cultures. These metallurgical extractions run under high reducing conditions, enabling the reduction of iron impurities present in copper ores, which are subsequently incorporated in the metallic bath. The raw copper obtained could be purified to iron contents down to ~0.5%, but further reduction was increasingly difficult and needless since it did not bring any noticeable improvement to the mechanical properties of the alloy (Northover, 2004).

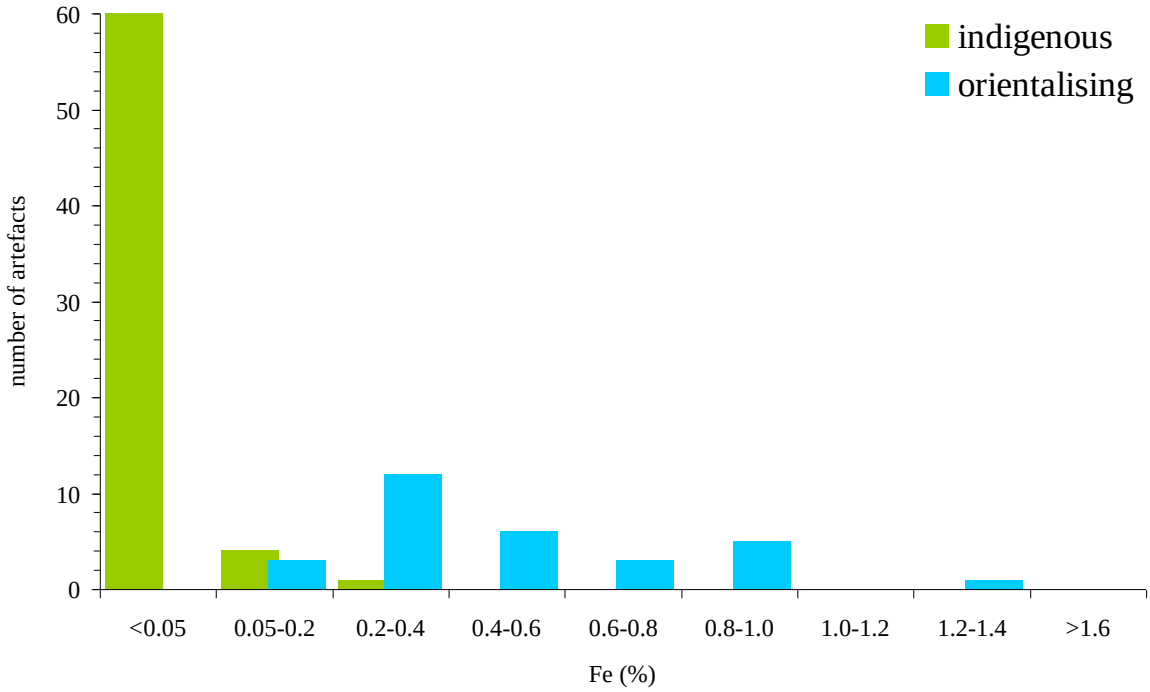

Figure 4.48. "Indigenous" *versus* "orientalising" – distribution of iron contents in copper-based artefacts from the "indigenous" cluster (65 artefacts from Entre Águas 5, Baleizão, Santa Margarida, Salsa 3, Quinta do Marcelo and Castro dos Ratinhos) and "orientalising" cluster (30 artefacts from Quinta do Almaraz and Palhais).

Earlier copper smelting "furnaces" operate under poor reducing conditions, which naturally produce copper with very low iron contents. In the Iberian Peninsula, copper smelting was conducted in the so-called crucible vases that were widely used until pre-Roman times (Delibes de Castro *et al.*, 2001; Rovira and Montero-Ruíz, 2003). The LBA production remains from the southern region of the Portuguese territory analysed in this work evidence a general absence of a strong reducing atmosphere. Furthermore, the socketed handle crucibles from Entre Águas 5

established the production of bronze inside these primitive crucible vases using a poor reducing atmosphere. Most metallic nodules confined inside the slagged material from those crucibles present low iron contents, comparable to the observed in the indigenous artefacts. The potential evidence of the use of these crucibles was also found in the Phoenician settlement of La Fonteta (Renzi *et al.*, 2009), which agrees with the absence of archaeological evidences regarding the replacement of crucibles by conventional furnaces during the EIA. However, it seems that the smelting of copper began to operate under more reducing conditions, which induced the increase of iron content of the bronze artefacts. It is possible that the need to improve the efficiency of smelting operations arise from the gradual exhaust of ores with high amounts of copper.

The majority of operational sequences applied to copper-based artefacts include forging plus annealing cycles, often terminating with a more or less evident final forging operation (Figure 4.47). Other operational sequences comprising annealing of the cast alloy followed or not by forging (i.e. C+A and C+A+F) are only residual, as has been noted in other studies concerning the early metallurgy in the Iberian Peninsula (Rovira, 2004). The more significant outcome is the fact that the replacement of "arsenical" coppers by bronzes does not produce any change in the manufacturing processes, i.e. the combined use of mechanical and thermal treatments remains customarily applied. Additionally, during the following chronological periods the differences observed between the bronze clusters at the southern Portuguese territory are not significant since as-cast artefacts from the "indigenous" group are related with typologies (balance weighs, rings, decorative parts of fibulae) and alloys with higher tin content, which are absent from the "orientalised" cluster. The fact that forging was not applied at artefacts with higher tin contents indicates a good knowledge of the technological aspects since these bronzes are more brittle and difficult to deform without fissuring.

This good technological knowledge involves the casting operation given that casting defects are rather uncommon. Two rings from Castro dos Ratinhos (D1/IIa/M4 and D2/IIa/M2) display high density of large pores due to low temperatures of mould and molten metal, while a knife from the same site (A2/IIc/M1) exhibits tin oxide inclusions probably from low casting temperature. These few exceptions remind us that even after several centuries, the casting of bronzes was not a straightforward operation. The major problem seems to be the lack of control over the cooling rate after pouring. These small artefacts will naturally cool at a very high rate, resulting in considerable coring of the as-cast microstructure (e.g. ring 392/12 from Baleizão), as well as in the formation of the $\alpha+\delta$ eutectoid (e.g. balance weight 392/25 from Baleizão), even in alloys with low tin content. However, slow cooling rates were already achievable, as the coarse microstructure of few artefacts clearly demonstrates (e.g. pendant D1/IIa/M2 from Castro dos Ratinhos). The heating of the mould

prior to the pouring operation will induce slower cooling rates. This constitutes a technological innovation of the LBA (Rovira, 2004).

Certain studied microstructures testimony that the temperatures and/or the time of operation were not enough to completely homogenise the alloy. In some extreme cases, alloys with low tin contents (e.g. needle S3/N18 from Salsa 3: 7.8% Sn; necklace-lock D1/Ib/M1 from Castro dos Ratinhos: 9.4% Sn) still exhibit the second phase richer in tin after being annealed. At the opposite edge, is the tranchet QM/1531 from Quinta do Marcelo, whose abnormal grain growth seems to indicate the use of an excessively high annealing temperature. Anyway, what seems more important is to verify that tools and weapons are almost always homogenised into a monophasic α matrix. This may indicate that the annealing operation was mastered, but only efficiently applied for typologies that require higher mechanical strength, while for certain ornaments, rings or specific tools (e.g. balance weights) the annealing operation seems to be of less importance. The only exception is the axe from 392/7 from Baleizão that presents a biphasic microstructure despite having a tin content (12.5%) that could have been completely homogenised. Finally, it should be mentioned that the fact that all "orientalising" artefacts present monophasic structures, is certainly more related with their lower tin content than with an improvement in the efficiency of annealing.

The hardness of a bronze artefact result from several factors (tin content of solid solution, precipitation of δ phase, grain size and degree of deformation). The integrated study of the hardness of metallic artefacts allows identifying which factors contribute more significantly to obtain a high hardness (Figure 4.49). Additionally, this study permits to obtain important considerations regarding the actual efficiency of operational sequences applied among "indigenous" and "orientalising" clusters. First of all, it seems quite evident that the tin content does not have a preponderant influence on the hardness of studied artefacts. Generally, the "high" tin bronzes present similar hardness to bronze alloys with lower tin contents. The results also evidence that the use of a final hammering is one of the major key factors regarding the hardness of an artefact. Strain hardened "indigenous" artefacts present a higher average hardness than recrystallized ones, i.e. 139 and 97 HV0.2, respectively. This indicates that commonly the final forging operation intended to increase the hardness of the material, instead of being merely a finishing operation (e.g. to remove surface defects). The increased hardness due to the final hammering is not so obvious at "orientalising" artefacts. Nevertheless, both strain hardened and recrystallized "orientalising" artefacts (161 and 125 HV0.2, respectively) present higher average values than the comparable "indigenous" ones. The major difference seems to be related with a smaller grain size of some "orientalising" microstructures that result in higher hardness. This suggests that the typical efficiency of the forging and annealing cycles increased, i.e. further deformation through hammering together with the correct control over the temperature and time of annealing. This

important technological evolution means that bronze artefacts from the "orientalising" cluster could be produced with good mechanical properties even with tin contents lower than the ones used by indigenous tradition. This implies that the overall reduction of the tin content in copper-based artefacts, either intended or resulting from scarcity of tin, would not be a problem in the manufacture of this type of simple artefacts. Finally, it should be mentioned that the different typologies studied do not allow discriminating between ornaments, tools or weapons, nor even among the same type of artefact (e.g. needles present variable hardness values, 94 – 164 HV0.2).

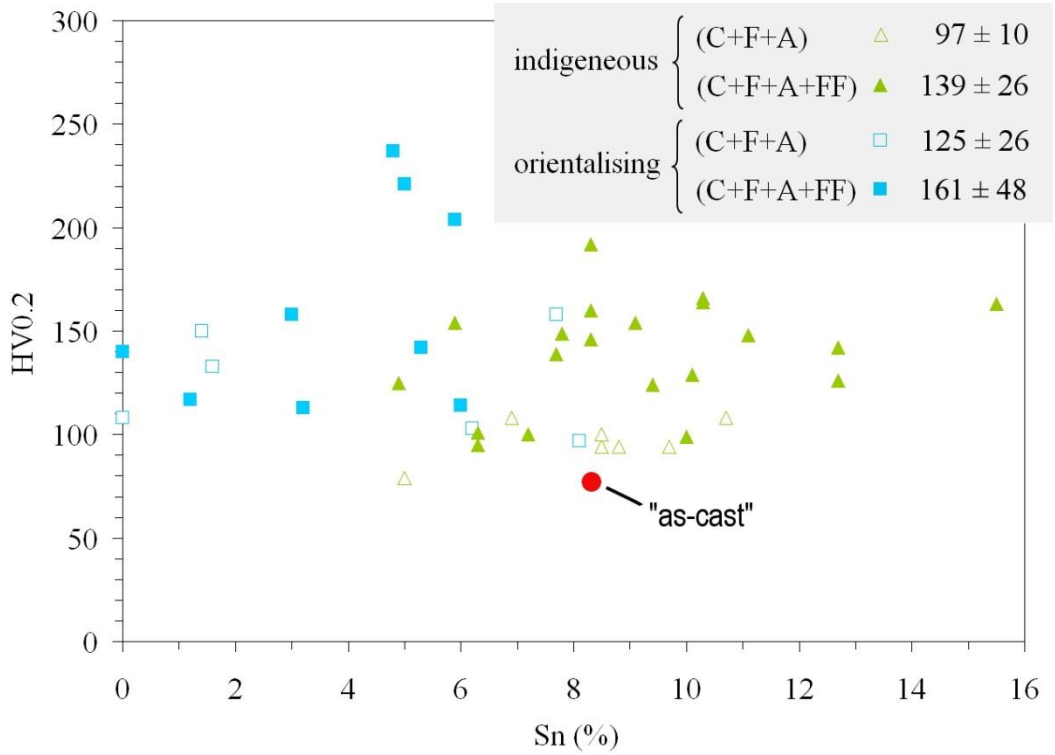

Figure 4.49. "Indigenous" *versus* "orientalising" – hardness values (average ± standard deviation) of "indigenous" artefacts (28 examples from Entre Águas 5, Baleizão, Salsa 3, Quinta do Marcelo and Castro dos Ratinhos) and "orientalising" artefacts (15 examples from Quinta do Almaraz and Palhais).

As mentioned before, the common presence of Cu-S inclusions in LBA and EIA copper-based artefacts does not necessarily imply the use of ores from primary sulphidic deposits, which usually are located deeper in the mineralization. However, the absence of Cu-S inclusions in earlier copper-based artefacts, namely from the EBA/MBA, suggests some modification involving the raw materials or the smelting conditions with the introduction of the LBA bronzes. In general, the difference might result from the selection of more pure oxidic copper ores during the earlier period, whereas the Cu-S inclusions in LBA and EIA artefacts should arise from the use of increasingly deeper oxidic ores naturally associated with sulphidic impurities. The LBA production remains from Entre Águas 5 confirm the use of these oxidic ores with significant amounts of sulphides, which are replicated in the higher amounts of Cu-S inclusions among the local bronze artefacts.

The results obtained in the present work allow, for the first time, to establish the evolution of the bronze metallurgy in the south region of the Portuguese territory. Indeed, the majority of LBA artefacts from the southern Portuguese territory are made of copper-tin alloys with suitable tin contents, i.e. 9.8±2.3% Sn. This type of metallurgy is very similar to the one present in the neighbouring areas, namely, to the north, the centre of the Portuguese territory and, to the east, the southwestern Spain (Figure 4.50).

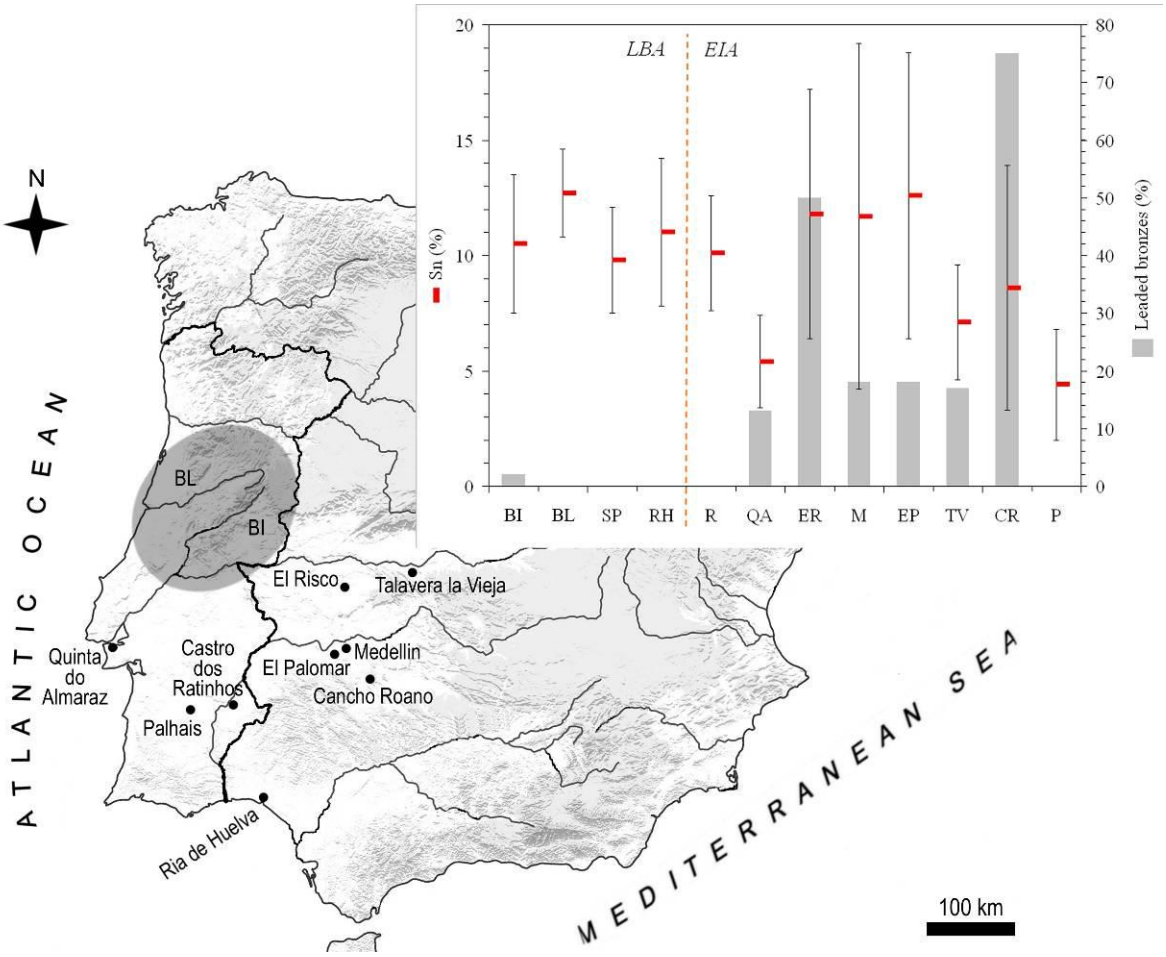

Figure 4.50 Tin contents (average ± standard deviation) and frequency of leaded bronzes in collections of bronze artefacts belonging to the LBA (BI: Beira Interior, n=81 (Vilaça, 1997); BL: Beira Litoral, n=86 (Figueiredo, 2010); SP: Southern Portugal, n=28 (this work); RH: Ria de Huelva, n=387 (Rovira, 1995) and EIA (R: Castro dos Ratinhos, n=36 (this work); QA: Quinta do Almaraz, n=15 (this work); ER: El Risco (Montero-Ruíz *et al.*, 2003); M: Medellin (Montero-Ruíz *et al.*, 2003); EP: El Palomar, n=53 (Rovira *et al.*, 2005); TV: Talavera la Vieja, n=18 (Montero-Ruíz and Rovira, 2006); CR: Cancho Roano, n=114 (Montero-Ruíz *et al.*, 2003) and P: Palhais, n=7 (this work).

The LBA collection from Beira Interior (81 artefacts from Cachouça, Castelejo, Alegrios, Monte do Frade and Moreirinha (Vilaça, 1997): mostly binary bronzes with 10.5±3.0% Sn), together with the collection from Beira Litoral (86 artefacts from Castro de São Romão, Santa Luzia, Baiões and Medronhal (Figueiredo, 2010): mainly binary bronzes with 12.7±1.9% Sn) characterise the LBA metallurgy at the Central Portuguese region. The metallic collection composed of nearly 400 artefacts from Ria de Huelva (SW Spain) typify the LBA metallurgical tradition at southwestern

Spain, being composed mainly by binary bronzes with ‘‘suitable’’ tin contents, i.e. 11.0±3.2% (Rovira, 1995). This establishes a LBA metallurgical tradition of binary bronzes with ~10-13% Sn, whilst pure copper artefacts are somewhat scant and leaded bronzes are even scarcer.

During the EIA the scenery changes considerably, the keyword being diversification (that is why the Orientalising sites at Figure 4.50 are presented individually, contrary to LBA sites, which are presented in groups). Initially, the more obvious modification is the increased tendency to use leaded bronzes. The specificities of some collections can induce some exaggerations, i.e. the nearly exclusive use of leaded bronzes at Cancho Roano is attributed to the high incidence of “as-cast” artefacts, namely small statuary items (Montero-Ruíz *et al.*, 2003). However, the general increasing trend is quite obviously shared by all mentioned artefact collections.

Concerning the binary bronze metallurgy, the 9th-8th centuries BC collection from Castro dos Ratinhos continues to present an average tin value similar to the LBA cluster. Furthermore, the same is still observed in the 7th-6th centuries BC collections of El Risco, Medellin (Montero-Ruíz *et al.*, 2003) and El Palomar (Rovira *et al.*, 2005), despite an somewhat extended variability in this tin content (increased standard deviation, see Figure 4.50). On the contrary, the 9th-7th collection from Quinta do Almaraz, in addition to the 6th century BC collections from Palhais, Talavera la Vieja (Montero-Ruíz and Rovira, 2006) and Cancho Roano (Montero-Ruíz *et al.*, 2003) present a reduced average tin content.

These results evidence the tendency to use poorer bronzes during the EIA, but more important they establish that the evolution of the bronze metallurgy was a rather slow and unequal process. Indigenous communities, especially those who inhabited the inland areas (e.g. Castro dos Ratinhos, El Risco, Medellin and El Palomar) persist with some aspects of the LBA metallurgical tradition until very late. By the contrary, Phoenician seaboard settlements (e.g. Quinta do Almaraz) present from the start a metallurgy that uses different alloys (coppers, bronzes and leaded bronzes), together with dissimilar tin contents. According to the available data this diversification only seems to be completely widespread on the studied region by the 6th century BC.

5. GOLD ARTEFACTS

5.1. Introduction

The gold used during pre-historic and proto-historic periods usually comes from nuggets collected from alluvial deposits, while mining operations to exploit the primary gold deposits only seem to commence during the Roman period (Montero-Ruíz and Rovira, 1991). The first gold artefacts recovered from the archaeological record are thin metal sheets hammered from native gold during the last centuries of the CA (Soares *et al.*, 1996). Native gold contains variable amounts of silver, which could reach up to 40% in some regions of Asia (Tylecote, 1987). At the Iberian Peninsula only very few gold artefacts belonging to the earlier metallurgical periods present silver contents above 20-25% (Montero-Ruíz and Rovira, 1991). Copper is also a common constituent of native gold and usually it may reach up to 1% (Tylecote, 1987). Consequently, despite not being straightforward to distinguish among native and alloyed gold based merely on the elemental contents of silver and copper, the above mentioned boundaries are generally used as an indication of its origin.

The gold-silver alloys are always composed of a monophasic solid solution (α) because silver is completely soluble in gold (Figure 5.1). The copper is also totally soluble in gold, while for very slow cooling rates a low temperature ordered phase can be formed – Cu_3Au, CuAu or $CuAu_3$ (Figure 5.2). This ordered phase is harder than the α solid solution so the gold alloy becomes more brittle and difficult to hammer. Fortunately, the copper content of pre-historic gold artefacts is commonly below the limit of the $CuAu_3$ phase (~8% Cu) so pre-historic gold alloys with copper are usually composed by the α solid solution.

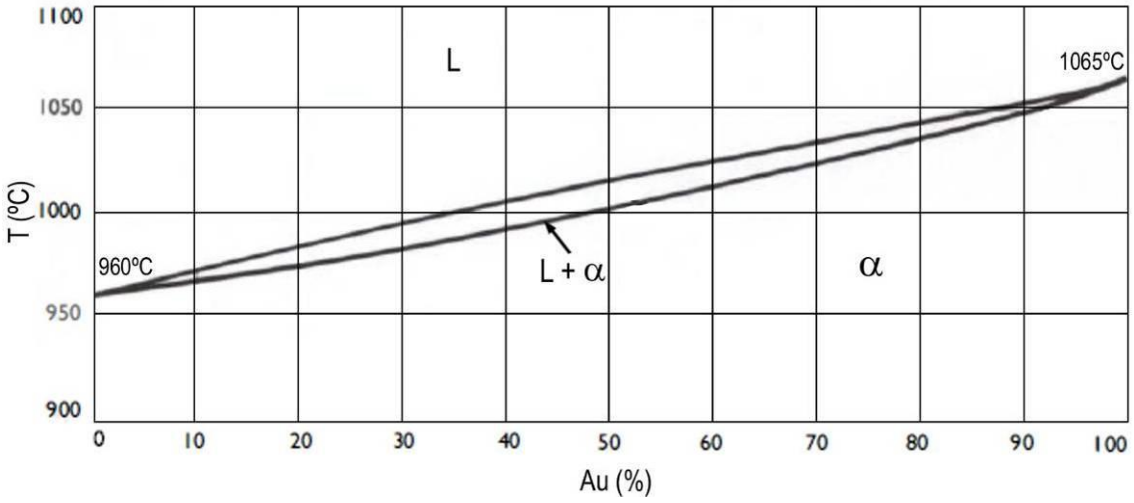

Figure 5.1. Gold-silver phase diagram with melting points of gold and silver (adapted from AMS, 1973).

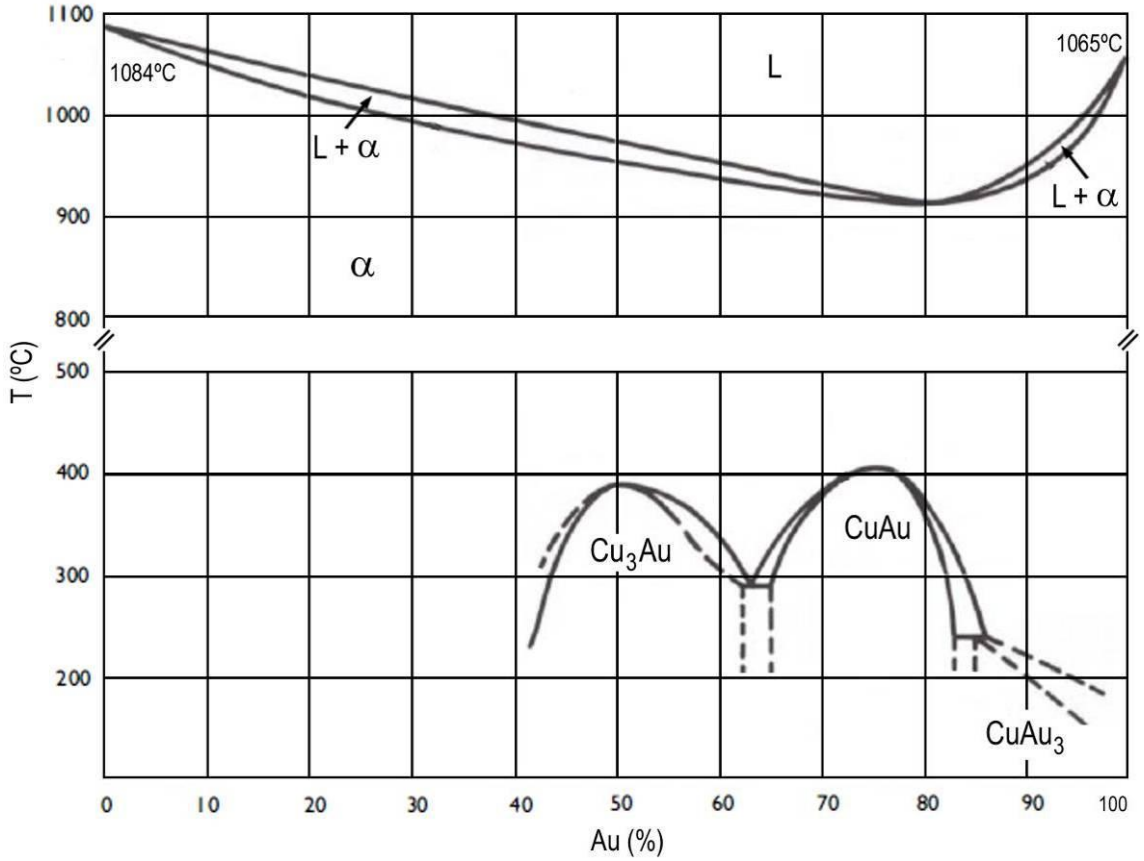

Figure 5.2. Gold-copper phase diagram with melting points of gold and copper (adapted from AMS, 1973).

Adding silver or copper to gold produces a decrease of the *solidus* and *liquidus* temperatures of the alloy (Figure 5.3). This reduction is more marked when alloying with copper than with silver, e.g. Au-20%Ag alloy presents a solidus temperature of 1040ºC, while Au-20%Cu alloy starts to melt at much lower temperatures (~910ºC). Consequently, during pre-history Au-Ag, Au-Cu and Au-Ag-Cu alloys were used as solder to connect the different components of gold artefacts (Perea, 1990).

Additionally, taking into consideration the symbolic nature of ancient gold artefacts, the effect of silver and copper in the colour of gold alloys must not be forgotten. The addition of silver to gold turns the golden colour more brownish, while the addition of copper makes the gold alloy more reddish (Figure 5.3).

The following sections present the elemental characterisation of several gold artefacts belonging to different chronological periods (CA, LBA and EIA). Occasionally, an artefact already fragmented could be sampled for OM and SEM-EDS characterisation to resolve specific issues. This includes the welding process used to join the different components of EIA gold buttons or the manufacturing operations utilised to make Chalcolithic metal sheets.

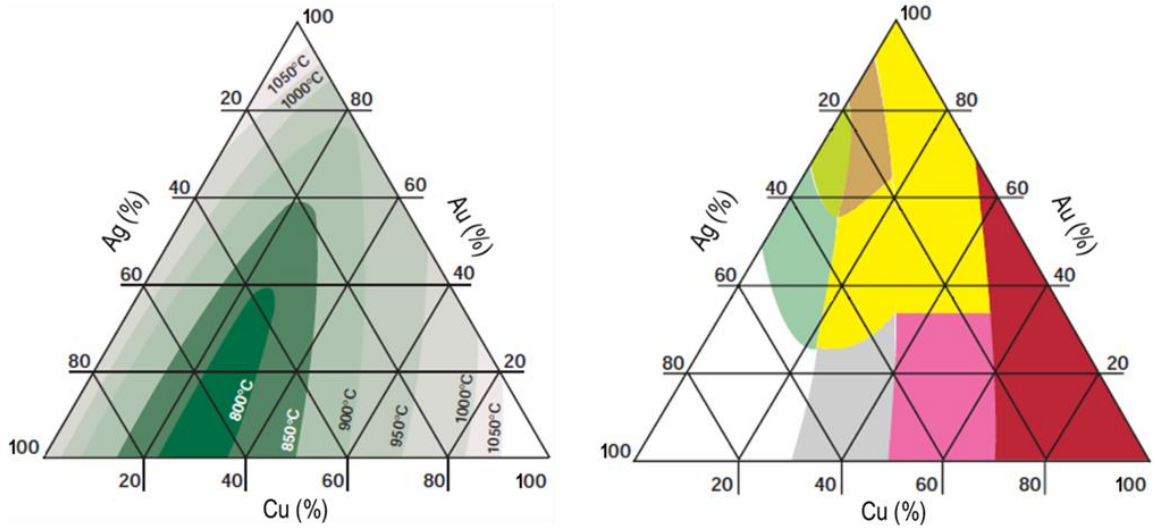

Figure 5.3. Ternary diagrams with *liquidus* temperatures and chromatic trends of Au-Ag-Cu alloys (Grimwade, 2000).

5.2. Perdigões

Archaeological works conducted since 1997 at the archaeological site of Perdigões (Reguengos de Monsaraz) revealed a complex necropolis composed by a sequence of concentric ditches and several tombs (Lago *et al.*, 1998). The architectural features of negative structures, together with the material culture typology, assign this necropolis to the CA period.

The collection of gold artefacts studied comprises 12 metal sheets with different dimensions (Figure 5.4). The largest ones are also the thicker (11450 and 11511), presenting the shape of long bands. The majority of the gold sheets present evidences of being connected to a support material, which completely decomposed during the long burial time – riveting holes and tarnished surfaces, most likely contaminated by decay of the support material.

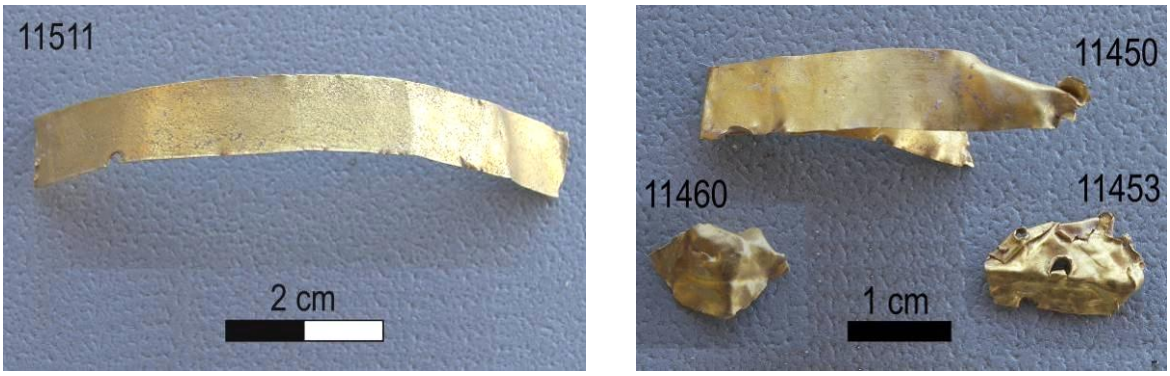

Figure 5.4. Gold artefacts belonging to the archaeological site of Perdigões.

Non-invasive EDXRF analyses were conducted at these gold artefacts to establish their elemental composition (Table 5.1). The results evidence a very pure gold with traces of copper (<0.10%) and moderately variable contents of silver (0.6-5.5%). However, the composition of all these gold artefacts clearly indicates a native origin for the gold used, which is perfectly compatible with the CA period to which they belong.

Table 5.1. Results of EDXRF analyses of gold artefacts from Perdigões (values in %).

Artefact	Reference	Context	Au	Ag	Cu
sheet metal	11041	CA	96.0	3.9	<0.10
sheet metal	11450	CA	96.9	3.0	<0.10
sheet metal	11451	CA	99.1	0.8	<0.10
sheet metal	11452	CA	99.0	0.9	<0.10
sheet metal	11453	CA	99.2	0.7	<0.10
sheet metal	11454	CA	99.3	0.6	<0.10
sheet metal	11455	CA	96.7	3.2	<0.10
sheet metal	11456	CA	96.7	3.2	<0.10
sheet metal	11458	CA	97.0	2.9	<0.10
sheet metal	11459	CA	96.8	3.1	<0.10
sheet metal	11460	CA	99.2	0.7	<0.10
sheet metal	11511	CA	94.4	5.5	<0.10

Two of the thinner gold sheets (11454 and 11458) were sampled for microstructural characterisation. These artefacts present recrystallized microstructures with annealing twins (Figure 5.5), evidencing the use of mechanical and thermal treatments. The manufacturing process involved hammering of a ticker sheet into a thinner one. Then this sheet was annealed to allow additional deformation without cracking. The consecutive cycles of hammering and annealing continue until the gold sheet attains the desired thickness.

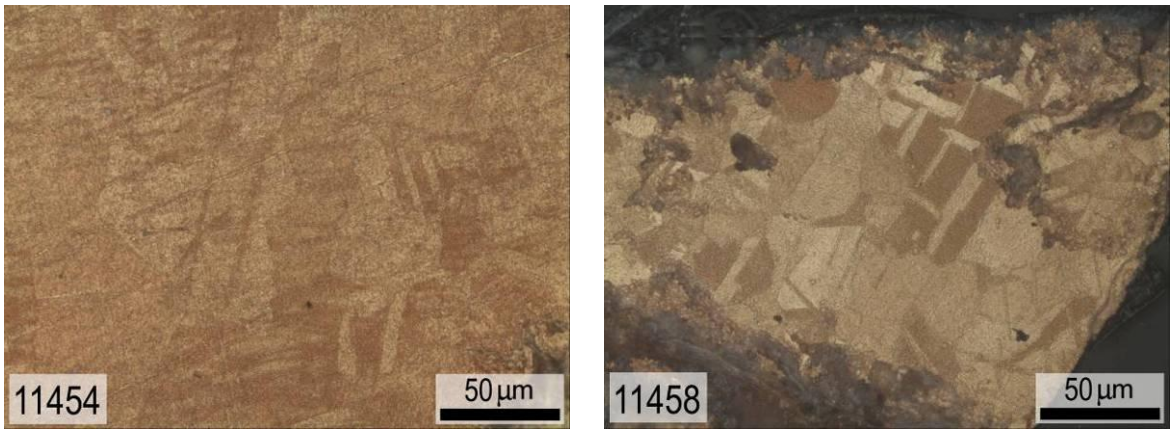

Figure 5.5. OM images of gold sheets 11454 and 11458 from Perdigões (both OM-BF, etched).

5.3. Baleizão

As it was mentioned in the section dealing with the copper-based artefacts, the collection discovered at Baleizão also includes 11 gold artefacts with typologies that are typical to the LBA period of the Portuguese territory (Vilaça and Lopes, 2005). This gold collection comprises several large and massive artefacts, including a necklace (1182), bracelet (1183) and ear-ring (1184), together with a small ingot (1185), 2 segments of rolled double-wire (1186a/b) and 5 small fragments of metal sheet (1187a/b/c/d/e) (Figure 5.6).

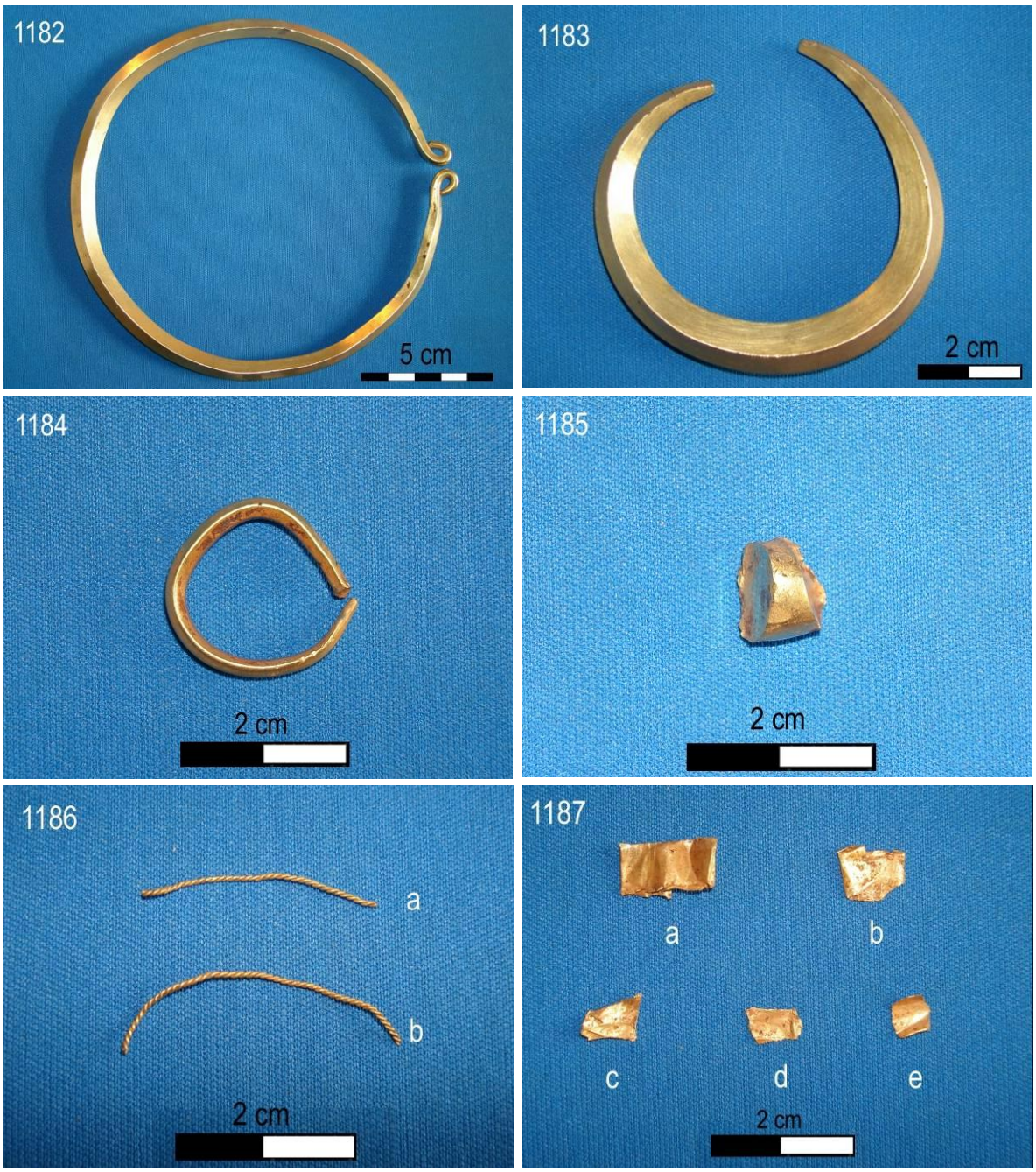

Figure 5.6. Gold artefacts belonging to the collection of Baleizão.

EDXRF analyses established that the artefacts are composed by gold alloys with rather high contents of silver and copper (Table 5.2). The ingot presents the lower silver and copper contents (11.4 and 1.4%, respectively), a composition very similar to the necklace (13.3% and 1.2%, respectively). The copper contents of all these gold artefacts (>1%) seem to indicate the possible alloying of gold with copper. Furthermore, the metal sheets (1187a/b/c/d/e) and rolled double-wires (1186a/b) present high silver contents that are very close to the limit of native gold (25% Ag).

Table 5.2. Results of EDXRF analyses of gold artefacts from Baleizão (values in %; * with ~2% Zn).

Artefact	Reference	Context	Au	Ag	Cu
Necklace	1182	LBA	85.5	13.3	1.2
Bracelet	1183	LBA	80.7	18.0	1.4
ear-ring	1184	LBA	78.4	18.2	3.4
Ingot	1185	LBA	87.2	11.4	1.4
double-wire*	1186a	LBA	71.7	24.1	2.4
double-wire*	1186b	LBA	73.3	21.9	2.9
sheet metal	1187a	LBA	75.0	21.9	3.2
sheet metal	1187b	LBA	72.7	25.2	2.2
sheet metal	1187c	LBA	73.8	24.2	2.1
sheet metal	1187d	LBA	74.6	23.2	2.3
sheet metal	1187e	LBA	72.4	25.7	1.9

The two segments of rolled double-wire (1186a and 1186b) from Baleizão also exhibit around 2% Zn. Gold nuggets can be very pure, such as the examples from Casas de Don Pedro (SW Spain) – 0.01% As; 0.02% S; 0.35% Bi; 0.016% Fe; 0.8% Ag; 0.05% Sb and 0.04% Te, which seem to characterise the gold outcrops employed by goldsmiths to manufacture the EIA treasure of Aliseda, discovered at the southwestern Iberian Peninsula (Garcia-Guinea *et al.*, 2005). On the other hand, native gold can also present highly variable amounts of other elements, mainly silver and copper, but other impurities as well, like tin or platinum (Montero-Ruíz and Rovira, 1991). Anyway, zinc seems to be an uncommon impurity among pre-historic gold artefacts from the Iberian Peninsula. It was found in a laminar fragment (~0.9-1.8% Zn) of a proto-historic pendant from Cancho Roano (Perea, 2003). Technologically, the presence of small amounts of zinc (up to 2% Zn) do not cause a pronounced change in the colour of these gold-silver-copper alloys, while it produces beneficial effects on the casting behaviour and quality of castings obtained (Raub and Ott, 1983). Summarily, it can be assumed that this is not a customary composition of a LBA gold artefact.

5.4. Castro dos Ratinhos[8]

A collection of seven gold buttons was recovered in the ruins of a large palace-like building that stands up at the highest place of the settlement of Castro dos Ratinhos (Berrocal-Rangel and Silva, 2010). The archaeological record suggests that this gold treasure was hidden during the 7th century BC, when the large building was abandoned, probably due to a violent event. A clay fragment exhibiting the imprint of a woven fabric was discovered in association with the gold buttons, suggesting that they were originally tied to a woven tissue. Additionally, a small hollow bead without decoration was discovered at surface level after the end of archaeological excavations.

Furthermore, the gold buttons are easily recognisable as a single collection due to their remarkable similar typology (Figure 5.7). These buttons (∅~10mm; weight~0.4g) were made with different components: main body, peripheral rod and tab. The main body exhibits a central spherical decoration enclosed by several engraved circles. It is connected to a peripheral decorated rod composed by a twisted wire (Figure 5.7A). The tab seems to be made with a fragment of the twisted wire previously flattened by hammering (Figure 5.7B). Sometimes this hammering was so intense that the original twisted decoration almost disappeared.

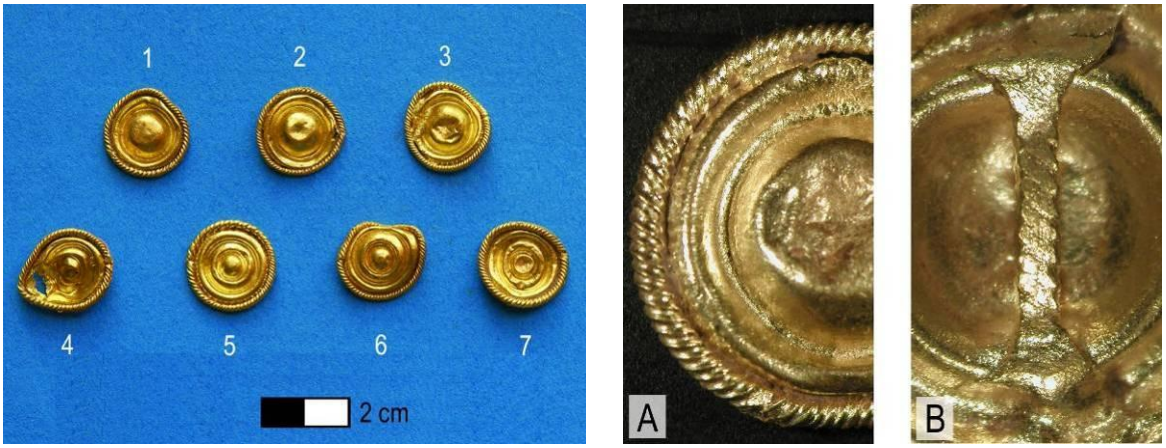

Figure 5.7. Gold buttons belonging to the archaeological site of Castro dos Ratinhos (A and B: detail of button decoration and decorated tab, respectively).

The buttons from Castro dos Ratinhos were analysed by micro-PIXE[9] with especial attention on the reverse faces so that it would be possible to investigate possible compositional differences between disk, peripheral rod, tab and welded areas. The micro-PIXE analyses did not identify any significant compositional differences among the different button components (see some examples in Figure 5.8). Additionally, the welded areas exhibit compositions that are similar to the

[8] Part of the content from this section was previously published (Valério *et al.*, 2010d; Soares *et al.*, 2010).

[9] Micro-PIXE analyses were made at ITN by Luis Cerqueira Alves.

composition of surrounding components, indicating the absence of a solder alloy. Nevertheless, the solder material can be restricted to a small area between the two attached components, i.e. it is possible that the solder material would not be reachable by this non-invasive approach.

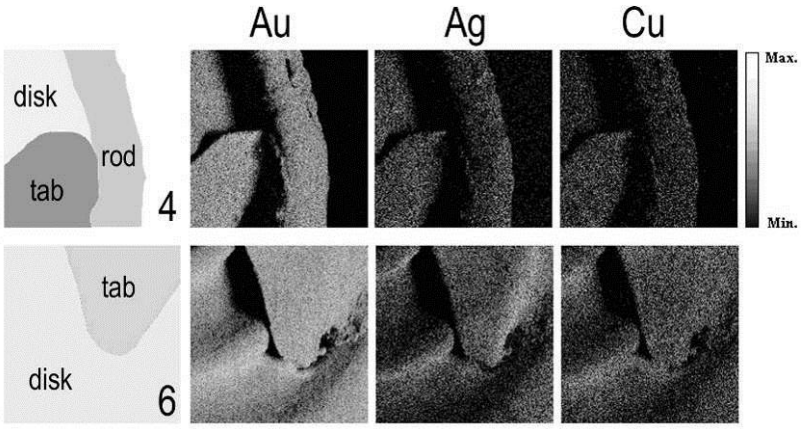

button 2	Au	Ag	Cu
disk	89.3	9.4	1.3
rod	89.4	9.2	1.4
tab	88.2	10.0	1.7

Figure 5.8. Maps of gold, silver and copper distribution (buttons 4 and 6) and point analyses (button 2) obtained by Micro-PIXE at reverse faces of gold buttons from Castro dos Ratinhos (values in %).

Due to the diameter of the incident beam, each EDXRF analysis corresponds to the entire face of the button, thus including more than one component. However, since micro-PIXE analyses established that the button components are composed of similar gold alloys and no solder materials could be detectable, it was considered that EDXRF analyses would give reliable results. Moreover, EDXRF results could be compared with the other collections of gold artefacts presented in this work.

Gold buttons from Castro dos Ratinhos were analysed by EDXRF at the obverse and reverse faces (Table 5.3). Initially, it was ascertained that the different geometries at the obverse and reverse faces do not introduce significant deviations. In fact, both faces of each button present comparable results. The minor differences observed could be explained by geometric effects (non-flat surfaces) and small compositional changes from superficial alteration processes that in gold alloys result in the removal of the less noble elements (silver and copper) from the superficial layer. The presence of a superficial layer enriched in gold is confirmed by the higher gold contents obtained by Micro-PIXE analyses when compared with EDXRF analyses (see results of button 2 in Figure 5.8 and Table 5.3, respectively). Micro-PIXE analysis concerns a more superficial layer due to the low penetration depth of the protons when compared with the X-rays used by EDXRF (Araújo *et al.*, 1993). EDXRF results established that all buttons are composed of almost identical gold alloys with ~13-16% Ag and 1.3-1.9% Cu. Furthermore, the gold bead discovered afterwards at Castro dos Ratinhos is composed of a very similar gold alloy (~12% Ag and 1.8% Cu).

Table 5.3. Results of EDXRF analyses of gold artefacts from Castro dos Ratinhos (*a*: obverse face; *b*: reverse face; values in %).

Artefact	Reference	Context		Au	Ag	Cu
button	1	EIA	*a*	83.4	15.0	1.6
			b	83.0	15.1	1.9
button	2	EIA	*a*	83.8	14.9	1.3
			b	84.1	14.4	1.6
button	3	EIA	*a*	83.3	15.0	1.8
			b	83.1	15.2	1.7
button	4	EIA	*a*	83.5	14.8	1.7
			b	83.0	15.1	1.8
button	5	EIA	*a*	83.9	14.4	1.7
			b	82.9	15.2	1.9
button	6	EIA	*a*	85.1	13.2	1.8
			b	85.4	12.9	1.7
button	7	EIA	*a*	83.1	15.3	1.7
			b	82.5	15.7	1.9
bead	8	-	-	86.4	11.8	1.8

5.5. Outeiro da Cabeça

The treasure of Outeiro da Cabeça (Torres Vedras) was discovered during the plowing of a field in the thirties of last century (Heleno, 1935). This gold treasure comprises two small ingots, together with many buttons, a necklace, ear-rings and bracelets, whose typology is familiar to the EIA. The small gold buttons deserve a special emphasis since it was their typology (similar to the buttons from Castro dos Ratinhos) that led us to study this collection. Part of this gold treasure now belongs to the *Museu Municipal de Torres Vedras*, while a second fraction is currently at display at *Museu Nacional de Arqueologia*. From the first, a collection was selected comprising 13 gold buttons, 2 ear-rings, an ingot and a necklace comprising of a hollow cylinder, 2 rings and a coiled wire (Figure 5.9). The collection selected for study from the treasure of Outeiro da Cabeça was completed with 10 gold buttons and 1 ingot (206: Figure 5.9).

Buttons from Outeiro da Cabeça (∅~16mm; weight~0.8g) are bigger than the ones from Castro dos Ratinhos, but the typology is analogous, comprising the main body, peripheral rod and tab. The main body exhibits a central spherical decoration enclosed by several engraved circles, whereas one or two of these circles are decorated by small punched points instead of a continuous circle. Similarly to the buttons from Castro dos Ratinhos, the peripheral rod is composed by a twisted wire, whereas the tab consists of a flattened twisted wire. The majority of the selected buttons present a single tab (1711; 1713; 1714; 1717; 1718; A; B; C; 199; 200; 201; 202; 203 and 593), while others have a double one (1707; 1712; 1715; 1716; 198; 204 and 205).

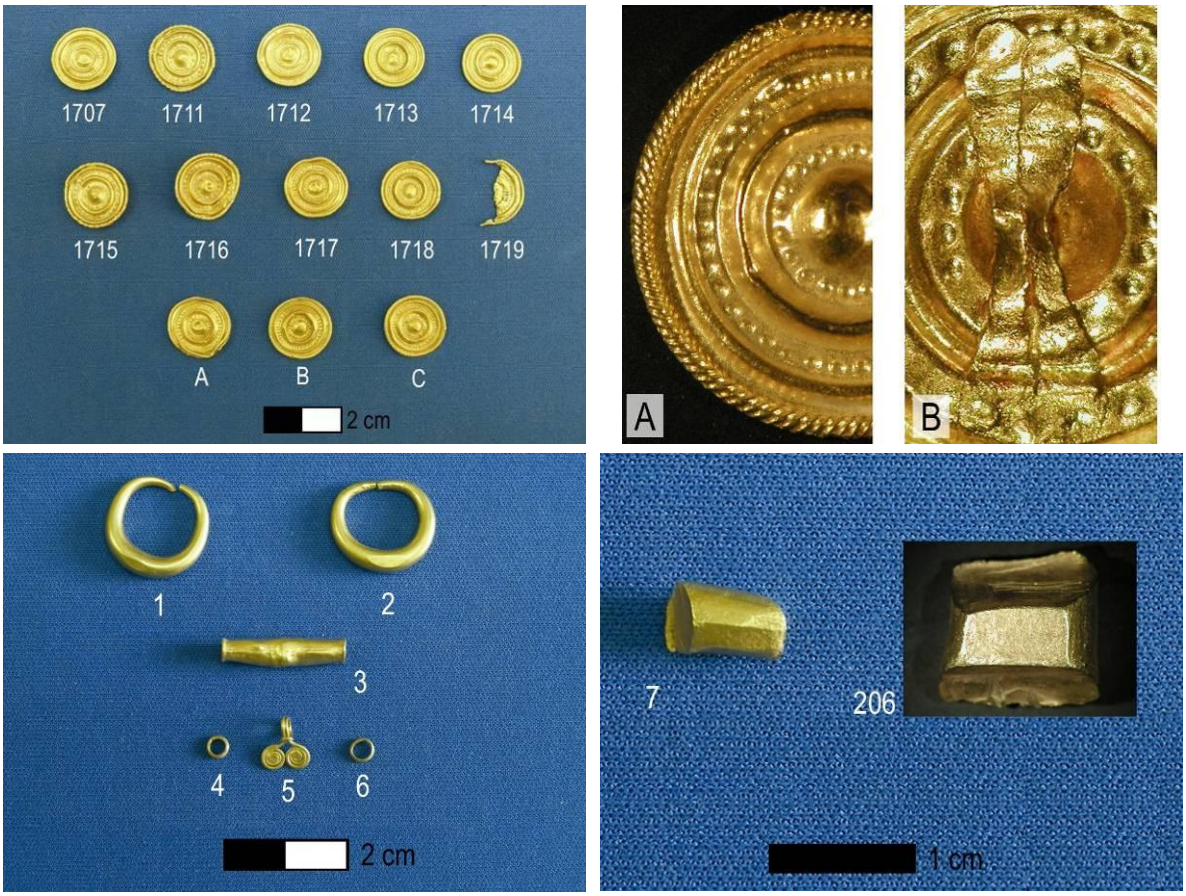

Figure 5.9. Gold artefacts belonging to the treasure of Outeiro da Cabeça (artefacts at *Museu Municipal de Torres Vedras* and ingot 206 from *Museu Nacional de Arqueologia*; A and B: detail of button decoration and double tab, respectively).

The gold artefacts from Outeiro da Cabeça were analysed by EDXRF to determine the alloy composition (Table 5.4). The two ingots present low copper (0.4-1.1%) and silver (10.2-15.1%) contents, suggesting a probable native origin and possibly the base contents for the formulation of some of these gold alloys. Accordingly, the ear-ring 1, hollow cylinder and ring 4 were certainly made with alloyed gold due to their very high copper contents (2.4-2.9%).

Table 5.4. Results of EDXRF analyses of gold artefacts from Outeiro da Cabeça (values in %).

Artefact	Reference	Context	Au	Ag	Cu
ear-ring	1	EIA	83.1	14.0	2.9
ear-ring	2	EIA	87.7	11.1	1.2
hollow cylinder	3	EIA	85.0	12.2	2.8
ring	4	EIA	78.8	18.8	2.4
ring	5	EIA	78.7	19.4	1.9
coiled wire	6	EIA	80.7	18.2	1.1
ingot	7	EIA	83.8	15.1	1.1
ingot	206	EIA	89.4	10.2	0.4

The buttons from Outeiro da Cabeça were also analysed by EDXRF at the obverse and reverse faces to establish eventual deviations (Table 5.5). These would be mostly due to the different button components since the analyses of buttons from Castro dos Ratinhos had already established that the deviations due to the different geometries of obverse and reverse faces are not significant.

Table 5.5. Results of EDXRF analyses of gold artefacts from Outeiro da Cabeça (*a*: obverse face; *b*: reverse face; values in %; +: reverse was not analysed since it is attached to a geologic material).

Artefact	Reference	Context		Au	Ag	Cu
button	1707	EIA	*a*	84.5	13.5	2.0
			b	85.6	12.2	2.2
button	1711	EIA	*a*	86.3	12.9	0.8
			b	87.1	11.8	1.1
button	1712	EIA	*a*	84.3	13.9	1.8
			b	85.6	12.6	1.8
button	1713	EIA	*a*	87.6	11.5	0.9
			b	88.5	10.5	1.0
button	1714	EIA	*a*	85.6	11.7	2.7
			b	85.8	11.3	2.9
button	1715	EIA	*a*	85.9	13.0	1.1
			b	86.3	12.7	1.0
button	1716	EIA	*a*	85.9	13.1	1.0
			b	86.0	13.0	1.0
button	1717	EIA	*a*	86.6	12.7	0.7
			b	86.7	12.5	0.8
button	1718	EIA	*a*	84.8	13.2	2.0
			b	84.8	13.3	1.9
button	1719	EIA	*a*	87.3	11.5	1.2
			b	87.7	11.0	1.3
button	A	EIA	*a*	87.3	11.8	0.9
			b	87.6	11.6	0.8
button	B	EIA	*a*	86.6	12.7	0.7
			b	86.4	12.7	0.9
button	C	EIA	*a*	86.2	12.0	1.8
			b	86.2	11.9	1.9
button	197^{+}	EIA	*a*	86.8	11.7	1.5
			b	-	-	-
button	198	EIA	*a*	84.5	13.7	1.8
			b	84.6	13.7	1.7
button	199	EIA	*a*	87.5	11.2	1.3
			b	87.9	11.0	1.1
button	200	EIA	*a*	87.0	12.3	0.7
			b	87.5	11.8	0.7
button	201	EIA	*a*	87.8	11.4	0.8
			b	88.0	11.2	0.8
button	202	EIA	*a*	85.3	13.3	1.4
			b	86.1	12.5	1.4
button	203	EIA	*a*	86.9	11.3	1.8
			b	87.7	10.5	1.8
button	204	EIA	*a*	84.8	13.4	1.8
			b	84.3	14.1	1.6
button	205	EIA	*a*	86.4	12.8	0.8
			b	88.0	11.2	0.8
button	593	EIA	*a*	85.3	13.2	1.5
			b	87.2	11.5	1.3

Similarly to the buttons from Castro dos Ratinhos, the EDXRF results from obverse and reverse faces of each button from Outeiro da Cabeça are comparable, suggesting that the main body, peripheral rod and tab are composed by gold alloys of similar composition. Additionally, this indicates that their joining did not imply a welding alloy with a different composition (i.e. gold alloy richer in copper, silver or in both). Generally, the buttons present comparable silver compositions (~10-14%), which are perfectly compatible with the gold ingots recovered among this treasure. However, the copper contents are more variable (0.8-2.9%) indicating a probable use of alloying, at least in the gold buttons that are richer in copper.

Since the button 1719 was already broken, it was possible to acquire a small sample for OM and SEM-EDS analyses. The microstructural characterisation intents to establish the welding process used to connect the button components, given that this was not completely ascertained by the non-invasive study of buttons from Castro dos Ratinhos. OM observations clearly identify the cross-sections of the two button components – main body and peripheral rod (Figure 5.10). Both components present twinned grains from hammering and heat treatments. In the second image it is visible the cross-section of the end of the main body tangled upon itself to obtain a perfect link with the peripheral rod.

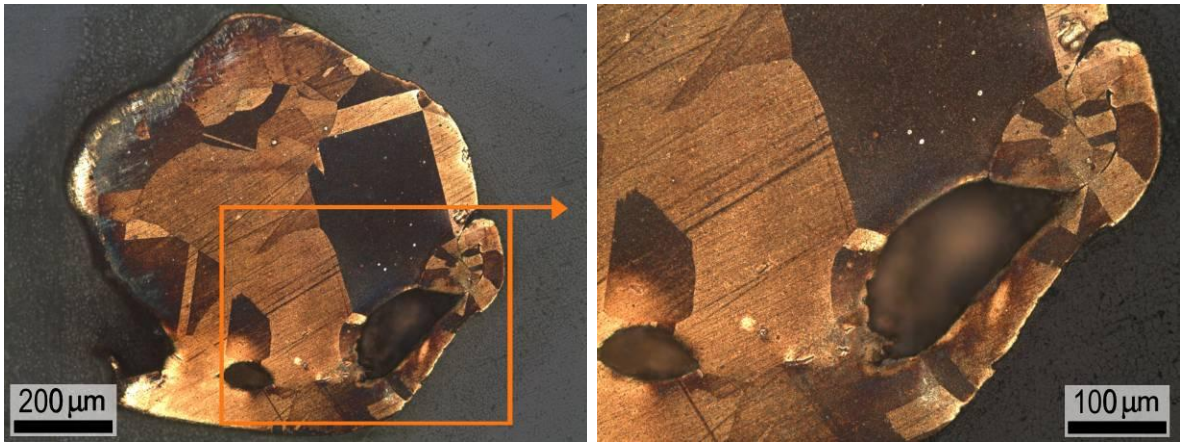

Figure 5.10. OM-BF (etched) images of button 1719 (main body and peripheral rod cross-sections) from Outeiro da Cabeça.

Several SEM-EDS line-scans and point analyses performed along the contact region between the main body and peripheral rod display almost constant gold, silver and copper contents (Figure 5.11). The small variations observed in the line-scans are due to topographic effects, namely the presence of pores and fissures. The constant elemental profiles prove that the main body and wire are composed by gold alloys with very similar contents. Furthermore, it was established that no solder alloy was used to connect this two components.

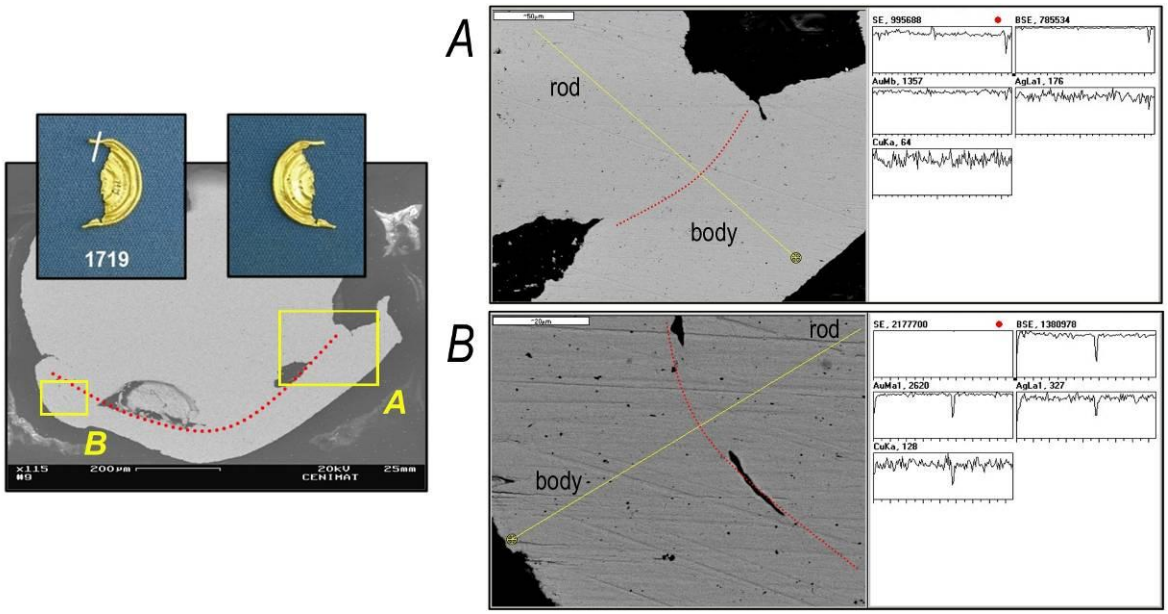

Figure 5.11. SEM-BSE images and EDS line-scans of button 1719 from Outeiro da Cabeça.

5.6. Fortios

The treasure of Fortios (Portalegre) was inside a clay pot raised during the plowing of a field in the early seventies of last century (Veiga Ferreira, 1974). This treasure was composed of several tens of EIA gold buttons. Some of them enter private collections, while others were acquired by the *Museu Nacional de Arqueologia*. The buttons from Fortios exhibit a diameter of about 20mm (weight~1.4g), being larger than the ones from Castro dos Ratinhos and Outeiro da Cabeça. Their typology is composed by several concentric circles surrounding the central spherical decoration (Figure 5.12). The peripheral rod consists of a twisted wire, while the tabs are smooth and exhibit flattened ends to fit perfectly into the reverse face of the decorated main body. Some of these flattened ends exhibit traces of being melted due to excessive heat during welding.

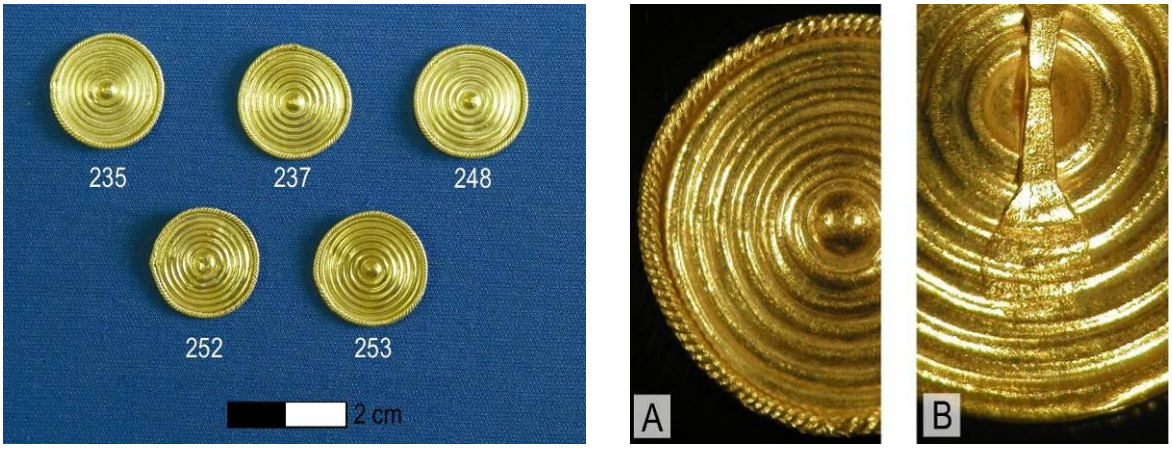

Figure 5.12. Gold artefacts belonging to the treasure of Fortios (A and B: detail of decoration and partially melted tab).

The gold buttons from Fortios were analysed by EDXRF to determine the alloy composition (Table 5.6). Similarly to the other studied collections, the obverse and reverse faces of each button give comparable results. This suggests that the button components were made with similar gold alloys and that no welding alloy was used to join them. Furthermore, these gold buttons present exceptionally analogous silver and copper contents, ranging from ~13-14% Ag and 1.2-1.4% Cu.

Table 5.6. Results of EDXRF analyses of gold artefacts from Fortios (*a*: obverse face; *b*: reverse face; values in %).

Artefact	Reference	Context		Au	Ag	Cu
button	235	EIA	*a*	84.9	13.9	1.2
			b	85.2	13.5	1.3
button	237	EIA	*a*	84.7	14.0	1.3
			b	85.2	13.5	1.3
button	248	EIA	*a*	85.4	13.2	1.4
			b	85.8	12.8	1.4
button	252	EIA	*a*	85.4	13.3	1.3
			b	85.8	12.9	1.3
button	253	EIA	*a*	85.6	13.1	1.3
			b	85.7	12.9	1.4

5.7. Fonte Santa and Quinta do Almaraz

The archaeological excavations conducted during 1972 at the necropolis of Fonte Santa (Ourique) discovered a gold button inside one of the tombs (Beirão, 1986). The gold button was accompanied by bronze bracelets, several bead necklaces, a scarab and silver artefacts, including a silver pendant shaped as an acorn, which is almost identical to the one found in the 6th century BC necropolis of Palhais. The material culture recovered by archaeological excavations at Quinta do Almaraz (Almada) includes a small crucible that suggests the local production of gold artefacts, but the only gold artefact recovered until now was a small hollow bead (Araújo *et al.*, 2004).

The gold button from Fonte Santa (∅~25mm; weight~1g) is somewhat different from the other studied examples since the peripheral rod is absent, instead being simulated by a punched relief along the periphery of the circular body (Figure 5.13). Furthermore, originally its reverse face was connected to a silver sheet containing the tab, which meanwhile disappeared, leaving only some traces of a molten area in the centre of the reverse face, probably due to the original welding of both components.

Figure 5.13. Gold button from the necropolis of Fonte Santa (A and B: detail of simulated peripheral rod and traces of welding at the reverse face, respectively).

These gold artefacts were analysed by EDXRF to determine their elemental composition (Table 5.7). The reverse face of the button seems to be richer in silver and copper, probably due to the presence of the relics of a solder alloy, as mentioned before. Therefore, only the result from the obverse face will be considered representative of this button. Anyway, this gold button is composed by a gold alloy very rich in silver and copper, such as the small gold bead from Quinta do Almaraz. These elemental compositions clearly indicate the use of alloyed gold instead of native one.

Table 5.7. Results of EDXRF analyses of gold artefacts from Fonte Santa and Quinta do Almaraz (*a*: obverse face; *b*: reverse face/; values in %).

Artefact	Reference	Context		Au	Ag	Cu
button	982	EIA	*a*	68.1	28.7	3.2
			b	62.6	33.1	4.3
bead	ALZ1	EIA	-	71.6	25.8	2.6

5.8. Discussion

The elemental composition of gold artefacts analysed in this work allows significant considerations regarding the evolution of the gold metallurgy at the southern Portuguese region. The artefacts belonging to the CA present very simple typologies – small sheets of metal – mostly composed of pure gold with minor amounts of silver (up to 5%) (Figure 5.14). The manufacture of these thinner sheets involved annealing and hammering cycles. The use of thermal treatment to facilitate additional mechanical deformation evidences the good technological expertise of the goldsmiths from this early chronological period. Many centuries later, the composition of gold artefacts seem to become remarkably different since the LBA artefacts analysed present increased silver and copper contents. The majority of LBA artefacts exhibit silver contents among 20-25% and copper contents above 1%, indicating that these LBA artefacts are made with alloyed gold. Additionally,

the single LBA ingot presents silver and copper contents lower than most of the remaining artefacts, which also seems to point to the use of alloying. In the following chronological period, the majority of the artefacts studied presents lower silver contents (10-15%), while the distribution of the EIA copper contents is similar to the observed at the earlier period (it must be noted that the EIA collection, mostly composed by buttons, is much larger than CA and LBA collections). Once more, the ingots (especially the 206) present copper and silver percentages lower than the average values of the artefacts. The gold artefact with higher silver and copper contents (button 982) belongs to the chronologically latter necropolis of Fonte Santa, being obviously made with alloyed gold.

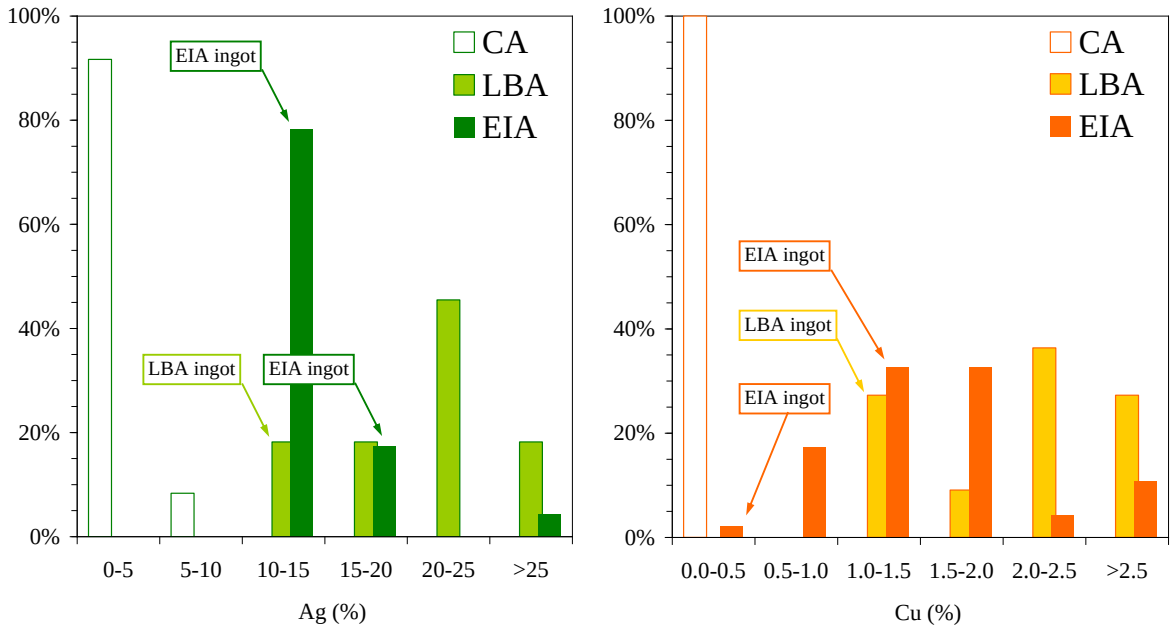

Figure 5.14. Distribution of silver and copper contents in gold artefacts from the southern Portuguese region (69 artefacts comprising 12 CA, 11 LBA and 46 EIA examples).

In order to better establish the evolution of gold artefacts at southern Portuguese territory, our results should be analysed together with other significant data from the same region. Accordingly, a systematic study gathering pre-historic gold artefacts with a known chronology from this region was used (Soares *et al.*, 1996). The data available comprises 104 analyses made by the SAM project (Hartmann, 1982), which increase the significance of CA and LBA collections, but above all, introduced the EBA/MBA chronology on this research. The results obtained by the OES technique used during the SAM project are comparable to the obtained by EDXRF (e.g. button 1719 from Outeiro da Cabeça – EDXRF: 11% Ag and 1.2% Cu, while OES: 10%Ag and 1.3% Cu). The compilation of these results evidences that the rise of the silver contents in gold artefacts started during the EBA/MBA, whose majority of artefacts present 10-15% Ag (Figure 5.15). During the LBA, the most representative group remains unchanged (10-15% Ag) but the clusters richer in silver are better represented, evidencing the continuous tendency towards a general increase of the silver contents. The more obvious modification during the EIA is the higher

homogeneity of the silver contents (mostly belonging to the 10-15% Ag cluster), which could be related with the predominance of buttons in our collection. Regarding the copper content, the more significant modification seems to occur during the LBA, whose artefacts present significantly higher copper contents than the artefacts from previous periods.

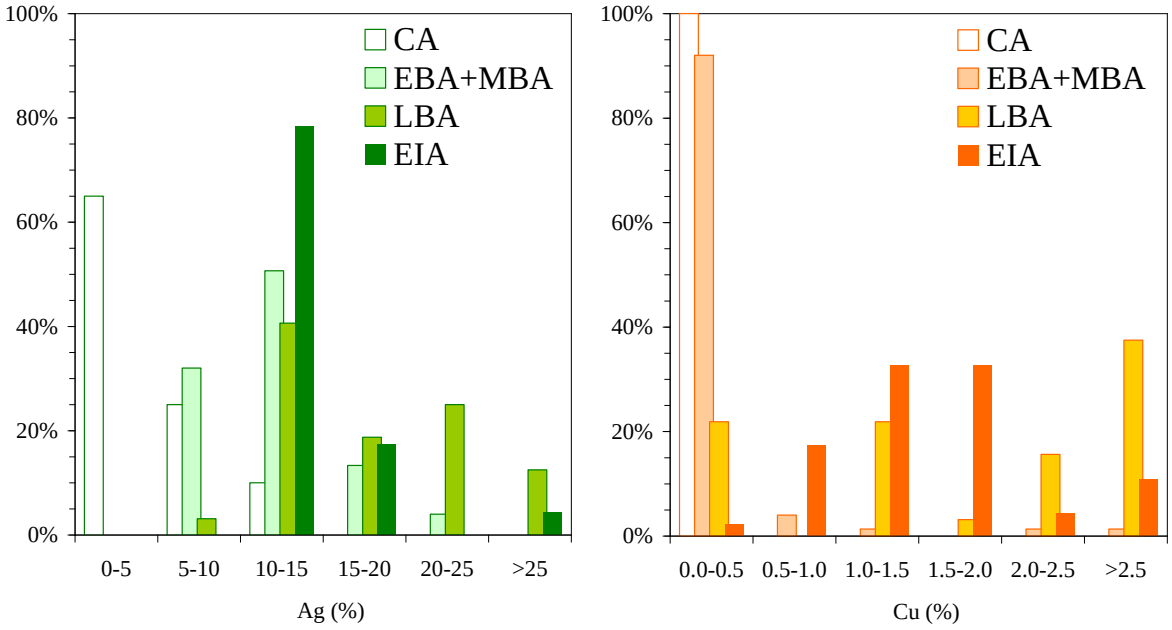

Figure 5.15. Distribution of silver and copper contents in gold artefacts from the southern Portuguese region (173 artefacts, comprising 20 CA, 75 EBA/MBA, 32 LBA and 46 EIA examples).

The increased amount of copper and, especially, of silver in the studied gold alloys produces a reduction in the *liquidus* temperature (Figure 5.16). Artefacts richer in silver present a *liquidus* temperature between 1000ºC and 950ºC, while pure gold melts at 1065ºC. Another outcome of the increased silver content is the more greenish colour of these gold artefacts (Figure 5.16).

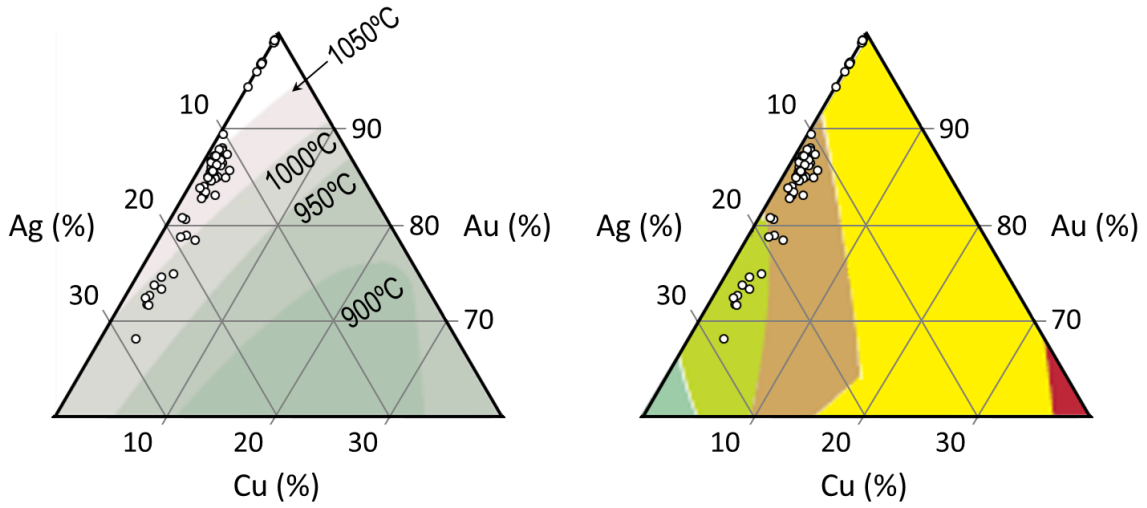

Figure 5.16. Ternary diagrams with the gold alloys studied in this work, evidencing the lower *liquidus* temperature and "greenish" colour of gold artefacts richer in silver (ternary diagrams from Grimwade, 2000).

A study involving the elemental composition of several hundred pre-historic gold artefacts from Spain allow to define the major trends observed throughout different chronological periods in most of the remaining Iberian Peninsula (Montero-Ruíz and Rovira, 1991). The database comprises 24 analyses made by these authors, together with 446 analyses published by the SAM project (Hartmann, 1982). The first significant alteration regarding gold artefact composition only occurs during the LBA, consisting on a generalized increase in the silver contents – the majority of EBA/MBA artefacts exhibit 5-10% Ag, while LBA silver contents mostly range from 10-15% (Figure 5.17). This increase of the silver contents of gold artefacts occurred earlier at the southern Portuguese territory (during the EBA/MBA), probably as the result of looking for better alloys to work with. The increase in the copper content of LBA gold artefacts from Spain is also noticeable, but there is still little tendency to alloy gold with copper since only 25% of LBA artefacts have more than 1% Cu. Therefore, the obvious increase of copper impurities in LBA gold artefacts (i.e. 0.25-1% Cu) might instead be related with the recycling of gold artefacts richer in copper (Montero-Ruíz and Rovira, 1991). Contrary, the majority (80%) of coeval artefacts from the southern Portuguese territory present copper contents above 1%, evidencing the copper richer raw materials used in this last region. Despite being impossible to completely determine the natural or artificial nature of these gold alloys, the composition of the ingot seems to support the alloying alternative in the southern Portuguese territory.

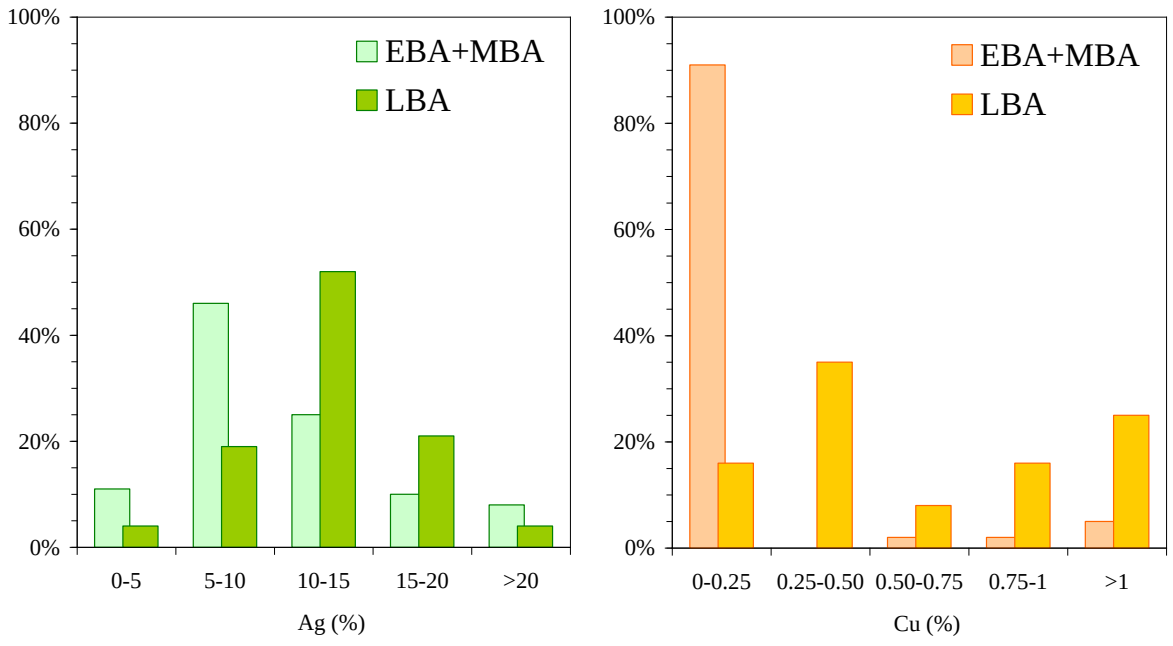

Figure 5.17. Distribution of silver and copper contents in gold artefacts from Spain (modified from Montero-Ruíz and Rovira, 1991).

During the EIA the main characteristic features of gold artefacts from Spain are the preponderance of copper rich alloys, simultaneously with an elevated differentiation among different regions and

collections (Montero-Ruíz and Rovira, 1991). The homogeneous alloy composition of most EIA gold artefacts from the southern Portuguese territory, namely the buttons from Castro dos Ratinhos, Outeiro da Cabeça and Fortios, together with the remarkable similar typology, seems to suggest a common gold workshop for these artefacts. The augmented heterogeneity encountered among EIA gold collections was interpreted as a consequence of the rising influences from the Orientalising region at the Iberian Peninsula (Perea, 2005). The bead from the Phoenician settlement of Quinta do Almaraz, being composed of a poorer gold alloy, seems to support this suggestion.

The introduction of an incipient welding technique was one of the innovations of the LBA period (Montero-Ruíz and Rovira, 1991). A study of pre-historic and proto-historic gold artefacts from the south of the Iberian Peninsula identified different types of welding (Perea, 1990). Generally, a solder alloy was used – a gold-silver, gold-copper or gold-silver-copper alloy with a melting point lower than the melting point of the components to be joined. A typical proto-historic solder alloy was identified in a gold torc (26-27% Ag and 1-2% Cu) from Chaves (Alves *et al.*, 2002) – the solder alloy is much richer in copper (~20% Ag and ~20% Cu) thus presenting a *liquidus* temperature (~850ºC) much inferior than the one of the torc alloy (~1020ºC).

Contrary, the analytical study of the gold buttons from Castro dos Ratinhos, Outeiro da Cabeça and Fortios evidences the absence of a solder alloy. Besides a homogeneous elemental composition identified at buttons welding regions, the OM and SEM-EDS characterisation of one button shows a completely homogeneous interface between the main body and decoration rod. Two gold components with similar melting points can be welded without a solder alloy due to the low propensity of this noble metal to become oxidised, even at high temperatures. If temperatures below the melting point are used the welding is due to solid state diffusion. However, even with temperatures very close to the melting point, it will take too long to close the spaces between the microscopically uneven surfaces and a complete elimination of the interface will take place (Tylecote, 1978). Therefore, the use of a somewhat higher temperature to produce a partial melting of the areas to be joined will significantly expedite the welding procedure. The concentration of the heat could be achieved with the help of a blowpipe to direct the flame in the areas to be welded. However, some of the ends of the tabs are totally melted proving that it should be very difficult to maintain a proper control over the welding temperature. Anyway, the overall manufacture of these beautiful gold buttons is a clear indication of the high metallurgical expertise of those ancient goldsmiths.

6. CONCLUSIONS

An integrated use of non-invasive and microanalytical techniques was able to characterise an important archaeological collection of artefacts belonging to the southern area of the Portuguese territory. The methodology selected to analyse the different type of materials, namely metallic artefacts (copper-based and gold) and production remains (copper-based), produced innovative and significant archaeometallurgical results without harming these valuable cultural items. Moreover, the analytical approach comprised a conservation treatment of those materials that are more predisposed to corrosion processes, namely the copper-based artefacts, to further minimize the impact of analytical studies.

The main focus of this work involves the evolution of the copper-based metallurgy from the LBA to the EIA in the southern region of the Portuguese territory. However, other studied issues provided important knowledge as well concerning early chronological periods and different metallurgies at this region. The study of gold artefacts evidenced the increased use of alloyed gold, especially with copper, during the LBA and EIA. Moreover, the annealing operation was already among the operational sequences used during the CA. There is no reason to think that these practices could not be transmitted and adapted to the copper-based metallurgy (and vice versa), so it should be kept in mind that those ancient LBA metallurgists already possessed a knowledge accumulated along two millennia of trial and error.

In fact, the few copper-based artefacts studied belonging to the period before the full adoption of the bronze alloys confirm that the results of hammering and annealing operations were already well understood. The edges of the MBA sword from Horta do Folgão were much more worked than the central section, thus creating a harder edge that was able to endure stronger impacts. However, there are still some evidences of a rather primitive control of the different metallurgical operations. Inverse segregation of arsenic evidences uncontrolled cooling rates during the casting operation, which complicates latter thermal homogenisation. Arsenic retained in oxide inclusions and arsenic-rich phases do not contribute to the solid solution, thus reducing the improvement of mechanical properties obtained by arsenic on copper.

The study of LBA production remains, principally the microstructural characterisation of slags, enabled an innovative approach about the bronze production at this region. All studied slags revealed a highly heterogeneous and immature nature, evidencing poor and changeable redox conditions within the smelting vases. These high viscosity slags detain a high amount of metallic prills, whose composition displays very low iron contents since the redox conditions were not sufficient to reduce the iron impurities present in the reaction vase. Metallic artefacts manufactured

with raw materials obtained by those early smelting operations will naturally exhibit very low iron contents. This was precisely the case of the "indigenous" cluster of bronze artefacts from this region, which includes all studied LBA collections together with the large EIA set from Castro dos Ratinhos. Despite the obvious Mediterranean influences present at this EIA settlement, the bronze artefacts recovered are still strongly correlated with the indigenous metallurgy inherited from the previous period.

Additionally, the analytical evidences strongly point to the co-smelting of copper ores with cassiterite inside primitive socketed handle crucibles at Entre Águas 5. The production of bronze alloy using co-smelting was already identified in other coeval sites from Central Portugal and Southwestern Iberian Peninsula, being possibly the more common method to produce bronzes during the LBA. The use of this method is entirely compatible with an almost exclusive presence of binary bronze alloys among the "indigenous" LBA metallurgy of this region. The variable metal content of copper ores and tin ores, in addition to somewhat changeable smelting conditions will make more difficult to obtain a "suitable" tin content. However, several centuries of metallurgical knowledge seem to enable the production of bronze alloys with a narrow range of tin contents.

The indigenous metallurgy at the southern Portuguese territory comprises binary bronzes with a "normal" distribution of tin contents around an average of ~10%, while the central region of the Portuguese territory presents a similar metallurgical tradition, but with slightly higher average tin contents (~13%, Figueiredo, 2010). Only the future analyses of a higher number of artefacts will be able to ascertain if there is actually a statistically significant difference between these two metallurgical traditions. If so, the reduction of tin contents at the southern region might be related with a higher distance to the sources of tin. Despite an apparent suitable supply of tin, evidenced by good tin contents of the bronzes from this southern region, it is possible that recycling of bronze scrap was somewhat more common than in the tin rich central region of the Portuguese territory.

The microstructural characterisation evidenced a superior knowledge over the mechanical and physical implications of adding tin to copper. The few alloys with higher tin contents produced were used in typologies that do not require high mechanical strength (e.g. "finger-rings", balance weights and fibulae), whilst these alloys were often not worked since they are more brittle and difficult to deform without fissuring. Tools and functional ornaments usually present lower tin contents that can easily be thermally homogenized. Additionally, the lighter colour of these high tin alloys could be considered more suitable for prestige artefacts.

The good technological knowledge commences with the casting operation given that casting defects due to low temperatures of mould and molten metal are rather uncommon. Afterwards, the

majority of operational sequences include forging and annealing cycles, often terminating with a more or less evident final forging operation. Certain microstructures testimony that the annealing treatment applied was not sufficient to completely homogenise the alloy (i.e. still display the α±δ). However, tools and weapons are usually composed by α matrix, which might indicates that the annealing operation was mastered, but only efficiently applied for significant typologies.

The metallurgy at the southern region of the Portuguese territory evidences a rising attendance of unalloyed coppers and leaded bronzes with the establishment of Phoenician colonies. The binary bronzes still constitute the more commonly used alloy, but commence to exhibit lower average tin contents (5.1 ± 2.1% Sn). In theory, the decrease of the tin content can be related with a significant use of bronze recycling without adding fresh tin. However, there are no archaeological evidences of significant problems with the supply of tin and there is still a lack of analytical studies concerning EIA copper-based production remains that could further explain the decrease of tin contents in bronze alloys.

Nevertheless, this study provides a number of primary clues regarding the metallurgical innovations induced by Phoenician contacts. The first evidence comes from the increased iron contents of "orientalising" bronze artefacts. Despite the absence of archaeological evidences regarding the replacement of crucibles by conventional furnaces during the EIA, the general increase of the iron content of bronze artefacts seems to indicate that the smelting operations began to operate under more efficient conditions. The second fact arises from the integrated study of the hardness of "indigenous" and "orientalising" artefacts from this region. Results seem to point out that the tin content do not present a ruling effect on the hardness of these artefacts. Moreover, some of the lower tin content "orientalising" artefacts present higher hardness than the "indigenous" ones. This higher hardness was attained by increasing the efficiency of both the hammering and annealing operations – additional deformation through hammering together with the correct control over the temperature and time of annealing. In practice, this means that even low tin bronzes could be worked to present somewhat good mechanical properties. It must be noted that the bronze alloy was already used among cultures from the Middle East since around 2600 BC. Therefore, it should be expected that the experienced Phoenician metallurgists, coming from a region with lack of tin sources, learned long ago how to beneficiate those low tin bronzes.

For the first time, the results obtained in the present work allow to establish a change of metallurgical technology during the EIA in the Portuguese territory. The adoption of innovative technologies was a rather slow process since indigenous communities, especially those who inhabited the inland areas, persist with some aspects of the LBA metallurgical tradition until very late. In fact, the diversification of copper-based alloys among the local communities was also an

unequal process, very dependent on cultural and socio-economical characteristics of indigenous settlements from the southwestern Iberian Peninsula. The inland 7th-6th centuries BC settlements of El Risco, Medellin (Montero-Ruíz *et al.*, 2003) and El Palomar (Rovira *et al.*, 2005) present a significant use of leaded bronzes, while binary bronzes do not seem to vary. On the contrary, the 6th century BC collections of Talavera la Vieja (Montero-Ruíz and Rovira, 2006) and Cancho Roano (Montero-Ruíz *et al.*, 2003) already present a reduced average tin content.

The diversification of metallic alloys also was encountered among EIA gold collections, being interpreted too as a consequence of the rising influences from the Phoenician people (Perea, 2005). Certainly, this diversification could not be found among the EIA gold artefacts from the southern region of the Portuguese territory analysed in this work because this collection was intentionally focused on a particular typology.

In the future, the integrated study of EIA slags and other production remains is needed to better understand the evolution of metallurgical practices. This will allow finding out if the metallurgical evolution comprises the increased use of alloying over co-smelting of copper-ores with cassiterite. The early evidence of alloying of metallic copper and tin was identified at the 8th-7th centuries BC site of Carmona (Rovira, 2005). The production of bronze alloys though different methods (co-smelting, cementation and alloying) would certainly originate in a wider range of bronze alloys, but further analytical studies are needed to corroborate this suggestion.

Additionally, the archaeometallurgical research must include provenance studies to identify the sources of metal exploited during pre-historic and proto-historic times. Provenance studies involving the lead isotopic composition compare the isotopic composition of artefacts with possible ore deposits. The lead isotopic composition of an ore is not modified by metallurgical processes used during the manufacture of an artefact (e.g. smelting, melting and casting) thus it can be used as a fingerprint of an ore deposit.

Finally, this work represents a significant step forward in the comprehension of the metallurgical evolution at the Portuguese territory. Innovative analytical data and interpretations contribute to the increased knowledge about the metal production and use among those ancient people, at last allowing to incorporate the southern region of the Portuguese territory amongst the well-studied regions from the Iberian Peninsula.

7. REFERENCES

Almagro-Bash, M.A. 1966. Sobre el origen possible de las más antiguas fíbulas anulares hispánicas. *Ampurias* 28, 215-236.

Alves, L.C., Araújo, M.F., Soares, A.M.M. 2002. Estudo de um torques proveniente do noroeste peninsular - aplicação de métodos instrumentais de análise química não destrutivos. *O Arqueólogo Português* 20, 115-134.

AMS 1973. *Metals Handbook 8: Metallography, Structures and Phase Diagrams*. Metals Park, OH, American Society for Metals International.

Araújo, M.F., Alves, L.C., Cabral, J.M.P. 1993. Comparison of EDXRF and PIXE in the analysis of ancient gold coins. *Nuclear Instruments and Methods in Physics Research B* 75, 450-453.

Araújo, M.F., Barros, L., Teixeira, A.C., Melo, A.A. 2004. EDXRF study of prehistoric artefacts from Quinta do Almaraz (Cacilhas, Portugal). *Nuclear Instruments and Methods in Physics Research B* 213, 741-746.

Arruda, A.M. 2008. Estranhos numa terra (quase) estranha: os contactos pré-coloniais no sul do território actualmente português. In: Celestino, S., Rafel, N., Armada, X.-L. (Eds.) *Contacto cultural entre el Mediterráneo y el Atlántico (siglos XII-VIII ane)*, CSIC, Madrid, 355-370.

Barros, L. 1998. *Introdução à Pré e Proto-História de Almada*. Núcleo de Arqueologia e História da Câmara Municipal de Almada, Almada.

Barros, L., Cardoso, J.L., Sabrosa, A. 1993. Fenícios na margem sul do Tejo: Economia e integração cultural do povoado de Almaraz-Almada, *Estudos Orientais* 4, 143-181.

Barros, L., Soares, A.M. 2004. Cronologia absoluta para a ocupação orientalizante da Quinta do Almaraz, no estuário do Tejo (Almada, Portugal). *O Arqueólogo Português* 22, 333-352.

Bayley, J., Rehren, T. (Eds.) 2007. *Towards a functional and typological classification of crucibles*. Archetype Publications, Oxford.

Beirão, C.M.M. 1986. *Une civilisation protohistorique du sud du Portugal (1er Âge du Fer)*. De Boccard, Paris.

Berrocal-Rangel, L., Silva, A.C. 2010. O Castro dos Ratinhos (Barragem do Alqueva, Moura). Escavações num povoado proto-histórico do Guadiana, 2004-2007. *O Arqueólogo Português Suplemento* 6, Museu Nacional de Arqueologia, Lisboa.

Bosi, C., Garagnani, G.L., Imbeni, V., Martini, C., Mazzeo, R., Poli, G. 2002. Unalloyed copper inclusions in ancient bronze artefacts. *Journal of Materials Science* 37, 4285-4298.

Bronk, H., Rohrs, S., Bjeoumikhov, A., Langhoff, N., Schmalz, J., Wedell, R., Gorny, H.E., Herold, A., Waldschlager, U. 2001. ArtTAX - A new mobile spectrometer for Energy-Dispersive Micro X-Ray Fluorescence spectrometry on art and archaeological objects. *Fresenius Journal of Analytical Chemistry* 371, 307-316.

Budd, P. 1991. Eneolithic arsenical copper: Heat treatment and the metallographic interpretation of manufacturing processes. In: Pernika, E., Wagner, G.A. (Eds.) Proceedings of Archaeometry 90. Basel, Birkhaüser, 35-44.

Budd, P., Ottaway, B.S. 1995. Eneolithic arsenical copper: chance or choice? In: Jovanovic, B. (Ed.) *International Symposium Ancient Mining and Metallurgy in Southeast Europe*. Archaeological Institute, Donji Milanovac, 95-102.

Calado, M., Mataloto, R. 2001. *Carta Arqueológica do Concelho do Redondo*. Câmara Municipal de Redondo, Redondo.

Canberra 2003. *WinAxil Operational Guide*. Canberra Eurisys Benelux N.V., Canberra.

Canha, A., Valério, P., Araújo, M.F. 2007. Testemunhos de metalurgia no povoado de Canedotes (Bronze Final). *Revista Portuguesa de Arqueologia* 10, 159-178.

Cardoso, J.L. 2000. The fortified site of Leceia (Oeiras) in the context of the Chalcolithic in Portuguese Estremadura. *Oxford Journal of Archaeology* 19, 37-55.

Cardoso, J.L., Braz Fernandes, F. 1995. Estudo arqueometalúrgico de um lingote de cobre de Leceia (Oeiras). *Estudos Arqueológicos de Oeiras* 5, 153-164.

Cardoso, J.L., Gradim, A. 2009. A anta do malhão (Alcoutim) e o "Horizonte de Ferradeira". *XELB* 10, 55-72.

Cardoso, J.L., Gradim, A. 2008. A necrópole de cistas da Idade do Bronze das Soalheironas (Alcoutim). Primeira notícia dos trabalhos realizados e dos resultados obtidos. *Promontoria* 6, 223-248.

Cardoso, J.L., Guerra, M.F., Bragança, F. 1992. O depósito de Bronze Final de Alqueva e a tipologia das lanças do Bronze Final português. *Mediterraneo* 1, 231-250.

Coffyn, A. 1985. *Le Bronze Final Atlantique dans la Péninsule Ibérique*. Centre Pierre Paris, Bordeaux.

Coghlan, H.H. 1975. *Notes on the metallurgy of copper and bronze in the Old World*. The University Press, Oxford.

Craddock, P.T. 1995. *Early metal mining and production*. The University Press, Cambridge.

Craddock, P.T., Meeks, N.D. 1987. Iron in ancient copper. *Archaeometry* 29, 187-204.

Delibes de Castro, G., Fernández-Manzano, J., Romero-Carnicero, F., Herrán-Martínez, J.I., Ramírez-Ramírez, M.L. 2001. Metal production at the end of the Late Bronze Age in the central Iberian Peninsula. *Journal of Iberian Archaeology* 3, 73-95.

Deus, M., Antunes, A.S., Soares, A.M.M. in press. Santa Margarida 3 (Serpa) no contexto do povoamento do Bronze Final do Sudoeste. In: V Encontro de Arqueologia do Sudoeste Peninsular, Almodôvar.

Deus, M., Antunes, A.S., Soares, A.M.M. 2009. A Salsa 3 (Serpa) no contexto dos povoados abertos do Bronze Final do Sudoeste. In: Pérez Macías, J.A., Bomba, E.R. (Eds.) IV Encuentro de Arqueología del Suroeste Peninsular, Universidad de Huelva, Huelva, 514-543 (CD-ROM).

Dungworth, D. 2000. Serendipity in the foundry? Tin oxide inclusions in copper and copper alloys as an indicator of production process. *Bulletin of the Metals Museum* 32, 1-5.

Etiégni, L., Campbell, A.G. 1991. Physical characteristics of wood ash. *Bioresource Technology* 37, 173-178.

Figueiredo, E. 2010. *A Study on Metallurgy and Corrosion of Ancient Copper-based Artefacts from the Portuguese Territory*. PhD thesis, Universidade Nova de Lisboa, Lisboa (unpublished).

Figueiredo, E., Melo, A.Á., Araújo, M.F. 2007. Artefactos metálicos do Castro de Pragança: um estudo preliminar de algumas ligas de cobre por espectrometria de fluorescência de raios X. *O Arqueólogo Português* 25, 195-215.

Figueiredo, E., Silva, R.J.C., Braz Fernandes, F.M., Araújo, M.F., Senna-Martinez, J.C., Vaz J.L.I. 2010. Smelting and recycling evidences from the Late Bronze Age habitat site of Baiões (Viseu, Portugal). *Journal of Archaeological Science* 37, 1623-1634.

Garcia-Guinea, J., Correcher, V., Rojas, R.M., Fierro, J.L.G., Fernandez-Martin, C., López-Arce, P., Rovira, S. 2005. Chemical tracers in archaeological and natural gold: Aliseda Tartesos treasure and new discovered nuggets (SW Spain). *Gold Bulletin* 38, 23-28.

García-Martínez, M.S., Ros-Sala, M.M. 2010. Gestión del combustible leñoso e impacto medioambiental asociados a la metalurgia protohistórica de Punta de los Gavilanes (Mazarrón, Murcia). *Trabajos de Prehistoria* 67, 545-559.

Giardino, C. 1995. *The West Mediterranean between the 14th and the 8th Centuries B.C.* (BAR International Series 612) Tempvs Reparatvm, Oxford.

Giumlia-Mair, A. 2005a. Copper and copper alloys in the Southeastern Alps: an overview. *Archaeometry* 47(2), 275-292.

Giumlia-Mair, A. 2005b. On surface analysis and archaeometallurgy. *Nuclear Instruments and Methods in Physics Research B* 239, 35-43.

Gomes, M.V. 1993. O estabelecimento fenício-púnico do Cerro da Rocha Branca (Silves). *Estudos Orientais* IV, 73-107.

Gómez-Ramos, P. 1999. *Obtención de Metales en la Prehistoria de la Península Ibérica* (BAR International Series 753) Archaeopress, Oxford.

Gonçalves, V.S., Valério, P., Araújo, M.F. 2005. The copper metallurgy of Monte Novo dos Albardeiros. *O Arqueólogo Português* 23, 231-256.

González de Canales, F., Serrano, L., Llompart, J. 2006. The pre-colonial Phoenician Emporium of Huelva ca 900-770 BC. *BABesch* 81, 13-29.

Grimwade, M. 2000. A plain man's guide to alloy phase diagrams: their use in jewellery manufacture - part 2. *Gold Technology* 30, 8-15.

Hanning, E., Gaub, R., Goldenberg, G. 2010. Metal from Zambujal: experimentally reconstructing a 5000-year-old technology. *Trabajos de Prehistoria* 67, 287-304.

Hanson, D., Pell-Walpole, W.T. 1951. *Chill-Cast Tin Bronzes*. Edward Arnold, London.

Hartmann, A. 1982. *Prähistorische goldfunde aus Europa*. Studien zu den Anfängen der Metallurgie 3(2), Gebrüder Mann Verlag, Berlin.

Hauptmann, A. 2007. *The Archaeometallurgy of Copper*. Springer-Verlag, Berlin.

Heleno, M. 1935. Joias pré-Romanas. *Ethnos* I, 229-257.

Hook, D. 2007. The composition and technology of selected Bronze Age and early Iron age copper alloy artefacts from Italy. In: Sestieri, A.M.B., Mcnamara, E. (Eds.) *Prehistoric Metal Artefacts from Italy (3500-720BC) in the British Museum*. (British Museum Research Publications 159) The British Museum, London, 308-323.

Hunt-Ortiz, M.A. 2003. *Prehistoric Mining and Metallurgy in South West Iberian Peninsula*. BAR International Series 1188, Archaeopress, Oxford.

Ingo, G.M., De Caro, T., Riccucci, C., Angelini, E., Grassini, S., Balbi, S., Bernardini, P., Salvi, D., Bousselmi, L., Cilingiroglu, A., Gener, M., Gouda, V.K., Al Jarrah, O., Khosroff, S., Mahdjoub, Z., Al Saad, Z., El-Saddik, W., Vassiliou, P. 2006. Large scale investigation of chemical composition, structure and corrosion mechanism of bronze archeological artefacts from Mediterranean basin. *Applied Physics A* 83, 513-520.

IUPAC 1978. Analytical Chemistry Division, Nomenclature, symbols, units and their usage in spectrochemical analysis. *Spectrochimica Acta B* 33, 242-245.

Junghans, S., Sangmeister, E., Schröder, M. 1974. *Kupfer und Bronze in der frühen Metallzeit Europas*. Studien zu den Anfängen der Metallurgie 2(4), Gebrüder Mann Verlag, Berlin.

Junghans, S., Sangmeister, E., Schröder, M. 1968. *Kupfer und Bronze in der frühen Metallzeit Europas*. Studien zu den Anfängen der Metallurgie 2(1-3), Gebrüder Mann Verlag, Berlin.

Kassianidou, V. 1993. Monte Romero, a silver-production workshop of the seventh century B.C. in south-west Spain. *Institute of Archaeo-Metallurgical Studies Newsletter* 18, 7-10.

Kayafa, M. 2003. The technology of copper-based alloys in Bronze Age western Peloponnese, Greece. In: Proceedings of the International Conference Archaeometallurgy in Europe, Vol 2, AIM, Milan, 1-10.

Kearns, T., Martinón-Torres, M., Rehren, T. 2010. Metal to mould: alloy identification in experimental casting moulds using XRF. *Historical Metallurgy* 44, 48-58.

Kevex 1992. *Kevex 771-EDX spectrometer users guide*. Kevex Instruments, Valencia.

Klein, S., Hauptmann, A. 1999. Iron Age leaded tin bronzes from Khirbet Edh-Dharih, Jordan. *Journal of Archaeological Science* 26, 1075-1082.

Kristiansen, K. 2003. *Europe before History*. Cambridge University Press, Cambridge.

Lago, M., Duarte, C., Valera, A., Albergaria, J., Almeida F., Carvalho, A.F. 1998. Povoado dos Perdigões (Reguengos de Monsaraz): dados preliminares dos trabalhos arqueológicos realizados em 1997. *Revista Portuguesa de Arqueologia* 1, 45-152.

Lechtman, H. 1996. Arsenic bronze: dirty copper or chosen alloy? A view from the Americas. *Journal of Field Archaeology* 23, 477-514.

Lechtman, H., Klein, S. 1999. The production of copper-arsenic alloys (arsenic bronze) by cosmelting: modern experiment, ancient practice. *Journal of Archaeological Science* 26, 497-526.

Maddin, R., Stech, T., Muhly, J.D. 1991. Çayönü Tepesi. The earliest archaeological metal artifacts. In: Éluère, C., Mohen, J.-P. (Eds.) *Découverte du Métal*. Picard, Paris, 375-386.

Mckerrell, H., Tylecote, R.F. 1972. The working of copper-arsenic alloys in the Early Bronze Age and the effect of the determination of provenance. *Proceedings of the Prehistoric Society* 38, 209–218.

Melo, A.Á. 2000. Armas, utensílios e esconderijos. Alguns aspectos da metalurgia do Bronze Final: o depósito do Casal dos Fiéis de Deus. *Revista Portuguesa de Arqueologia* 3, 15-120.

Melo, A.Á., Valério, P., Barros, L., Araújo, M.F. in press. Práticas metalúrgicas na Quinta do Almaraz (Cacilhas, Portugal): vestígios orientalizantes. In: Actas do VI Congresso Internacional de Estudos Fenício Púnicos, Lisboa, 136-149.

Mohen, J.-P. 1990. *Métallurgie préhistorique*. Masson, Paris.

Monteagudo, L. 1953. Album grafico de Carmona por G. Bonsor. *Archivo Español de Arqueologia* XXVI, 350-370.

Montero-Ruíz, I. 2008. Ajuares metálicos y aspectos tecnológicos en la metalurgia del Bronce Final-Hierro en el Sudeste de la Península Ibérica. In: Lorrio, A. (Ed.) *Querénima. El Bronce Final del Sureste de la Península Ibérica*. Real Academia de la Historia, Madrid, 499-516.

Montero-Ruíz, I. 1994. *Estudio Arqueometalurgico en el Sudeste de la Peninsula Ibérica*. Instituto de Estudios Almerienses, Almeria.

Montero-Ruíz, I., Perea, A., 2007. Brasses in early metallurgy of the Iberian Peninsula. In: La Niece, S., Hook, D., Craddock, P. (Eds.) *Metals and Mines: Studies in Archaeometallurgy*. Archetype Publications, London, 136-139.

Montero-Ruíz, I., Gómez-Ramos, P., Rovira, S. 2003. Aspectos de la metalurgia orientalizante en Cancho Roano. In: Pérez, S. (Ed.) *Cancho Roano IX. Los Materiales Arqueológicos II*. Instituto de Historia, Madrid, 195-210.

Montero-Ruíz, I., Rovira, S. 2006. Comentários sobre las composiciones de los metales del conjunto. In: Jimenez-Ávila, J. (Ed.) *El Conjunto Orientalizante de Talavera la Vieja (Cáceres)*. Junta de Extremadura, Cáceres, 109-114.

Montero-Ruíz, I., Rovira, S. 1991. El oro y sus aleaciones en la orfebrería preromana. *AEspA* 64, 7-21.

Moreno-Onorato, A., Contreras-Cortés, F., Renzi, M., Rovira, S., Cortés-Santiago, H. 2010. Preliminary study of slags and slaggy layers on ceramics from the Bronze Age metallurgical site of Peñalosa (Baños de la Encina, Jaén). *Trabajos de Prehistoria* 67, 305-322.

Morgenroth, U. 1999. Southern Iberia and the Mediterranean trade-routes. *Oxford Journal of Archaeology* 18, 395-401.

Müller, R., Goldenberg, G., Bartelheim, M., Kunst, M., Pernicka, E. (eds) 2007. *Zambujal and the Beginnings of Metallurgy in Southern Portugal*. Archetype Publications, Oxford.

Neville, A. 2007. *Mountains of Silver and Rivers of Gold. The Phoenicians in Iberia*. Oxbow Books, Oxford.

Nijboer, A.J., Van der Plicht, J. 2006. An interpretation of the radiocarbon determinations of the oldest indigenous-Phoenician stratum thus far, excavated at Huelva, Tartessos (south-west Spain). *BABesch* 81, 31-36.

Nocete, F., Queipo, G., Sáez, R., Nieto, J.M., Inácio, N., Bayona, M.R., Peramo, A., Vargas, J.M., Cruz-Auñón, R., Gil-Ibarguchi, J.I., Santos, J.F. 2008. The smelting quarter of Valencina de la Concepción (Seville, Spain): the specialised copper industry in a political centre of the Guadalquivir Valley during the Third millennium BC (2750–2500 BC). *Journal of Archaeological Science* 35, 717-732.

Northover, J.P. 2004. Metallography of two experimentally cast bronze swords of Ewart Park type. In: Faoláin, S.Ó. (Ed.) *Bronze Artefact Production in Late Bronze Age Ireland* (BAR British Series 382) Archaeopress, Oxford, 96-102.

Northover, J.P. 1989. Properties and use of arsenic-copper alloys. In: Hauptmann, A., Pernicka, E., Wagner, G.A. (Eds.) *Old World Archaeometallurgy*, Deutsches Bergbaumuseum, Bochum, 111-118.

Nunes, S., Corga, M., Basílio, L., Ferreira, M.T., Couto, R., Almeida, M., Neves, M.J. 2007. Fossas escavadas na rocha do Casarão da Mesquita 4 (S. Manços, Évora). *Al-madan online* 15, 9-10.

Paço, A. 1955. Castro de Vila Nova de São Pedro. VII – Considerações sobre o problema da metalurgia, *Zephyrus* 6, 27-40.

Pellicer-Catalán, M. 2000. El proceso orientalizante en el occidente ibérico. *Huelva Arqueológica* 16, 89-134.

Penhallurick, R.D. 1986. *Tin in Antiquity*. Institute of Metals, London.

Perea, A. 2005. Relaciones tecnológicas y de poder en la producción y consumo de oro durante la transición Bronce Final-Hierro en la fachada atlántica peninsular. *Anejos de AEspA* XXXV, 1077-1087.

Perea, A. 2003. Cancho Roano: estudio tecnológico de los objetos de oro. In: Celestino Pérez, S. (Ed.) *Cancho Roano VIII. Los Materiales Arqueológicos*. Junta de Extremadura & Consejería de Cultura, Madrid, 195-228.

Perea, A. 1990. Estudio microscópico y microanalítico de las soldaduras y otros procesos técnicos en la orfebrería prehistórica del Sur de la Península Ibérica. *Trabajos de Prehistoria* 47, 103-160.

Pérez, J.A., Rivera, T., Romero, E. 2002. Crisoles-hornos en el Bronce del Suroeste. *Bolskan* 19, 65-73.

Plesters, J. 1956. Cross-sections and chemical analysis of paint samples. *Studies in Conservation* 2, 110-157.

Ponte, S. 2006. *Corpus Signorum das Fíbulas Proto-históricas e Romanas de Portugal*. Caleidoscópio, Coimbra.

Ponte, T.R.N., Soares, A.M.M., Araújo, M.F., Frade, J.C., Ribeiro, I., Rodrigues, Z., Silva, R.J.C., Valério, P. in press. O Bronze Pleno do Sudoeste da Horta do Folgão (Serpa, Portugal). Os Hipogeus Funerários. *Revista Portuguesa de Arqueologia*.

Radivojevic, M., Rehren, T., Pernicka, E., Sljivar, D., Brauns, M. 2010. On the origins of extractive metallurgy: new evidence from Europe. *Journal of Archaeological Science* 37, 2775-2787.

Raub C.J., Ott, D. 1983. Gold casting alloys. The effect of zinc additions on their behaviour. *Gold Bulletin* 16, 46-51.

Rebelo, P., Santos, R., Neto, N., Fontes, T., Soares, A.M.M., Deus, M., Antunes, A.S. 2009. Dados preliminares da intervenção arqueológica no sítio do Bronze Final de Entre Águas 5 (Serpa). In: Pérez Macías, J.A., Bomba, E.R. (Eds.) IV Encuentro de Arqueología del Suroeste Peninsular, Universidad de Huelva, Huelva, 463-488 (CD-ROM).

Renfrew, C. 1983. *Les Origines de L'Europe*. Flammarion, Paris.

Renzi, M. 2007. A typological and functional study of the tuyeres from the site of La Fonteta (Guardamar del Segura, Alicante). *Trabajos de Prehistoria* 64, 165-177.

Renzi, M., Montero-Ruíz, I., Bode, M. 2009. Non-ferrous metallurgy from the Phoenician site of La Fonteta (Alicante, Spain): a study of provenance. *Journal of Archaeological Science* 36, 2584-2596.

Robbiola, L., Portier, R. 2006. A global approach to the authentication of ancient bronzes based on the characterisation of the alloy–patina–environment system. *Journal of Cultural Heritage* 7, 1-12.

Roberts B., 2008. Creating traditions and shaping technologies: understanding the earliest metal objects and metal production in Western Europe. *World Archaeology* 40, 354-372.

Rodriguez-Diaz, A., Pavon-Soldevila, I., Merideth, C., Tresserras, J.J.I. 2001. *El Cerro de San Cristobal, Logrosan, Extremadura, Spain* (BAR International Series 922) Archaeopress, Oxford.

Rovira, S. 2005. Bronze production in prehistory. In: VI Congresso Ibérico de Arqueometría, Girona, 21-35.

Rovira, S. 2004. Tecnología metalúrgica y cambio cultural en la Prehistoria de la Península Ibérica. *Norba. Revista de Historia* 17, 9-40.

Rovira, S. 2002. Metallurgy and society in prehistoric Spain. In: Ottaway, B.S., Wager, E.C. (Eds.) *Metals and Society* (BAR International Series 1061) Archaeopress, Oxford.

Rovira, S. 1995. Estudio arqueometalurgico del deposito de la Ria de Huelva. In: Priego, M.R.-G. (Ed.) *Ritos de Paso y Puntos de Paso. La Ria de Huelva en el Mundo del Bronce Final Europeu*. Universidad Complutense, Madrid, 33-57.

Rovira, S., Gómez-Ramos, P. 1998. Metalurgia calcolítica en Carmona (Sevilla). *SPAL. Revista de Prehistoria y Arqueologia* 7, 67-79.

Rovira, S., Montero-Ruíz, I. 2003. Natural tin-bronze alloy in Iberian Peninsula metallurgy: potentiality and reality. In: Giumlia-Mair, A., Lo Schiavo, F. (Eds.) *The Problem of Early Tin* (BAR International Series 1199) Archaeopress, Oxford, 15-22.

Rovira, S., Montero-Ruíz, I., Ortega, J., Jimenez-Ávila, J. 2005. Bronce y trabajo del bronce en el poblado orientalizante de "El Palomar" (Oliva de Mérida, Badajoz). *Anejos de AEspA* XXXV, 1231-1240.

Rovira, S., Montero-Ruíz, I., Renzi, M. 2009. Experimental co-smelting to copper-tin alloys. In: Kienlin, T.L., Roberts, B.W. (Eds.) *Metals and Societies. Studies in honour of Barbara S. Ottaway*. Universitätsforschungen zur Prähistorischen Archäologie 169, Bonn, 407-414.

Ruíz-Taboada, A., Montero-Ruíz, I. 1999. The oldest metallurgy in western Europe. *Antiquity* 73, 897-902.

Santos, F.J.C., Antunes, A.S.T., Grilo, C., Deus, M. 2009. A necrópole da I Idade do Ferro de Palhais (Beringel, Beja). Resultados preliminares de uma intervenção de emergência no Baixo-Alentejo. In: Pérez-Macías, J.A., Bomba, E.R. (Eds.) IV Encuentro de Arqueología del Suroeste Peninsular, Huelva, 746-804 (CD-ROM).

Santos, F.J.C., Arez, L., Soares, A.M.M., Deus, M., Queiroz, P.F., Valério, P., Rodrigues, Z., Antunes, A.S., Araújo, M.F. 2008. O Casarão da Mesquita 3 (S. Manços, Évora): um sítio de fossas "silo" do Bronze Pleno/Final na Encosta do Albardão. *Revista Portuguesa de Arqueologia* 11, 55-86.

Sarabia-Herrero, F.J. 1992. Arqueología experimental. La fundición de bronce en la Prehistoria Reciente. *Revista de Arqueología* 130, 12-22.

Sarabia-Herrero, F.J., Martín-Gil, J., Martín-Gil, F.J. 1996. Metallography of ancient bronzes: Study of pre-Roman metal technology in the lberian Peninsula. *Materials Characterization* 36, 335-347.

Senna-Martinez, J.C. 2007. Aspectos e problemas das origens e desenvolvimento da metalurgia do bronze na fachada atlântica peninsular. *Estudos Arqueológicos de Oeiras* 15, 119-134.

Senna-Martinez, J.C., Pedro, I. 2000. Between myth and reality: the foundry area of Senhora da Guia de Baiões and Baiões/Santa Luzia metallurgy. *Trabalhos de Arqueologia da EAM* 6, 61-77.

Sieso, J.P. 2005. Entre la fascinación y el rechazo: la aculturación entre las propuestas de interpretación del periodo orientalizante. *Anejos de AEspA* XXXV, 167-187.

Soares, A.M.M., Araújo, M.F., Alves 2004. Análise química não-destrutiva de artefactos em ouro pré e proto-históricos: alguns exemplos. *Revista Portuguesa de Arqueologia* 7, 125-138.

Soares, A.M.M., Araújo, M.F., Alves, L., Ferraz, M.T. 1996. Vestígios metalúrgicos em contextos calcolíticos e da Idade do Bronze no sul de Portugal. In: Maciel, M.J. (Ed.) *Miscellanea em Homenagem ao Professor Bairrão Oleiro*. Edições Colibri, Lisboa, 553-579.

Soares, A.M.M., Araújo, M.F., Cabral, J.M.P. 1985. O Castelo Velho de Safara: vestígios da prática da metalurgia. *Arqueologia* 11, 87-94.

Soares, A.M.M., Cabral, J.M.P. 1993. Cronologia absoluta para o Calcolítico da Estremadura e do Sul de Portugal. In: *1º Congresso de Arqueologia Peninsular, Actas dos Trabalhos de Antropologia e Etnologia* XXXIII, Porto, 217-235.

Soares, A.M.M., Martins, J. 2010. A cronologia absoluta para o Castro dos Ratinhos: Datas de radiocarbono. In: Berrocal-Rangel, L., Silva, A.C. (Eds.) *O Castro dos Ratinhos (Barragem do Alqueva, Moura). Escavações num povoado proto-histórico do Guadiana, 2004-2007*. O Arqueólogo Português Suplemento 6, 409-414.

Soares, A.M.M., Santos, F.J.C., Dewulf, J., Deus, M., Antunes, A.S. 2009. Práticas rituais no Bronze do Sudoeste – alguns dados. *Estudos Arqueológicos de Oeiras* 17, 433-456.

Soares, A.M.M., Valério, P., Araújo, M.F. 2005. Um novo vestígio da prática da metalurgia no Castelo Velho de Safara (Moura). *Revista Portuguesa de Arqueologia* 8, 215-224.

Soares, A.M.M., Valerio, P., Frade, J.C., Oliveira, M.J., Patoilo, D., Ribeiro, I., Arez, L., Santos, F.J.C., Araujo, M.F. 2007. A Late Bronze Age stone mould for flat axes from Casarão da Mesquita 3 (São Manços, Évora, Portugal). In: Proceedings of 2nd International Conference Archaeometallurgy in Europe, Associazione Italiana di Metallurgia, Aquileia (CD-ROM).

Soares, A.M.M., Valério, P., Silva, R.J.C., Alves, L.C., Araújo, M.F. 2010. Early Iron Age gold buttons from South-Western Iberian Peninsula. Identification of a gold metallurgical workshop. *Trabajos de Prehistoria* 67, 501-510.

Sousa, A.C., Valério, P., Araújo, M.F. 2004. Metalurgia antiga do Penedo do Lexim (Mafra). Calcolítico e Idade do Bronze. *Revista Portuguesa de Arqueologia* 7, 97-117.

Subramanian, P.R., Laughlin, D.E. 1988. The As-Cu (Arsenic-Copper) system. *Bulletin of Alloy Phase Diagrams* 9, 605-617.

Tate, J. 1986. Some problems in analysing museum material by nondestructive surface sensitive techniques. *Nuclear Instruments and Methods in Physics Research B* 14, 20-23.

Torres-Ortiz, M. 1998. La cronologia absoluta europea y el inicio de la colonización fenicia en Occidente. Implicaciones cronológicas en Chipre y el próximo Oriente. *Complutum* 9, 49-60.

Tylecote, R.F. 1992. *The History of Metallurgy*. The Institute of Materials, London.

Tylecote, R.F. 1987. *The Early History of Metallurgy in Europe*. Longman, London.

Tylecote, R.F. 1978. The solid phase bonding of gold to metals. *Gold Bulletin* 11, 74-80.

Tylecote, R.F., Ghaznavi, H.A., Boydell, P.J. 1977. Partitioning of trace elements between the ores, fluxes, slags and metal during the smelting of copper. *Journal of Archaeological Science* 4, 305-333.

Urbina, D., Morín, J., Ruíz, L.A., Agustí, E., Montero, I. 2007. El yacimiento de Las Camas, Villaverde, Madrid. Longhouses y elementos orientalizantes al inicio de la Edad del Hierro, en el valle medio del Tajo. *Gerión* 25, 45-82.

Valério, P., Alves, L.C., Soares, A.M.M., Araújo, M.F. 2010d. Os metais dos Ratinhos. II. Os botões em ouro. In: Berrocal-Rangel, L., Silva, A.C. (Eds.) *O Castro dos Ratinhos (Barragem do Alqueva, Moura). Escavações num povoado proto-histórico do Guadiana, 2004-2007*. O Arqueólogo Português Suplemento 6, 381-388.

Valério, P., Araújo, M.F., Canha, A. 2007. EDXRF and Micro-EDXRF studies of Late Bronze Age metallurgical productions from Canedotes (Portugal). *Nuclear Instruments and Methods in Physics Research B* 263, 477-482.

Valério, P., Araújo, M.F., Melo, A.Á., Barros, L. 2003. Archaeometallurgical studies of pre-historical artefacts from Quinta do Almaraz (Cacilhas, Portugal). In: *Proceedings of the International Conference Archaeometallurgy in Europe*, Vol 1. Associazione Italiana di Metallurgia, Milan, 327-336.

Valério, P., Araújo, M.F., Senna-Martinez, J.C., Inês Vaz, J.L. 2006. Caracterização química de produções metalúrgicas do Castro da Senhora da Guia de Baiões (Bronze Final). *O Arqueólogo Português* 24, 289-319.

Valério, P., Araújo, M.F., Silva, R.J.C., Soares, A.M.M. 2010a. Os metais dos Ratinhos I. A metalurgia do bronze. In: Berrocal-Rangel, L., Silva, A.C. (Eds.) *O Castro dos Ratinhos (Barragem do Alqueva, Moura). Escavações num povoado proto-histórico do Guadiana, 2004-2007*. O Arqueólogo Português Suplemento 6, 369-380.

Valério, P., Silva, R.J.C., Araújo, M.F., Soares, A.M.M., Barros L. 2012. A multianalytical approach to study the Phoenician bronze technology in the Iberian Peninsula – a view from Quinta do Almaraz. *Materials Characterization* 67, 74-82.

Valério, P., Silva, R.J.C., Araújo, M.F., Soares, A.M.M., Braz Fernandes, F.M. 2010b. Microstructural signatures of bronze archaeological artifacts from the southwestern Iberian Peninsula. *Materials Science Forum* 636-637, 597-604.

Valério, P., Silva, R.J.C., Soares, A.M.M., Araújo, M.F., Braz Fernandes, F.M., Gregório, A., Rebelo, P., Neto, N., Santos, R., Fontes, T. 2009. The beginning of bronze metallurgy in southern Portugal – Preliminary results from Entre Águas 5 (Serpa). *Proceedings of Archaeometallurgy: Technological, Economic and Social Perspectives in Late Prehistoric Europe*, CSIC, Madrid, 57.

Valério, P., Silva, R.J.C., Soares, A.M.M., Araújo, M.F., Braz Fernandes, F.M., Silva, A.C., Berrocal-Rangel, L. 2010c. Technological continuity in Early Iron Age bronze metallurgy at the South-Western Iberian Peninsula – a sight from Castro dos Ratinhos. *Journal of Archaeological Science* 37, 1811-1919.

Valério, P., Soares, A.M.M., Araújo, M.F., Silva, C.T., Soares, J. 2007. Vestígios arqueometalúrgicos do povoado calcolítico fortificado do Porto das Carretas (Mourão). *O Arqueólogo Português* 25, 177-194.

Veiga Ferreira, O. 1974. Notícia da descoberta de jóias auríferas no distrito de Portalegre. *Estudos Italianos em Portugal* 37, 79-82.

Vilaça, R. 2003. Acerca da existência de ponderais em contextos do Bronze Final / Ferro Inicial no território português. *O Arqueólogo Português* 21, 245-286.

Vilaça, R. 1997. Metalurgia do Bronze Final da Beira Interior: revisão dos dados à luz de novos resultados. *Estudos Pré-Históricos* V, 123-154.

Vilaça, R., Lopes, M.C. 2005. The treasure of Baleizão, Beja (Alentejo, Portugal). *Journal of Iberian Archaeology* 7, 177-184.

Walker, R. 1980. Corrosion and preservation of bronze artifacts. *Journal of Chemical Education* 4, 277-280.

Williamson, R.A., Nickens, P.R. 2000. *Science and Technology in Historic Preservation*. Klumer Academic/Plenum Publishers, New York.